VOLUME 37 MAY 1959 NUMBER 5

Canadian Journal of Chemistry

Editor: LÉO MARION

Associate Editors:

HERBERT C. BROWN, *Purdue University*
A. R. GORDON, *University of Toronto*
C. B. PURVES, *McGill University*
SIR ERIC RIDEAL, *Imperial College, University of London*
J. W. T. SPINKS, *University of Saskatchewan*
E. W. R. STEACIE, *National Research Council of Canada*
H. G. THODE, *McMaster University*
A. E. VAN ARKEL, *University of Leiden*

Published by THE NATIONAL RESEARCH COUNCIL

OTTAWA CANADA

Canadian Journal of Chemistry

Under the authority of the Chairman of the Committee of the Privy Council on Scientific and Industrial Research, the National Research Council issues THE CANADIAN JOURNAL OF CHEMISTRY and five other journals devoted to the publication, in English or French, of the results of original scientific research. Matters of general policy concerning these journals are the responsibility of a joint Editorial Board consisting of: members representing the National Research Council of Canada; the Editors of the Journals; and members representing the Royal Society of Canada and four other scientific societies.

The Chemical Institute of Canada has chosen the Canadian Journal of Chemistry as its medium of publication for scientific papers.

EDITORIAL BOARD

Representatives of the National Research Council

I. McT. Cowan, *University of British Columbia*
A. Gauthier, *University of Montreal*
H. G. Thode (Chairman), *McMaster University*
D. L. Thomson, *McGill University*

Editors of the Journals

D. L. Bailey, *University of Toronto*
T. W. M. Cameron, *Macdonald College*
H. E. Duckworth, *McMaster University*
K. A. C. Elliott, *Montreal Neurological Institute*
Léo Marion, *National Research Council*
R. G. E. Murray, *University of Western Ontario*

Representatives of Societies

D. L. Bailey, *University of Toronto*
Royal Society of Canada
T. W. M. Cameron, *Macdonald College*
Royal Society of Canada
H. E. Duckworth, *McMaster University*
Royal Society of Canada
Canadian Association of Physicists
K. A. C. Elliott, *Montreal Neurological Institute*
Canadian Physiological Society
P. R. Gendron, *University of Ottawa*
Chemical Institute of Canada
R. G. E. Murray, *University of Western Ontario*
Canadian Society of Microbiologists
T. Thorvaldson, *University of Saskatchewan*, Royal Society of Canada

Ex officio

Léo Marion (Editor-in-Chief), *National Research Council*
J. B. Marshall (Administration and Awards), *National Research Council*

Manuscripts for publication should be submitted to Dr. Léo Marion, Editor-in-Chief, Canadian Journal of Chemistry, National Research Council, Ottawa 2, Canada.
(For instructions on preparation of copy, see **Notes to Contributors** (inside back cover).)

Proof, correspondence concerning proof, and orders for reprints should be sent to the Manager, Editorial Office (Research Journals), Division of Administration and Awards, National Research Council, Ottawa 2, Canada.

Subscriptions, renewals, requests for single or back numbers, and all remittances should be sent to Division of Administration and Awards, National Research Council, Ottawa 2, Canada. Remittances should be made payable to the Receiver General of Canada, credit National Research Council.

The journals published, frequency of publication, and prices are:

Canadian Journal of Biochemistry and Physiology	Monthly	$9.00 a year
Canadian Journal of Botany	Bimonthly	$6.00 a year
Canadian Journal of Chemistry	Monthly	$12.00 a year
Canadian Journal of Microbiology	Bimonthly	$6.00 a year
Canadian Journal of Physics	Monthly	$9.00 a year
Canadian Journal of Zoology	Bimonthly	$5.00 a year

The price of regular single numbers of all journals is $2.00.

Canadian Journal of Chemistry

Issued by THE NATIONAL RESEARCH COUNCIL OF CANADA

VOLUME 37 MAY 1959 NUMBER 5

PYRIDINIUM BETAINES OF 1,3-INDANDIONE SERIES[1]

GERASSIMOS FRANGATOS AND ALFRED TAURINS

ABSTRACT

2-Bromo- (II) and 2,2-dibromo-1,3-indandione (III) react with pyridine, 3- and 4-methylpyridine, and 2-, 3-, and 4-pyridinecarboxylic acids to give 1-(3-hydroxy-1-oxo-2-indenyl)-pyridinium hydroxide betaines. In the betaines derived from pyridinecarboxylic acids the negative charge is located not in the carboxylic group but on the carbonyl oxygen atoms.

INTRODUCTION

Stafford (1) has obtained 1-(3-hydroxy-1-oxo-2-indenyl)pyridinium hydroxide, betaine (I), by brominating 1,3-indandione in the presence of pyridine and subsequently treating the intermediate salt with alkali. He assumed that the addition of bromine to pyridine resulted in the formation of pyridine bromide perbromide which formed 2-bromo-1,3-indandione with 1,3-indandione; the latter compound reacted further with pyridine to form a pyridinium salt. These steps appear plausible, but no experimental proof was given to support these assumptions.

It is known, however, that 1,3-indandione produces with bromine only 2,2-dibromo-1,3-indandione (2) and that 2-bromo-1,3-indandione (3) has never been isolated as an intermediate in this bromination. However, this does not exclude the presence of 2-bromo-1,3-indandione in some intermediate steps in the formation of 1-(3-hydroxy-1-oxo-2-indenyl)pyridinium bromide.

A similar reaction of pyridine with 5,5-dibromobarbituric acid produced the betaine of 1-(4-hydroxy-2,6-dioxo-5-tetrahydropyrimidyl)pyridinium hydroxide and 4-pyridylpyridinium bromide hydrobromide. 5-Bromo-5-nitrobarbituric acid and pyridine gave the same products, but 5-bromobarbituric acid did not react (4).

It has been found by Metro and Taurins (5) that 2-bromo-2-nitro-1,3-indandione reacted with pyridine by a different mechanism yielding the pyridinium salt of 2-nitro-1,3-indandione, pyridine hydrobromide, and a black tar containing nitrogen, bromine, and oxygen.

The objective of the present work was to investigate the formation of (I) and similar betaines by the direct interaction of 2-bromo- (II) and 2,2-dibromo-1,3-indandione with pyridine, methylpyridines, and pyridinecarboxylic acids.

DISCUSSION

When 2-bromo-1,3-indandione (II) was added to pyridine, a yellow solution was obtained, the color of which deepened gradually as the reaction proceeded. Upon standing at 20° for several hours, or short heating at 100°, the solution turned very dark. It was

[1]*Manuscript received January 14, 1959.*
Contribution from the Department of Chemistry, McGill University, Montreal, Quebec, with the financial assistance of the National Research Council of Canada, Ottawa, Canada.

felt that 1-(1,3-dioxo-2-indanyl)pyridinium bromide should be formed from (II) in the first step of the reaction as the result of a simple nucleophilic attack by pyridine. Therefore, attempts were made to isolate the bromide by sublimation of the residue obtained after removal of excess pyridine. On sublimation a white pyridinium hydrobromide appeared first and at a higher temperature the betaine (I) sublimed in the form of lustrous yellow crystals. The isolation of these products led to the conclusion that the intermediate 1-(1,3-dioxo-2-indanyl)pyridinium bromide is very reactive and is dehydrobrominated by pyridine in the first stages of the reaction. Furthermore, the isolation of these two products indicates that the bromine atom in (II) can be released also in the form of anion (Formulae sheet I, steps (*c*) and (*d*)).

2,2-Dibromo-1,3-indandione reacted slowly with pyridine at water bath temperature and the color of the mixture deepened gradually. From the reaction mixture two products were isolated, 1-(3-hydroxy-1-oxo-2-indenyl)pyridinium hydroxide, betaine (I), and pyridinium hydrobromide. The latter compound was isolated by removing the excess pyridine *in vacuo* and crystallizing the semisolid residue from alcohol. Both compounds could also be isolated by fractional sublimation. The residue after sublimation was a black tar which contained nitrogen and bromine.

The formation of the betaine may be considered as an elimination of two bromine atoms from each molecule of 2,2-dibromo-1,3-indandione by the action of pyridine. Steps (*c*) and (*d*) are also valid for the reaction of 2-bromo-1,3-indandione with pyridine.

The essential point in this mechanism is that the first bromine atom is removed as Br^+ leaving two electrons at the carbon atom. The second bromine is removed as Br^- in a displacement reaction with pyridine. The formation of two products (betaine I and pyridine hydrobromide) indicates that the mechanism is a two-step elimination. Protons which are necessary for step (*b*) are formed in the bromination reaction of pyridine by Br^+. There is always a black tar formation in the reaction of bromine Br_2 with pyridine (6).

We found that it was impossible to synthesize betaines of the 1,3-indandione series from three isomer methylpyridines using the Stafford procedure. In all cases, even at 0°, there was a rapid tar formation. From the black semisolid products only methylpyridine hydrobromides were isolated by sublimation. Contrary to that, the interaction of 2-bromo- and 2,2-dibromo-1,3-indandione with 3- and 4-methylpyridines gave the corresponding betaines. 2-Methylpyridine produced a black resin with both the reagents, although reactions were attempted under varying conditions of temperature, solvent, and time. 4-Methylpyridine reacted easily with 2,2-dibromo-1,3-indandione in boiling ethanol. On cooling of the red solution, a crystalline compound precipitated which was crystallized and obtained as pure yellow crystals. The reaction occurred also in toluene, but the yield was only about 40%, compared with 67% in ethanol.

3-Methylpyridine was less reactive with 2,2-dibromo-1,3-indandione than its 4-isomer and therefore a longer time and a higher temperature was necessary. Therefore the reaction was carried out in isoamyl alcohol at reflux temperature for 7 hours. The yield of the betaine under such conditions was 77%. The reaction did not occur in methyl or ethyl alcohol resulting in almost quantitative recovery of the starting materials.

The reactions of 3- and 4-methylpyridines with 2-bromo-1,3-indandione were carried out without any solvent at room temperature for 24 hours. Under such conditions 4-methylpyridine reacted with greater ease than pyridine.

The formation of betaines of 2-, 3-, and 4-pyridinecarboxylic acids with 2,2-dibromo-1,3-indandione were of interest because carboxylic groups could be considered as a potential negative center in the betaine. Since pyridinecarboxylic acids have an inner

FORMULAE SHEET I

REACTION OF 2-BROMO-1,3-INDANDIONE AND 2,2-DIBROMO-1,3-INDANDIONE WITH PYRIDINE

(a)

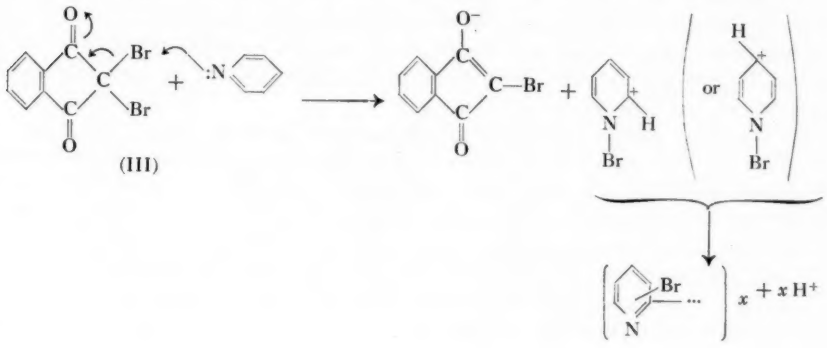

(III)

(b)

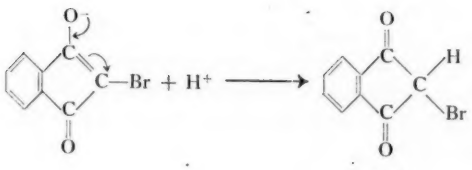

(II)

(c)

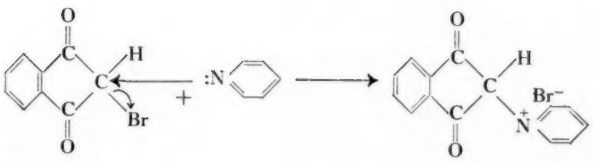

(d)

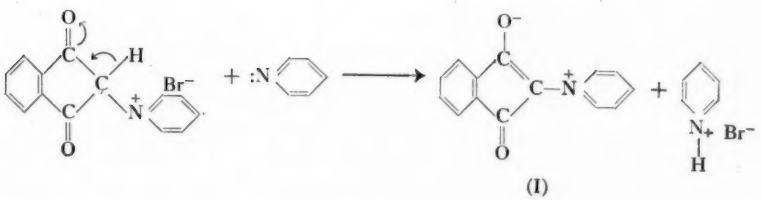

(I)

salt structure it was expected that the reaction of 2,2-dibromo-1,3-indandione with these acids would proceed with difficulty. This was confirmed experimentally. Higher temperatures and longer reaction time in refluxing isoamyl or *n*-butyl alcohol were necessary for the reaction to be completed. When the reaction mixture had been cooled, the golden-colored product precipitated together with the unreacted excess of pyridinecarboxylic acid. The latter was removed from the mixture by extracting with boiling water or more effectively by treatment with strong mineral acids. Any unreacted 2,2-dibromo-1,3-indandione was removed by extracting with chloroform. 2-Pyridinecarboxylic acid gave a poor yield of the betaine and the reaction was accompanied by fairly strong tar formation.

The presence of the carboxylic group in these betaines was detected by infrared spectroscopy. The betaine of 2-carboxy-1-(3-hydroxy-1-oxo-2-indenyl)pyridinium hydroxide showed weak bands at 2840, 2580, 2470, 2380, and 2300 cm^{-1} given by the stretching vibrations of the hydroxyl of the carboxyl group; 3- and 4-carboxy-isomers gave similar bands at slightly different positions. Also, there was a strong band present at 1725–1732 cm^{-1} in each one of the three betaines derived from pyridinecarboxylic acids. This band was given by the carbonyl of the carboxyl group. The carbonyl absorption of the unsubstituted betaine (Stafford compound) and 4-methyl derivative was very weak at 1725 and 1733 cm^{-1} respectively.

The electronic absorption spectra of the betaines obtained from methylpyridines or pyridinecarboxylic acids were determined and a great similarity in the patterns of these spectra was revealed. In each spectrum the absorption maxima occurred in the regions of 237–243, 311–316, and 386–418 mμ, and the molecular extinction coefficients were of the same order of magnitude. 1-(3-Hydroxy-1-oxo-2-indenyl)4-methylpyridinium hydroxide, betaine, showed a fourth absorption maximum in the region of 300 mμ (Table I and Figs. 1 and 2).

TABLE I

Electronic spectra of betaines of 1-(3-hydroxy-1-oxo-2-indenyl)pyridinium hydroxides (in absolute ethanol solution)

Substituent in the pyridine ring	λ_{max}, mμ	$\log_{10} \epsilon_{max}$
4-CH_3	273, 300, 316, 386	4.53; 3.34; 3.45; 4.13
3-CH_3	241, 313, 400	4.85; 3.36; 3.95
4-COOH	243, 315, 418	4.49; 3.28; 4.09
3-COOH	241, 312, 398	4.81; 3.44; 4.05
2-COOH	240, 311, 396	4.79; 3.33; 4.04

The similarity in spectra of betaines derived from methylpyridines and those obtained from pyridinecarboxylic acids serves to confirm the structures assigned to the latter group of betaines, and leaves no doubt that the carboxylic group does not participate in the formation of the inner salt by becoming the negative center of the dipole.

The absorption spectra of the betaines were determined in absolute alcohol. When attempts were made to measure the absorption spectra in chloroform, it was found that the wavelengths at which the absorption maxima appeared were reproducible but the molecular extinction coefficients were not.

EXPERIMENTAL

For the synthesis of the pyridine betaines of the 1,3-indandione series, three procedures, A, B, and C, were used.

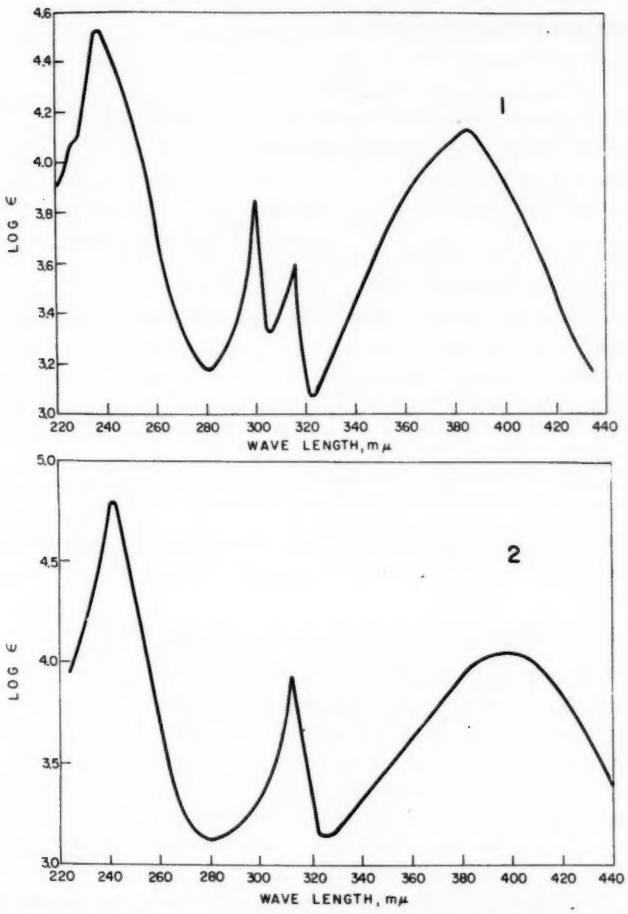

FIG. 1. Electronic absorption spectrum of 1-(3-hydroxy-1-oxo-2-indenyl)4-methylpyridinium hydroxide, betaine.

FIG. 2. Electronic absorption spectrum of 3-carboxy-1-(3-hydroxy-1-oxo-2-indenyl)pyridinium hydroxide, betaine.

Procedure A.—This procedure was applied to the reaction of 2-bromo-1,3-indandione with pyridine and methylpyridines. The method consisted of direct interaction of compounds in the absence of solvents, followed by the removal of excess unreacted materials by extraction, and isolation of the corresponding betaines. The reaction temperature was either 20° for 24 hours, or 100° for 4–6 minutes.

Procedure B.—This method consisted of the direct interaction of 2,2-dibromo-1,3-indandione with excess of pyridine and methylpyridines at 100° for several hours. The excess pyridine compound was removed by distillation in vacuum and the betaine was isolated by sublimation of the residue in vacuum.

Procedure C.—According to this method, 2,2-dibromo-1,3-indandione and pyridine derivatives were dissolved in a solvent (ethyl, *n*-butyl, or isoamyl alcohol, or toluene) and refluxed for 3 to 8 hours. The solvent was removed by distillation at reduced pressure.

The results are summarized in Table II.

TABLE II

Betaines of 1-(3-hydroxy-1-oxo-2-indenyl)pyridinium hydroxides

No.	Substituent in the pyridine ring	Procedure No.	Solvent	Temp., °C	Time	Yield, %	M.p., °C (decomp.)	Empirical formula	Elementary analysis C, % Calc.	C, % Found	H, % Calc.	H, % Found	N, % Calc.	N, % Found
1	3-CH_3	A	No solvent	100	4 min.	82								
		B	No solvent	100	4 hr.	65.8	218	$C_{16}H_{11}NO_2$	75.95	76.20	4.67	4.62	5.90	6.15
		C	Isoamyl alcohol		7 hr.									
		A	No solvent	20	24 hr.	71.7								
2	4-CH_3	C	Ethyl alcohol	78	2 min.		258	$C_{16}H_{11}NO_2$	75.95	76.22	4.67	4.74	5.90	6.19
3	2-COOH	C	*n*-Butyl alcohol	117	3 hr.	27	312	$C_{16}H_9NO_4$	67.41	67.15	4.34	4.17	5.24	4.92
4	3-COOH	C	Isoamyl alcohol	132	6 hr.		317	$C_{16}H_9NO_4$	67.41	67.46	4.34	4.21	5.24	5.02
5	4-COOH	C	Isoamyl alcohol	132	6 hr.	58	351	$C_{16}H_9NO_4$	67.41	67.18	4.34	4.18	5.24	5.04

1-(3-Hydroxy-1-oxo-2-indenyl)pyridinium Hydroxide, Betaine (I)

1. Reaction of 2-Bromo-1,3-indandione with Pyridine (Procedure A)

2-Bromo-1,3-indandione (1.139 g, 0.005 moles) and 3 ml of pyridine were heated on a steam bath for 6 minutes. The dark red solution was poured into 50 ml of water and refluxed for 10 minutes. After being allowed to cool to room temperature, the solution was extracted with three 10-ml portions of ether. The aqueous layer was separated and made alkaline (pH 11) with sodium hydroxide solution. On cooling for 10 hours, the solution deposited 0.75 g of the betaine in 67% yield. The melting point of the substance after crystallizing from ethanol was 257° (decomp.), in agreement with the literature (1). The betaine (I) can be also obtained if the reaction is carried out at room temperature for 24 hours.

2. Reaction of 2,2-Dibromo-1,3-indandione with Pyridine (Procedure B)

(*a*) A sample of 2,2-dibromo-1,3-indandione (1 g, 3.3 millimoles) was added to 3 ml of pyridine and the solution was heated on a steam bath for 3 hours. The excess pyridine was removed under reduced pressure. The solid dark residue was dried in a vacuum desiccator over concentrated sulphuric acid. The material was crystallized from 12 ml of ethyl alcohol and the betaine (I) was obtained in pure form, melting point 257° (decomp.). The yield of (I) was 0.34 g (46.5% of the theoretical).

(*b*) The other product of the reaction, pyridine hydrobromide, was isolated by sublimation (at 120–125° and 1 mm pressure) of the dried reaction mixture in all-glass apparatus. The yield of the substance was 0.475 g. It was purified by repeated sublimations or by recrystallization from a hot mixture of chloroform and styrene. The second fraction, betaine I (0.5 g), sublimed at 185–190° under 1 mm pressure. A black resinous material remained (0.5 g) in the sublimation apparatus. It did not crystallize from various solvents and the analysis showed the presence of nitrogen and anionic bromine.

1-(3-Hydroxy-1-oxo-2-indenyl)3-methylpyridinium Hydroxide, Betaine

1. Reaction of 2-Bromo-1,3-indandione with 3-Methylpyridine (Procedure A)

The betaine weighed 0.97 g (82% yield) and melted at 218° (decomp.).

2. Reaction of 2,2-Dibromo-1,3-indandione with 3-Methylpyridine

(*a*) *Procedure B.*—The first fraction obtained by the sublimation of the residue from the reaction mixture was 3-methylpyridine hydrobromide (yield 0.23 g). The second fraction was the betaine of 1-(3-hydroxy-1-oxo-2-indenyl)3-methylpyridinium hydroxide, melting point 218° (decomp.). The yield was 0.78 g (65.8%). The black resinous residue which did not crystallize weighed 0.64 g.

(*b*) *Procedure C.*—Five milliliters of 3-methylpyridine was added to a solution of 1.53 g (0.005 moles) of 2,2-dibromo-1,3-indandione in 40 ml of warm isoamyl alcohol. The orange reaction mixture was refluxed for 7 hours, then most of the isoamyl alcohol was distilled at reduced pressure and the viscous orange solution was cooled in an ice bath. The solid material which separated was filtered by suction and washed with two 10-ml portions of ether. On recrystallization from ethyl alcohol it melted at 218° (decomp.). The yield was 0.91 g (0.77%).

1-(3-Hydroxy-1-oxo-2-indenyl)4-methylpyridinium Hydroxide, Betaine

1. By Procedure A

The betaine crystallized from ethyl alcohol in yellow elongated prisms, melting point 258° (decomp.). The yield was 71.7%.

2. By Procedure C

(*a*) 2,2-Dibromo-1,3-indandione (1.53 g, 0.005 moles) was dissolved in 20 ml of ethyl alcohol by refluxing. To this solution 4 ml of 4-methylpyridine was added over a period of 10 minutes. The betaine was isolated in the usual way and melted at 258° with decomposition. The yield was 0.82 g (67% of the theoretical). Molecular weight determination: Calc. for $C_{15}H_{11}NO_2$: 237. Found by the Rast method: 234.

(*b*) In toluene, at reflux temperature of 110.6°, the reaction of the substances mentioned above gave the betaine in a 39% yield.

(*c*) The fractional sublimation of the reaction product gave 0.37 g of 4-methylpyridinium hydrobromide.

2-Carboxy-1-(3-hydroxy-1-oxo-2-indenyl)pyridinium Hydroxide, Betaine

Procedure C.—A sample of 2,2-dibromo-1,3-indandione (0.76 g; 2.5 millimoles) was allowed to react with an excess (2 g) of 2-pyridinecarboxylic acid in 30 ml of boiling *n*-butyl alcohol (b.p. 117°) for 3 hours. The alcohol was removed by distillation under reduced pressure. A solid residue consisting of betaine and excess 2-pyridinecarboxylic acid was left. It was extracted with 8 ml of boiling water to remove the acid. The betaine was dried in vacuum and crystallized several times from *n*-butyl alcohol. A yield of 0.18 g (27% of the theoretical) of the betaine, m.p. 312° (decomp.), was obtained.

3-Carboxy-1-(3-hydroxy-1-oxo-2-indenyl)pyridinium Hydroxide, Betaine

Procedure C.—This compound was prepared in isoamyl alcohol from 3-pyridinecarboxylic acid and 2,2-dibromo-1,3-indandione. It melted at 317° (decomp.) after crystallization from isoamyl alcohol.

4-Carboxy-1-(3-hydroxy-1-oxo-2-indenyl)pyridinium Hydroxide, Betaine

Procedure C.—The betaine was synthesized from 4-pyridinecarboxylic acid and 2,2-dibromo-1,3-indandione in isoamyl alcohol, m.p. 351°.

REFERENCES

1. STAFFORD, W. H. J. Chem. Soc. 580 (1952).
2. WISLICENUS, W. Ann. **246**, 354 (1888).
3. ROSER, W. and HASELDORF, E. Ann. **247**, 140 (1888).
4. TAYLOR, E. C., JR., PAUDLER, W. W., and CAIN, C. K. J. Org. Chem. **20**, 264 (1955).
5. METRO, S. J. and TAURINS, A. Can. J. Chem. **30**, 466 (1952).
6. MCELVAIN, M. S. and GOESE, M. A. J. Am. Chem. Soc. **65**, 2227 (1943).

A GAS CHROMATOGRAPHIC STUDY OF THE ADSORPTIVE PROPERTIES OF A SERIES OF ACTIVATED CHARCOALS[1]

HENRY W. HABGOOD[2] AND JAMES F. HANLAN[3]

ABSTRACT

From measurements of the gas chromatographic retention volumes, the initial slopes of the adsorption isotherms of nitrogen and the simpler hydrocarbons on a series of steam-activated coconut charcoals were determined. The initial heats of adsorption were obtained in the usual way from the temperature dependence. It was found for all gases that both the initial slope of the isotherm and the initial heat of adsorption decreased with increasing degree of activation of the charcoal (i.e. with increasing surface area per g). This suggests that the higher affinity for the very small pores in less activated material more than counterbalances the lower total surface.

Measurements at several different carrier gas flow rates of the relative band width for the charcoals of least and of greatest activation demonstrated, as might be expected, a greater resistance to mass transfer for the former. However, the apparent diffusion coefficients calculated on the assumption that all transport is by gas phase in the pores were nearly the same for each charcoal and showed relatively little variation among the different gases.

INTRODUCTION

The technique of gas chromatography which, in recent years, has been so useful in analytical chemistry may also be applied to some problems in physical chemistry. We have used gas–solid (gas adsorption) elution chromatography to study the adsorptive properties of a series of varyingly activated coconut charcoals. A systematic investigation has been made of the elution peaks obtained for a number of simple hydrocarbon gases from columns of each of the charcoals at a series of temperatures. Each peak is characterized by two quantities, its retention volume and its relative width. The former may be readily identified with the gas–solid distribution coefficient while the latter depends in part on the rate of adsorption.

The retention volume for any given eluate is related to its distribution coefficient between the moving and stationary phases. Cremer and Prior (1) have examined this relationship for gas–solid chromatography, but the best-known development is that for gas–liquid chromatography of Martin and Synge (2). Their simple relationship may be written in the following form to apply to gas–solid chromatography:

$$[1] \qquad \alpha = (V^0_R - V^0_d)/W \,.\, 273/T$$

where α is the initial slope of the adsorption isotherm in cc (S.T.P.) adsorbed per g, atm; V^0_R is the limiting value of the retention volume for small samples at column temperature, T, and pressure corrected to zero pressure drop through the column (3); V^0_d is similarly the retention volume for a non-adsorbed component; and W is the weight of adsorbent. Thus α is the net retention volume corrected to standard temperature per g of column material. Porter, Deal, and Stross (4) and others (5, 6, 7) have demonstrated the validity of the equivalent relationship for gas–liquid chromatography provided the sample volume is small compared with the total column volume.

Gas–solid chromatography has the complication of a curved isotherm—i.e. a variable distribution coefficient—and hence equation [1] will only apply to the limiting retention

[1]*Manuscript received October 20, 1958.*

Contribution No. 92 from the Research Council of Alberta, Edmonton, Alberta. Based on a paper presented at the 41st Annual Conference and Exhibition of the Chemical Institute of Canada, Toronto, May 26–28, 1958.

[2]*Associate Research Officer, Research Council of Alberta, and Special Lecturer, Department of Chemical and Petroleum Engineering, University of Alberta.*

[3]*Summer Research Assistant, Summer 1957. Present Address: University of California, Berkeley, California.*

volume at small sample pressure. The shape of the tail, which is characteristic of the asymmetric peaks usually found with gas–solid chromatography, may give some information about the complete isotherm (8, 9).

While the theory of gas–solid chromatography follows from that for gas–liquid chromatography, it may also be developed directly in terms of the apparent volume of the adsorbate in the presence of the adsorbent (10) by applying the Steele and Halsey equation of state approach to high temperature physical adsorption (11, 12).

The heat of adsorption is obtained from the slope of the log α–$1/RT$ plot. From the definition of α this is seen to be the limiting value at zero coverage of the isosteric heat of adsorption.[4,5]

Generally speaking, the initial slope of the adsorption isotherm is proportional to the product of two quantities, the total surface area and the affinity of the sorbate for the surface. Since the latter is directly related to the heat of adsorption, it is possible, in principle, given a particular model for the adsorption process, to determine the surface area from measurements of α at various temperatures. Steele and Halsey (11, 12), assuming an inverse third power attraction between hard spheres and a smooth surface, fitted the initial slopes of isotherms of the noble gases over a range of temperatures to surface areas fairly close to standard Brunauer–Emmett–Teller areas. Hanlan and Freeman in a paper to be published (10) have applied this method with some additional refinements to the present chromatographic data.

The use of gas–solid chromatography to study the rates of adsorption is based on an interpretation of the relative band widths which follows from the analysis of van Deemter, Zuiderweg, and Klinkenberg (14). These authors, from a development of the "plate" theory of chromatography, related the height equivalent to a theoretical plate, H, to the relative band width, $\Delta S^0/V^0_R$ where ΔS^0 is the volume of carrier gas corresponding to the base of the chromatographic elution peak and V^0_R is the volume to the maximum of the peak. For very small sample volumes giving symmetrical Gaussian peaks the relationship assumes the simple form:

$$[2] \qquad H = L(\Delta S^0/V^0_R)^2/16$$

where L is the length of the column.

The authors showed, from a comparison of the "plate" and "rate" theories, that H is expected to be a function of carrier gas velocity, u, as follows:

$$[3] \qquad H = A + B/u + Cu$$

where A, B, and C are constants for any particular system and may be interpreted respectively in terms of "eddy diffusion", molecular diffusion, and resistance to mass transfer. The last of these determines the rate of adsorption in gas–solid chromatography. A variation of H with u of the form of equation [3] has been obtained by several workers for gas–liquid chromatography (14, 15, 16, 17).

In the present work a tentative interpretation of C in terms of an apparent gas phase diffusion coefficient in the charcoal pores is attempted.

Figure 1 shows a typical chromatogram replotted from the chart record to illustrate the quantities α and H. This chromatogram also illustrates the small but distinct asym-

[4]*Cremer and Prior (1) and more recently Greene and Pust (13) have plotted what is equivalent to log αT against $1/T$ and accordingly obtained a ΔH which is smaller by an amount RT. This difference was not sufficient to influence the linearity of the plots obtained nor the comparison of the ΔH's with literature values.*

[5]*In gas–liquid chromatography an equivalent procedure, i.e. a plot of the logarithm of the retention volume corrected to standard temperature against reciprocal temperature, gives the heat of solution of the solute in the stationary liquid (4).*

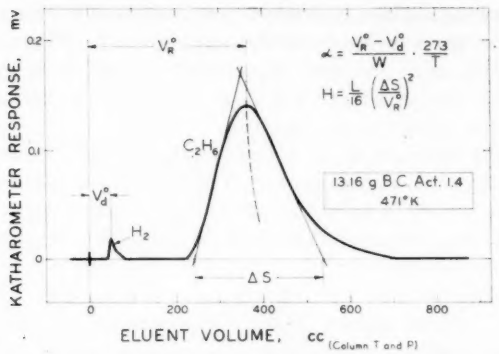

FIG. 1. A typical chromatogram obtained for a mixture of ethane and hydrogen. The usual time–base record is replotted in terms of carrier gas volume. The shoulder on the hydrogen peak results from a trace of air.

metry similar to that generally found with gas–solid chromatograms. Although the treatment referred to above was developed only for symmetrical elution chromatograms we were encouraged to apply it in the present case by the fact that H was found to be independent of sample size over a considerable range.

A major experimental advantage of gas chromatography is its relative speed and simplicity. It is best suited to conditions of fairly mild interaction in order that excessive band broadening and asymmetry do not obscure the center of the peak. This also corresponds to adsorption at temperatures well above the critical where the initial curvature of the isotherm is slight. However, by proper choice of the amount of adsorbent and of the gas flow rate a considerable range of temperatures may be covered.

The activated charcoals used in this study were taken from a series of coconut charcoals which had been steam-activated to varying degrees.[6] Lemieux and Morrison (18), Nay and Morrison (19), and Morrison and Miller (20) had previously studied the adsorptive properties of similar series of charcoals.[7] Their results suggested molecular sieve effects with the charcoals of lower activation; for example, the apparent surface areas for small molecules such as methane and nitrogen were found to be larger than for propane and butane.

By way of confirming the method, measurements were made on a sample of Columbia L-activated coconut charcoal[8] for comparison with the published isotherms of Ray and Box (21).

EXPERIMENTAL

The chromatography column was a copper tube 26 cm long by 1.015 cm inside diameter. It was preceded by a 15-in. length of coiled $\frac{1}{8}$-in. copper tubing and the whole was contained inside a 30-in. furnace made from a copper tube wound uniformly with resistance wire and insulated. There were thermocouples at each end of the column and a thermocouple well ran the length of the heater. The maximum temperature variation over the column was less than 1.0° and usually less than 0.5°.

[6] *These charcoals were kindly provided by Dr. J. L. Morrison of the Department of Chemistry, University of Alberta (now with Connaught Medical Research Laboratories, Toronto), who had obtained them from the Barnebey-Cheney Company, Cassady at Eighth, Columbus 19, Ohio.*

[7] *Unlike the earlier series these new charcoals were not prepared entirely from a single batch of nut shells. There is, therefore, some possibility of non-systematic variation through the series although the results of our work show no indication of this.*

[8] *From Union Carbide and Chemicals Co., Division of Union Carbide Corporation.*

Helium was used as a carrier gas, and flows were measured with a soap-bubble manometer corrected for the vapor pressure of the soap solution. The usual flow rate was around 100 cc per minute and retention volumes were found to be independent of flow rate over a considerable range around this value. A Gow-Mac katharometer was used as detector in conjunction with a 1-mv recorder.

The sample volume, 0.185 cc, was the volume of the bore of a two-way stopcock plug which was fitted into the shell of a three-way T-stopcock, the midtube of which led to the gas inlet and a manometer. A constant volume of sample at a known pressure could thus be introduced into the helium stream by turning the plug through 90° while simultaneously closing the helium bypass.

The Barnebey-Cheney charcoals were received as $-6+14$ mesh. This is much coarser than usually used for chromatography. Some preliminary investigations were made to determine the effect of grinding on the chromatographic properties of the charcoal. The finer fractions behaved generally like charcoals of higher activity in the series. Presumably the more highly activated portions of the granules are more fragile and easily broken up. All tests were subsequently carried out with the original material screened to exclude particles larger than 8 mesh. It was hoped that the slight degree of fractionation involved here would not invalidate comparison with conventional measurements made on the whole sample. The relatively large diameter column permitted a fairly uniform packing of this rather coarse material. Furthermore, the use of large particles magnified the effects of diffusional resistances in the charcoal pores.

Each charcoal was dried at 300° and chromatograms were determined at approximately 50° intervals down to as low a temperature as would yield measurable peaks for each gas.

Each solute was introduced as a mixture with hydrogen. While one might introduce a mixture of several non-overlapping gases at once, it is possible that the resultant volumes would be low due to competition for the available surface. Some brief studies of this point, although rather inconclusive, suggested that such effects were slight.

In many cases, particularly with the less active charcoals, several samples of each gas were run at various pressures down to the lowest pressure which would give a detectable peak (from 3–4 mm to 10 cm, depending on the retention volume and subsequent band broadening). It was thus possible to extrapolate the retention volumes to zero concentration. The variation in retention volume was usually less than 1 or 2% but in a few cases with the less active charcoals variations of up to 10% were noted and the limiting values were consequently more uncertain.

EXPERIMENTAL RESULTS

Retention volumes of nitrogen, methane, ethane, propane, the butanes, acetylene, ethylene, and propylene were measured for a sample of Columbia L-activated coconut charcoal, 35–50 mesh. The corresponding values of α from equation [1] are plotted on a logarithmic scale against reciprocal temperature in Fig. 2. Measurements made with a small glass column holding approximately one quarter as much charcoal yielded α's coincident with those from the copper column. For comparison, several values of the estimated initial slopes of the isotherms of Ray and Box (19) are included. The measurements of these authors did not always extend to low adsorbate concentrations, so that except at the higher temperatures there is some uncertainty in drawing the initial slopes. Nevertheless, the general agreement is satisfactory.

The results of Ray and Box for propane and propylene were rather surprising. At 38° and 66° C the adsorption of propylene was greater than that of propane at all pressures

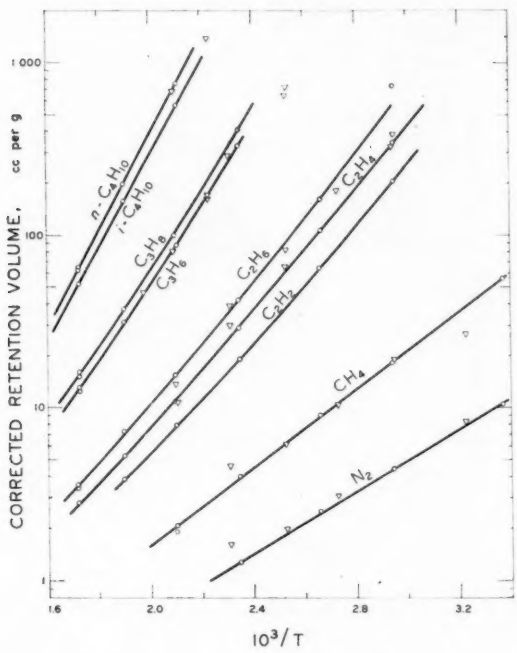

FIG. 2. Corrected retention volume per g (= α from equation [1]) vs. reciprocal temperature for Columbia L charcoal. Also shown (∇) are initial slopes of the isotherms of Ray and Box (21) for all gases except i-C_4H_{10} and C_2H_2. (Only two points are given for C_3H_6 and these lie just below the corresponding C_3H_8 points.)

investigated. At 93° the two were almost identical and at higher temperatures the propane isotherm lay above that of propylene. Lewis, Gilliland, Chertow, and Cadogan (22) found propylene to be more strongly adsorbed at 25°. They suggested that this indicated a special affinity of the carbon surface for double bonds such as that shown by silica gel. However, it may possibly reflect only a greater monolayer capacity resulting from a smaller molecular adsorption area for propylene—the methyl group perhaps projecting free of the surface. The chromatographic measurements are in the region where propane lies above propylene but the slopes of the plot do not give any suggestion of a crossing over at lower temperatures.

The limiting values of the isosteric heats of adsorption at zero coverage follow from the slopes in Fig. 2. The slight curvature in some of the plots is in the direction of decreasing ΔH with temperature. The average heat of adsorption over the interval 200–300° C is plotted in Fig. 3 against the number of carbons in the adsorbate. For comparison the figure includes the calorimetric differential heats of adsorption at 5% coverage for the normal paraffins from ethane to pentane on channel black (Spheron 6) as determined by Schaeffer, Polley, and Smith (23) at 0° C. There does not seem to be any comparable set of measurements reported for activated coconut charcoal. As noted below, the initial isosteric heats of adsorption determined for the Barnebey-Cheney charcoals vary with degree of activation over a range of around twenty-five per cent. Consequently precise agreement with the measurements on carbon black is not to be expected for any particular charcoal.

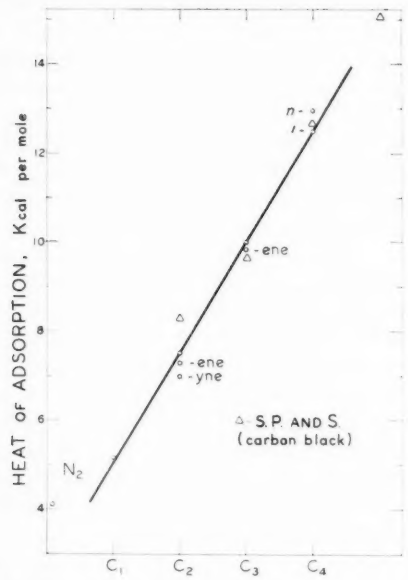

FIG. 3. The initial heats of adsorption on Columbia L charcoal compared with calorimetric values for carbon black at 5% coverage.

The charcoals in the Barnebey-Cheney series on which measurements were made had chloropicrin activities of 0, 1.4, 4.5, 9.5, 51.7, and 89.6. These numbers are times in minutes to break-through for the accelerated chloropicrin test in a standard procedure (air containing 0.286 moles per liter chloropicrin, flowing at 1 liter per minute per cm^2 through a 10-cm column). Since this test is based on a unit volume of packed charcoal the activities were converted to a weight basis using the densities reported by the manufacturer. For comparison with the α values the activities were then expressed as average concentrations at break-through in cc (S.T.P. assuming ideal gas behavior) per g of charcoal and the respective values are then 0, 1.4, 4.7, 10.1, 59.4, 149.0.[9]

For each charcoal a plot similar to Fig. 2 was obtained, and nearly all plots were straight lines. The results with acetylene were erratic. Frequently no peak appeared above 100° and measurements were not continued due to fear of possible polymerization affecting the charcoal surface. The difficulty may have been reaction with the copper tubing. The measurements with the Columbia charcoal which were made near the beginning of the work gave peaks up to 250° C.

The results are summarized in Figs. 4 and 5. Figure 4 shows the values of α for two selected temperatures plotted as functions of the revised chloropicrin activity. Figure 5 shows the heat of adsorption also against activity. Measurements with nitrogen were not always made to low enough temperatures to permit accurate slopes to be drawn.

Morrison and Myshok (24), using conventional methods, studied the adsorption at room temperature and lower of nitrogen and the C_2 hydrocarbons by some charcoals of this series and observed similar trends in initial isotherm slopes and in isosteric heats of adsorption. Their work is being prepared for publication but they have, in the mean-

[9]*The chloropicrin activity of Columbia L charcoal is given by the manufacturers as between 40 and 60 minutes, which corresponds to an average concentration at break-through of 61 to 76 cc/g.*

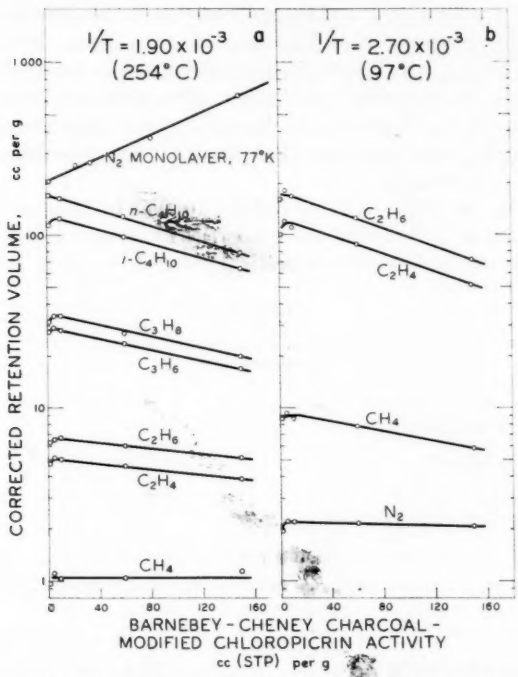

FIG. 4. Corrected retention volumes per g for the Barnebey-Cheney charcoals at 254° C (*a*) and 97° C (*b*). Nitrogen monolayers at 77° K (24) are also shown.

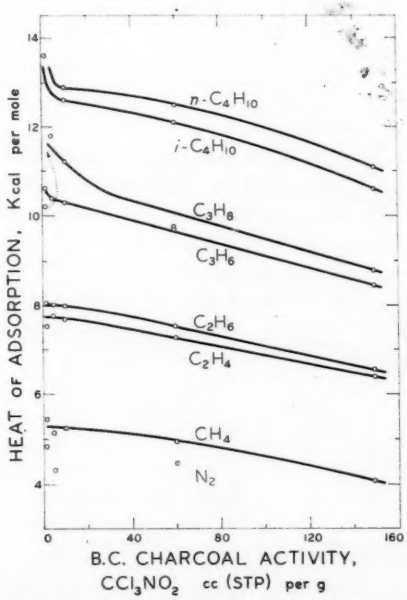

FIG. 5. Initial heats of adsorption for the Barnebey-Cheney charcoals as determined from the slopes of the log α–$1/T$.

time, provided us with values for the nitrogen monolayer capacities at 77° K for several of the charcoals and these are shown in Fig. 4*a*.

The zero activity charcoal which presumably had been only carbonized but not steam-activated showed some traces of slow adsorption. The retention volumes were within a few cubic centimeters of that of hydrogen in all cases but the peaks showed marked tailing. Conventional adsorption measurements (24) showed that adsorption was very slow but apparently quite considerable.

The variation in relative band width with flow rate was investigated for the charcoals of activities 1.4 and 149 cc/g. Some of the properties of these charcoals are summarized in Table I. The height equivalent to a theoretical plate, H as given by equation [2], was

TABLE I

Characteristics of charcoals of least and greatest activation

Chloropicrin activity, cc/g	1.4	149
Bed density (8–14 mesh granules) cc/g	0.660	0.373
Granule density cc/g (with mercury)	1.110	0.611
Charcoal density cc/g (with helium)	1.87 (100°) 1.969 (25°)	2.075 (100°)
(With CCl_4)	1.299 (25°)	2.095 (25°)

found to be independent of sample pressure over at least a 20-fold range. H is plotted against flow rate for several gases at three temperatures in Fig. 6. Because of the skew-

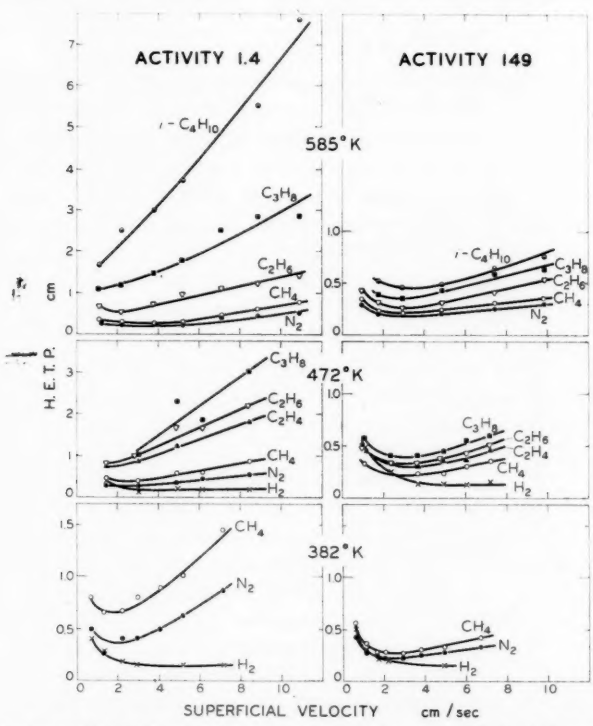

FIG. 6. Variation of H.E.T.P. with flow rate for several gases at 312°, 199°, and 109° C using columns of Barnebey-Cheney charcoals of 1.4 and 149 cc/g activities.

ness of the peaks (cf. Fig. 1) the retention volume is not identical with the volume corresponding to the intersection of the inflection point tangents and we have for convenience used the retention volume in calculating H. The band-spreading in the connecting tubing has also been neglected but the effect on H of these two factors is likely to be small. It was difficult to get enough measurements at low velocities to determine B in equation [3] so that the values of A and C which are summarized in Table II were ob-

TABLE II

Resistance to mass transfer

H.E.T.P. = $A + B/u + Cu$ (fitted only at the high-velocity end)

	Charcoal activity 1.4 cc/g					Charcoal activity 149 cc/g			
				D_p cm² sec⁻¹ ×10²					
Solute	α cc g⁻¹ atm⁻¹	A cm⁻¹	C sec	(a)	(b)	α cc g⁻¹ atm⁻¹	A cm⁻¹	C sec	D_p cm² sec⁻¹ ×10²
				585° K					
N_2	0.16	0.05	0.045	1.21	3.36		0.13	0.018	—
CH_4	0.56	−0.15	0.085	2.19	6.09	0.74	0.13	0.023	3.62
C_2H_6	2.9	0.25	0.112	3.13	8.70	2.79	0.13	0.038	4.36
C_3H_8	12.0	0.30	0.268	1.50	4.17	8.8	0.13	0.056	3.64
i-C_4H_{10}	30.6	0.32	0.630	0.66	1.83	23.8	0.13	0.066	3.34
				472° K					
N_2	0.44	0.12	0.050	2.59	7.20	—	—	—	—
CH_4	1.74	0.10	0.090	3.23	8.96	1.70	0.02	0.047	2.65
C_2H_4	11.0	0.60	0.158	2.50	6.95	7.90	0.05	0.058	3.40
		(0.15)	(.195)	(2.03)	(5.64)				
C_2H_6	15.3	0.60	0.195	2.08	5.77	10.6	0.05	0.065	3.14
		(0.15)	(0.245)	(1.65)	(4.58)				
C_3H_8	98	0.05	0.355	1.19	3.30	54.0	0.10	0.071	3.16
				382° K					
N_2	1.51	0.02	0.118	2.16	6.01	1.75	0.13	0.028	4.03
CH_4	6.9	0.13	0.175	2.14	5.96	5.00	0.13	0.041	4.24

(a) Based on pore volume from helium density.
(b) Based on pore volume from carbon tetrachloride density.

tained from the limiting tangent at high velocities. With few exceptions the A values are close to the limiting H for a non-sorbing gas, 0.10 to 0.15 cm.

To further interpret the coefficient C we have assumed the total resistance to mass transfer to lie in diffusion along the charcoal pores and have calculated apparent gas phase diffusion coefficients to describe such movement. Use was made of the following equation developed by van Deemter *et al.* (14, equation [49]) for ion-exchange chromatography which describes the resistance due to diffusion in a spherical particle of ion exchange resin:

$$C = \frac{d^2}{2\pi^2} \frac{F_I}{(1-F_I)} \frac{K}{D_{II}} \frac{1}{(1+KF_I/F_{II})^2}$$

where d = particle diameter,
F_I = volume fraction of moving phase,
F_{II} = volume fraction of stationary phase,
K = distribution coefficient, concentration in moving phase/concentration in stationary phase,
and D_{II} = diffusion coefficient in the stationary phase.

To modify this equation to fit the present case the ratio D_{II}/K which describes diffusion

in the stationary phase in terms of equivalent concentrations in the moving phase was replaced by D_p which accordingly refers directly to gas phase diffusion in the pores. At the same time a factor ϵ was introduced to represent the fraction of external particle surface represented by pore mouths together with a tortuosity factor $\sqrt{2}$ to allow for the greater diffusion path along a system of random pores and the quantity KF_I/F_{II} was replaced by the equivalent expression for gas–solid chromatography. Thus the following expression was obtained:

$$[4] \qquad C = \frac{d^2}{\sqrt{2}\pi^2} \frac{F_I}{(1-F_I)} \frac{1}{\epsilon D_p} \frac{1}{(1+273F_I/\alpha T\rho_b)^2}$$

where ϵ = void fraction in a single granule determined from the densities in mercury and helium or carbon tetrachloride,

D_p = apparent gas phase diffusion coefficient in the charcoal pores, (i.e. all movement along a pore is assumed to occur via the gas phase),

ρ_b = density of the packed bed,

and α = distribution coefficient as given by equation [1].

Values of D_p calculated according to equation [4] are included in Table II. For the 1.4-activity charcoal two sets of values are calculated corresponding to ϵ's determined from the helium and carbon tetrachloride densities.

DISCUSSION

Equilibrium Properties

The somewhat unexpected finding from this work is that the initial slopes of the isotherms all decrease with increasing surface areas of the charcoals. Qualitatively this means that the specific affinity decreases more rapidly than the surface area increases in order that the product of the two should decrease. This decrease in affinity is, of course, reflected in the decreasing heat of adsorption with increasing activation.

As pointed out earlier, α, ΔH, and the surface area are related quantities. It may be shown in the following way that the chromatographically determined α's and ΔH's are consistent with the conventionally measured nitrogen monolayer capacities at 77° K. Consider a simplified form of the initial part of the Langmuir isotherm (25):

$$\alpha = v_m A(T) e^{\Delta H/RT}$$

where v_m is the adsorbate monolayer capacity in cc (S.T.P.) per g. For any given adsorbate at a particular temperature v_m may reasonably be assumed to be a constant fraction of the nitrogen monolayer capacity at 77° K (apart from molecular sieve exclusion effects which may operate with the finer charcoals), and $A(T)$ should be reasonably constant for all charcoals. Consequently the following relationship should hold:

$$\log \alpha - \log v_{m,N_2\,77°} = \text{constant} + \Delta H/RT.$$

Figure 7 shows plots of the left-hand side for the α's and nitrogen monolayer values shown in Fig. 4 against the corresponding ΔH's. The straight lines are arbitrarily drawn in at the correct slopes and, at least for the higher activity charcoals, they fit the points reasonably well. It is doubtful whether any significance should be attached to the actual values of the intercepts, although they seem to be of approximately the correct order of magnitude required by the relationship of Fowler and Guggenheim referred to above (25). The success of this rather crude correlation encourages one to hope that surface areas could in some cases be determined from chromatographic measurements alone.

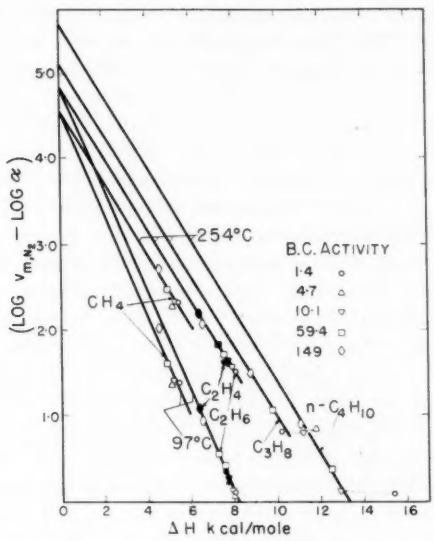

FIG. 7. A test of consistency of the α, ΔH, and nitrogen monolayer capacities (at 77° K) for $1/T = 1.90$ and 2.70×10^{-3}.

This possibility is examined in more detail from a somewhat different point of view in a paper to be published (10).

There is no reason to assume any difference in the chemical nature of the surface as the result of further activation. Therefore, the higher heat of adsorption for the lower activity charcoals is probably due to stronger adsorption in the narrower pores. The initial heat of adsorption with graphitic adsorbents is frequently almost twice the limiting value at higher concentrations, suggesting that the first adsorbate molecules are held by both sides of a narrow crevice. Similar sites will be present, although in smaller proportion, even on the most fully activated charcoals and consequently the range of initial heats is relatively small.

As can be seen from Fig. 4, the variation in surface area (to nitrogen) is much less than the variation in chloropicrin activity. For the most active charcoal the average chloropicrin adsorption at break-through is 149 cc/g. The chloropicrin monolayer capacity was estimated from rough measurements to be around 180 cc/g, which is consistent with the nitrogen monolayer capacity of 630 cc/g. However, when the average chloropicrin concentration at break-through is only 5 cc/g the nitrogen monolayer value is still over 200 cc/g. This discrepancy probably reflects both the slower rates of diffusion in the less active charcoals as well as a relatively lower surface area for chloropicrin due to its exclusion from the smallest pores. By comparing the nitrogen surface areas with those for the previous charcoal series (19), it would appear that significant exclusion of butane would be found only in charcoals of activity less than 5. Exclusion of chloropicrin which is not much larger would hardly extend to much higher activities so that the main reason for the increasing disparity between chloropicrin activities and nitrogen monolayer values must be slower diffusion.

It is perhaps worth considering a little further to what extent a dynamic chromatographic measurement can reflect the true equilibrium adsorption relationship. The

usual argument is that equilibrium exists at the center of a peak because here the overall rate of transfer is zero (26). This is probably true for a uniform stationary phase. However, each charcoal contains a range of pore sizes. Diffusion in and out of the smaller pores is very slow and consequently broadens the peak but, since this diffusion also opens up a larger surface for adsorption, the broadening is asymmetric in the direction of larger retention volume. In an extreme case, as with the inactivated charcoal, the broadening may be so great as to become indistinguishable from the base line. Thus the asymmetry of a gas–solid chromatogram is at least partly due to the nature of the solid as well as to the curvature of the adsorption isotherm.

This suggests that our method of extrapolation of the peak retention volume to zero sample pressure may be inadequate fully to take account of the retention in the narrowest pores. An alternative procedure considered was to draw in the center line of the peak and take as the retention volume its intersection with the base line. This point was found to be very uncertain, particularly with the less active charcoals, due to the curvature of the center line near the base. We feel, in any case, that the use of such a refinement would change the results relatively little. The direction of any change would be to increase the α's, more so for the less active charcoals and at lower temperatures. Consequently the trend in α and the trend in ΔH may be somewhat stronger than shown in Figs. 4 and 5.

Diffusion Coefficients

The apparent gas phase diffusion coefficients in Table II have been calculated on the assumption of pores of a single size extending through the charcoal granule. For this simplified picture the diffusion coefficients for the 1.4-activity charcoal are slightly larger than those for the 149-activity (taking the values based on the carbon tetrachloride void volumes since transport through channels inaccessible to carbon tetrachloride is likely to be negligible). This is in contrast to the much larger transfer resistance, as shown by the H values, for the 1.4-activity charcoal. However, this resistance, as expressed by C, depends on the total transfer load per unit volume of bed as well as on the specific resistance. The lower α's and lower density of the high-activity charcoal make this load smaller while the greater pore volume increases the cross section for transfer.

The extreme simplifications involved in this picture (e.g. the neglect of the macropore system in the charcoal structure) cast considerable uncertainty on the absolute values of D_p. However, the approximate equality of the values for the two charcoals is consistent with the rather limited range in micropore diameters which appears to be characteristic of steam-activated coconut charcoals. Measurements on an earlier series showed for each charcoal a very narrow spread in micropore sizes around a median diameter which increased only from 18 Å to 25 Å over the series (20).

The mechanism of transient gas flow in small capillaries is usually assumed to be a process of Knudsen diffusion modified by adsorption on the pore walls and by diffusion of the adsorbed phase (27). The apparent gas phase diffusion coefficients corresponding to Knudsen diffusion are decreased by adsorption on the pore walls and increased by diffusion in the adsorbed film. The experimental coefficients vary only a little for the various gases which cover more than a 100-fold range in α values. This suggests that the two factors must nearly balance each other and that diffusion in the adsorbed film is probably quite considerable for strongly adsorbed gases. At these relatively high temperatures this is not unreasonable.

A more detailed analysis of transport properties in these charcoals is not warranted by the present measurements. We believe, however, that this work has demonstrated the usefulness of gas chromatography in the study of kinetic as well as equilibrium aspects of adsorption.

ACKNOWLEDGMENTS

We wish to thank Dr. J. L. Morrison for his co-operation during this work as well as for giving us samples of the charcoals and, together with Mr. N. W. Myshok, making available some experimental measurements prior to publication. We are grateful to Dr. M. P. Freeman for several helpful suggestions. The co-operation of the Barnebey-Cheney Company in preparing this series of charcoals is also appreciated.

REFERENCES

1. CREMER, E. and PRIOR, F. Z. Elektrochem. **55**, 66 (1951).
2. MARTIN, A. J. P. and SYNGE, R. L. M. Biochem. J. **35**, 1358 (1941).
3. JAMES, A. T. and MARTIN, A. J. P. Biochem. J. **50**, 679 (1952).
4. PORTER, P. E., DEAL, C. H., and STROSS, F. H. J. Am. Chem. Soc. **78**, 2999 (1956).
5. BRADFORD, B. W., HARVEY, D., and CHALKLEY, D. E. J. Inst. Petrol. **41**, 80 (1955).
6. LITTLEWOOD, A. B., PHILLIPS, C. S. G., and PRICE, D. T. J. Chem. Soc. 1480 (1955).
7. ANDERSON, J. R. A. and NAPIER, K. H. Australian J. Chem. **10**, 250 (1957).
8. GLUECKAUF, E. Nature, **156**, 748 (1945).
9. SANGSTER, D. F. Atomic Energy Research Establ. (Gt. Britain), C/M 280 (1956).
10. HANLAN, J. F. and FREEMAN, M. P. Can. J. Chem.
11. STEELE, W. A. and HALSEY, G. D., JR. J. Chem. Phys. **22**, 979 (1954).
12. STEELE, W. A. and HALSEY, G. D., JR. J. Phys. Chem. **59**, 57 (1955).
13. GREENE, S. A. and PUST, H. J. Phys. Chem. **62**, 55 (1958).
14. VAN DEEMTER, J. J., ZUIDERWEG, F. J., and KLINKENBERG, A. Chem. Eng. Sci. **5**, 271 (1956).
15. KEULEMANS, A. I. M. and KWANTES, A. *In* Vapour phase chromatography. *Edited by* D. H. Desty. Butterworth Scientific Publications, London. 1957. p. 150.
16. BRENNAN, D. and KIMBALL, C. J. Inst. Petrol. **44**, 14 (1958).
17. DE WET, W. J. and PRETORIUS, V. Anal. Chem. **30**, 325 (1958).
18. LEMIEUX, R. U. and MORRISON, J. L. Can. J. Research, B, **25**, 440 (1947).
19. NAY, M. A. and MORRISON, J. L. Can. J. Research, B, **27**, 205 (1949).
20. MORRISON, J. L. and MILLER, D. M. Can. J. Chem. **33**, 330 (1955).
21. RAY, G. C. and BOX, E. O., JR. Ind. Eng. Chem. **42**, 1315 (1950).
22. LEWIS, W. K., GILLILAND, E. R., CHERTOW, B., and CADOGAN, W. P. Ind. Eng. Chem. **42**, 1326 (1950).
23. SCHAEFFER, M. D., POLLEY, W. H., and SMITH, W. R. J. Phys. Chem. **54**, 227 (1950).
24. MYSHOK, N. W. M.Sc. Thesis, University of Alberta, Edmonton. September 1958.
25. FOWLER, R. and GUGGENHEIM, E. A. Statistical thermodynamics. Cambridge: The University Press, London. 1949. p. 427.
26. TURKEL'TAUB, N. M., SHWARTSMAN, V. P., NAUMOVA, V. V., and ZHUKOVITSKII, A. A. Zhur. Fiz. Khim. **30**, 417 (1956).
27. BARRER, R. M. and GROVE, D. M. Trans. Faraday Soc. **47**, 826 (1951).

THE PARTIAL STRUCTURES OF ACONITINE AND ACONITOLINE[1]

HANS MAYER[2] AND LÉO MARION

ABSTRACT

In aconitoline ($C_{33}H_{41}O_{10}N$), the product of the oxidation of aconitine with chromic acid, the presence of an $\alpha\beta$-unsaturated carbonyl group has been confirmed. The determination of the basic strengths of aconitoline and its various hydrolytic and reduction products revealed a very strong influence of the carbonyl on the basicity of the alkaloid. It was concluded that the secondary hydroxyl that becomes oxidized must be located in close proximity to the nitrogen. Partial structures are suggested to represent both aconitine and aconitoline.

The alkaloid aconitine ($C_{34}H_{47}O_{11}N$) is known to contain three free hydroxyls, four methoxyl groups, an acetate, and a benzoate group. It has further been shown to contain an N-ethyl group so that its empirical formula can be expanded to $C_{19}H_{19}N.C_2H_5$-$(OH)_3(OCH_3)_4(O.COCH_3)(O.COC_6H_5)$ (cf. ref. 1). If in this formula all the oxygenated substituents be replaced by hydrogen the resulting compound would be expressed by $C_{21}H_{33}N$. Similarly, the alkaloid lycoctonine ($C_{25}H_{41}O_7N$) is also expressed by $C_{21}H_{33}N$ when its oxygenated substituents are replaced by hydrogen. It therefore seems legitimate to assume that there is a great deal of similarity between the carbon–nitrogen skeletons of both alkaloids.

Indeed, Schneider (2) has assumed that aconitine possesses the same carbon–nitrogen skeleton as that derived for lycoctonine by X-ray crystallography (3). Of the nine oxygenated substituents of aconitine he has assumed that seven occupied the same positions as the seven oxygenated substituents in lycoctonine, and has assigned to the remaining two positions on the heterocyclic ring I (2, 4). Further, because of the inertness of aconitine towards lead tetraacetate and periodic acid (5), he arranged the substituents in such a way as to avoid the presence of a vicinal glycol in the alkaloid.

It has long been known that aconitine is oxidized by chromic acid to the ketone aconitinone (6), which very readily loses the elements of methanol and gives rise to aconitoline (6, 7, 8). Since β-methoxy ketones were known to eliminate methanol readily and thus gave rise to $\alpha\beta$-unsaturated ketones, Majima and Tamura (6) concluded that aconitoline was an $\alpha\beta$-unsaturated ketone, and that aconitine contained a β-methoxy secondary alcohol system. Schneider (4), who also prepared aconitoline, claimed that the characteristic absorption of the carbonyl group in the infrared and ultraviolet spectra confirmed the presence of an $\alpha\beta$-unsaturated ketone, and he proposed to represent aconitoline by structure II.

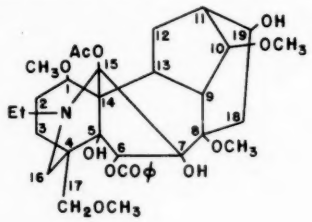

I

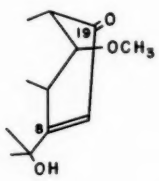

II

[1]*Manuscript received January 20, 1959.*
Contribution from the Division of Pure Chemistry, National Research Council, Ottawa, Canada.
Issued as N.R.C. No. 5118.
[2]*National Research Council of Canada Postdoctorate Fellow.*

In order to find further evidence regarding the location of the two substituents which by oxidation and loss of methanol give rise to an unsaturated ketone, a fresh study of the oxidation of aconitine with chromic acid has been undertaken.

In our hands the oxidation of aconitine with chromic acid always gave aconitoline directly. The analytical figures confirmed the empirical formula ($C_{33}H_{41}O_{10}N$) already reported (6, 8) and the melting point agreed with that given in the literature. The infrared spectrum of aconitoline contained, besides the ester carbonyl absorption at 1720 and 1730 cm^{-1}, bands at 1677 cm^{-1} (carbonyl) and 720 cm^{-1} (double bond). The ultraviolet spectrum contained four maxima including λ_{max} 232 mμ, log ϵ 4.35 and λ_{max} 305 mμ, log ϵ 2.35. Saponification of aconitoline removed the acetyl and benzoyl groups and gave rise to demethanolaconinone, $C_{24}H_{35}O_8N$, which in the infrared showed a single strong band at 1680 cm^{-1} (carbonyl). Its ultraviolet spectrum showed two maxima (λ_{max} 236 mμ, log ϵ 3.99; λ_{max} 310 mμ, log ϵ 2.34). It has been established that $\alpha\beta$-unsaturation caused a shift of *ca.* 30–40 wave-numbers in the carbonyl absorption in the infrared of six-membered cyclic ketones (9) and the ultraviolet spectrum of demethanolaconinone is characteristic of that of an $\alpha\beta$-unsaturated ketone. Indeed, dihydrodemethanolaconinone ($C_{24}H_{37}O_8N$), the product of the catalytic hydrogenation of demethanolaconinone, in which the double bond is no longer present, shows in the infrared a carbonyl absorption band at 1710 cm^{-1}. This is displaced by 30 wave-numbers from the carbonyl band in the infrared spectrum of demethanolaconinone. β-Methoxyketones are known to eliminate the elements of methanol readily and give rise to $\alpha\beta$-unsaturated ketones. Hence aconitine must contain a secondary hydroxyl located in β-position to a methoxyl, as other workers had previously concluded (4, 6, 8).

We have now observed that whereas the pK_a of aconitine is 7.72, that of aconitoline is 3.85. This very marked influence on the basic strength is due to the formation of the carbonyl group, since dihydrodemethanolaconitinone, $C_{33}H_{43}O_{10}N$, prepared by the catalytic hydrogenation of aconitoline, in which the double bond is no longer present has a pK_a 3.85. Furthermore, the action of sodium borohydride either on aconitoline or on dihydrodemethanolaconitinone gave rise to dihydrodemethanolaconitine, $C_{33}H_{45}O_{10}N$, which contained no double bond and in which the carbonyl group had been converted back to a secondary alcohol, and the pK_a of this compound was 6.0. Its ultraviolet absorption spectrum was essentially the same as that of aconitine, and its saponification product, dihydrodemethanolaconine, $C_{24}H_{39}O_8N$, isolated as its hydrochloride, showed no carbonyl absorption in the infrared.

The alkaloid delcosine, which is very closely related to lycoctonine (10, 11), has a pK_a 6.49. It contains a secondary hydroxyl in position 10 (formula I) which[3] is remote from the nitrogen, and when this is oxidized to a carbonyl group (dehydrodelcosine) the pK_a drops to 5.75. The drop in pK_a is only 0.75 unit, whereas a drop of 3.87 units accompanies the formation of aconitoline. Such a dramatic effect on the basic strength indicates that the secondary hydroxyl that becomes oxidized to a carbonyl must be located close to the nitrogen. Hence the location by Schneider of the β-methoxy secondary alcohol system involved in the formation of aconitoline in positions as remote to the nitrogen as carbons 8 and 19 (structure II) is not compatible with these observations.

A β-aminoketone has a much lower basic strength than the hydroxylic base from which it arises, as illustrated by tropine (pK_a 9.80) and tropinone (pK_a 6.98).[4] If then,

[3] *The numbering of the lycoctonine carbon–nitrogen skeleton has been arrived at in consultation with Professor R. C. Cookson and Dr. O. E. Edwards.*

[4] *The basic strengths of tropine and tropinone were determined in 50% ethanol by titration with .055 N p-toluenesulphonic acid in 50% ethanol.*

like Schneider (2) we assume as a working hypothesis that the carbon–nitrogen structure of aconitine be the same as that of lycoctonine, it appears highly probable that the β-methoxy alcohol system involved in the oxidation to aconitoline is located in ring A, and that that ring is substituted as in partial structure III. That the methoxyl and hydroxyl groups should be as shown in III, and not in the reversed positions, is apparent from the fact that the presence of a hydroxyl in position 1, provided it has the right orientation, should on oxidation lead to the formation of an internal ether as in delcosine (10) and in delsoline (12) and such an internal ether has not been obtained from aconitine. Consequently, aconitoline is represented as IV which is a β-aminoketone.

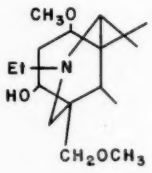

III

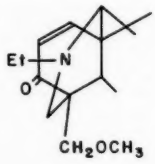

IV

The wave-length at which the maximum (λ_{max} 236 mμ, log ε 3.99) occurred in the ultraviolet spectrum of demethanolaconinone, however, indicated a possible further substituent in the α or β position of the αβ-unsaturated ketone system of aconitoline. Since in aconitine the β-position is already substituted with a methoxyl, a second substituent would be more likely to be found in the α-position. Furthermore, such a substituent should be a methoxyl, since were it a hydroxyl it would have been oxidized in the course of the formation of aconitoline. It is well known that α-methoxy-αβ-unsaturated ketones are readily hydrolyzed by acids to α-diketones but aconitoline was recovered quantitatively from such a treatment. Also, the Wolff–Kishner reaction on α-methoxyketones is accompanied by elimination of the methoxyl and formation of a double bond (13). Dihydrodemethanolaconinone was, therefore, reduced by the Wolff–Kishner reaction but the product, $C_{24}H_{39}O_7N$, which showed no carbonyl absorption in the infrared, had the same number of methoxyl groups as the starting material. Hence, there is no substituent between the hydroxyl and methoxyl of ring A in aconitine, and aconitoline is IV.

The location of the acetoxy group in Schneider's proposed structure on the α-position to the nitrogen in the heterocylic ring is also unacceptable. Were the acetoxy group to occupy that position, the hydrochloride of benzoylaconine should be an anhydronium salt and the spectroscopic and other evidence, to be discussed in a later communication, clearly indicate that it is not.

EXPERIMENTAL

All infrared absorption spectra were determined on nujol mulls, unless otherwise mentioned, with a Perkin–Elmer Model 21B spectrometer. For the measurement of the ultraviolet spectra the substances were dissolved in methanol. Basic strengths were determined by titration with .05 *N* *p*-toluenesulphonic acid of solutions of the compounds in 95% ethanol (except when otherwise mentioned).

The aconitine used in the following experiments was recrystallized from methanol–water from which it separated as colorless prisms, m.p. 198–199°[5] (decomp.), when

[5]*Melting points are uncorrected.*

immersed in the bath at 180°. Its pK_a was 7.7, $[\alpha]_D^{24}$ +18.2° (*c*, 1.5 in chloroform). Infrared absorption: 3470 cm^{-1} (OH), 1718 cm^{-1} (ester carbonyls), 1610, 710 cm^{-1} (benzene ring). The homogeneity of the base was tested with a paper chromatogram developed with the organic phase of the mixture isoamyl alcohol, glacial acetic acid, and water (40:15:45). The chromatogram gave only one spot (R_F 0.84).

Aconitoline (*Demethanolaconitinone*)

Aconitine (4.493 g) was dissolved in acetone (100 ml) and cooled in ice and salt. To the cold solution chromium trioxide (4.50 g) dissolved in cooled acetone (50 ml) was added. The reaction mixture was allowed to stand at room temperature for 3 days, after which the solvent was evaporated under reduced pressure. The dark brown residue was triturated with sulphurous acid (100 ml), sulphur dioxide was bubbled into the mixture, and the resulting dark green solution was extracted with ether (500 ml).

The aqueous liquor was then alkalized with finely powdered sodium carbonate and the precipitate filtered and dried. The dried precipitate was extracted with chloroform (100 ml) in a Soxhlet apparatus. The filtrate was extracted with chloroform (250 ml) and the two chloroform extracts combined and evaporated to dryness. There was left a light yellow froth (3.64 g, 85.5%) that crystallized in contact with ether and *n*-hexane. The product melted at 105–110°, resolidified, and melted again at 205–210° (decomp.). After two recrystallizations from methanol–water, it consisted of colorless prisms (wt., 2.506 g), m.p. 218–220°, $[\alpha]_D^{25}$ +69.0° (*c*, 1.85 in chloroform), pK_a 3.85. Found: C, 64.96; H, 6.75; N, 2.33. Calc. for $C_{33}H_{41}O_{10}N$: C, 64.80; H, 6.76; N, 2.29%. Infrared absorption: 3470 cm^{-1} (OH), 1730, 1720 cm^{-1} (ester carbonyls), 1677 cm^{-1} (six-membered $\alpha\beta$-unsaturated ketone), 1605 and 720 cm^{-1} (benzene).

Ultraviolet spectrum: λ_{max} 232 mμ, log ϵ 4.35; λ_{max} 273 mμ, log ϵ 3.09; λ_{max} 281 mμ, log ϵ 3.0; λ_{max} 305 mμ, log ϵ 2.35.

Aconitoline formed a hydriodide which crystallized in long needles from acetone–ether, m.p. 225–226° (decomp.) when immersed at 200°.

Demethanolaconinone

To a solution of aconitoline (155 mg) in ethanol (10 ml), heated to boiling in a slow stream of nitrogen, was added dropwise an alcoholic *N*-potassium hydroxide solution (0.56 ml), and the reaction mixture was refluxed for 2 hours. The light yellow solution was evaporated to dryness *in vacuo*, water (10 ml) was added, and the solution brought to pH 6 by the dropwise addition of 2 *N* hydrochloric acid. The solution was extracted five times with 25 ml of ether, saturated with sodium carbonate, and extracted five times with 25 ml of chloroform. After drying with sodium sulphate, the chloroform solution was evaporated to dryness *in vacuo*. It left a crystalline froth (115.5 mg, 98% yield) that could not be induced to crystallize.

The froth was dissolved in water (10 ml), the solution was filtered and brought to pH 6 with 2 *N* hydrochloric acid. After evaporation *in vacuo* there remained 126 mg (99% yield) of demethanolaconinone hydrochloride, which crystallized on contact with absolute ethanol, m.p. 220–221° (decomp.). After two recrystallizations from absolute ethanol – ether the colorless needles (95 mg) melted at 220–221° (decomp.), $[\alpha]_D^{24}$ +66.5° (*c*, 1.97 in water). Found: C, 57.37; H, 7.15. Calc. for $C_{24}H_{35}O_8N$. HCl: C, 57.42; H, 7.23%. Infrared absorption: 3320, 3160 cm^{-1} (OH), and a sharp band at 1680 cm^{-1} (six-membered $\alpha\beta$-unsaturated ketone), 720 cm^{-1} (double bond). Ultraviolet spectrum: λ_{max} 229 mμ, log ϵ 3.94; λ_{max} 301 mμ, log ϵ 2.62.

Some of the hydrochloride (38 mg) was dissolved in water (5 ml), the solution was

saturated with sodium carbonate and extracted five times with 20 ml of chloroform. Evaporation of the chloroform left a residue of 34.5 mg (98% yield) of pure demethanolaconinone, which could not be induced to crystallize. Its ultraviolet spectrum showed λ_{max} 236 mμ, log ϵ 3.99; λ_{max} 310 mμ, log ϵ 2.34.

A quantity of demethanolaconinone was converted to the hydriodide, which crystallized from methanol–ether as colorless prismatic needles, m.p. 240–241° (decomp.) when immersed at 220°. The salt crystallized as a hydrate from which it was not possible to remove all the water. The hydrate dried in air only was used for analysis, $[\alpha]_D^{25}$ +59.2° ±1.5° (*c*, 1.04 in water). Found: C, 44.91; H, 6.53. Calc. for $C_{24}H_{35}O_8N.HI.3H_2O$: C, 44.53; H, 6.54%. Infrared absorption: 3320, 3420 cm^{-1} (OH, H_2O), 1650 cm^{-1} (H_2O), 1680 cm^{-1} (six-membered $\alpha\beta$-unsaturated ketone).

Dihydrodemethanolaconitinone

Aconitoline (113 mg) dissolved in 95% ethanol (5 ml) was hydrogenated at room temperature in the presence of 30% palladium–charcoal (28 mg). After 3.5 hours the reaction was completed (hydrogen uptake 4.28 ml; calc. for 1 mole, 4.55 ml). The catalyst was removed by filtration and the filtrate evaporated to dryness. There was left a colorless froth, 114 mg, which crystallized in contact with ether. After three recrystallizations from aqueous methanol, the product consisted of colorless needles (73 mg), m.p. 220–221° (decomp.) when immersed at 180°, $[\alpha]_D^{25}$ −50° (*c*, 1.1 in chloroform), pK_a 3.85. Found: C, 64.97; H, 7.40. Calc. for $C_{33}H_{43}O_{10}N$: C, 64.58; H, 7.06%. Infrared absorption (fluorolube mull): 3470 cm^{-1} (OH), 1720, 1733 cm^{-1} (ester carbonyl), shoulder at 1705 cm^{-1} (six-membered ketone).

Dihydrodemethanolaconinone

To a solution of dihydrodemethanolaconitinone (363 mg) in ethanol (20 ml) under reflux in a stream of nitrogen, 1.3 ml (2.2 equiv.) of *N*-alcoholic potassium hydroxide was added dropwise and the refluxing continued for 2 hours. The solution was evaporated to dryness *in vacuo* and the residue dissolved in water (10 ml). The aqueous solution was acidified with 10% hydrochloric acid, extracted five times with 20 ml of ether, saturated with sodium carbonate, and extracted five times with 20 ml of chloroform. On evaporation the chloroform solution left a colorless gum (271 mg, 98% yield) which crystallized from acetone – *n*-hexane. After recrystallization from the same mixture, the product consisted of colorless rhombohedral leaflets (255 mg), m.p. 131–133° (decomp.), $[\alpha]_D^{25}$ −52.2° (*c*, 1.11 in chloroform). Found: C, 60.31; H, 7.80. Calc. for $C_{24}H_{37}O_8N.\frac{1}{2}H_2O$: C, 60.48; H, 8.03%. It was not possible to remove all the water by drying *in vacuo* without causing some decomposition. Infrared absorption (in chloroform): 3420 cm^{-1} (OH) and 1710 cm^{-1} (six-membered cyclic ketone).

Dihydrodemethanolaconitine

(*a*) *Reduction of Aconitoline with Sodium Borohydride*

Sodium borohydride (200 mg) was added to a solution of aconitoline (498 mg) in 80% aqueous methanol (40 ml). After the reaction mixture had been left for 1 hour at room temperature the solution was evaporated to dryness *in vacuo* and the residue dissolved in 2 *N* sulphuric acid (20 ml). The solution was extracted five times with 25 ml of ether, saturated with sodium carbonate, and extracted five times with 25 ml of chloroform. Evaporation of the chloroform extract gave a colorless froth (500 mg) which crystallized in contact with ether. The product was recrystallized twice from methanol–water, from which it separated as colorless prisms (321 mg), m.p. 173–174 (decomp.), $[\alpha]_D^{27}$

+23° (*c*, 1.31 in chloroform), pK_a 6.0±0.1. Found: C, 64.53; H, 7.51. Calc. for $C_{33}H_{45}O_{10}N$: C, 64.38; H, 7.37%. Infrared absorption: 3460 cm^{-1} (OH), 1715, 1730 cm^{-1} (ester carbonyls), 1608 and 702 cm^{-1} (benzene ring). Ultraviolet spectrum: λ_{max} 230 mμ, log ε 4.24; λ_{max} 274 mμ, log ε 3.09; λ_{max} 281 mμ, log ε 3.02.

(*b*) *Reduction of Dihydrodemethanolaconitinone with Sodium Borohydride*

To a solution of dihydrodemethanolaconitinone (101 mg) in 80% aqueous methanol (10 ml), sodium borohydride (50 mg) was added. After the solution had been left for 1 hour at room temperature, it was evaporated to dryness and the residue dissolved in 2 *N* sulphuric acid (10 ml). The solution was washed five times with 20 ml of ether, saturated with sodium carbonate, and extracted five times with 20 ml of chloroform. On evaporation the dried chloroform solution yielded a colorless froth (101 mg) which crystallized when triturated with ether – *n*-hexane. After two recrystallizations from methanol–water the product (47 mg) consisted of colorless prismatic needles, m.p. 171–173° (decomp.), $[\alpha]_D^{27}$ +23.7° (*c*, 1.42 in chloroform). Found: C, 64.48; H, 7.18. Calc. for $C_{33}H_{45}O_{10}N$: C, 64.38; H, 7.37%. The melting point was unchanged by mixture with the dihydrodemethanolaconitine obtained above (*a*) and the infrared absorption spectra were superimposable.

Dihydrodemethanolaconine Hydrochloride

Pure dihydrodemethanolaconitine (148 mg) was hydrolyzed in alkaline solution, as described under demethanolaconinone. The product (106 mg, 95% yield) was a colorless froth. It was dissolved in water (5 ml) and the solution made just acid by the dropwise addition of 10% hydrochloric acid. Evaporation of the acid solution left a colorless froth which crystallized after addition of a few drops of methanol. The crystalline product (108 mg) was recrystallized three times from methanol–ether from which it separated as colorless needles, m.p. 212–213° (decomp.), $[\alpha]_D^{25}$ −19.0±0.6° (*c*, 1.72 in water). Found: C, 56.91; H, 7.87. Calc. for $C_{24}H_{39}O_8N$.HCl: C, 56.96; H, 7.97%. The infrared spectrum contained no absorption attributable to carbonyl or unsaturation.

Attempted Saponification of Demethanolaconinone Hydrochloride

Pure demethanolaconinone hydrochloride (69 mg) was dissolved in 2 *N* hydrochloric acid (10 ml), and the solution refluxed for 2 hours. The solution was then evaporated and the residual colorless froth crystallized from ethanol, from which it separated as colorless needles, m.p. 220–221° when immersed at 200° (decomp.) either alone or in admixture with the starting material. The infrared spectrum of the product was identical with that of the starting material and so was its optical rotation, $[\alpha]_D^{24}$ +66.8° (*c*, 1.53 in water).

Wolff–Kishner Reduction of Dihydrodemethanolaconinone

A mixture of dihydrodemethanolaconinone (101 mg), triethylene glycol (3 ml), and 95% hydrazine (1.2 ml) was immersed in a metal bath preheated to 145°, the temperature raised to 150° and maintained for 1 hour. Potassium hydroxide (520 mg) was then added, the temperature raised gradually to 190°, and maintained between 190–195° for a further 3 hours while a slow stream of nitrogen was passed into the reaction flask. After cooling, the light yellow solution was diluted with water (20 ml), acidified with 2 *N* sulphuric acid, and extracted 10 times with 20 ml of chloroform. The aqueous solution was then alkalized and saturated with solid sodium carbonate and extracted five times with 20 ml of ether. The ether extract when evaporated left a colorless oil which crystallized on addition of some drops of acetone and water (54 mg, yield 55%), colorless

needles, m.p. 104° (decomp., after beginning to shrink at 80°). Recrystallization from a very concentrated acetone solution gave dihydrodemethanoldehydroxyaconine as rhombohedral leaflets, m.p. 104–106° (decomp.), $[\alpha]_D^{22}$ +21.4° (*c*, 1.04 in chloroform). Found: C, 62.97; H, 8.41; OCH_3, 20.65. Calc. for $C_{24}H_{39}O_7N$: C, 63.55; H, 8.67; 3 OCH_3, 20.53%. The infrared spectrum contained no carbonyl absorption.

ACKNOWLEDGMENTS

We are indebted to Mr. R. Lauzon and Mr. H. Seguin of these laboratories for preparing the infrared spectra and for the microanalyses, respectively. We wish to express our gratitude to Dr. Raymond Paul, Rhône-Poulenc, Paris, who kindly helped us in securing our first supply of aconitine.

REFERENCES

1. STERN, E. S. *In* The alkaloids. Vol. IV. *Edited by* R. H. F. Manske and H. L. Holmes. Academic Press, Inc., New York. 1954.
2. SCHNEIDER, W. Archiv. Pharm. **289**, 703 (1956).
3. PRZYBYLSKA, M. and MARION, L. Can. J. Chem. **34**, 185 (1956).
4. SCHNEIDER, W. and TAUSEND, H. Naturwiss. **44**, 512 (1957).
5. SCHNEIDER, W. Naturwiss. **44**, 492 (1957).
6. MAJIMA, R. and TAMURA, K. Ann. **545**, 1 (1940).
7. LAWSON, A. J. Chem. Soc. 80 (1936).
8. JACOBS, W. A. and CRAIG, L. C. J. Biol. Chem. **136**, 323 (1940).
9. JONES, R. N., WILLIAMS, V. Z., WHALEN, M. J., and DOBRINER, K. J. Am. Chem. Soc. **70**, 2024 (1948).
10. ANET, R., CLAYTON, D. W., and MARION, L. Can. J. Chem. **35**, 397 (1957).
11. SKARIC, V. and MARION, L. J. Am. Chem. Soc. **80**, 4434 (1958).
12. SPARATORE, F., GREENHALGH, R., and MARION, L. Tetrahedron, **4**, 157 (1958).
13. WARNHOFF, E. W. and WILDMAN, W. C. Chem. & Ind. 1293 (1958).

CARBONYL AND THIOCARBONYL COMPOUNDS

I *a*. REACTION OF 9-DIAZOXANTHENE WITH *o*-QUINONES

b. THE DIRECT PREPARATION OF HALOGENATED CYCLIC ETHERS FROM CERTAIN THIONES AND THEIR MOLLUSCICIDAL ACTIVITY[1]

NAZIH LATIF AND IBRAHIM FATHY

ABSTRACT

The preparation and properties of 9-diazoxanthene are described. It reacts with tetrachloro- and tetrabromo-*o*-benzoquinone, 4-triphenylmethyl-1,2-benzoquinone, and phenanthraquinone to give the cyclic ethers III*a*, III*b*, IV, and V respectively. The action of hydrochloric acid – dioxane solution on the products is stressed.

Tetrachloro- and tetrabromo-*o*-benzoquinone react with xanthione forming the halogenated cyclic ethers III*a* and III*b* respectively. A 1,2-benzopyran derivative IX is obtained by the action of tetrachloro-*o*-quinone on coumarin-2-thione. IX is toxic to *Biomphalaria boissi* snails in high dilution.

Reaction of 9-Diazoxanthene with o-Quinones

The reactions of diazomethane and diphenyldiazomethane with *o*-quinones have been described by various authors (1). Schönberg and Latif (2) investigated the action of 9-diazofluorene on *o*-quinones and found that it reacts readily with *o*-benzoquinone and β-naphthoquinone derivatives to give methylenedioxy derivatives in good yield, but it fails to react with phenanthraquinone under the same conditions.

9-Diazoxanthene has not been described before. It could be prepared by the oxidation of xanthone hydrazone with mercuric oxide in the presence of alkali at room temperature. However, microanalysis could not be carried out, since the substance decomposes at room temperature with the formation of the ketazine. In contrast to diazofluorene, it reacts readily with phenanthraquinone to give the cyclic ether V. It also reacts, but more vigorously, with tetrachloro- I*a*, and tetrabromo-*o*-benzoquinone I*b*, and 4-triphenylmethyl-1,2-benzoquinone II, to give, in excellent yield, the analogous products III*a*, III*b*, and IV, respectively, according to scheme A (2).

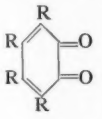

I*a*; R = Cl
I*b*; R = Br

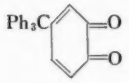

II

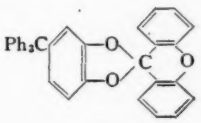

IV

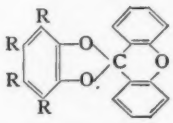

III*a*; R = Cl
III*b*; R = Br

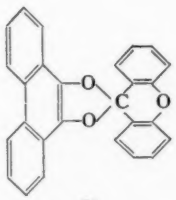

V

[1]*Manuscript received December 9, 1958.*
Contribution from the Organic Chemistry Department, National Research Centre, Dokki, Cairo, Egypt, U.A.R.

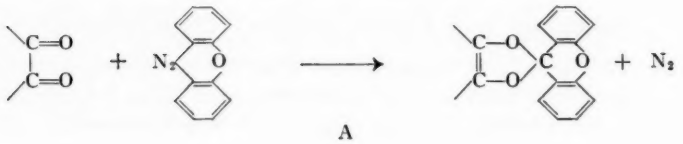

A

The constitution of the products formed is based on the following facts:

(*a*) they are colorless or nearly so,

(*b*) they are readily hydrolyzed by acids, and

(*c*) III*a* and III*b* can be obtained by the reaction between 9,9-dichloroxanthene and the corresponding tetrahalogenocatechol according to scheme B.

The identity of the products obtained from reactions A and B is established by analysis, melting point and mixed melting point, and by their identical infrared spectra.

R = Cl or Br

B

It is observed that all the cyclic ethers obtained in this reaction are readily and quantitatively cleaved by hydrochloric acid in dioxane; for example, when III*a* or III*b* are boiled for 30 minutes with a mixture of concentrated hydrochloric acid and dioxane (1:5), xanthone and the corresponding catechol are obtained in quantitative yield. In the case of V, xanthone and phenanthraquinone are obtained after air oxidation. This is rather remarkable as the analogous products VI and VII obtained by the action of diphenyl- (3) and diphenylene-diazomethane (2) on tetrachloro-*o*-quinone are not similarly attacked. This may be explained by assuming that the proton attacks first the ethereal

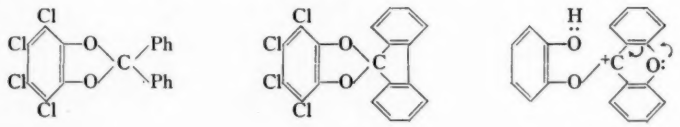

VI VII VIII

oxygen atom and this is followed by the heterolytic fission of the C–O bond, to give a carbonium ion which is stabilized by resonance with the unshared electron pair of the oxygen of the xanthyl residue (4) (cf. VIII for III*a*). However, it is observed that these products are not appreciably cleaved by concentrated sulphuric acid at room temperature, as usually happens with the other methylenedioxy derivatives obtained by the action of diazomethanes on *o*-quinones. This may be attributed to the formation of an oxonium salt which is rather stable under the conditions of the experiment, a property generally shown by xanthenes.

The Direct Preparation of Halogenated Cyclic Ethers from Certain Thiones

Several reactions of thioketones have been described (5), but it is believed that nothing is mentioned about the action of *o*-quinones on cyclic thiones. It is found that the high potential quinones, tetrachloro- and tetrabromo-*o*-benzoquinone, react with xanthione

in dry benzene at room temperature with the formation of III*a* and III*b*, respectively, according to scheme C.

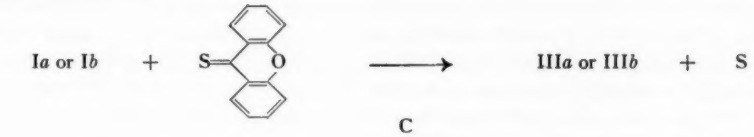

C

However, the reaction is slow at room temperature, but is remarkably accelerated by heat. Thus when I*a* and xanthione are boiled in dry benzene for 1 hour, an 80% yield of III*a* is obtained, whereas, at room temperature, a 75% yield is reached only after 5 days. The reaction of I*b* with xanthione is affected by temperature in almost a similar way. III*a* can also be obtained by heating I*a* and xanthione without a solvent in a carbon dioxide atmosphere.

The identity of the compounds obtained in this reaction with those obtained by either reaction A or B is established by analysis, melting point and mixed melting point, and by similar infrared spectra.

It is found also that tetrachloro-*o*-quinone reacts similarly with coumarin-2-thione in boiling benzene with the formation of a 1,2-benzopyran derivative IX in good yield. The constitution of the product obtained is based on analogy, as well as on the fact that it is colorless and easily hydrolyzed by hydrochloric acid in dioxane to coumarin and tetrachlorocatechol. The absence of sulphur and of the characteristic frequency band of a *d*-lactone (1755 cm^{-1} nujol) (6) shown by coumarin excludes structure X of a 1,4-dioxane, which may result by the addition of the quinone to the double bond of the lactone ring. Addition of *o*-quinones to the double bond in ethylenes, benzofurans, isocoumarins, etc. is well known. However, it is reported that coumarin fails to react with phenathraquinone (7).

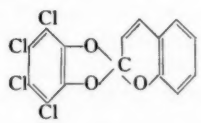

IX

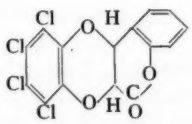

X

The Molluscicidal Activity of Halogenated Cyclic Ethers

Halawani and Latif (8) found that halogenated *o*-benzoquinone and benzodioxole derivatives are toxic to *Biomphalaria boissi* snails—the intermediate host of *Schistosoma mansoni* in Egypt—in high dilutions. The toxicity of the above-mentioned halogenated cyclic ethers has been investigated. It is found that IX kills the snails in concentrations as low as 20 p.p.m. in water during a 24-hour-exposure period to the drug followed by a 72-hour-observation period in fresh water. III*a*, III*b*, IV, and V could not be tested, since they are almost insoluble in the solvents usually used for the test. Details of these experiments will be published separately.

EXPERIMENTAL

Melting points are not corrected. Microanalyses were carried out by A. Bernhardt, Germany.

Preparation of 9-diazoxanthene.—Xanthone hydrazone (4 g), mercuric oxide (7 g), and anhydrous sodium sulphate (1 g) were ground together in a dry mortar, and transferred

to a dry 100-ml R.B.F. guarded with a calcium chloride tube and containing 50 ml dry ether. One milliliter of a freshly prepared saturated solution of potassium hydroxide in absolute alcohol was added while shaking the mixture for 2 minutes at room temperature (20° C), then stirring for 30 minutes at 10°. The green ethereal solution was filtered off and the residue washed with dry ether. The combined ethereal solutions were concentrated under reduced pressure in the cold, when green crystals of 9-diazoxanthene separated, and filtered. The compound is soluble in most organic solvents in the cold, melts with decomposition at about 60° C (red melt), and turns orange-red when left at room temperature for a few hours.

Xanthone ketazine.—9-Diazoxanthene (0.1 g) was left in a watch glass exposed to air for 24 hours. The orange-red crystals formed were washed with ether and recrystallized from benzene when xanthone ketazine was obtained (m.p. 285° not depressed when admixed with an authentic sample prepared according to Schönberg and Stolpp (9)).

Reaction of tetrachloro-o-quinone with 9-diazoxanthene.—Tetrachloro-*o*-quinone (10) (0.8 g) was added slowly to a dry ethereal solution of diazoxanthene (1.1 g). A vigorous reaction with evolution of gas took place and after a few seconds a yellowish crystalline solid separated. On recrystallization from xylene 9,9-(tetrachloro-*o*-phenylenedioxy) xanthene III*a* separated in colorless crystals,* m.p. 286° (yield almost quantitative). It is difficultly soluble in cold alcohol, acetone, or benzene. Calc. for $C_{19}H_8O_3Cl_4$: C, 53.52; H, 1.87; Cl, 33.3. Found: C, 53.43; H, 2.17; Cl, 32.87%. It dissolves in concentrated sulphuric acid with a deep yellow color and when the solution was kept overnight at room temperature (20° C) and then poured into ice, above 75% of the substance was recovered unchanged.

Hydrolysis of IIIa.—To a solution of concentrated hydrochloric acid (sp. gr. 1.19) (1 ml) in dioxane (5 ml) was added III*a* (0.15 g), the mixture boiled for 30 minutes, and then left to cool. It was then poured into ice and the colorless precipitate formed was filtered, dried, and dissolved in the least amount of boiling methyl alcohol and left to cool. The colorless crystals separated proved to be xanthone (m.p. and mixed m.p. 174°). On addition of dilute hydrochloric acid to the mother liquor a white precipitate was formed. After filtering, drying, and refluxing with acetic anhydride for 30 minutes, the mixture was left to cool, and then poured into ice. The solid formed was recrystallized from methyl alcohol and proved to be the diacetyl derivative of tetrachlorocatechol (melting point and mixed melting point). Using methyl alcohol instead of dioxane, hydrolysis was partial and about 50% of the substance was recovered unchanged.

Reaction between tetrachlorocatechol and 9,9-dichloroxanthene.—Tetrachlorocatechol (0.1 mole) and 9,9-dichloroxanthene (0.1 mole from thionyl chloride and xanthone) were heated together in a test tube protected from moisture at 150° (oil bath) for 1 hour. The reaction mixture was left to cool, washed several times with acetone, and recrystallized from xylene when III*a* was obtained (m.p. 286° undepressed when admixed with an authentic sample prepared by the action of diazoxanthene on tetrachloro-*o*-quinone) (yield about 80%). The product and the authentic sample have identical infrared spectra. Calc. for $C_{19}H_8O_3Cl_4$: C, 53.52; H, 1.87; Cl, 33.3. Found: C, 54.32; H, 2.08; Cl, 32.6%.

Reaction of tetrabromo-o-quinone with 9-diazoxanthene.—Tetrabromo-*o*-quinone (11) (1 g) was added to a crude ethereal solution of diazoxanthene (from 2 g of xanthone hydrazone). A vigorous reaction took place with evolution of gas and the immediate separation of a yellowish deposit. This was filtered off, washed with boiling acetone,

**In a parallel experiment carried out using the crude ethereal solution obtained from the oxidation of xanthone hydrazone as described above, instead of diazoxanthene crystals, the same yield of IIIa was obtained. In the coming experiments this crude ethereal solution will be generally used.*

and recrystallized from xylene (using charcoal) when 9,9-(tetrabromo-*o*-phenylenedioxy) xanthene III*b* separated in almost colorless crystals, m.p. 280° (decomp.). Yield almost quantitative. The compound dissolves in concentrated sulphuric acid with a yellow color and most of it was recovered unchanged when poured into ice as in the case of the chloro-analogue. Calc. for $C_{19}H_8O_3Br_4$: C, 37.74; H, 1.32; Br, 52.98. Found: C, 37.68; H, 1.75; Br, 53.24%. When III*b* was boiled with concentrated hydrochloric acid – dioxane as in the case of the chloro-analogue, xanthone and tetrabromocatechol (identified as its diacetyl derivative) were obtained.

Reaction of tetrabromocatechol with 9,9-dichloroxanthene.—Tetrabromocatechol (4 g) and dichloroxanthene (from 2 g of xanthone and thionyl chloride) were dissolved in dry benzene (20 ml), and a few drops of piperidine added. The mixture was refluxed for 3 hours, concentrated, and left to cool. The solid separated was washed with boiling acetone and recrystallized from xylene (using charcoal) when III*b* was obtained in colorless crystals, m.p. 280° (decomp.). Its infrared spectrum is identical with that of the product obtained from diazoxanthene.

Reaction of 4-triphenylmethyl-1,2-benzoquinone with 9-diazoxanthene.—The quinone (12) (1.2 g) was added in very small portions to a crude ethereal solution of diazoxanthene (from 2 g of xanthone hydrazone). A new portion was only added when the reaction from a previous addition had subsided. After all the quinone was added, the reaction mixture was left for 2 hours at room temperature with occasional shaking. The color of the quinone disappeared and a colorless solid was formed. This was recrystallized from xylene when 9,9-(4-triphenylmethyl-*o*-phenylenedioxy) xanthene IV was obtained in colorless crystals, m.p. 264° (yield about 60%). Calc. for $C_{38}H_{26}O_3$: C, 86.01; H, 4.94. Found: C, 86.45; H, 5.28%.

Reaction of phenanthraquinone with 9-diazoxanthene.—The quinone (0.5 g) was added in very small portions to a crude ethereal solution of diazoxanthene (from 2 g xanthone hydrazone) with mild stirring at 37°. When all the quinone had been added, stirring of the reaction mixture was continued for 2 hours. The yellowish solid formed was washed several times with boiling acetone and recrystallized from xylene when (V) was obtained in almost colorless crystals, m.p. 298°. It is insoluble in most organic solvents and gives a deep yellow color with concentrated sulphuric acid. Calc. for $C_{27}H_{16}O_3$: C, 83.5; H, 4.15. Found: C, 84.1; H, 4.35%. V (0.2 g) was refluxed with hydrochloric acid – dioxane solution as above, the reaction mixture was left to cool and then poured into ice. The yellowish solid formed was filtered off using the pump and suction was allowed to continue for 1 hour to facilitate air oxidation. The product was then pressed on a porous plate and recrystallized from benzene. The resulting orange crystals proved to be phenanthraquinone (melting point and mixed melting point). It gives olive green color with concentrated sulphuric acid.

Reaction of tetrachloro-o-quinone with xanthione.—Method "a". The quinone (2.4 g) and xanthione (2.2 g) in dry benzene (15 ml) were refluxed together for 1 hour on the water bath. The red color of the quinone disappeared and the solution became dark brown; it was left to cool. The crystalline solid formed was filtered off and the mother liquor concentrated to obtain another crop of crystalline solid.* The whole crude reaction product was washed with acetone several times and recrystallized from xylene in colorless crystals which proved to be III*a* (m.p. 286° undepressed when admixed with an authentic sample prepared in the above experiments. The product and the authentic sample have

**When the mother liquor was evaporated to dryness under reduced pressure and the residue heated in a carbon dioxide atmosphere at 150° (oil bath) for 1 hour, sulphur collected on the cooler parts of the reaction vessel. Xanthione is stable when heated alone under the same conditions.*

identical infrared spectra.). Yield above 80%. Calc. for $C_{19}H_8O_3Cl_4$: C, 53.52; H, 1.87; Cl, 33.3. Found: C, 53.51; H, 2.07; Cl, 33.04%. *Method "b"*. Tetrachloro-*o*-quinone (0.61 g) and xanthione (0.5 g) were mixed together in a dry test tube protected from moisture. The mixture was heated for 2 hours at 200° (oil bath) while passing carbon dioxide, and then left to cool. The solid mass obtained was ground well, washed with acetone, and recrystallized from xylene (using charcoal) when III*a* was obtained in colorless crystals, m.p. 286° (yield about 50%).

Reaction of tetrabromo-o-quinone with xanthione.—The quinone (1 g) and xanthione (0.5 g) in dry benzene (20 ml) were refluxed together for 1 hour on the water bath. The reaction mixture became dark brown, and yellowish crystals separated. These were filtered off, and the filtrate concentrated and left to cool when another crop of crystals was obtained. The combined crude product was washed with boiling acetone and recrystallized from xylene (using charcoal) when III*b* was obtained in almost colorless crystals, m.p. 280° (decomp.). Its infrared spectrum is identical with that of the products obtained by reactions A and B.

When the quinone and the thione in dry benzene were kept at room temperature in a carbon dioxide atmosphere for 3 days about 75% yield of III*b* separated.

Reaction of tetrachloro-o-quinone with coumarin-2-thione.—The quinone (1.2 g) and the thione (0.8 g) in dry benzene (10 ml) were refluxed for 3 hours. The reaction mixture was filtered while hot, concentrated, and left to cool. The crystals that separated were washed with acetone and recrystallized from benzene when 2,2-(tetrachloro-*o*-phenylenedioxy) benzopyran IX was obtained in colorless crystals, m.p. 214° C. It is soluble in hot acetone, benzene, and chloroform, difficultly soluble in alcohol. Calc. for $C_{15}H_6O_3Cl_4$: C, 47.87; H, 1.59; Cl, 37.7. Found: C, 47.88; H, 1.64; Cl, 37.38%.

Hydrolysis of IX.—IX (0.2 g) was refluxed with a solution of hydrochloric acid in dioxane as usual. The reaction mixture was then poured into ice and filtered and the filtrate left to concentrate slowly at room temperature. The separated colorless crystals were recrystallized from petroleum ether (30–50°) and proved to be coumarin (melting point and mixed melting point). Diluted hydrochloric acid was added to the mother liquor and the white solid obtained was filtered off, dried, and refluxed with acetic anhydride when the diacetyl derivative of tetrachlorocatechol was obtained.

ACKNOWLEDGMENTS

The authors wish to express their appreciation to Dr. E. Bickert, Max-Planck Institut fur Biochemie, München, and to Professor F. G. Baddar, Faculty of Science, A'in Schams University, Cairo, for the determination of infrared spectra.

REFERENCES

1. ADAMS, R. Organic reactions. Vol. VIII. John Wiley & Sons, Inc., New York. p. 364.
2. SCHÖNBERG, A. and LATIF, N. J. Chem. Soc. 446 (1952). HORNER, L. and LINGNAU, E. Ann. **573**, 30 (1951).
3. SCHÖNBERG, A., AWAD, W. I., and LATIF, N. J. Chem. Soc. 1368 (1951).
4. ALEXANDER, E. R. Principles of ionic organic reactions. John Wiley & Sons, Inc., New York. 1950. p. 214.
5. CAMPAIGN, E. Chem. Revs. **39**, 1 (1946). SCHÖNBERG, A. *In* Houben-Weyl. Methoden Der Organishen Chemie. IX. George Thieme Verlag, Stuttgart. 1955. p. 704.
6. BELLAMY, L. J. The infrared spectra of complex molecules. John Wiley & Sons, Inc., New York. 1954. p. 153.
7. SCHÖNBERG, A. and MUSTAFA, A. Chem. Revs. **40**, 181 (1947). SCHÖNBERG, A. *et al.* J. Chem. Soc. 1364 (1951).
8. HALAWANI, A. and LATIF, N. J. Egypt. Med. Assoc. **37**, 957 (1954).
9. SCHÖNBERG, A. and STOLPP, TH. Ber. **63**, 3102 (1930).
10. JACKSON, C. L. and MACLAURIN, R. D. Am. Chem. J. **37**, 7 (1907).
11. ZINCKE, TH. Ber. **20**, 1777 (1887).
12. ZINCKE, TH. and WUGK, E. Ann. **363**, 284 (1908).

INFRARED SPECTRA OF ORGANO-PHOSPHORUS COMPOUNDS

III. PHOSPHORAMIDATES, PHOSPHORAMIDOTHIONATES, AND RELATED COMPOUNDS[1, 2]

R. A. McIvor and C. E. Hubley

ABSTRACT

Examination of a number of new phosphorus compounds has provided additional confirmation for many of the group frequencies reported previously. In certain cases additional information has been obtained on the effect of environment on the band positions, and some previously unassigned bands have been attributed to specific structures. In particular, bands previously assigned to P(S), P(S)X, C—H deformation, P—O—(C), P—C, P—S—H, P—S(P), P—N, C—S(P), and C—N(P) are discussed.

INTRODUCTION

In Parts I and II of this series, characteristic bands were given for various functional groups of organo-phosphorus compounds, in particular P—O—P, P→S, P—O—(C), and P—Cl. A number of new compounds containing P—N bonds has been examined, in addition to those previously discussed, which makes further and revised group frequency assignments possible.

These assignments are simply empirical, based on observations of compounds containing particular atomic groupings. No fundamental studies have been carried out by us to test which particular parts, if any, of the large groupings are responsible for the bands. Thus, for example, while it is always possible to say that compounds containing an isopropoxy group attached to phosphorus will exhibit a triplet of bands between 1100 and 1200 cm^{-1}, the assignment of these bands to specific vibrations has not been attempted and for convenience they have been grouped under R—O—(P), since many other authors in this field have considered at least one band in this region as being a C—O—(P) absorption. Where groups of bands occur in a specific region for many closely related compounds, it is often convenient to discuss all such bands together. More recently, however (1, 2), the strong 1000–1100 cm^{-1} band has been postulated as the C—O—(P) band, while bands near 830 cm^{-1} are considered to be P—O—(C) stretching bands. This C—O assignment seems more in line with the absorption of this grouping in non-phosphorus compounds, but not consistent with the assignment of a 940 cm^{-1} band to P—O(P) and P—O—(H). It should also be noted that the 1000–1100 cm^{-1} band occurs at progressively lower frequencies in the series MeOP, EtOP, *i*-PrOP, whereas the band attributed to C—O stretching in alcohols shifts to higher frequencies with increasing substitution (3).

EXPERIMENTAL

The preparation of some of these compounds is described elsewhere (4, 5). A Baird double-beam recording spectrophotometer was used for all spectra. Band positions are cited to the nearest 0.01 μ for sharp bands and to the nearest 0.05 μ for broad bands. All but three samples, which are marked in the tables, were run as thin films. The solid samples were run as KBr pellets. These were prepared by mixing one part of the sample with 100 parts of KBr in an agate mortar for approximately 1 minute, and then pressing at 75,000–90,000 lb/in.^{2} in a Hilger & Watts evacuated die.

[1]*Manuscript received December 17, 1958.*
Contribution from the Defence Research Chemical Laboratories, Ottawa, Canada.
Issued as D.R.C.L. Report No. 258A.
[2]*Part II, Can. J. Chem.* **36**, *820 (1958).*

RESULTS AND DISCUSSION

(*a*) P→S

An additional 43 compounds containing P→S have been examined. These compounds have bands in the 740–830 cm^{-1} region with various intensities. However, since the corresponding P→O compounds frequently have similar bands in this region, our earlier assignment of this band to P→S seems less certain. The spectra of most P→S compounds containing *n*-PrO do not have bands in the 770–830 cm^{-1} region, but have one in the 715–770 cm^{-1} region.

A number of compounds of types I and II have been examined both here and in other laboratories (5, 6, 7). I can be converted to II by heating, and the progress of the isomerization can be followed in the infrared. During the isomerization of these compounds there

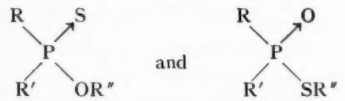

I II

is usually a disappearance of one or more bands in the 740–830 cm^{-1} region with concomitant appearance of P—O and C—S—P bands (see section (*k*) below). Thus compound I (R = Me_2N; R′ = *n*-PrO; R″ = CH_2—CH_2NEt_2) has a very weak band at 790 cm^{-1} which disappears on conversion to the corresponding II isomer.

Since this work was completed a paper by Hooge and Christen (8) has assigned the band discussed in section (*b*) to the P→S link, and related its frequency to the mass of the remaining substituents. This seems to be an excellent suggestion, and consistent with all our observations. The nature of the 740–830 cm^{-1} band remains in doubt.

The 740–830 cm^{-1} band is particularly intense in compounds containing MeO and EtO groups, which usually have an additional strong band in this region, attributed recently to P—O—(C) stretching (1, 2). Such intensification has been frequently noted when two bands associated with the same small group of atoms have closely related frequencies. In this case, however, the effect may be one of simple summation of two superimposed bands. *n*-Propyl and *n*-butyl phosphorus esters have no strong band in this region.

Several additional observations have been made concerning this absorption. As a general rule acids absorb below 770 cm^{-1}. Dichlorides absorb at lower frequencies than the corresponding full esters for any one ester group. For the ester groups absorption usually occurs in this region in the following order of increasing frequency: *n*-propyl > isopropyl > ethyl > methyl. Compounds containing alkyl groups attached to P absorb at lower frequencies than the corresponding phosphates, but since many methylphosphonates have a sharp band near 794 cm^{-1} and a broad one near 758 cm^{-1} the association of either of these with the P→S grouping is dubious. Bands believed to be characteristic are listed in Table I.

(*b*) (O)—P—Cl, (O)—P—S—
S S

Many new compounds have been examined containing these groupings which are particularly useful for analytical purposes. Further to the information previously reported (7), more examples of phosphonate half-esters are available, all of which absorb

strongly in the 630 to 641 cm^{-1} region, and two dimethylphosphoramidochloridothionates which absorb near 633 cm^{-1} in contrast with simple phosphorothionates and thionyl dichlorides which absorb near 666 cm^{-1}. Phosphonothionic acids and phosphorothionic acids also absorb in this region but with somewhat lesser intensity. As these compounds probably have the P(S)OH structure primarily, this band (which occurs near 606 cm^{-1} in the phosphonothioic acids) is probably of this type rather than a P—S—(H) stretching as suggested previously (7). Two compounds which possibly contain P—S—P groupings have a doublet at 658 cm^{-1} and 630 cm^{-1}, the components of which retain the same relative intensities during purification procedures. Compounds containing the structure $P(S)CF_3$ also exhibit this band. This band has recently been assigned by Hooge and Christen (8) to the P→S stretching vibration.

Observed bands are listed in Table I.

TABLE I

S
↑
P→S and P—X Bands

Compounds	Band positions in cm^{-1}	
Methyl phosphorodichloridothionate	830	725
		704
Ethyl phosphorodichloridothionate	799	728
		699
n-Propyl phosphorodichloridothionate	758?*	730
		694
i-Propyl phosphorodichloridothionate	775	722
		685
n-Butyl phosphorodichloridothionate	800?	714
	746?	694
O,O-Dimethyl phosphorodithioic acid	780?	658
O,O-Diethyl phosphorodithioic acid	767	658
O,O-Di-*n*-propyl phosphorodithioic acid	741	658
O,O-Di-*i*-propyl phosphorodithioic acid	757	649
O,O-Di-*n*-butyl phosphorodithioic acid	730	658
Sodium O,O-diethyl phosphorodithioate (P)†	775?	730?
	769?	694?
	746?	
Triethylammonium diethyl phosphorothioate	766	649
Triethylammonium di-*n*-propyl phosphorothioate	746	656
Triethylammonium di-*n*-butyl phosphorothioate	735?	658
Triethylammonium ethyl methylphosphonothioate	758?	
Sodium ethyl trifluoromethylphosphonothioate (P)	754	<625
Ethylphosphonothionyl dichloride	779	645
Dimethylphosphoramidothionyl dichloride	766	671
Diethylphosphoramidothiony[1] dichloride	790?	662
	741	
Diethyl dimethylphosphoramidochloridothionate	806	633
	752?	
n-Propyl dimethylphosphoramidochloridothionate	769	633
Ethyl methylphosphonochloridothionate	794	629
γ-Fluoropropyl methylphosphonochloridothionate	794	637
Cyclohexyl methylphosphonochloridothionate	797	641
β-Fluoroethyl methylphosphonochloridothionate	797	634
Ethyl dimethylphosphoramidothioic acid	758	662?
Ethyl methylphosphonothioic acid	790	602
Dimethyl phosphorothioic acid	810	Not examined
Ethyl trifluoromethylphosphonothioic acid	794	Not examined
β-Fluoropropyl methylphosphonothioic acid	793	606
γ-Fluoropropyl methylphosphonothioic acid	790	606
Diethyl dimethylphosphoramidothionate	813	
Diethyl diethylphosphoramidothionate	806	
Diethyl diisopropylphosphoramidothionate	763	
Di-*n*-propyl diethylphosphoramidothionate	790	
Di-*n*-propyl diisopropylphosphoramidothionate	787 wk	
	735?	
Diisopropyl diethylphosphoramidothionate	787	
Diisopropyl diisopropylphosphoramidothionate	755	
Di-*n*-butyl diethylphosphoramidothionate	806	
Di-*n*-butyl diisopropylphosphoramidothionate	787	
Diethyl ethylphosphonothionate	794	
Diethyl methylphosphonothionate	800	
OOOO-Tetraethyl trithiopyrophosphate	830	660
	797?	631
OOOO-Tetraisopropyl trithiopyrophosphate	778	658
	800?	629
O-Ethyl-O-β-diethylaminoethyl dimethylphosphoramidothionate	806	
O-Propyl-O-β-diethylaminoethyl dimethylphosphoramidothionate	794	
Diethyl trifluoromethylphosphonate	830	649

*In this and subsequent tables the symbol ? indicates that the cited band is beyond the normal range for this grouping, or is one of several possible choices. wk = Weak, sh = shoulder, br = broad.

†(P) indicates the spectrum was run as KBr pellet.

(*c*) C—H *Deformation*

Some additional observations have been made in this region, and the characteristic band positions are listed in Table II.

TABLE II
C—H Deformations

Group	Observed bands in cm^{-1}	
Et—P(O)	1460 1399	
Et—P(S)	1453 1389 sh	1381
Me_2N—P	1481 sh 1453	1412 v wk
Et_2N—P(S)	1453 1389 sh	1381
i-Pr_2N—P(S)	1462 1406	1389 sh or wk 1366

Me_2N—P(O) and Me_2N—P(S) absorb at the same positions but in P(S) compounds the 1481 cm^{-1} shoulder is only about one-half the intensity of the neighboring band, whereas in P(O) compounds it is of approximately equal intensity.

(*d*) P—O—(H) *and* P—O—(C) (*900 to 1100 cm*$^{-1}$)

1. EtO *Bands.*—In an earlier paper (7) the occurrence of two bands was mentioned, one between 1100 and 1000 cm^{-1} and another between 1000 and 900 cm^{-1}. Since most Et-containing compounds without EtO—P groupings have weak bands between 1000 and 900 cm^{-1} thought to be associated with a C—C vibration, it is postulated that in P—O—Et compounds this second band is intensified by interaction with the vibration giving rise to the strong absorption between 1000 and 1100 cm^{-1}. P—OEt groups and possibly P—N—C—C groups are the only ones examined that invariably give a band or shoulder in the 962–980 cm^{-1} region for pentavalent compounds and near 917 cm^{-1} for trivalent P compounds. β-Fluoroethoxy phosphorus compounds (two examples) have bands in this region.

2. Acidic compounds.—POOH and PSOH acids and salts generally have a band near 943 cm^{-1} which may be a symmetric P—O stretching for the ions and a P—O(H) stretching in the acids.

(*e*) P—C (*Alkyl*) *and* C—C (*Alkyl*) *Bands*

Examination of more than a dozen new compounds has confirmed the earlier assignments for P—methyl and P—ethyl bands (7). In addition, all compounds containing isopropyl groups (either P—O—*i*-Pr or P—N—*i*-Pr) also have a medium intensity band near 893 cm^{-1} for O—*i*-Pr and near 877 cm^{-1} for P—N—*i*-Pr compounds. P—N—*i*-Pr compounds also have two medium intensity bands in the 625–666 cm^{-1} region. These bands are listed in Table III.

(*f*) P—S—(H)

A number of new examples have been obtained and are listed with other dithioic acids in Table IV.

(*g*) P—S—(P)

Two compounds, although not analytically pure, obtained by reacting dicyclohexylcarbodiimide with diethyl and diisopropyl phosphorodithioic acids had spectra which were different from those of the starting material and the corresponding OOS-trialkyl

TABLE III

P—C and C—C Bands

Compound	Band positions in cm^{-1}	
Tetraisopropyl monothionopyrophosphate	889	
Diisopropyl dimethylmonothionopyrophosphate	893 (P—Me?)	
Di(isopropyl methylphosphonothionyl) methylphosphonothioate	870	
Isopropyl methylphosphonochloridothionate	897	
Diisopropyl methylphosphonothionate	909?	
	893 sh	
Diisopropyl phosphorochloridothionate	893	
O,O-Diisopropyl phosphorodithioic acid	893	
Sodium diisopropyl phosphate (P)	885	
Isopropyl phosphorodichloridothionate	894	
Diisopropyl diethylphosphoramidothionate	889	
Diisopropyl phosphorofluoridate	901	
Diisopropyl diisopropylphosphoramidothionate	890	664 wk
	877	652 wk
Diethyl diisopropylphosphoramidothionate	881	662
		654 sh
Di-*n*-butyl diisopropylphosphoramidothionate	893?	664
	881	654
Di-*n*-propyl diisopropylphosphoramidothionate	885	664
		654 sh

TABLE IV

P—S—(H) Bands

Compound	Band positions in cm^{-1}
O,O–Dimethyl phosphorodithioic acid	526
	493
O,O-Diethyl phosphorodithioic acid	541
	508
O,O-Di-*n*-propyl phosphorodithioic acid	543
	518
O,O-Di-*i*-propyl phosphorodithioic acid	548
	518
O,O-Di-*n*-butyl phosphorodithioic acid	546
	526

TABLE V

P—Cl Bands

Compound	Band positions in cm^{-1}	
Methylphosphonous dichloride	562 br	
	472 br	
n-Propyl phosphorothionyl dichloride	552?	500 sh
	529?	485
n-Butyl phosphorothionyl dichloride	552	488 wk
	529	
i-Propyl phosphorothionyl dichloride	549	500 sh
	526	488 sh
Ethyl dimethylphosphoramidochloridothionate		515
		465
Dimethylphosphoramidothionyl dichloride		513 br
		461
β-Fluoroethyl methylphosphonochloridothionate		505
		465
Ethyl methylphosphonochloridothionate		510
		469
γ-Fluoropropyl methylphosphonochloridothionate		510
		467

phosphorodithioate (which cannot be completely excluded as a by-product however) and contained weak diffuse bands near 488 cm^{-1}.

(*h*) P—Cl

New observations recorded in Table V confirm previous assignments.

(*i*) P—N—(C)

Holmstedt and Larsson (9) and Mayhood and Harvey (10) note two bands in P—N-containing compounds, one between 1006 and 989 cm^{-1} and the other between 730 and 704 cm^{-1}. They attribute the latter to P—N stretching, and Larsson (11) has shown that on hydrolysis of the P—N bond the intensity of this band is inversely proportional to the extent of hydrolysis. Mayhood and Harvey noted additional characteristic bands in the 2849–2747 cm^{-1} region for Me_2N and in the 2905–2890 cm^{-1} region for Et_2N compounds.

From electronegativity and mass considerations it is estimated that the P—N—(C) stretching vibration should be very close to the P—O(C) stretching bands. If the 1050 cm^{-1} bands can be attributed to the latter, the band near 1000 cm^{-1} would be the more likely candidate for the P—N stretching vibration. The "absence" of this band in Et_2N compounds noted by Mayhood and Harvey may be due to a perturbation by the 962 cm^{-1} C—C band mentioned earlier, and the P—N stretching is possibly contained in the 1030 cm^{-1} P—O or the 962 cm^{-1} C—C band. Et_2N—P compounds generally have three bands in this region near 1025, 952, and 926 cm^{-1}. In the P—N isopropyl compounds the band near 1000 cm^{-1} is again present.

Since the question of assignments of P—O—(C) and C—O—(P) stretching bands is still controversial, analogies based on these bands are not too useful for assigning P—N—(C) and C—N—(P) bands. The strong band near 943 cm^{-1} in all compounds containing a P—O—P link is consistent with the assignment of P—O—(C) to the 1000–1100 cm^{-1} band. This band is usually not symmetrical, and it is conceivable that the C—O—(P) band should also absorb in this region, particularly since the P—O—(C) band possesses a certain amount of "double bond character".

The 714–770 cm^{-1} band in our experience is mainly associated with N-dimethylamino groups, where it appears in the range 704–725 cm^{-1} for $Me_2NP(O)$ compounds and near 740–769 cm^{-1} for $Me_2NP(S)$ compounds. In $Et_2NP(S)$ compounds a band appears at 714–719 cm^{-1} and in *i*-Pr_2N—P(S) compounds the doublet mentioned previously in section (*e*) is found. From Mayhood and Harvey's work, it appears that the low frequency band is shifted bathochromically when C—P or additional Me_2NP links are present. Band positions are listed in Table VI.

(*j*) C—N—(P)

Bands attributed to groups containing this structure are very strong and tend to hide neighboring bands arising from similar R—O—alkyl structures. The position of these bands suggests that they arise from similar vibration modes as those for P—O—C compounds, previously discussed under R—O—(C) stretching.

1. Me_2N.—Mayhood and Harvey (10) mention bands at 1282–1316, 1190, and 1064 cm^{-1} as characteristic for C—N in Me_2N. All of these bands occur in regions where other absorptions take place so have to be interpreted with caution. Our examples are in agreement with these assignments.

2. Et_2N *and* *i*-Pr_2N.—Et_2N—P compounds all have intense bands near 1210 and 1175 cm^{-1} which are characteristic for this grouping. *i*-Pr_2N—P Compounds have a set

of five medium intensity bands near 1200, 1183, 1160, 1139 sh, and 1129 cm^{-1}, in addition to those mentioned for other regions of the spectrum. All compounds examined with these two groups contained P(S) as well, so there is a possibility of shifts in the spectra of the corresponding P(O) compounds.

TABLE VI

P—N and C—S—(P) Bands

Compound	Band positions in cm^{-1}	
Diethyl phosphoroamidate	1020?	
	962?	
Diethyl dimethylphosphoroamidate	990	700
Diethyl dimethylphosphoramidothionate	990	748
Ethyl dimethylphosphoramidochloridate	995	725
Ethyl dimethylphosphoramidochloridothionate	990	752
Propyl dimethylphosphoramidochloridothionate	985	766?
Dimethylphosphoramidothionyl dichloride	980	766?
Dimethylphosphoramidyl dichloride	990	725
O-Ethyl S-β-diethylaminoethyl dimethylphosphoramidothioate	985	714
		694
O-Ethyl O-β-diethylaminoethyl dimethylphosphoramidothioate	990	749
O-*n*-Propyl S-β-diethylaminoethyl dimethylphosphoramidothioate	985	714
		697
O-*n*-Propyl O-β-diethylaminoethyl dimethylphosphoramidothioate	990	752
Diethylphosphoramidothionyl dichloride	1026	917
	952	741?
O,O-Diethyl diethylphosphoramidothioate	1026	917 wk
	948	741
O,O-Di-*n*-propyl diethylphosphoramidothioate	1026	924
	948	719?
O,O-Diisopropyl diethylphosphoramidothioate	975?	924
	948 sh	714
O,O-Di-*n*-butyl diethylphosphoramidothioate	975?	924
	952	719
O,O-Diethyl diisopropylphosphoramidothioate	1000	
O,O-Di-*n*-propyl diisopropylphosphoramidothioate	995?	
O,O-Diisopropyl diisopropylphosphoramidothioate	971	
O,O-Di-*n*-butyl diisopropylphosphoramidothioate	995	

(*k*) C—S—(P)

In an earlier paper (7) we attributed a weak band near 641 cm^{-1} to the C—S(P) vibration. Further studies with compounds of type III have indicated that the intensity of a weak band between 667 and 714 cm^{-1} decreases with rupture of the P—S link. This band is tentatively assigned to the P—S—C grouping. It is weak or absent in compounds

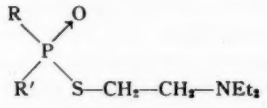

III

where R = R′ = alkoxy, but stronger where R = alkyl and R′ = alkoxy (6), and very prominent where R = Me_2N and R′ = alkoxy (5). Of the phosphonates, Et—P compounds give the strongest band. This may result from either addition to the Et—P and $Me_2NP(O)$ bands or an interaction as described in section (*a*) with concomitant increase in intensity. The formation of a very strong doublet at 714 and 694 cm^{-1} [P—S(C) and $Me_2NP(O)$] (Table VI) with disappearance of bands near 820 and 746 cm^{-1} [P(S) and Me_2N—P(S)] is the most characteristic spectral change during the isomerism IV→V.

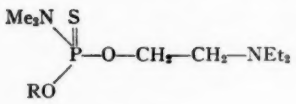

IV

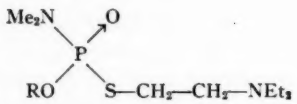

V

The principal group frequencies derived from the tables are summarized in Table VII.

TABLE VII

Group	Frequency range	Intensity
$P\rightarrow S$	740–830	Variable
$O—P(S)Cl_2$	485–488	Weak
	526–529	Strong
	549–552	Strong
	715–730	Strong
	685–705	Strong
$O_2P(S)S$	650–660	Strong
$NP(S)Cl_2$	660–670	Strong
	460–470	Strong
NP(S)Cl and OCP(S)Cl	505–515	Wk to medium
	630–640	Strong
OCP(S)OH	600–610	Strong
PO *i*-Pr	885–900	Wk to medium
PN *i*-Pr	652–654	Medium
	662–664	Medium
	875–885	Wk to medium
	980–990	Strong
	1129	Medium
	1139 sh	
	1160	
	1183	
	1200	
$P(O)NMe_2$	700–725	Strong
	980–990	Strong
$P(S)NMe_2$	745–755	Strong
	980–990	Strong
$PNEt_2$	715–740	Medium to strong
	915–925	Medium to strong
	948–950	Medium to strong
	1025	Strong
	1210	Medium
	1175	Medium
P(S)SH	525–550	Medium
	495–525	Medium

ACKNOWLEDGMENTS

The technical assistance of Mr. A. A. Grey of these laboratories in recording the infrared spectra is gratefully acknowledged. The authors are also indebted to Dr. H. J. Bernstein and Mr. L. C. Thomas for helpful comments, and to Dr. K. F. Jennings for samples of the fluorine-containing compounds.

REFERENCES

1. MAARSEN, J. W., SMIT, M. C., and MATZE, J. Rec. trav. chim. **76**, 713 (1957).
2. MORTIMER, F. S. Spectrochim. Acta, **9**, 270 (1957).
3. BELLAMY, L. J. The infra-red spectra of complex molecules. John Wiley & Sons, Inc., New York. 1954. p. 94.
4. McIVOR, R. A., McCARTHY, G. D., and GRANT, G. A. Can. J. Chem. **34**, 1819 (1956).
5. McIVOR, R. A., MILLER, R. K., and GRANT, G. A. Report in preparation.
6. TAMMELIN, L. E. Acta Chem. Scand. **11**, 1738 (1957).
7. McIVOR, R. A., GRANT, G. A., and HUBLEY, C. E. Can. J. Chem. **34**, 1611 (1956).
8. HOOGE, F. N. and CHRISTEN, P. J. Rec. trav. chim. **77**, 911 (1958).
9. HOLMSTEDT, B. and LARSSON, L. Acta Chem. Scand. **5**, 1179 (1951).
10. MAYHOOD, J. E. and HARVEY, R. B. Can. J. Chem. **33**, 1552 (1955).
11. LARSSON, L. Acta Chem. Scand. **6**, 1470 (1952).

THE SYNTHESIS OF 2-KETOCYCLOHEXYLSUCCINIC ACID AND RELATED SUBSTANCES

IV. STUDIES ON SOME *CIS*- AND *TRANS*-FUSED γ-LACTONES[1]

E. H. CHARLESWORTH, H. J. CAMPBELL, AND D. L. STACHIW

ABSTRACT

The *cis* and *trans* lactones of cyclohexanol-2-acetic acid and cyclohexanol-2-α-propionic acid have been subjected to alkaline hydrolysis to determine the relative ease of ring opening. In addition, a new synthesis by way of a Reformatsky reaction followed by dehydration and cyclization has been shown to yield the *cis* lactone. Finally, the first overtone band of the fundamental carbonyl stretching frequency has been identified.

INTRODUCTION

The reaction of sodiomalonic ester with cyclohexene oxide, followed by hydrolysis and decarboxylation, affords the *trans* lactone (I*a*) (1). An isomeric *cis* lactone (I*b*) is obtained by catalytic reduction of cyclohexanone-2-acetic acid (2).

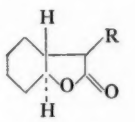

I*a*, R = H
II*a*, R = CH_3

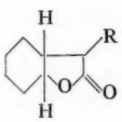

I*b*, R = H
II*b*, R = CH_3

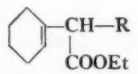

III*a*, R = H
III*b*, R = CH_3

This investigation has shown the latter compound to be identical with the lactone obtained by the acid-catalyzed cyclization of ethyl cyclohexene-1-acetate (III*a*). This substance was produced by a Reformatsky reaction between cyclohexanone and ethyl bromoacetate, followed by dehydration of the β-hydroxy ester with phosphorus pentoxide.

The *cis* and *trans* configurations shown for the lactones follow from (*a*) the known stereochemistry of the reaction of nucleophiles with epoxides (3); (*b*) the known stereochemistry of the catalytic reduction of substituted cyclohexanones (4); and (*c*) the greater ease with which (I*b*) is formed from the corresponding hydroxy acid (2, cf. 5). Similar arguments apply to the lactones (II*a*) (6) and (II*b*), available by essentially the same reactions.

Further support for these configurational assignments is given by studies on the rates of ring opening by alkali. In both cases the isomer assigned the *trans* configuration hydrolyzed more rapidly, as shown in Fig. 1. This was to be expected in view of the less stable *trans* configuration. The greater stability of the methyl-substituted ring is in accordance with the many analogous cases in the literature (7).

All lactones showed peak absorption at about 2.8 μ in the infrared region accessible to the Beckmann D.K. recording spectrophotometer. This is undoubtedly the first overtone (8) of the powerful carbonyl adsorption band observed for (I*a*) and (I*b*) at 5.62 μ and 5.70 μ respectively, by Brewster and Kucera (9). As in the case of the fundamental frequencies, a wavelength shift was observed for these 2.8 μ bands indicating the more strained condition of the *trans* form. Rasmussen and Brattain (10) noticed absorption in this 2.8 μ region by several lactones, but suggested that it might be due to traces of

[1]*Manuscript received January 9, 1959.*
Contribution from the Department of Chemistry, University of Manitoba, Winnipeg, Manitoba.

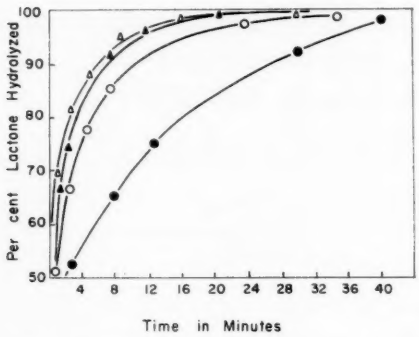

FIG. 1. Rates of hydrolysis of *cis–trans* γ-lactones by .0765 *N* NaOH at 20° C (△—I*a*, ○—I*b*, ▲—II*a*, ●—II*b*).

water. However, in a re-examination of the spectrum of γ-valerolactone in carbon tetrachloride, we find the peak at 2.8 μ to be unaffected by drying the solvent, while a less prominent band at 2.71 μ diminishes (but could not be eliminated altogether). The latter band is undoubtedly due to water, which in carbon tetrachloride alone causes absorption at 2.696 μ; the shift to longer wavelength in the presence of lactones is evidence of hydrogen-bonding between the two molecules.

TABLE I

Some physical constants and derivatives of the lactones

	γ-Lactone of cyclohexanol-2-acetic acid			γ-Lactone of cyclohexanol-2-α-propionic acid		
		cis I*b*			*cis* II*b*	
	trans (I*a*) Method (1)	Method (2)	Reformatsky method	*trans* (II*a*) Method (6)	Reformatsky method	Method (2)
B.p.(per mm)	131–132°/12	129–130°/13	128–128.5°/10	125–128°/10	131–134°/11	132–135°/13
D_4^{20}	1.0859	1.0921	1.0923	1.0519	1.0589	—
n_D^{20}	1.4752	1.4784	1.4773	1.4719	1.4756	1.4751
Position of C=O overtone in millimicrons	2802	2808	2808	2812	2819	2819
M.p. of hydroxy acid	105–106°	—	—	110–111°	—	—
M.p. of hydrazide	167–167.5°	140–141°	140–141°	191–192°	136–137°	—
M.p. of N-benzylamide	141–142°*	97–98°	97–98°*	—	—	—

*Brewster and Kucera (9).

EXPERIMENTAL

REFORMATSKY REACTIONS AND SUBSEQUENT PROCEDURE

Ethyl 1-Cyclohexanolacetate

Cyclohexanone (49 g), zinc filings (33 g), and dry benzene (200 ml) were placed in a 1-l. three-necked flask equipped with a stirrer and condenser. The mixture was heated to boiling and the addition of ethyl bromoacetate (167 g) containing a trace of iodine was begun. At the first sign of reaction, heating was discontinued, the stirrer started, and the addition continued at such a rate that moderate refluxing was maintained. Following addition of the ester, refluxing was continued for a further half hour. No attempt should

be made to dissolve the unreacted zinc by prolonged heating, as this decreases the yield and quality of the product. A little ice was added to the cooled solution and with the stirrer running, cold sulphuric acid (250 ml, 6 *N*) was added slowly. After half an hour the benzene layer was separated, washed with water and sodium carbonate solution, and dried over calcium chloride. The benzene was removed and the ethyl 1-cyclohexanolacetate (66.5 g, 72% yield) distilled *in vacuo* at 108–118° C (11 mm). Auwers and Ellinger (11) report 141° C (33 mm) and Charlesworth *et al.* (12) 143–146° C (37 mm).

Ethyl Cyclohexene-1-acetate (III*a*)

Ethyl 1-cyclohexanolacetate (50 g) was dissolved in dry benzene (150 ml), and phosphorus pentoxide (40 g) was added to the solution. It was refluxed on the water bath for 3 hours and allowed to cool. The benzene solution was decanted, the porous residue rinsed twice with benzene (25-ml portions), and the washings combined with the main solution. The benzene was removed and the unsaturated ester (30.5 g, 68%) was distilled at 93–95° C (10 mm). Wallach (13) reports 100° C (12 mm).

Lactone of cis-Cyclohexanol-2-acetic Acid (I*b*)

Ethyl cyclohexene-1-acetate (10 g) and sulphuric acid (60 ml, 50% by volume) were heated on the water bath under reflux with stirring for 1 hour. By this time the oily layer had disappeared and the solution was yellow-orange in color. Only a small amount of polymeric material clinging to the walls of the flask was observed. The solution was allowed to cool, water (150 ml) was added, and the solution heated to boiling. It was cooled and extracted four times with ether (50-ml portions). The ethereal extract was washed with saturated salt solution, sodium carbonate solution, and thoroughly dried with anhydrous potassium carbonate. The ether was removed and distillation gave a colorless liquid (5.0 g, 60% yield) with a characteristic smell, which boiled at 129–130° C (13 mm); $n_D^{20} = 1.4784$. It was neutral to litmus and solidified at −20° C into long white needles. The original ethyl cyclohexene-1-acetate does not solidify at −80° C. Found: C, 69.1; H, 8.72%. Calc. for the lactone $C_8H_{12}O_2$: C, 68.6; H, 8.57%.

When crude cyclohexene-1-acetic acid (m.p. 34–36° C) prepared by the hydrolysis of the ester according to the directions of Wallach (13) was treated with 50% sulphuric acid according to the above directions, there was considerably more darkening than with the ester. Acidification of the sodium carbonate washings showed that very little unlactonized acid was left. Distillation gave the lactone in slightly smaller yield (43%), but with the same properties and constants as before. Found: C, 68.8; H, 8.97%. There was more dark viscous distillation residue than in the previous case.

When ethyl 1-cyclohexanolacetate was lactonized according to the above conditions there was considerably more dark polymeric material produced than in the previous cases. The lactone was isolable as before, but only in about 26% yield.

Ethyl α-(1-Cyclohexanol) Propionate

This ester was obtained in 76% yield in a Reformatsky reaction with ethyl α-bromopropionate. It distilled at 115–119° C (11 mm). Wallach reported 125–127° C (12 mm).

Ethyl Cyclohexene-1-α-propionate (III*b*)

This was obtained in 70% yield by dehydration of the previous ester. It boiled at 97–99° C (11 mm) or 68–70° C (1 mm).

Lactone of cis-Cyclohexanol-2-α-propionic Acid (II*b*)

This was obtained in 66% yield by cyclization of the previous unsaturated ester with

50% sulphuric acid. It boiled at 131–134° C (11 mm); $n_D^{20} = 1.4756$. It did not solidify at −20° C. Found: C, 69.5; H, 9.24%. Calc. for $C_9H_{14}O_2$: C, 70.0; H, 9.15%.

γ-Lactones (Other than by Reformatsky Method)

The preparation of the *cis* lactones by the Reformatsky method (D. L. Stachiw) is described above. These samples were compared with *cis* lactones prepared from the corresponding keto acids by the catalytic hydrogenation method of Newman and Van der Werf (2) and found to be identical in all respects (Table I).

The *trans* lactones (I*a* and II*a*) were prepared by the method of Coffey (1) and of McRae, Charlesworth, and Alexander (6) from cyclohexene oxide.

γ-Lactone of trans-Cyclohexanol-2-methylmalonic Acid

This product was isolated prior to the decarboxylation step in the cyclohexene oxide synthesis of the *trans* lactone (II*a*). After recrystallization from benzene–ligroin, white crystals were obtained melting at 151–152° C. Found: C, 60.98; H, 7.22%; neut. equiv., 198.0. Calc. for $C_{10}H_{14}O_4$: C, 60.6; H, 7.12%; neut. equiv., 198.2.

trans-Cyclohexanol-2-acetic Acid

Upon alkaline hydrolysis and acidification of the *trans* lactone (I*a*) Newman and Van der Werf (2) obtained an acid of m.p. 105–106° C. They claimed that their product was not identical with the 97–102° melting acid obtained by Coffey (1) by hydrogen chloride treatment of the potassium salt of (I*a*) because the latter had a tendency to relactonize in solution. The two methods were repeated and, although several recrystallizations failed to raise the melting point of Coffey's product, a mixed melting point revealed little or no depression. It seems more reasonable, therefore, to view the instability of this low-melting acid as resulting merely from its impurity.

trans-Cyclohexanol-2-α-propionic Acid

The method previously outlined (2) was used to obtain an acid which, after recrystallization from water, melted at 110° C. Found: C, 63.0; H, 9.16%; neut. equiv., 173.5. Calc. for $C_9H_{16}O_3$: C, 62.8; H, 9.31%; neut. equiv., 172.2.

Hydrazide Derivatives

The method described by Coffey (1) was used. A 10% solution of the lactone in alcohol was boiled with hydrazine (95%) for a few minutes. When the solution was cooled, the hydrazide separated.

The Reformatsky-produced lactone (III*a* → I*b*) and the Newman *cis* lactone (I*b*) both gave a hydrazide which, when recrystallized from benzene–ligroin, melted at 140–141° C. Found: N, 16.12%. Calc. for $C_8H_{16}O_2N_2$: N, 16.26%. This derivative was far more soluble in polar and non-polar solvents than the corresponding *trans* hydrazide, which melted at 167.5°, as reported by Coffey (1).

The *trans* lactone of cyclohexanol-2-α-propionic acid (II*a*) gave a derivative which, upon recrystallization from water, melted at 191–192° C. Found: N, 14.76%. Calc. for $C_9H_{18}O_2N_2$: N, 15.04%.

The Reformatsky-produced *cis* lactone (III*b* → II*b*) yielded a hydrazide which, after two recrystallizations from benzene–ligroin, melted at 136–137° C. Found: N, 15.15%. Calc. for $C_9H_{18}O_2N_2$: N, 15.04%.

N-Benzylamide Derivatives

The method used was that of Dermer and King (14). The Reformatsky-produced lactone (1 g) was refluxed with benzylamine (3 ml) in the presence of ammonium chloride

(1 g). The amide, when recrystallized from benzene–ligroin, melted at 97–98° C. Brewster and Kucera (9) reported an identical melting point for the N-benzylamide prepared from Newman's *cis* lactone.

Hydrolyses of γ-Lactones

The technique used was adapted from that described by Kendall, Osterberg, and MacKenzie (15) for the determination of the rate of ring opening of a γ-lactone. The lactone (1/200 mole) was dissolved in ethanol (25 ml) and introduced into a flask containing .0860 *N* sodium hydroxide (200 ml), stirred gently, and thermostated at 20° C. At periodic intervals, 20-ml portions were withdrawn and run into hydrochloric acid (20 ml, .0896 *N*). The excess acid was then titrated with standard alkali and the hydrolysis rate plotted (Fig. 1).

Infrared Spectra

A Beckmann D.K. recording spectrophotometer was used to investigate the small portion of the infrared region up to 2.85 μ. A pair of quartz cells were used whose 100% line did not deviate more than 3% on either side. The lactone samples were weighed directly into the cell and a measured amount of solvent carbon tetrachloride added.

REFERENCES

1. COFFEY, S. Rec. trav. chim. **42**, 387 (1923).
2. NEWMAN, M. S. and VAN DER WERF, C. A. J. Am. Chem. Soc. **67**, 233 (1945).
3. GRIGSBY, W. E., HIND, J., CHANLEY, J., and WESTHEIMER, F. H. J. Am. Chem. Soc. **64**, 2606 (1942).
4. SIEGEL, S. J. Am. Chem. Soc. **75**, 1317 (1953).
5. ANGYAL, S. J. and MACDONALD, C. G. J. Chem. Soc. 686 (1952).
6. MCRAE, J. A., CHARLESWORTH, E. H., and ALEXANDER, D. S. Can. J. Research, B, **21**, 1 (1943).
7. ELIEL, E. L. Steric effects in organic chemistry. *Edited by* M. S. Newman. John Wiley & Sons, Inc., New York. 1956. p. 119.
8. MARION, L., RAMSAY, D. A., and JONES, R. N. J. Am. Chem. Soc. **73**, 305 (1951).
9. BREWSTER, J. H. and KUCERA, C. H. J. Am. Chem. Soc. **77**, 4564 (1955).
10. RASMUSSEN, R. S. and BRATTAIN, R. R. J. Am. Chem. Soc. **71**, 1073 (1949).
11. AUWERS, K. and ELLINGER, P. Ann. **387**, 200 (1911).
12. CHARLESWORTH, E. H., MCRAE, J. A., and MACFARLANE, H. M. Can. J. Research, B, **21**, 55 (1943).
13. WALLACH, O. Ann. **343**, 51 (1905).
14. DERMER, O. C. and KING, J. J. Org. Chem. **8**, 168 (1943).
15. KENDALL, E. C., OSTERBERG, A. E., and MACKENZIE, B. F. J. Am. Chem. Soc. **48**, 1384 (1926).

ON THE COUPLING BETWEEN F^{19} AND H^1 NUCLEI IN *p*-FLUOROTOLUENE[1]

T. SCHAEFER

ABSTRACT

The proton and fluorine high resolution nuclear magnetic resonance spectra of *p*-fluorotoluene are discussed in terms of the case $A_2A_2'X$. The 4×4 submatrices are diagonalized in analytical form and therefore explicit values for all energy levels can be obtained. The spectra are consistent with $J_m^{HF} = J_o^{HF}$, which may be of theoretical interest.

INTRODUCTION

The analysis of high resolution nuclear magnetic resonance spectra normally yields values of the spin–spin coupling constants and of the relative chemical shifts of the resonating nuclei. However, in some special cases the distribution of lines in the spectrum depends only on the sum of the coupling constants. The simplest example of this occurs in the case ABB' (terminology of Bernstein, Pople, and Schneider (1)), in which two nuclei seeing a field H_B may be unequally coupled to a third nucleus seeing a field H_A. Richards and Schaefer (2) analyzed the proton spectrum of 2,5-dichloronitrobenzene and showed that the protons at position 3 and 4 have the same shift and that the line splittings are equal to the average of the coupling constant between protons 3 and 6 and between 4 and 6: $(1/2)(J_m^{HH}+J_p^{HH})$. It does not follow that $J_m^{HH} = J_p^{HH}$.

The proton and fluorine spectra of fluorobenzene indicate a negligible shift between the protons. From the shape of the spectra Baker (3) suggested that the H–F coupling constants are equal. In general the coupling decreases as the number of bonds between the nuclei increases. In view of the work of Gutowsky *et al.* (4) a more likely explanation appears to be that of Roux (5), who interprets the splittings as the average of the H–F coupling constants $(1/5)(2J_o^{HF}+2J_m^{HF}+J_p^{HF})$ without analyzing the spectrum. This interpretation contains the implicit assumption that the signs of the coupling constants are equal. This need not be so (4).

A glance at the proton and fluorine spectra of *p*-fluorotoluene (Fig. 1) would suggest that here also the splittings are given by the average of the H–F coupling constants $(1/2)(J_o^{HF}+J_m^{HF})$. It is the purpose of the present work to show from an explicit analysis that, in fact, $J_o^{HF} = J_m^{HF}$ for this compound. Such a result may be of theoretical interest.

EXPERIMENTAL

p-Fluorotoluene of known purity was kindly loaned by Dr. H. W. Thompson. The proton and fluorine spectra of the pure compound were taken on the high resolution spectrometer in Dr. R. E. Richards' laboratory at Oxford (6). The proton resonance occurs at 29.92000 Mc.p.s. The measurement of line separations is accurate to 1%, while the intensity measurements are good to about 10%.

RESULTS

The proton and fluorine spectra are shown in Fig. 1. The line separations are given in c.p.s. and the number of the lines is such as is convenient for the discussion below.

[1]*Manuscript received January 22, 1959.*
Contribution from the Department of Chemistry, University of Manitoba, Winnipeg, Manitoba.

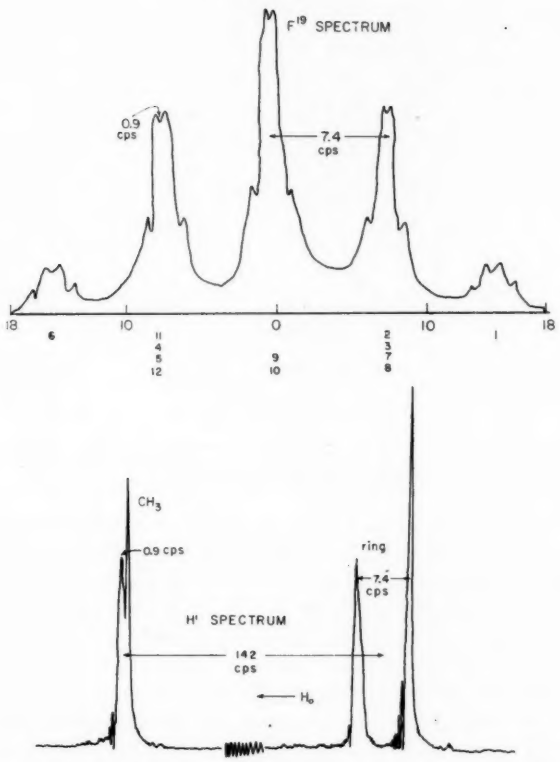

FIG. 1. Fluorine and proton resonance spectra of *p*-fluorotoluene.

DISCUSSION

The ring proton spectrum indicates a negligibly small chemical shift between the protons ortho and meta to the fluorine atom. The intensities of the two lines are the same within experimental error but one is slightly broader and this indicates a very small shift which can be neglected for our purposes. Protons in a methyl group situated ortho or para to a fluorine atom in the benzene ring are normally weakly coupled only to the fluorine nucleus but not to the ring protons (7). In the present instance this coupling is 0.9 c.p.s. Each line in the fluorine spectrum will therefore actually be a quadruplet, while the methyl resonance is a doublet. The splittings due to this coupling are the same in c.p.s., although, of course, not in gauss.

We are interested, however, primarily in the coupling between ring protons and the F^{19} nucleus. Information of a definite nature on this point requires the analysis of the case $A_2A_2'X$.

1. Analysis of the Case $A_2A_2'X$

We shall label the protons of the aromatic ring A and A' as shown in Fig. 2 and we shall call the fluorine atom X. The positions in the ring are numbered 1 to 5. Let the field experienced by nuclei A and A' be H_A such that in an applied field H_0, $H_A = H_0(1-\sigma_A)$, and similarly $H_x = H_0(1-\sigma_x)$. There are 10 coupling constants between these

nuclei and from symmetry we can write:

$$J_{14} = J_{23}, \quad J_{45} = J_{35};$$
$$J_{25} = J_{15}, \quad J_{24} = J_{13};$$
$$J_{12} = J_{34}.$$

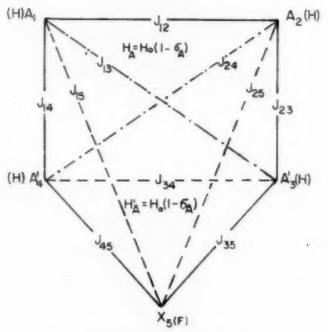

FIG. 2. Model for $A_2A_2'X$.

In the magnetic field H_0, a nucleus of magnetogyric ratio γ will have a nuclear resonance frequency ν_0, such that $\nu_0 = (\gamma/2\pi)H_0$. We shall use ν_0 for the resonance frequency for protons in the applied field and ν_0' for the frequency of the X nucleus resonance.

The initial wave functions are given in Table I together with the diagonal matrix elements. The off-diagonal elements are given in Table II. The matrix is similar to that given by Richards and Schaefer for the case A_2B_2X (8). It is given in full because reference will be made to specific matrix elements later on.

The initial choice of wave functions factorizes the secular determinant considerably. Further simplification arises from the condition that $\nu_0'\sigma_x$ is much larger than any of the spin coupling constants. This condition is of course amply fulfilled when X is fluorine. The determinant resolves itself into four 1×1, ten 2×2, and two 4×4 determinants.

Define positive quantities A, B, C, D, and angles θ, ϕ, ψ, γ, by:

$$\begin{aligned}
A\cos 2\theta &= (1/4)(J_{35}-J_{15}),\\
A\sin 2\theta &= (1/2)(J_{23}+J_{13});\\
B\cos 2\phi &= (1/4)(J_{15}-J_{35}),\\
B\sin 2\phi &= (1/2)(J_{23}+J_{13});\\
C\cos 2\psi &= (1/2)(J_{35}-J_{15}),\\
C\sin 2\psi &= (1/2)(J_{23}-J_{13});\\
D\cos 2\gamma &= (1/4)(J_{15}-J_{35}),\\
D\sin 2\gamma &= (1/2)(J_{13}-J_{23}).
\end{aligned} \qquad [1]$$

When the indicated orthogonal transformations are carried out, we obtain the stationary wave functions and energies given in Tables III and IV. Selection rules allow a maximum number of 110 transitions for the five nuclei. Of these, 46 are combination lines which, because of their weak intensity, will not be further considered. This leaves 16 transitions originating with the X nuclei, 12 of which can now be written down explicitly, whatever the value of the coupling constants. Similarly the A and A' nuclei give rise to 48 lines and 24 of these may now be explicitly tabulated. The 36 transitions are given in Tables V and VI. Later on we shall find explicit values for the other transitions for *p*-fluorotoluene in terms of the experimental parameters.

TABLE I

No.	Wave function (ψ)	Symmetry	Diagonal elements
1	$\alpha\alpha\alpha\alpha\alpha$	$(A_1)_{5/2}$	$(1/2)\nu_0\,(4-4\sigma_A)+(1/2)\nu_0'(1-\sigma_x)+(1/2)(J_{12}+J_{13}+J_{23}+J_{15}+J_{35})$
2	$\alpha\alpha\alpha\alpha\beta$	$(A_1)_{3/2}$	$(1/2)\nu_0\,(4-4\sigma_A)-(1/2)\nu_0'(1-\sigma_x)+(1/2)(J_{12}+J_{13}+J_{23}-J_{15}-J_{35})$
3	$\sqrt{(1/2)}(\alpha\alpha\alpha\beta\alpha+\alpha\alpha\beta\alpha\alpha)$	$(A_1)_{3/2}$	$(1/2)\nu_0\,(2-2\sigma_A)+(1/2)\nu_0'(1-\sigma_x)+(1/2)(J_{15}+J_{12})$
4	$\sqrt{(1/2)}(\beta\alpha\alpha\alpha\alpha+\alpha\beta\alpha\alpha\alpha)$	$(A_1)_{3/2}$	$(1/2)\nu_0\,(2-2\sigma_A)+(1/2)\nu_0'(1-\sigma_x)+(1/2)(J_{35}+J_{12})$
5	$\sqrt{(1/2)}(\alpha\alpha\alpha\beta\beta+\alpha\alpha\beta\alpha\beta)$	$(A_1)_{1/2}$	$(1/2)\nu_0\,(2-2\sigma_A)-(1/2)\nu_0'(1-\sigma_x)+(1/2)(-J_{15}+J_{12})$
6	$\sqrt{(1/2)}(\alpha\beta\alpha\alpha\beta+\beta\alpha\alpha\alpha\beta)$	$(A_1)_{1/2}$	$(1/2)\nu_0\,(2-2\sigma_A)-(1/2)\nu_0'(1-\sigma_x)+(1/2)(-J_{35}+J_{12})$
7	$\sqrt{(1/2)}(\alpha\beta\alpha\beta\alpha+\beta\alpha\beta\alpha\alpha)$	$(A_1)_{1/2}$	$(1/2)\nu_0'(1-\sigma_x)+(1/2)(J_{13}-J_{12}-J_{23})$
8	$\sqrt{(1/2)}(\beta\alpha\alpha\beta\alpha+\alpha\beta\beta\alpha\alpha)$	$(A_1)_{1/2}$	$(1/2)\nu_0'(1-\sigma_x)+(1/2)(-J_{13}-J_{12}+J_{23})$
9	$\alpha\alpha\beta\alpha\alpha$	$(A_1)_{1/2}$	$(1/2)\nu_0'(1-\sigma_x)+(1/2)(-J_{13}-J_{23}+J_{15}-J_{35}+J_{12})$
10	$\beta\beta\alpha\alpha\alpha$	$(A_1)_{1/2}$	$(1/2)\nu_0'(1-\sigma_x)+(1/2)(-J_{13}-J_{23}-J_{15}+J_{35}+J_{12})$
11	$\sqrt{(1/2)}(\alpha\beta\alpha\beta\beta+\beta\alpha\beta\alpha\beta)$	$(A_1)_{-1/2}$	$(1/2)\nu_0'(-1+\sigma_x)+(1/2)(J_{13}-J_{12}-J_{23})$
12	$\sqrt{(1/2)}(\beta\alpha\alpha\beta\beta+\alpha\beta\beta\alpha\beta)$	$(A_1)_{-1/2}$	$(1/2)\nu_0'(-1+\sigma_x)+(1/2)(-J_{13}-J_{12}+J_{23})$
13	$\beta\beta\alpha\alpha\beta$	$(A_1)_{-1/2}$	$(1/2)\nu_0'(1-\sigma_x)+(1/2)(J_{12}-J_{13}-J_{23}+J_{15}-J_{35})$
14	$\alpha\alpha\beta\beta\beta$	$(A_1)_{-1/2}$	$(1/2)\nu_0'(1-\sigma_x)+(1/2)(J_{12}-J_{13}-J_{23}-J_{15}+J_{35})$
15	$\sqrt{(1/2)}(\beta\beta\alpha\alpha\beta+\beta\beta\alpha\beta\alpha)$	$(A_1)_{-1/2}$	$(1/2)\nu_0\,(-2+2\sigma_A)+(1/2)\nu_0'(1-\sigma_x)+(1/2)(-J_{15}+J_{12})$
16	$\sqrt{(1/2)}(\alpha\beta\beta\beta\alpha+\beta\alpha\beta\beta\alpha)$	$(A_1)_{-1/2}$	$(1/2)\nu_0\,(-2+2\sigma_A)+(1/2)\nu_0'(1-\sigma_x)+(1/2)(-J_{35}+J_{12})$
17	$\beta\beta\beta\beta\alpha$	$(A_1)_{-3/2}$	$(1/2)\nu_0\,(-4+4\sigma_A)+(1/2)\nu_0'(1-\sigma_x)+(1/2)(J_{12}+J_{13}+J_{23}-J_{15}-J_{35})$
18	$\sqrt{(1/2)}(\beta\beta\alpha\beta+\beta\beta\alpha\beta\beta)$	$(A_1)_{-3/2}$	$(1/2)\nu_0\,(-2+2\sigma_A)-(1/2)\nu_0'(1-\sigma_x)+(1/2)(J_{15}+J_{12})$
19	$(1/\sqrt{2})(\beta\alpha\beta\beta\beta+\alpha\beta\beta\beta\beta)$	$(A_1)_{-3/2}$	$(1/2)\nu_0\,(-2+2\sigma_A)-(1/2)\nu_0'(1-\sigma_x)+(1/2)(J_{35}+J_{12})$
20	$\beta\beta\beta\beta\beta$	$(A_1)_{-5/2}$	$(1/2)\nu_0\,(-4+4\sigma_A)-(1/2)\nu_0'(1-\sigma_x)+(1/2)(J_{12}+J_{13}+J_{23}+J_{15}+J_{35})$
21	$(1/\sqrt{2})(\alpha\alpha\alpha\beta\alpha-\alpha\alpha\beta\alpha\alpha)$	$(B_2)_{3/2}$	$(1/2)\nu_0\,(2-2\sigma_A)+(1/2)\nu_0'(1-\sigma_x)+(1/2)(J_{15}-J_{12})$
22	$(1/\sqrt{2})(\beta\alpha\alpha\alpha\alpha-\alpha\beta\alpha\alpha\alpha)$	$(B_2)_{3/2}$	$(1/2)\nu_0\,(2-2\sigma_A)+(1/2)\nu_0'(1-\sigma_x)+(1/2)(J_{35}-J_{12})$
23	$(1/\sqrt{2})(\alpha\alpha\alpha\beta\beta-\alpha\alpha\beta\alpha\beta)$	$(B_2)_{1/2}$	$(1/2)\nu_0\,(2-2\sigma_A)-(1/2)\nu_0'(1-\sigma_x)+(1/2)(-J_{15}-J_{12})$
24	$(1/\sqrt{2})(\alpha\beta\alpha\alpha\beta-\beta\alpha\alpha\alpha\beta)$	$(B_2)_{1/2}$	$(1/2)\nu_0\,(2-2\sigma_A)-(1/2)\nu_0'(1-\sigma_x)+(1/2)(-J_{35}-J_{12})$
25	$(1/\sqrt{2})(\alpha\beta\alpha\beta\alpha-\beta\alpha\beta\alpha\alpha)$	$(B_2)_{1/2}$	$(1/2)\nu_0'(1-\sigma_x)+(1/2)(-J_{12}+J_{13}-J_{23})$
26	$(1/\sqrt{2})(\beta\alpha\alpha\beta\alpha-\alpha\beta\beta\alpha\alpha)$	$(B_2)_{1/2}$	$(1/2)\nu_0'(1-\sigma_x)+(1/2)(-J_{12}-J_{13}+J_{23})$
27	$(1/\sqrt{2})(\alpha\beta\alpha\beta\beta-\beta\alpha\beta\alpha\beta)$	$(B_2)_{-1/2}$	$(1/2)\nu_0'(-1+\sigma_x)+(1/2)(J_{13}-J_{12}-J_{23})$
28	$(1/\sqrt{2})(\beta\alpha\alpha\beta\beta-\alpha\beta\beta\alpha\beta)$	$(B_2)_{-1/2}$	$(1/2)\nu_0'(-1+\sigma_x)+(1/2)(-J_{13}-J_{12}+J_{23})$
29	$(1/\sqrt{2})(\beta\beta\beta\alpha\alpha-\beta\beta\alpha\beta\alpha)$	$(B_2)_{-1/2}$	$(1/2)\nu_0\,(-2+2\sigma_A)+(1/2)\nu_0'(1-\sigma_x)+(1/2)(-J_{12}-J_{15})$
30	$(1/\sqrt{2})(\alpha\beta\beta\beta\alpha-\beta\alpha\beta\beta\alpha)$	$(B_2)_{-1/2}$	$(1/2)\nu_0\,(-2+2\sigma_A)+(1/2)\nu_0'(1-\sigma_x)+(1/2)(-J_{12}-J_{35})$
31	$(1/\sqrt{2})(\beta\beta\beta\alpha\beta-\beta\beta\alpha\beta\beta)$	$(B_2)_{-3/2}$	$(1/2)\nu_0\,(-2+2\sigma_A)-(1/2)\nu_0'(1-\sigma_x)+(1/2)(J_{15}-J_{12})$
32	$(1/\sqrt{2})(\beta\alpha\beta\beta\beta-\alpha\beta\beta\beta\beta)$	$(B_2)_{-3/2}$	$(1/2)\nu_0\,(-2+2\sigma_A)-(1/2)\nu_0'(1-\sigma_x)+(1/2)(J_{35}-J_{12})$

TABLE II

Off-diagonal elements

$\mathfrak{H}_{23} = (1/\sqrt{2})J_{35}$, $\mathfrak{H}_{24} = (1/\sqrt{2})J_{15}$, $\mathfrak{H}_{34} = (1/2)(J_{23}+J_{13})$,
$\mathfrak{H}_{56} = (1/2)(J_{23}+J_{13})$, $\mathfrak{H}_{57} = \mathfrak{H}_{58} = (1/2)J_{15}$, $\mathfrak{H}_{59} = (1/\sqrt{2})J_{35}$,
$\mathfrak{H}_{5,10} = \mathfrak{H}_{69} = \mathfrak{H}_{9,10} = 0$, $\mathfrak{H}_{67} = \mathfrak{H}_{68} = (1/2)J_{35}$, $\mathfrak{H}_{6,10} = (1/\sqrt{2})J_{15}$,
$\mathfrak{H}_{7,8} = J_{12}$, $\mathfrak{H}_{7,9} = \mathfrak{H}_{7,10} = (1/\sqrt{2})J_{23}$, $\mathfrak{H}_{89} = \mathfrak{H}_{8,10} = (1/\sqrt{2})J_{13}$,
$\mathfrak{H}_{11,12} = J_{12}$, $\mathfrak{H}_{11,13} = \mathfrak{H}_{11,14} = (1/\sqrt{2})J_{23}$, $\mathfrak{H}_{11,15} = \mathfrak{H}_{12,15} = (1/2)J_{15}$,
$\mathfrak{H}_{11,16} = \mathfrak{H}_{12,16} = (1/2)J_{35}$, $\mathfrak{H}_{12,13} = \mathfrak{H}_{12,14} = (1/\sqrt{2})J_{13}$, $\mathfrak{H}_{13,14} = \mathfrak{H}_{13,16} = \mathfrak{H}_{14,15} = 0$,
$\mathfrak{H}_{13,15} = (1/\sqrt{2})J_{35}$, $\mathfrak{H}_{14,16} = (1/\sqrt{2})J_{15}$, $\mathfrak{H}_{15,16} = (1/2)(J_{23}+J_{13})$,
$\mathfrak{H}_{17,18} = (1/\sqrt{2})J_{35}$, $\mathfrak{H}_{17,19} = (1/\sqrt{2})J_{15}$, $\mathfrak{H}_{18,19} = (1/2)(J_{23}+J_{13})$,
$\mathfrak{H}_{21,22} = (1/2)(J_{23}-J_{13})$,
$\mathfrak{H}_{23,24} = (1/2)(J_{13}-J_{23})$, $\mathfrak{H}_{23,25} = \mathfrak{H}_{23,26} = (1/2)J_{15}$,
$\mathfrak{H}_{24,26} = -\mathfrak{H}_{24,25} = -(1/2)J_{35}$, $\mathfrak{H}_{25,26} = 0$,
$\mathfrak{H}_{27,28} = 0$, $\mathfrak{H}_{27,29} = \mathfrak{H}_{28,29} = -(1/2)J_{15}$,
$\mathfrak{H}_{27,30} = -\mathfrak{H}_{28,30} = -(1/2)J_{35}$, $\mathfrak{H}_{29,30} = (1/2)(J_{23}-J_{13})$,
$\mathfrak{H}_{31,32} = (1/2)(J_{13}-J_{23})$.

2. The Spectrum of p-Fluorotoluene

(a) Fluorine Resonance Spectrum

The fluorine spectrum has a 7.4-c.p.s. interval between the lines with an intensity distribution of 1:4:6:4:1 within experimental error. From the energies and intensities

TABLE III

Stationary wave functions and symmetry

3′	$(1/\sqrt{2})\{-\sin\theta(\beta\alpha\alpha\alpha+\alpha\beta\alpha\alpha)+\cos\theta(\alpha\alpha\beta\alpha+\alpha\alpha\beta\alpha)\}$	$(A_1)_{3/2}$
4′	$(1/\sqrt{2})\{\cos\theta(\beta\alpha\alpha\alpha+\alpha\beta\alpha\alpha)+\sin\theta(\alpha\alpha\beta\alpha+\alpha\alpha\beta\alpha)\}$	
5′	$(1/\sqrt{2})\{-\sin\phi(\alpha\beta\alpha\beta+\beta\alpha\alpha\beta)+\cos\phi(\alpha\alpha\beta\beta+\alpha\alpha\beta\alpha)\}$	$(A_1)_{1/2}$
6′	$(1/\sqrt{2})\{\cos\phi(\alpha\beta\alpha\beta+\beta\alpha\alpha\beta)+\sin\phi(\alpha\alpha\beta\beta+\alpha\alpha\beta\alpha)\}$	
15′	$(1/\sqrt{2})\{\cos\theta(\beta\beta\beta\alpha\alpha+\beta\beta\alpha\beta\alpha)+\sin\theta(\alpha\beta\beta\beta\alpha+\beta\alpha\beta\beta\alpha)\}$	$(A_1)_{-1/2}$
16′	$(1/\sqrt{2})\{-\sin\theta(\beta\beta\beta\alpha\alpha+\beta\beta\alpha\beta\alpha)+\cos\theta(\alpha\beta\beta\beta\alpha+\beta\alpha\beta\beta\alpha)\}$	
18′	$(1/\sqrt{2})\{\cos\phi(\beta\beta\beta\alpha\beta+\beta\beta\alpha\beta\beta)+\sin\phi(\beta\alpha\beta\beta\beta+\alpha\beta\beta\beta\beta)\}$	$(A_1)_{-3/2}$
19′	$(1/\sqrt{2})\{-\sin\phi(\beta\beta\beta\alpha\beta+\beta\beta\alpha\beta\beta)+\cos\phi(\beta\alpha\beta\beta\beta+\alpha\beta\beta\beta\beta)\}$	
21′	$(1/\sqrt{2})\{-\sin\psi(\beta\alpha\alpha\alpha\alpha-\alpha\beta\alpha\alpha\alpha)+\cos\psi(\alpha\alpha\alpha\beta\alpha-\alpha\alpha\beta\alpha\alpha)\}$	$(B_2)_{3/2}$
22′	$(1/\sqrt{2})\{\cos\psi(\beta\alpha\alpha\alpha\alpha-\alpha\beta\alpha\alpha\alpha)+\sin\psi(\alpha\alpha\alpha\beta\alpha-\alpha\alpha\beta\alpha\alpha)\}$	
23′	$(1/\sqrt{2})\{-\sin\gamma(\alpha\beta\alpha\alpha\beta-\beta\alpha\alpha\alpha\beta)+\cos\gamma(\alpha\alpha\alpha\beta\beta-\alpha\alpha\beta\alpha\beta)\}$	$(B_2)_{1/2}$
24′	$(1/\sqrt{2})\{\cos\gamma(\alpha\beta\alpha\alpha\beta-\beta\alpha\alpha\alpha\beta)+\sin\gamma(\alpha\alpha\alpha\beta\beta-\alpha\alpha\beta\alpha\beta)\}$	
29′	$(1/\sqrt{2})\{\cos\psi(\beta\beta\beta\alpha\alpha-\beta\beta\alpha\beta\alpha)+\sin\psi(\alpha\beta\beta\beta\alpha-\beta\alpha\beta\beta\alpha)\}$	$(B_2)_{-1/2}$
30′	$(1/\sqrt{2})\{-\sin\psi(\beta\beta\beta\alpha\alpha-\beta\beta\alpha\beta\alpha)+\cos\psi(\alpha\beta\beta\beta\alpha-\beta\alpha\beta\beta\alpha)\}$	
31′	$(1/\sqrt{2})\{\cos\gamma(\beta\beta\beta\alpha\beta-\beta\beta\alpha\beta\beta)+\sin\gamma(\beta\alpha\beta\beta\beta-\alpha\beta\beta\beta\beta)\}$	$(B_2)_{-3/2}$
32′	$(1/\sqrt{2})\{-\sin\gamma(\beta\beta\beta\alpha\beta-\beta\beta\alpha\beta\beta)+\cos\gamma(\beta\alpha\beta\beta\beta-\alpha\beta\beta\beta\beta)\}$	

TABLE IV

State		Energy
3′	$(A_1)_{3/2}$	$\nu_0(1-\sigma_A)+(1/2)\nu_0'(1-\sigma_x)+(1/4)(2J_{12}+J_{15}+J_{35})-A$
4′		$\nu_0(1-\sigma_A)+(1/2)\nu_0'(1-\sigma_x)+(1/4)(2J_{12}+J_{15}+J_{35})+A$
5′	$(A_1)_{1/2}$	$\nu_0(1-\sigma_A)-(1/2)\nu_0'(1-\sigma_x)+(1/4)(2J_{12}-J_{15}-J_{35})-B$
6′		$\nu_0(1-\sigma_A)-(1/2)\nu_0'(1-\sigma_x)+(1/4)(2J_{12}-J_{15}-J_{35})+B$
15′	$(A_1)_{-1/2}$	$\nu_0(-1+\sigma_A)+(1/2)\nu_0'(1-\sigma_x)+(1/4)(2J_{12}-J_{15}-J_{35})+A$
16′		$\nu_0(-1+\sigma_A)+(1/2)\nu_0'(1-\sigma_x)+(1/4)(2J_{12}-J_{15}-J_{35})-A$
18′	$(A_1)_{-3/2}$	$\nu_0(-1+\sigma_A)-(1/2)\nu_0'(1-\sigma_x)+(1/4)(2J_{12}+J_{15}+J_{35})+B$
19′		$\nu_0(-1+\sigma_A)-(1/2)\nu_0'(1-\sigma_x)+(1/4)(2J_{12}+J_{15}+J_{35})-B$
21′	$(B_2)_{3/2}$	$\nu_0(1-\sigma_A)+(1/2)\nu_0'(1-\sigma_x)+(1/4)(-2J_{12}+J_{15}+J_{35})-C$
22′		$\nu_0(1-\sigma_A)+(1/2)\nu_0'(1-\sigma_x)+(1/4)(-2J_{12}+J_{15}+J_{35})+C$
23′	$(B_2)_{1/2}$	$\nu_0(1-\sigma_A)-(1/2)\nu_0'(1-\sigma_x)+(1/4)(-2J_{12}-J_{15}-J_{35})-D$
24′		$\nu_0(1-\sigma_A)-(1/2)\nu_0'(1-\sigma_x)+(1/4)(-2J_{12}-J_{15}-J_{35})+D$
29′	$(B_2)_{-1/2}$	$\nu_0(-1+\sigma_A)+(1/2)\nu_0'(1-\sigma_x)+(1/4)(-2J_{12}-J_{15}-J_{35})+C$
30′		$\nu_0(-1+\sigma_A)+(1/2)\nu_0'(1-\sigma_x)+(1/4)(-2J_{12}-J_{15}-J_{35})-C$
31′	$(B_2)_{-3/2}$	$\nu_0(-1+\sigma_A)-(1/2)\nu_0'(1-\sigma_x)+(1/4)(-2J_{12}+J_{15}+J_{35})+D$
32′		$\nu_0(-1+\sigma_A)-(1/2)\nu_0'(1-\sigma_x)+(1/4)(-2J_{12}+J_{15}+J_{35})-D$

TABLE V

Transitions and intensities of nucleus X

	Transition	Energy relative to $\nu_0'(1-\sigma_x)$	Relative intensity
1	$2\rightarrow 1$	$+J_{15}+J_{35}$	1
2	$5'\rightarrow 3'$	$+(1/2)(J_{15}+J_{35})-A+B$	$(\cos\theta\cos\phi+\sin\phi\sin\theta)^2$
3	$6'\rightarrow 4'$	$+(1/2)(J_{15}+J_{35})+A-B$	$(\cos\theta\cos\phi+\sin\phi\sin\theta)^2$
4	$18'\rightarrow 15'$	$-(1/2)(J_{15}+J_{35})+A-B$	$(\cos\theta\cos\phi+\sin\phi\sin\theta)^2$
5	$19'\rightarrow 16'$	$-(1/2)(J_{15}+J_{35})-A+B$	$(\cos\theta\cos\phi+\sin\phi\sin\theta)^2$
6	$20\rightarrow 17$	$-(J_{15}+J_{35})$	1
7	$23'\rightarrow 21'$	$+(1/2)(J_{15}+J_{35})-C+D$	$(\cos\gamma\cos\psi-\sin\gamma\sin\psi)^2$
8	$24'\rightarrow 22'$	$+(1/2)(J_{15}+J_{35})+C-D$	$(\cos\gamma\cos\psi-\sin\gamma\sin\psi)^2$
9	$27\rightarrow 15$	0	1
10	$28\rightarrow 26$	0	1
11	$31'\rightarrow 29'$	$-(1/2)(J_{15}+J_{35})+C-D$	$(\cos\gamma\cos\psi-\sin\gamma\sin\psi)^2$
12	$32'\rightarrow 30'$	$-(1/2)(J_{15}+J_{35})-C+D$	$(\cos\gamma\cos\psi-\sin\gamma\sin\psi)^2$

calculation in Table V and the definitions of A, B, C, D, and angles θ, ϕ, ψ, γ, it is clear

that the only conditions on them consistent with experiment are:

$$\begin{aligned} &A = B = (1/2)(J_{23}+J_{13}),\\ &C = D = (1/2)(J_{23}-J_{13}),\\ &\theta = \phi = \psi = -\gamma = 45°,\\ &J_{15} = J_{35} = \pm 7.4 \text{ c.p.s.} \end{aligned} \qquad [2]$$

TABLE VI

Transitions and intensities of A and A' nuclei

Transitions		Energy relative to $\nu_0(1-\sigma_A)$	Relative intensity
17	$4' \rightarrow 1$	$+(1/4)(2J_{13}+2J_{23}+J_{15}+J_{35})-A$	$2(1+\sin 2\theta)$
18	$17' \rightarrow 16'$	$+(1/4)(-2J_{13}-2J_{23}+J_{15}+J_{35})-A$	$2(1-\sin 2\theta)$
19	$20 \rightarrow 19'$	$+(1/4)(-2J_{13}-2J_{23}-J_{15}-J_{35})-B$	$2(1-\sin 2\phi)$
20	$6' \rightarrow 2$	$+(1/4)(2J_{13}+2J_{23}-J_{15}-J_{35})-B$	$2(1+\sin 2\phi)$
21	$25 \rightarrow 21'$	$+(1/4)(-2J_{13}+2J_{23}+J_{15}+J_{35})-C$	$1+\sin 2\psi$
22	$26 \rightarrow 21'$	$+(1/4)(+2J_{13}-2J_{23}+J_{15}+J_{35})-C$	$1-\sin 2\psi$
23	$27 \rightarrow 23'$	$+(1/4)(-2J_{13}+2J_{23}-J_{15}-J_{35})-D$	$1-\sin 2\gamma$
24	$28 \rightarrow 23'$	$+(1/4)(2J_{13}-2J_{23}-J_{15}-J_{35})-D$	$1+\sin 2\gamma$
25	$29' \rightarrow 26$	$+(1/4)(-2J_{13}+2J_{23}+J_{15}+J_{35})-C$	$1+\sin 2\psi$
26	$29' \rightarrow 25$	$+(1/4)(2J_{13}-2J_{23}+J_{15}+J_{35})-C$	$1-\sin 2\psi$
27	$31' \rightarrow 27$	$+(1/4)(2J_{13}-2J_{23}-J_{15}-J_{35})-D$	$1+\sin 2\gamma$
28	$31' \rightarrow 28$	$+(1/4)(-2J_{13}+2J_{23}-J_{15}-J_{35})-D$	$1-\sin 2\gamma$
29	$3' \rightarrow 1$	$+(1/4)(2J_{13}+2J_{23}+J_{15}+J_{35})+A$	$2(1-\sin 2\theta)$
30	$5' \rightarrow 2$	$+(1/4)(2J_{13}+2J_{23}-J_{15}-J_{35})+B$	$2(1-\sin 2\phi)$
31	$17' \rightarrow 15'$	$+(1/4)(-2J_{13}-2J_{23}+J_{15}+J_{35})+A$	$2(1+\sin 2\theta)$
32	$20 \rightarrow 18'$	$+(1/4)(-2J_{13}-2J_{23}-J_{15}-J_{35})+B$	$2(1+\sin 2\phi)$
33	$25 \rightarrow 22'$	$+(1/4)(-2J_{13}+2J_{23}+J_{15}+J_{35})+C$	$1-\sin 2\psi$
34	$26 \rightarrow 22'$	$+(1/4)(+2J_{13}-2J_{23}+J_{15}+J_{35})+C$	$1+\sin 2\psi$
35	$27 \rightarrow 24'$	$+(1/4)(-2J_{13}+2J_{23}-J_{15}-J_{35})+D$	$1+\sin 2\gamma$
36	$28 \rightarrow 24'$	$+(1/4)(2J_{13}-2J_{23}-J_{15}-J_{35})+D$	$1-\sin 2\gamma$
37	$30' \rightarrow 25$	$+(1/4)(2J_{13}-2J_{23}+J_{15}+J_{35})+C$	$1+\sin 2\psi$
38	$30' \rightarrow 26$	$+(1/4)(-2J_{13}+2J_{23}+J_{15}+J_{35})+C$	$1-\sin 2\psi$
39	$32' \rightarrow 28$	$+(1/4)(-2J_{13}+2J_{32}-J_{15}-J_{35})+D$	$1+\sin 2\gamma$
40	$32' \rightarrow 27$	$+(1/4)(2J_{13}-2J_{23}-J_{15}-J_{35})+D$	$1-\sin 2\gamma$

A possible assignment is shown in Fig. 1. The four transitions involving the F^{19} nucleus which have not yet been calculated will have relative intensities of one and zero energies relative to $\nu_0'(1-\sigma_x)$ for consistency. This remains to be shown.

(*b*) *Proton Resonance Spectrum*

Of the 24 transitions in Table VI, 12 are of nonzero intensity under the conditions [2]. It is to be noted that these have energies $\pm(1/4)(J_{15}+J_{35})$ relative to $\nu_0(1-\sigma_A)$.

In order to calculate energies and intensities for the other 24 proton lines and the 4 flourine lines, the two 4×4 determinants must be solved. This is usually done numerically and would involve an assumption as to the values of J_{23}, J_{13}, and J_{12}. However, a solution in analytical form can be achieved in this case on the assumption that $J_{13} \leqslant 0.5$ c.p.s. and that J_{13} can therefore be neglected. This assumption is in accord with the same result obtained in a variety of other aromatic compounds. Orthogonal matrices can then be found which will diagonalize the two 4×4 matrices. The energies and corresponding eigenfunctions found in this way are given in Table VII. In Table VII quantities a, b, c, d, are related to experimental parameters by:

$$\begin{aligned} a &= J_{12}(-J_{23}+K)^{-1}, \qquad & b &= J_{23}(-J_{12}+K)^{-1};\\ c &= J_{12}(J_{23}+K)^{-1}, \qquad & d &= J_{23}(J_{12}+K)^{-1}; \end{aligned}$$

with

$$K = (J_{12}^2+J_{23}^2-J_{12}J_{23})^{\frac{1}{2}}.$$

Remembering that $\sin 2\phi = \sin 2\theta = 1$ and noting that $(1-c-d) = (1-ac-bd) = 0$, the only transitions with nonzero intensity involving these eight states are given in Table VIII. None of these depend on J_{12}. Counting of intensities in Tables V–VIII shows that the distribution and intensity of the predicted lines tallies with experiment. The predicted spectrum depends explicitly on the assumption that $J_o^{HF} = J_m^{HF}$.

TABLE VII

Energies and eigenfunctions for states 7′–14′

	Eigenfunction	Energy
7′	$(1+c^2+d^2)^{-1/2}[\psi_7-c\psi_8-(d/\sqrt{2})\psi_9-(d/\sqrt{2})\psi_{10}]$	$(1/2)\nu_0'(1-\sigma_x)+(1/2)(-J_{12}-J_{23})-K$
8′	$(1+a^2+b^2)^{-1/2}[\psi_7+a\psi_8+(b/\sqrt{2})\psi_9+(b/\sqrt{2})\psi_{10}]$	$(1/2)\nu_0'(1-\sigma_x)+(1/2)(-J_{12}-J_{23})+K$
9′	$(1/\sqrt{3})(\psi_7+\psi_8)+(1/\sqrt{6})(\psi_9+\psi_{10})$	$(1/2)\nu_0'(1-\sigma_x)+(1/2)(J_{12}+J_{23})$
10′	$(1/\sqrt{2})(\psi_9-\psi_{10})$	$(1/2)\nu_0'(1-\sigma_x)+(1/2)(J_{12}-J_{23})$
11′	$(1+c^2+d^2)^{-1/2}[\psi_{11}-c\psi_{12}-(d/\sqrt{2})\psi_{13}-(d/\sqrt{2})\psi_{14}]$	$(1/2)\nu_0'(-1+\sigma_x)+(1/2)(-J_{12}-J_{23})-K$
12′	$(1+a^2+b^2)^{-1/2}[\psi_{11}+a\psi_{12}+(b/\sqrt{2})\psi_{13}+(b/\sqrt{2})\psi_{14}]$	$(1/2)\nu_0'(-1+\sigma_x)+(1/2)(-J_{12}-J_{23})+K$
13′	$(1/\sqrt{3})(\psi_{11}+\psi_{12})+(1/\sqrt{6})(\psi_{13}+\psi_{14})$	$(1/2)\nu_0'(-1+\sigma_x)+(1/2)(J_{12}+J_{23})$
14′	$(1/\sqrt{2})(\psi_{13}-\psi_{14})$	$(1/2)\nu_0'(-1+\sigma_x)+(1/2)(J_{12}-J_{23})$

TABLE VIII

Transitions involving states 7′–14′

Transition	Energy	Relative intensity
10′→3′	$\nu_0(1-\sigma_A)+(1/4)(2J_{23}+J_{15}+J_{35})-A$	$1+\sin 2\theta$
9′→4′	$\nu_0(1-\sigma_A)+(1/4)(-2J_{23}+J_{15}+J_{35})+A$	$3(1+\sin 2\theta)$
14′→5′	$\nu_0(1-\sigma_A)+(1/4)(2J_{23}-J_{15}-J_{35})-B$	$1+\sin 2\phi$
13′→6′	$\nu_0(1-\sigma_A)+(1/4)(-2J_{23}-J_{15}-J_{35})+B$	$3(1+\sin 2\phi)$
15′→9′	$\nu_0(1-\sigma_A)+(1/4)(2J_{23}+J_{15}+J_{35})-A$	$3(1+\sin 2\theta)$
16′→10′	$\nu_0(1-\sigma_A)+(1/4)(-2J_{23}+J_{15}+J_{35})+A$	$1+\sin 2\theta$
18′→13′	$\nu_0(1-\sigma_A)+(1/4)(2J_{23}-J_{15}-J_{35})-B$	$3(1+\sin 2\phi)$
19′→14′	$\nu_0(1-\sigma_A)+(1/4)(-2J_{23}-J_{15}-J_{35})+B$	$1+\sin 2\phi$
14′→10′	$\nu_0'(1-\sigma_x)$	1
13′→10′	$\nu_0'(1-\sigma_x)$	1
12′→8′	$\nu_0'(1-\sigma_x)$	1
11′→7′	$\nu_0'(1-\sigma_x)$	1

ACKNOWLEDGMENTS

I should like to thank Dr. R. E. Richards for the use of his spectrometer and Dr. J. Leane for the measurement of the spectra shown in Fig. 1.

REFERENCES

1. BERNSTEIN, H. J., POPLE, J. A., and SCHNEIDER, W. G. Can. J. Chem. **35**, 65 (1957).
2. RICHARDS, R. E. and SCHAEFER, T. J. Molecular Phys. **1**, 331 (1958).
3. BAKER, E. B. J. Chem. Phys. **23**, 984 (1955).
4. GUTOWSKY, H. S., HOLM, C. H., SAIKA, A., and WILLIAMS, G. A. J. Am. Chem. Soc. **79**, 4596 (1957).
5. ROUX, D. Helv. Phys. Acta, **31**, 511 (1958).
6. LEANE, J., RICHARDS, R. E., and SCHAEFER, T. J. Sci. Instr. (In press).
7. RICHARDS, R. E. and SCHAEFER, T. Trans. Faraday Soc. **54**, 1447 (1958).
8. RICHARDS, R. E. and SCHAEFER, T. Proc. Roy. Soc. A, **246**, 429 (1958).

NOTE ADDED IN PROOF: Under highest resolution the high field line of the CH_3 doublet can be resolved further, with splittings of about 0.2 c.p.s. The CH_3 protons appear to be coupled to the ring protons ortho to the CH_3 group. This effect is under investigation and the interpretation is not obvious. The conclusions arrived at above still hold.

THE LIMITING CONDUCTANCE OF AQUEOUS SOLUTIONS OF POTASSIUM IODATE, POTASSIUM CHLORATE, AND SILVER NITRATE AT 35.00° C[1]

E. Bock and A. N. Campbell

ABSTRACT

Measurements have been made of the equivalent conductances of aqueous solutions of potassium iodate, potassium chlorate, and silver nitrate at 35.00° C at concentrations ranging from 0.8×10^{-4} to 16×10^{-4} *N*. From these, the limiting equivalent conductances and association constants *A* as obtained by the use of the Fuoss–Shedlovsky extrapolation procedure were found to be at 35.0° C:

$\Lambda_0KIO_3 = 138.62$ mhos, $A = 0.8$ l.,
$\Lambda_0KClO_3 = 165.70$ mhos, $A = 0.5$ l.,
$\Lambda_0AgNO_3 = 161.53$ mhos, $A = 0.9$ l.

INTRODUCTION

The fact that aqueous solutions of some salts, especially salts of the oxyacids, behave as moderately strong electrolytes has long been recognized. Several attempts have been made to calculate the association constants of these electrolytes, from conductance data. The various suggested treatments of the experimental data differ from one another in the way in which the effect of ionic attraction on the equivalent conductance is calculated. Thus, in the method proposed by Davis (1), *K*, the dissociation constant, is obtained through the use of a modified Ostwald dilution law, viz.,

$$K = \frac{\Lambda^2 f_\pm^2}{\Lambda'(\Lambda' - \Lambda)}. \qquad [1]$$

Here Λ is the experimentally determined equivalent conductance at concentration *c*, Λ' the conductance of one equivalent of free ions, calculated by means of an empirical equation, and *f* the mean activity coefficient of the electrolyte, usually obtained by means of the Debye–Hückel relationship or modification thereof.

Another treatment, that adopted in the present paper, was suggested by Fuoss and Shedlovsky (2). These authors use a slightly modified Onsager equation in which resistance instead of conductance is considered in its derivation, in combination with the law of mass action. The association constant as well as the limiting equivalent conductance is obtained from a plot of ΛS vs. $c(\Lambda^2 S^2 f_\pm^2)$ where

$$\Lambda S = \Lambda_0 - [c(\Lambda^2 S^2 f_\pm^2)/K\Lambda_0]. \qquad [2]$$

Here Λ, Λ_0, *c*, and $f_\pm$ have their usual meaning. *S* is the Shedlovsky (2) function and *K* is the dissociation constant.

In the present paper Λ_0 and *A* for the three electrolytes were determined through the use of eq. [2]; the activity coefficient in each case was calculated from the Debye–Hückel approximation

$$\log_{10} f_\pm = -0.5190\sqrt{(\theta c)} \qquad [3]$$

where $\theta = S(\Lambda/\Lambda_0)$ is the degree of dissociation.

[1]*Manuscript received January 26, 1959.*
Contribution from the Chemistry Department of the University of Manitoba, Winnipeg, Manitoba.

EXPERIMENTAL

The experimental technique has been described elsewhere (3). Potassium iodate and potassium chlorate, both Fisher certified reagents of the highest purity, whose total impurities—mostly ionic in nature—were less than 0.01%, were dried carefully at 150° C and stored over phosphorus pentoxide. The silver nitrate, also a high quality Fisher certified reagent, was fused in darkness and also stored over phosphorus pentoxide.

EXPERIMENTAL RESULTS

Our results are contained in Tables I, II, and III given below.

DISCUSSION

Potassium Iodate

When the results for potassium iodate given in Table I are plotted in the form Λ

TABLE I

Equivalent conductance of potassium iodate at 35.00° C

Concentration in moles/liter $\times 10^4$	Equivalent conductance in mhos
1.3035	137.397
2.1329	137.040
2.4340	136.948
3.6615	136.584
4.0939	136.431*
5.1986	136.194*
5.6073	136.061
6.6614	135.838
7.1539	135.717
8.3134	135.519
8.7871	135.398
9.9599	135.212
10.425	135.121
11.605	134.944
12.169	134.858
13.342	134.680
16.235	134.282

*These points were not included in the least square calculation since their deviation from the mean is greater than three times the mean deviation.

versus $\sqrt{c}$ the usual straight line plot is obtained. When the best straight line (derived by the method of least squares) is drawn and extrapolated to zero concentration Λ_0 results as 138.62_2 mhos and the slope of the line has a value of -108.03. The Onsager tangent on the other hand has the value -107.43. Thus, to use the language of Fuoss (4), the phoreogram is catabatic to the latter, indicating ion association. When the conductance results are plotted, using eq. [2], a straight line plot again results which on extrapolation yields $\Lambda_0 = 138.61_7$ mhos. The mean deviation from the line, again obtained by the method of least squares as were all subsequent lines, is less than 0.01 of a ΛS unit. The difference between the two Λ_0's is within the experimental error, which is estimated to be 0.01% to 0.02%. This agreement is not surprising since as $c \rightarrow 0$, $S \rightarrow 1$ and $\Lambda \rightarrow \Lambda_0$, so that the intercepts should be identical. Taking the value for the limiting conductance for the potassium ion to be 88.21 mhos (5) the limiting conductance of the iodate ion follows as 50.41 mhos. The association constant as obtained from the slope of the graph of eq. [2] is equal to 0.8 l. It should be pointed out, however, that this association constant is forced to carry all the inadequacy or approximations of eq. [2]. A more realistic association constant and perhaps a slightly better value for Λ_0 would have been obtained

if the recently proposed treatment of conductance data, derived by Fuoss (6) and based on the latest extension of the conductance equation by Fuoss and Onsager (7), had been employed, but this treatment requires, especially for moderately strong electrolytes whose association constant approaches unity, conductance data in low dielectric constant media, and these are at present lacking. The value of Λ_0 may be taken with confidence to be within 0.02% of its "true" value, but the association constant gives only the order of magnitude.

We greatly regret that in our recent paper (3) on the conductance of potassium iodate at 25° C we overlooked the work of Krieger and Kilpatrick (8), Monk (9), and Spiro (10) on the same subject. We did not encounter the difficulties in the dilute region of concentration experienced by Krieger and Kilpatrick and by Monk. Neither did we observe a scatter as noticed by the former workers nor did we find a change in slope of the curve ΛS vs. $c(\Lambda^2 S^2 f_\pm^2)$ with increase in dilution as reported by Monk, either at 25° C or at 35° C. The mean deviation of ΛS when plotted versus $c(\Lambda^2 S^2 f_\pm^2)$ from a straight line was found to be less than 0.01 of a ΛS unit. The dissociation constant for potassium iodate at 25° C calculated from our data results as 2.0 l.$^{-1}$, a value intermediate between those obtained by the above workers.

Potassium Chlorate and Silver Nitrate

The behavior of these electrolytes was found to be, in general, similar to that of potassium iodate. In both cases the limiting conductances, as obtained by the two

TABLE II

Equivalent conductance of potassium chlorate at 35.00° C

Concentration in moles/liter $\times 10^4$	Equivalent conductance in mhos
0.82043	164.497*
2.3006	163.840*
3.6084	163.355*
5.2357	162.882
6.3990	162.592
7.9999	162.242
9.5265	161.963
10.772	161.734
12.402	161.467
13.814	161.236
15.088	161.067
16.021	160.930

*See footnote of Table I.

extrapolation methods, agree to within the experimental error. Thus for potassium chlorate, Λ_0 derived from the Λ vs. $\sqrt{c}$ plot is 165.45_3 mhos whereas Λ_0 obtained by extrapolation of eq. [2] is 165.47 mhos. Similarly for silver nitrate, Λ_0 obtained by the former procedure, 161.55_3 mhos, is identical within the experimental error, with Λ_0 derived by employing the latter procedure, viz. 161.53_1 mhos. The association constants for potassium chlorate and silver nitrate were found to be 0.5 l. and 0.9 l. respectively. The phoreogram for potassium chlorate was found to be anabatic to the Onsager tangent. Yet the fact that A is equal to 0.5 would seem to indicate that potassium chlorate is associated. A similar behavior was noticed by Fuoss and Kraus (11) for sodium bromate. Moreover, if conductance values for potassium chloride (12), a salt usually taken to be completely dissociated in dilute aqueous solutions, are plotted using eq. [2] a very small A, in fact, one approaching zero, is obtained. Thus it seems that whenever

TABLE III

Equivalent conductance of silver nitrate at 35.00° C

Concentration in moles/liter $\times 10^4$	Equivalent conductance in mhos
0.84902	160.544*
1.1126	160.346
1.6349	160.148*
2.1291	159.856
2.6514	159.652*
3.1565	159.524
4.8132	159.029
4.8641	159.026
6.1714	158.708
6.4389	158.633
7.4173	158.419
9.1949	158.064
11.075	157.728
12.636	157.479
14.638	157.150

*See footnote of Table I.

eq. [2] yields a slope of reasonable magnitude one is justified in suspecting ion association. For silver nitrate the phoreogram was found to be catabatic to the Onsager tangent, indicating ion association unequivocally.

CONCLUSION

Since the graph obtained by plotting eq. [2] is much more sensitive to errors, especially in the ordinates, than is the graph obtained by plotting Λ vs. $\sqrt{c}$ it is suggested that the limiting equivalent conductance derived from the former be taken as being closer to its "true" value than that derived from the latter. Subtracting from the limiting conductance of potassium iodate and of potassium chlorate the limiting conductance of the potassium ion (viz. 88.2_1 mhos) and from that of silver nitrate the known value of the nitrate ion (13) (viz. 85.48 mhos) there result the following individual limiting ionic conductances at 35.00° C:

$$\lambda_0 IO_3^- = 50.41 \text{ mhos}$$
$$\lambda_0 ClO_3^- = 77.50 \text{ mhos}$$
$$\lambda_0 Ag^+ = 76.05 \text{ mhos.}$$

ACKNOWLEDGMENT

One of us (E.B.) is indebted to the National Research Council of Canada for the award of a student summer research grant.

REFERENCES

1. DAVIS, C. W. Trans. Faraday Soc. **23**, 351 (1927). ROBINSON, R. A. and DAVIS, C. W. J. Chem. Soc. 574 (1937).
2. FUOSS, R. M. and SHEDLOVSKY, T. J. Am. Chem. Soc. **71**, 1496 (1949).
3. CAMPBELL, A. N. and BOCK, E. Can. J. Chem. **36**, 1277 (1958).
4. FUOSS, R. M. J. Chem. Educ. **32**, 527 (1955).
5. GORDON, A. R. and BENSON, G. C. J. Chem. Phys. **13**, 473 (1945).
6. FUOSS, R. M. J. Am. Chem. Soc. **79**, 3301 (1957).
7. FUOSS, R. M. and ONSAGER, L. J. Phys. Chem. **61**, 668 (1957).
8. KRIEGER, K. A. and KILPATRICK, M. J. Am. Chem. Soc. **64**, 7 (1942).
9. MONK, C. B. J. Am. Chem. Soc. **70**, 3281 (1948).
10. SPIRO, M. J. Phys. Chem. **60**, 976, 1673 (1956).
11. FUOSS, R. M. and KRAUS, C. A. J. Am. Chem. Soc. **79**, 3304 (1957).
12. SHEDLOVSKY, T. J. Am. Chem. Soc. **54**, 1411 (1932).
13. CAMPBELL, A. N. and BOCK, E. Can. J. Chem. **36**, 330 (1958).

THE CONSTITUTION OF A HEMICELLULOSE FROM SUGAR MAPLE (ACER SACCHARUM)[1]

T. E. TIMELL

ABSTRACT

Partial hydrolysis of the main hemicellulose constituent of sugar maple (*Acer saccharum*) has yielded D-xylose, D-galacturonic acid, 4-*O*-methyl-D-glucuronic acid, and 2-*O*-(4-*O*-methyl-α-D-glucosyluronic acid)-D-xylose. Hydrolysis of the fully methylated polysaccharide gave a mixture of 2-*O*- and 3-*O*-methyl-D-xylose, 2,3-di-*O*-methyl-D-xylose, 2,3,4-tri-*O*-methyl-D-xylose, and 2-*O*-(2,3,4-tri-*O*-methyl-α-D-glucosyluronic acid)-3-*O*-methyl-D-xylose in a mole ratio of 3:111:1:12. The number-average degrees of polymerization of the native and the methylated polysaccharide were 205 and 149, respectively. These data indicate that the hemicellulose is composed of a linear chain of 1,4-linked β-D-xylose residues and that on the average every tenth residue of the chain carries a terminal 4-*O*-methyl-D-glucuronic acid residue attached through its C_2. The structure of the polysaccharide is similar to that of the main hemicellulose component of European beech, white birch, and yellow birch.

Sugar maple is an important hardwood species in the northeastern part of this continent. Ritter and co-workers (1, 2) have studied the general composition of various hemicellulose fractions from this wood and chromatographic evidence for the presence of 4-*O*-methyl glucuronic acid has been reported by Nelson and Schuerch (3). The structure of the same hemicellulose has been studied by Neubauer and Purves (4), who concluded that the polysaccharide was composed of a branched backbone of 1,4-linked xylose residues, some of which carried terminal *O*-methyl glucuronic acid residues. In a previous investigation (5) the molecular properties of a native cellulose from sugar maple were studied. The present paper is concerned with the constitution and properties of the main hemicellulose component of this species.

RESULTS AND DISCUSSION

The high pentosan content of the wood (18.5%) indicated that the preponderant hemicellulose was a xylan. When the wood was extracted with alkali, a hemicellulose was obtained in a yield of 12.4%, giving D-xylose and three uronic acid compounds on partial hydrolysis. The sugar acids were separated from the xylose on an anion exchange resin and the mixture obtained was resolved on a charcoal column to yield galacturonic acid, 4-*O*-methyl glucuronic acid, and an aldobiouronic acid. The hexuronic acids were identified chromatographically whereas the structure of the aldobiouronic acid was proved by the following experiments.

Reduction of the methyl glycoside methyl ester of the aldobiouronic acid followed by hydrolysis gave D-xylose and 4-*O*-methyl-D-glucose. When the neutral disaccharide was methylated to completion and hydrolyzed, 3,4-di-*O*-methyl-D-xylose and 2,3,4,6-tetra-*O*-methyl-D-glucose were obtained. This evidence, together with the specific rotation of the compound (+100°) (6), showed that the acid was 2-*O*-(4-*O*-methyl-α-D-glucosyluronic acid)-D-xylose.

Methanolysis of the fully methylated hemicellulose gave a mixture of glycosides which was saponified and resolved into an acidic and a neutral fraction on an exchange resin. The acid fraction contained only one compound, the ester glycoside of which was reduced with lithium aluminum hydride to yield a crystalline disaccharide, identified as methyl

[1]*Manuscript received January 20, 1959.*
Contribution from the Division of Industrial and Cellulose Chemistry, McGill University, and the Wood Chemistry Division, Pulp and Paper Research Institute of Canada, Montreal, Quebec.

Can. J. Chem. Vol. 37 (1959)

2-*O*-(2,3,4-tri-*O*-methyl-α-D-glucosyl)-3-*O*-methyl-D-xylopyranoside. Hydrolysis of this compound gave the expected 3-*O*-methyl-D-xylose and 2,3,4-tri-*O*-methyl-D-glucose.

The mixture of neutral glycosides was hydrolyzed and resolved by paper chromatography to yield a mixture of 2-*O*- and 3-*O*-methyl-D-xylose, which could be resolved by paper ionophoresis, 2,3-di-*O*-methyl-D-xylose and 2,3,4-tri-*O*-methyl-D-xylose. A quantitative estimation (7), together with the weight of the acidic fraction, indicated a molar ratio of 3:111:1:12 between the mono-, di-, and tri-*O*-methylated xyloses and the latter.

The large quantity of 2,3-di-*O*-methyl-D-xylose, together with the high negative rotation (−80°) of the hemicellulose as well as its consumption of periodate, indicated the presence of 1,4-linked β-D-xylose residues, while the 2,3,4-tri-*O*-methyl-D-xylose undoubtedly originated from the non-reducing end groups. Since no monouronic acids were formed during the methanolysis, the presence of the mono-*O*-methyl xyloses could be accounted for only by incomplete methylation, demethylation, or branching. The fact that their number exceeded that of the tri-*O*-methyl xylose made it certain that branching was not the only factor involved. When the molecular weight of the methylated hemicellulose was determined by osmometry, a value of 27,300 was obtained, corresponding to a number-average degree of polymerization of 149. This was a value somewhat higher than that indicated by the number of non-reducing end groups present (127) and showed that no branching was involved. The mono-*O*-methyl xyloses were therefore artifacts, probably caused by demethylation (8, 9).

The structure of the aldobiouronic acid indicated that the hemicellulose contained residues of 4-*O*-methyl-α-D-glucuronic acid linked by 1,2-glycosidic bonds to the anhydroxylose units. The fact that the 4-hydroxyl was unsubstituted in the xylose moiety of the partly methylated aldobiouronic acid obtained from the methylated hemicellulose, while a methoxyl group was present in this position in the corresponding, fully methylated acid, showed that the acid groups were linked *directly* to the xylan framework. The methoxyl and uronic anhydride content, the yield of aldobiouronic acid from the methylated polysaccharide, and the amount of periodate consumed on oxidation of the hemicellulose all indicated the presence of an average number of 10 xylose residues per acid side chain.

The number-average molecular weight of the acetate derivative of the hemicellulose was 49,300, corresponding to a degree of polymerization of 205. Values of 205 and 217 were obtained from viscosity measurements in cupriethylenediamine and dimethyl sulphoxide, respectively.

Summarizing the above evidence, a tentative structure can now be assigned to the 4-*O*-methyl glucuronoxylan present in sugar maple wood. This polysaccharide consists of a linear framework of approximately 200 1,4-linked β-D-xylose residues. Every tenth residue on the average is linked through its 2-position to a single side chain of 4-*O*-methyl-α-D-glucuronic acid. From recent evidence (10, 11) it appears probable that the polysaccharide contains acetyl groups in its native state and the possibility that at least a portion of it is linked to lignin cannot be excluded (12, 13).

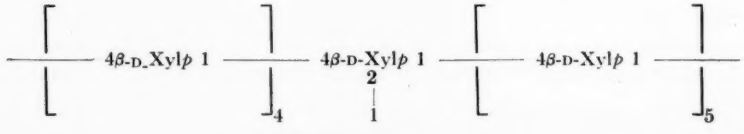

4-*O*-Me-α-D-G*p*A

The present polysaccharide is very similar to the 4-*O*-methyl glucuronoxylans previously isolated from the woods of European beech (14), white birch (15), and yellow birch (16) and it is also similar to the main hemicellulose components of Finnish birch (17) and white elm (18). The corresponding polysaccharide of American beech (19), on the other hand, has been claimed to possess a branched xylan backbone and that of trembling aspen (20) evidently contains terminal L-arabofuranose residues. The number-average molecular weight of the hemicellulose is approximately the same as that of other hardwood glucuronoxylans so far studied (21). It is not known, however, whether the alkali used in the extraction of the hemicellulose from the wood has any noticeable depolymerizing effect (22, 23), nor has the weight-average degree of polymerization been determined for any native, undegraded xylan.

EXPERIMENTAL

General experimental conditions were the same as described previously (24). Solvents (v/v) used for separating sugars on the paper chromatogram were (A) ethyl acetate – acetic acid – water (9:2:2), (B) butan-1-ol – pyridine – water (10:3:3), (C) butan-1-ol – ethanol – water (40:11:19), and (D) butan-2-one – water (89:11).

Composition of the Wood

Analyses according to standard methods (9, 15) indicated the following composition of the wood: pentosan (18.5), lignin (22.7), acetyl (2.9), ash (0.3), uronic anhydride (4.4), galactan (trace), glucan (51.7), mannan (2.3), araban (0.8), and xylan (14.8%).

Isolation of the Hemicellulose

Extractive-free wood meal from a sound, 25-year-old specimen of sugar maple* (500 g, 40–60 mesh) was exhaustively extracted by shaking with 24% (w/w) aqueous potassium hydroxide (3.5 liters) as described previously (15, 16, 24). The recovered product was dried from petroleum ether *in vacuo* to give 57 g (12.3%) of a white powder. Anal.: uronic anhydride, 12.05%; methoxyl, 2.09%; $[\alpha]_D^{20}$ −80° (*c*, 1.0 in 2.5% sodium hydroxide). Examination by paper chromatography (solvents A and B) of the hydrolyzate of the hemicellulose suggested the presence of xylose and three uronic acids, two of which corresponded chromatographically to galacturonic acid and 4-*O*-methyl glucuronic acid.

Isolation of the Aldobiouronic Acid

Wood meal (500 g) was treated with 72% sulphuric acid (100 ml) for 24 hours after which the solution was diluted to 2 liters and boiled under reflux for 10 hours. After neutralization with barium hydroxide, filtration through Celite, and evaporation, the solution was added to the top of a cocoanut charcoal column (7.5×25 cm) (25). Most of the neutral sugars were removed with water. Elution with 2% aqueous ethanol removed galacturonic acid and a portion of the 4-*O*-methyl glucuronic acid. Further elution with 4% and 10% ethanol yielded a chromatographically pure aldobiouronic acid (5 g). Anal. Calc. for $C_{12}H_{20}O_{11}$: OCH_3, 9.1; equiv. wt., 340. Found: OCH_3, 9.1; equiv. wt., 326; $[\alpha]_D^{20}$ +100° (*c*, 1.0 in water).

Identification of Hydrolysis Products from the Reduced Aldobiouronic Acid

The aldobiouronic acid (4 g) was boiled under reflux with 2.5% methanolic hydrogen chloride (150 ml) for 7 hours. After neutralization with silver carbonate and filtration through Celite and evaporation, the sirupy ester glycoside was reduced with lithium

**Kindly donated by Mr. Ken Murray, Fitch Bay, Quebec.*

aluminum hydride (4 g) (26) in dry tetrahydrofuran (100 ml) to yield a sirup (3.6 g). A portion of the reduced glycoside (1.2 g) was hydrolyzed with *N* sulphuric acid to give a sugar mixture (1.1 g) which was resolved on sheets of filter paper (solvent A) to yield D-xylose $[\alpha]_D^{20}$ +18° (*c*, 1.0 in water), and 4-*O*-methyl-D-glucose, $[\alpha]_D^{20}$ +58° (*c*, 1.0 in water). The xylose dibenzylidene dimethyl acetal (27) had m.p. and mixed m.p. 210° C and the 4-*O*-methyl-D-glucosazone had m.p. and mixed m.p. 157° C. The infrared spectrum of the latter was identical with that of an authentic specimen.

Methylation and Hydrolysis of the Ester Glycoside of the Aldobiouronic Acid

The ester glycoside of the aldobiouronic acid (2.0 g) was dissolved in dry dimethyl formamide (100 ml) and shaken in the dark with methyl iodide (10 ml) and silver oxide (10 g) (28). The product was recovered as described by Kuhn (28). After addition of chloroform to the reaction mixture, silver salts were removed by filtration. Extraction with aqueous potassium cyanide followed by three extractions with water gave a chloroform solution which was dried with anhydrous sodium sulphate and evaporated to dryness to yield a yellow sirup. Anal. Calc. for $C_{18}H_{34}O_{10}$: OCH_3, 52.8%. Found: OCH_3, 51.0%. The ester glycoside was reduced with lithium aluminum hydride to yield a sugar mixture which was resolved by paper chromatography (solvent C) to give two compounds, chromatographically indistinguishable from a di-*O*-methyl xylose (110 mg) and a tetra-*O*-methyl glucose (130 mg).

Identification of 3,4-Di-O-methyl-D-xylose and 2,3,4,6-Tetra-O-methyl-D-glucose

The di-*O*-methyl xylose, $[\alpha]_D^{20}$ +15° (*c*, 1.0 in water), gave a crystalline 3,4-di-*O*-methyl-*N*-phenyl-D-xylosylamine, m.p. 115° C (29). The tetra-*O*-methyl glucose, $[\alpha]_D^{20}$ +83° (*c*, 3.1 in water), crystallized, melting point and mixed melting point after three recrystallizations from petroleum ether 88–90° C. Anal. Calc. for $C_{10}H_{20}O_6$: OCH_3, 52.7%. Found: OCH_3, 50.0%. The 2,3,4,6-tetra-*O*-methyl-*N*-phenyl-D-glucosylamine had m.p. and mixed m.p. 135–136° C.

Methylation of the Hemicellulose

The hemicellulose (20 g) was dissolved in 40% (w/w) aqueous sodium hydroxide (300 ml) in an atmosphere of nitrogen, after which dimethyl sulphate (200 ml) was added dropwise at 0° C over a period of 8 hours. This treatment was repeated six times at room temperature. The recovered product was dissolved in tetrahydrofuran (2 liters) and powdered sodium hydroxide (200 g) and dimethyl sulphate (300 ml) were added (30). This treatment was repeated twice. The solvent was removed by distillation, and the remainder was washed with water and dissolved in chloroform. The solution was dried and poured into petroleum ether to yield a white, fluffy product (22 g). Anal. Calc. for the fully methylated sodium salt of the hemicellulose: OCH_3, 37.3%. Found: OCH_3, 37.8%. The infrared spectrum indicated the absence of hydroxyl groups.

Hydrolysis and Separation of Acidic and Neutral Sugars

Methylated hemicellulose (10 g) was treated with methanolic hydrogen chloride and the mixture of glycosides (10.8 g) was de-esterified with barium hydroxide (31). The mixture obtained was resolved on a column of Dowex 1-X4 anion exchange resin (acetate form) to yield a mixture of neutral sugars (7.8 g) and an acidic compound (1.7 g).

Identification of Methyl 2-O-(2,3,4-Tri-O-methyl-α-D-glucosyl)-3-O-methyl-α,β-D-xylopyranoside

The above acid compound was converted to its methyl ester methyl glycoside which was reduced with lithium aluminum hydride. The colorless sirup obtained crystallized

immediately, m.p. and mixed m.p. 167–168° C after recrystallization from ethyl acetate. Anal. Calc. for $C_{16}H_{30}O_{10}$: OCH_3, 40.6%. Found: OCH_3, 40.4%; $[\alpha]_D^{20}$ +93° (*c*, 1.0 in water). The infrared spectrum and the X-ray powder diagram were identical with those of an authentic (31) specimen of methyl 2-*O*-(2,3,4-tri-*O*-methyl-α-D-glucopyranosyl)-3-*O*-methyl-α,β-D-xylopyranoside.

A portion of the disaccharide (600 mg) was hydrolyzed to yield a mixture of methylated sugars which was resolved on the paper chromatogram (solvent D), giving two compounds chromatographically identical with a mono-*O*-methyl xylose and a tri-*O*-methyl glucose. 3-*O*-Methyl-D-xylose, $[\alpha]_D^{20}$ +15° (*c*, 1.0 in water) gave a crystalline aniline derivative, m.p. 134°. The 2,3,4-tri-*O*-methyl-D-glucose had $[\alpha]_D^{20}$ +78° (*c*, 1.0 in water) and aniline derivative with m.p. and mixed m.p. 143°.

Separation and Identification of the Neutral Components

The mixture of neutral glycosides was hydrolyzed and resolved by paper chromatography (solvent D) to yield three fractions. One was a mixture of 2-*O*- and 3-*O*-methyl-D-xylose, resolvable by paper ionophoresis in a borate buffer (32). The main fraction consisted of 2,3-di-*O*-methyl-D-xylose, $[\alpha]_D^{20}$ +25° (*c*, 3.0 in water). Anal. Calc. for $C_7H_{14}O_5$: OCH_3, 34.9%. Found: OCH_3, 35.0%. The 2,3-di-*O*-methyl-*N*-phenyl-D-xylopyranosylamine had m.p. 126–127° C. The last fraction, 2,3,4-tri-*O*-methyl-D-xylose could not be induced to crystallize. Anal. Calc. for $C_8H_{16}O_5$: OCH_3, 48.4%. Found: OCH_3, 47.2%. The infrared spectrum of the sirupy aniline derivative was indistinguishable from that of an authentic specimen.

Quantitative Analysis of the Neutral Components

A small portion of the mixture of neutral sugars was resolved on the paper chromatogram with solvent mixture C. Each paper strip was eluted with water and the concentration of the sugar was determined by the *o*-aminodiphenyl method (7). The average value of three determinations was used. With solvent system D high paper blanks were obtained.

Periodate Oxidation of the Hemicellulose

Periodate oxidations were carried out in the dark with 0.05 *M* solutions of both trisodium paraperiodate and sodium metaperiodate. The amount of periodate consumed, as determined by the arsenite method, was extrapolated to zero time, giving in both cases a consumption of 10.5 mole of oxidant per repeating unit.

Acetylation of the Hemicellulose

Acetylation of the hemicellulose was carried out as described previously (24) essentially according to the method of Carson and Maclay (33). Two acetylations gave a product soluble in chloroform–ethanol (9:1 v/v). Anal. Calc. for the fully acetylated hemicellulose: acetyl, 37.8%. Found: acetyl, 38.3%.

Determination of Molecular Weights

The molecular weights of the original hemicellulose and of its methyl derivative were carried out by osmotic pressure measurements as described elsewhere (24, 34). The results obtained are presented in Table I. Degrees of polymerization were calculated as shown earlier (15).

Estimation of the Intrinsic Viscosity of the Hemicellulose

Intrinsic viscosities were determined with a Craig–Henderson (35) viscometer in *M* cupriethylenediamine and in anhydrous dimethyl sulphoxide as described elsewhere

(34). The relationship $\bar{P}_n = K[\eta]$, where $[\eta]$ was the intrinsic viscosity and K was 212 and 346, respectively, was used for estimating the degree of polymerization ($\bar{P}_n$).

TABLE I

Osmometry data

Hemicellulose			Methylated hemicellulose		
w*	h†	h/w	w	h	h/w
3.469	1.905	0.549	3.500	3.996	1.142
2.948	1.586	0.538	3.108	3.423	1.102
2.568	1.394	0.543	2.695	2.854	1.059
2.304	1.282	0.556	2.077	2.127	1.024
1.612	0.892	0.553	1.768	1.810	1.024
1.522	0.784	0.515	1.324	1.323	0.999
0	—	0.52	0	—	0.94

*Concentration in g/kg solution (chloroform–ethanol 9:1).
†Osmotic height in cm solvent.

ACKNOWLEDGMENTS

The author wishes to express his gratitude to Mr. W. Steyn and Mr. D. Stoltzenburg for technical assistance.

REFERENCES

1. Mitchell, R. L. and Ritter, G. J. J. Am. Chem. Soc. **62**, 1958 (1940).
2. Mitchell, R. L., Rogers, S. C., and Ritter, G. J. Ind. Eng. Chem. **40**, 1528 (1948).
3. Nelson, R. and Schuerch, C. Tappi, **40**, 419 (1957).
4. Neubauer, L. G. and Purves, C. B. Can. J. Chem. **35**, 388 (1957).
5. Timell, T. E. Pulp Paper Mag. Can. **59** (No. 8), 139 (1958).
6. Gorin, P. A. J. and Perlin, A. S. Can. J. Chem. **36**, 999 (1958).
7. Timell, T. E., Glaudemans, C. P. J., and Currie, A. L. Anal. Chem. **28**, 1916 (1956).
8. Lindberg, B. Private communication.
9. Barth, F. W. and Timell, T. E. J. Am. Chem. Soc. **80**, 6320 (1958).
10. Hägglund, E., Lindberg, B., and MacPherson, J. Acta Chem. Scand. **10**, 1160 (1956).
11. Bouveng, H. and Lindberg, B. Acta Chem. Scand. **10**, 1283 (1956).
12. Lindgren, B. O. Acta Chem. Scand. **12**, 447 (1958).
13. Hayashi, A. and Tachi, I. Tappi, **41** (No. 9), 173 A (1958).
14. Aspinall, G. O., Hirst, E. L., and Mahomed, R. S. J. Chem. Soc. 1734 (1954).
15. Glaudemans, C. P. J. and Timell, T. E. J. Am. Chem. Soc. **80**, 941, 1209 (1958).
16. Timell, T. E. To be published.
17. Saarnio, J., Wathen, K., and Gustafsson, Ch. Acta Chem. Scand. **8**, 825 (1954).
18. Gillham, J. K. and Timell, T. E. Can. J. Chem. **36**, 1467 (1958).
19. Adams, G. A. Can. J. Chem. **35**, 556 (1957).
20. Jones, J. K. N., Merler, E., and Wise, L. E. Can. J. Chem. **35**, 634 (1957).
21. Timell, T. E., Glaudemans, C. P. J., and Gillham, J. K. Pulp Paper Mag. Can. **59** (No. 10), 242 (1958).
22. Whistler, R. L. and Corbett, W. M. J. Am. Chem. Soc. **78**, 1003 (1956).
23. Aspinall, G. O., Carter, M. E., and Los, M. J. Chem. Soc. 4807 (1956).
24. Currie, A. L. and Timell, T. E. Can. J. Chem. **37**, 922 (1959).
25. Barth, F. W. and Timell, T. E. Can. J. Chem. **36**, 1321 (1958).
26. Smith, F. J. Chem. Soc. 2646 (1951).
27. Breddy, L. J. and Jones, J. K. N. J. Chem. Soc. 738 (1945).
28. Kuhn, R., Trischmann, H., and Löw, I. Angew. Chem. **67**, 32 (1955).
29. Jones, J. K. N. and Wise, L. E. J. Chem. Soc. 3389 (1952).
30. Falconer, E. L. and Adams, G. A. Can. J. Chem. **34**, 338 (1956).
31. Dutton, G. G. S. and Smith, F. J. Am. Chem. Soc. **78**, 3744 (1956).
32. Foster, A. B. Advances in Carbohydrate Chem. **12**, 81 (1957).
33. Carson, J. F. and Maclay, W. D. J. Am. Chem. Soc. **68**, 1015 (1946).
34. Glaudemans, C. P. J. and Timell, T. E. Svensk Papperstidn. **61**, 1 (1958).
35. Craig, A. W. and Henderson, D. A. J. Polymer Sci. **19**, 215 (1956).

ISOTHERMS OF BROMINE ON GRAPHITE[1]

J. G. HOOLEY

ABSTRACT

The isotherms of bromine on eight carbon blacks and on natural graphite have been related to the known structures of these materials. The surface areas can be calculated from the adsorption isotherms and the size of the graphite crystals can be estimated from the extent of hysteresis on desorption. The isosteric heats of adsorption on the surface and between the layers are each 11 kcal mole^{-1}. The formation of residue compounds displaces the isotherms equally at all pressures.

INTRODUCTION

The isotherm of bromine on a natural graphite at 28.8° C has been determined by Reyerson (6) along with the changes in magnetic susceptibility that occur during the process. The purpose of the present work was to study the isotherm at various temperatures and to include carbon blacks of various areas and crystal sizes. A recording vacuum thermobalance (3) and spoon gauge (4) were specially designed for such measurements with bromine and other corrosive vapors.

MATERIALS

1. Carbon black.—G. Cabot Inc., of Boston, donated samples from three sources, each heat-treated to two or three different temperatures. The data supplied with them included an estimate from X-ray data of the average thickness L_c and width L_a of the volumes in which the carbon atoms had the graphite structure. The area of the aggregates of these crystals per gram as calculated from electron microscope data and from B.E.T. adsorption data for N_2 was also given. The effect of heat-treatment on these properties is described elsewhere (7).

2. Graphite.—Natural crystals about 2 mm across were obtained through G. Cabot Inc. from a deposit near Willsboro, N.Y.

3. Bromine.—Analytical material was doubly distilled.

PROCEDURE

A 0.5- to 1-gram sample was weighed, suspended in the balance, evacuated to 0.001 cm, and thermostated to the desired temperature. The positions of the weight- and pressure-measuring transformers were then adjusted and the primary voltage to be applied to each was selected to give suitable sensitivities—all as described in refs. 3 and 4. When the recorded weight had settled down to a constant value, bromine was admitted at any desired pressure up to the saturation value. The pressure and the sample weight were then followed as a function of time by application of the known conversion factors to the millivolt records. At any time the bromine pressure could be increased by opening the tap to the reservoir or decreased by opening the tap to a liquid nitrogen trap at 0.001 cm. Leaving this latter tap open is referred to as reducing the pressure to zero.

For all runs a weight sensitivity of 3.4 mv mg^{-1} and a pressure sensitivity of 3.6 mv mm^{-1} was used. With no sample on the balance pan, any variation in the weight record was less than 0.2 mv over a period of several days. With a sample at 0.001 cm the record was equally constant after any initial loss of volatile material. The buoyancy correction

[1]*Manuscript received January 26, 1959.*
Contribution from the Department of Chemistry, University of British Columbia, with financial assistance from the National Research Council of Canada.

for the spring-pan system was found to be 0.33 mg per cm of mercury of bromine vapor with the reactor tube at 80° C or 25° C. No buoyancy correction was applied to the sample itself because its maximum value would be equivalent to only 0.1 atoms of bromine per 1000 carbon atoms. Adsorption and desorption isotherms were determined at temperatures from 0° C to 80° C. The uptake was plotted as gram atoms of bromine per 1000 g-atoms of carbon and will be referred to as the number of bromine atoms.

RESULTS

The following aspects of the isotherms are related where possible to other known properties of the adsorbent.

1. Hysteresis

(*a*) *Natural Graphite, Untreated*

This material showed rapid, reversible but only relatively slight bromine adsorption below a critical pressure dependent on temperature. Thus at 25° C less than 0.5 atoms of bromine (per 1000 carbon atoms) were adsorbed below 1 cm pressure. The critical pressures at 50°, 60°, and 80° C were 6 cm, 12 cm, and above 18 cm, respectively. Above these critical pressures bromine was very slowly adsorbed to a maximum value which increased with the pressure and with the reciprocal of temperature. Then on reducing the pressure, bromine slowly left the material until at zero pressure an amount remained that was independent of time and of temperatures up to 120° C. This is the residue compound studied by Hennig (2). When the cycles were repeated with a single sample of the residue compound obtained by debromination from 15 cm at 25° C the points in Fig. 1 were obtained. Below the critical pressure at a given temperature, less than 0.5 additional bromine atoms were adsorbed and above this pressure a slow adsorption occurred, followed by a hysteresis loop on desorption. The residue composition after each cycle was the same value of 30 bromine atoms. The two loops at 50° and 60° are reproducible in any order if sufficient time is allowed to establish equilibrium. This was as high as 24 hours for large amounts of bromine. For points that are critical in establishing the general shape of a loop, it was shown that no further change occurred in an additional 12 hours. The desorption side of the loop does not close at the critical pressure where adsorption started but continues on down to 2 cm or less before reaching the residue composition. There are five points in this region at 50° and 60° and their compositions were shown to be constant for 24 hours. The curves for 25° were not completed because of the great time required for the larger amounts of bromine adsorbed at this temperature.

(*b*) *Carbon Blacks*

These materials showed a rapid adsorption even at the lowest pressure used—0.03 cm. The subsequent isotherm showed hysteresis only if the pressure exceeded the critical value noted for natural graphite. Thus there was no hysteresis at 80° below at least 18 cm and none at 25° below 1 cm. Isotherms at three temperatures for Sterling M.T. 3100 are shown in Fig. 2. The equilibrium values involving hysteresis were reached in an hour or less, which is very rapid compared with the time required for natural graphite. Similar curves were obtained for other carbon blacks, although the amount of hysteresis varied. If the maximum vertical distance between adsorption and desorption curves at 25° C is taken as a measure of hysteresis then its value, listed in Table I, increases with crystal size. Unfortunately the data are insufficient to evaluate the relationship. All that can be said is that the defined hysteresis is proportional to a power of L_a between one and two.

Hysteresis was also observed when the temperature was changed at constant pressure. The compositions were simply those found on the adsorption and desorption curves for the particular pressure used. With natural graphite the change from one curve to another at constant pressure was extremely slow. Even after 24 hours the change from a 50° curve in Fig. 1 to a 60° curve had progressed only half way and was not followed any further because its rate had dropped to such a low value.

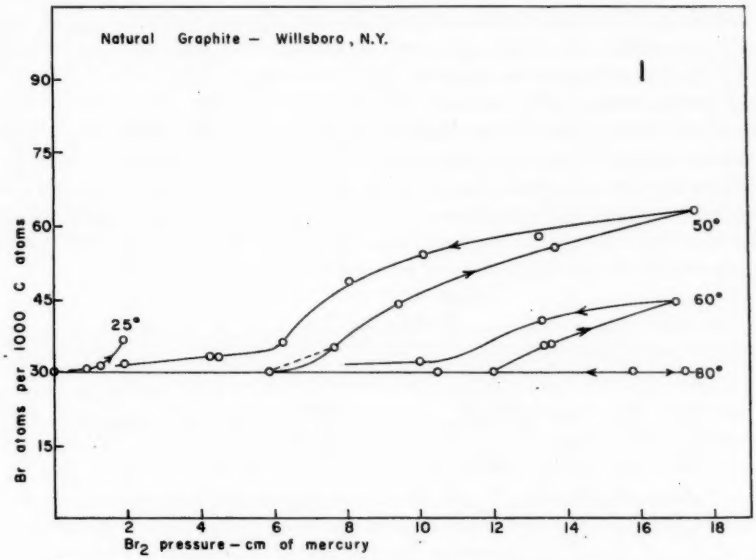

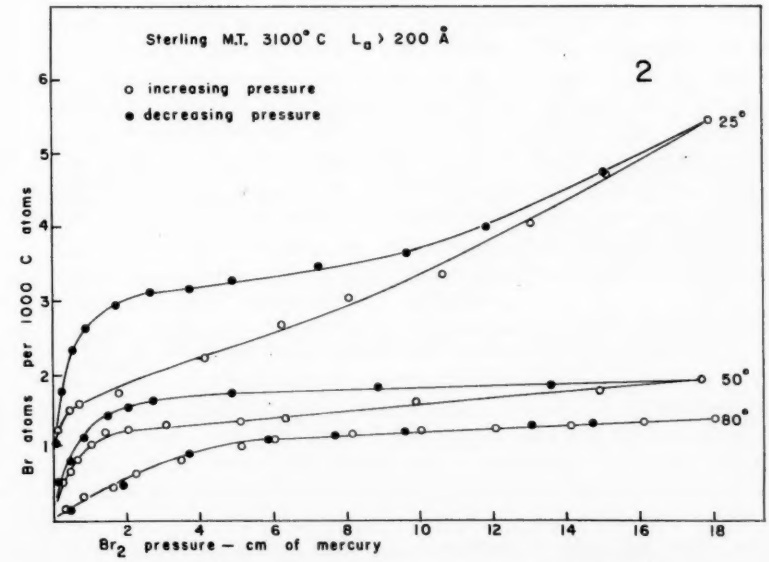

FIG. 1. Isotherms for a residue compound of natural graphite.
FIG. 2. Isotherms for Sterling M.T. 3100° C.

2. Residue Compounds

This refers to the bromine that is not removed to a liquid nitrogen trap in a system at 0.001 cm pressure. The time required to reach equilibrium varied up to 24 hours and the final composition was a function of the following conditions. For a given material it increased with the amount of bromine adsorbed before reducing the pressure to zero and with the time of exposure to bromine as reported by Hennig (2). The uptake after 24 hours was zero or very small. The source of carbon black and the temperature of heat-treatment before bromination are also factors. This is shown in Table I where the residue compositions are those obtained after 24 hours' exposure to bromine at 17 cm and 25° C. The values show that for a given source of carbon black the residual bromine content decreases as the temperature of heat-treatment increases.

The effect of the formation of these residue compounds on the isotherms was simply to displace them vertically by an amount equal to the residual bromine content. Any additional effect was not detected. As a result adsorption isotherms were only reproduced in case nothing was done to change the residue composition. In the subsequent use of the isotherms to determine area and isosteric heats only the amount of bromine adsorbed in excess of the residual amount was used in the calculations.

TABLE I

	L_a (Å)	L_c (Å)	Area, meter² g⁻¹ N_2	Area, meter² g⁻¹ Electron microscope	Area, meter² g⁻¹ Br_2	Hysteresis*	Isosteric heat (kcal mole⁻¹) Adsorption	Isosteric heat (kcal mole⁻¹) Desorption	Residual bromine*
Spheron 6 Original	23	13	114	105	124	<0.5	9.5±0.7		15
Spheron 6 1000° C	36	15	91		85	<0.5	10.1±0.9		7
Spheron 6 2700° C	79	48	84		75	0.5	11.2±0.2		0.4
Sterling F.T. Original	28	17	14.5	15.4	25	<0.2	11.2±0.7		8
Sterling F.T. 1500° C	62	39	12.9	16.2	13	0.2	11.2±0.4		0.3
Sterling F.T. 2700° C	132	88	12.5	16.6	12	0.7	8.7±1.4	10.8±0.9† 18.7±3.3‡	0.1
Sterling M.T. Original	34	15	6.6	5.7	6.5	<0.2	11.4±0.7		0.8
Sterling M.T. 3100° C	>200	>200	6.3		7.5	1.2	11.1±1.1	14.6±0.9† 18.8±3.2‡	0.5
Natural graphite							11.7±0.3	16±2‡	30

*Bromine atoms per 1000 carbon atoms.
†Below monolayer value.
‡Above monolayer value.

3. Area Calculations

The B.E.T. equation was applied to the carbon black isotherms at 80° by plotting $p\{\mathrm{Br}/\mathrm{C}(p_0-p)\}^{-1}$ against p/p_0 between partial pressures of 0.03 and 0.12. From the slope of this straight line the areas in Table I were calculated using 12.2 Å² as the average area covered per atom of bromine. Except for Sterling F.T. Original the values average (5±10)% higher than the areas from N_2 adsorption data and (10±20)% lower than the electron microscope areas. When similar calculations were made for adsorption isotherms below 80°, larger areas were obtained whenever the plot included pressures above the critical value. Thus the area of Sterling M.T. 3100° calculated from the 0° isotherm was 12.4 and from the 25° isotherm 7.9 meter² g⁻¹. The higher values are caused by lamellar adsorption, which will be shown later to occur only above the critical pressure.

4. Isosteric Heats

These were calculated from the adsorption isotherms at 25°, 50°, and 80°. The results are summarized in Table I, where each recorded value is the average for a range of Br/C values from 0.2 to 1.5 monolayers. For Spheron 6 2700° the linearity of the Arrhenius plot is excellent and the standard deviation of the calculated heats at various Br/C values is only 2%. This good behavior is a result of the relatively large surface area, negligible hysteresis, and low residue composition associated with the sample. These combine to make lamellar adsorption and errors in the weighing and in the residue composition less significant. The situation is somewhat less satisfactory for the other carbon blacks. There is, however, no detectable trend of the heat with Br/C content or with temperature. Only on desorption from the two largest crystals and natural graphite is a trend with Br/C content noticeable and that toward lower values as bromine is removed. In Table I the average slopes above and below the monolayer value are used to calculate the two recorded heats of desorption for each of these three samples. All that can be said is that the value is the same as for adsorption below the monolayer value and higher by about 6 kcal per mole above it.

CONCLUSIONS

Because the critical pressure above which hysteresis occurs is the same for natural graphite and for all the carbon blacks it is concluded that the common lamellar structure of these materials is responsible for this behavior. Specifically, intercalation of bromine between the layers occurs only above the critical pressure and because the reverse process is hindered there is hysteresis. As one would expect, the hysteresis increases with the area of the carbon lamella and indeed the extent of hysteresis can be used to estimate the crystal dimension normal to the C axis. Furthermore the transport of bromine in and out of the layers should be and is much slower than the surface adsorption that is the main process below the critical pressure.

The isotherm for this surface adsorption can be used to calculate the surface area from the B.E.T. equation. The values for eight carbon blacks are, with one unexplained exception, within experimental error of the areas calculated from nitrogen adsorption data at low temperature or from electron microscope measurements of the size of the aggregates of graphite crystals. The average area occupied per bromine atom is of course critical in this calculation. The value of 12.2 $Å^2$ used is calculated from the density of the liquid assuming six co-ordination. However, one could equally well use the 11.8 $Å^2$ area per bromine atom in the halogen complexes of violanthrene studied by Professor H. Akamatu (1). He found evidence for a complex with two molecules of bromine to one molecule of the above hydrocarbon with its nine benzene rings. It is also interesting to note that placing bromine molecules over alternate pairs of graphite hexagons gives an average area per bromine atom of 10.5 Å. The atoms would be 0.09 Å from the center of each hexagon.

The isosteric heats in Table I show that the value for adsorption on the surface is within 10% of the value for adsorption between the layers. The best value for the carbon blacks of 11.2 ± 0.2 kcal $mole^{-1}$ agrees well with the 11.4 kcal $mole^{-1}$ reported by Reyerson (5) for adsorption on steam-activated charcoal. These values are only about 4 kcal higher than the heat of vaporization of bromine.

The bromine content of the residue compound increases with the pressure of bromine to which the sample had been exposed. However, the various isotherms for these different contents can be brought to coincidence by subtracting the residue composition at all pressures. This means that the total area available to bromine on the outer surfaces of

the crystal aggregates and the intercalating properties of the carbon layers are not changed noticeably by formation of the residue compound.

REFERENCES

1. AKAMATU, H., INOKUCHI, H., and MATSUNAGA, Y. Bull. Chem. Soc. Japan, **29**, 2, 213 (1956).
2. HENNIG, G. J. Chem. Phys. **20**, 1438 (1952).
3. HOOLEY, J. G. Can. J. Chem. **35**, 374 (1957).
4. HOOLEY, J. G. Can. J. Chem. **35**, 1414 (1957).
5. REYERSON, L. H. and CAMERON, A. E. J. Phys. Chem. **39**, 181 (1935).
6. REYERSON, L. H., WERTZ, J. E., WELTNER, W., and WHITEHURST, H. J. Phys. Chem. **61**, 1334 (1957).
7. SCHAEFFER, W. D., SMITH, W. R., and POLLEY, M. H. Ind. Eng. Chem. **45**, 1721 (1953).

STERIC INHIBITION OF RESONANCE

III. CALCULATION OF RESONANCE ENERGIES AND BOND LENGTHS[1]

JAMES TROTTER[2]

ABSTRACT

In many aromatic nitro compounds steric effects prevent the attainment of complete coplanarity and inhibit resonance interaction between the nitro group and the aromatic π-electrons. The variations with nitro group tilt of resonance energy, electron distribution, and π-bond order in this type of molecule have been calculated by molecular orbital methods, and the corresponding bond length variations have been deduced. The calculated bond lengths for 9,10-dinitroanthracene and 9-nitroanthracene are compared with those measured by X-ray analyses.

INTRODUCTION

Investigations of the crystal and molecular structures of 9-nitroanthracene and 9,10-dinitroanthracene have shown that the nitro groups are tilted markedly out of the planes of the aromatic rings due to the steric effects of neighboring carbon and hydrogen atoms (1, 2), and the resultant decreases in resonance interaction between the nitro groups and the aromatic π-electrons have been correlated with the variations in the characteristic vibration frequencies of the nitro groups (3). Further detailed examination of the bond lengths in these molecules, especially the C–N distances, suggests that the resonance is almost completely inhibited in 9-nitroanthracene, where the nitro group is tilted about the C–N bond 85° from the coplanar position, but that in the 9,10-dinitro derivative, where the tilts are 64°, there is a small but measurable resonance interaction (4).

The changes in the resonance energy and in the bond lengths in aromatic nitro compounds when the nitro group is tilted out of the plane of the aromatic ring may be calculated by molecular orbital methods, and the first section of the present paper describes the calculation of the variation of resonance energy and bond lengths with nitro group tilt (θ) in aromatic nitro compounds in general, nitrobenzene being used as a simple example. Subsequent sections describe the application of these methods to 9-nitroanthracene and 9,10-dinitroanthracene.

NITROBENZENE

In nitrobenzene (Fig. 1) each carbon and oxygen atom contributes one p_z electron to the π-molecular-orbital system, while the nitrogen atom contributes two, so that nine molecular orbitals accommodate 10 electrons. The secular equations

$$\sum c_r^i(H_{rs}-ES_{rs}) = 0$$

were set up in the usual way, using the parameters given in Table I, overlap integrals being taken as zero, and inductive effects neglected (this point will be discussed later). Since the nitrogen atom contributes two electrons its coulomb integral has been taken as $\alpha + \beta$ instead of the usual $\alpha + \frac{1}{2}\beta$ (8). The resonance integral H_{17} varies of course with the angle of tilt, being a maximum when $\theta = 0°$ and a minimum when $\theta = 90°$. By resolving the p_z atomic orbitals along axes at right angles, it can be shown that the value of this resonance integral for any value of θ is given approximately by

$$\beta^\theta = \beta^0, \cos\theta.$$

[1]*Manuscript received October 31, 1958.*
Contribution from the Division of Pure Physics, National Research Council, Ottawa, Canada.
Issued as N.R.C. No. 5133.
[2]*National Research Council Postdoctorate Fellow.*

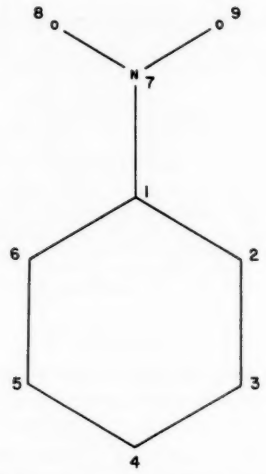

FIG. 1. Numbering used in the computations for nitrobenzene.

TABLE I

Parameters for nitrobenzene

	Coulomb integrals		Resonance integrals
H_{11}	α	H_{12}	β
H_{22}	α	H_{23}	β
H_{33}	α	H_{34}	β
H_{44}	α	H_{45}	β
H_{55}	α	H_{56}	β
H_{66}	α	H_{61}	β
H_{77}	$\alpha+\beta$	H_{17}	$\beta.\cos\theta$
H_{88}	$\alpha+\beta$	H_{78}	$\sqrt{2}\beta$
H_{99}	$\alpha+\beta$	H_{79}	$\sqrt{2}\beta$

The determinant Δ formed by the coefficients of the c_r^i is of the ninth order, and by writing $x = (\alpha - E_i)/\beta$ the molecular energy levels were obtained in terms of β by solving the equation $\Delta = 0$. Using determinants of the variety known as continuants, as described by Goodwin and Vand (5), the secular determinant for nitrobenzene was readily expanded to

$$\Delta_{\text{nitrobenzene}} = \Delta_{\text{benzene}} \cdot \Delta_{\text{nitro group}} - \cos^2\theta(x+1)^2 \cdot P_5$$
$$= (x+1)^3(x-1)[P_5+P_4-5P_3+2P_2+7P_1-11P_0-\cos^2\theta(P_3-P_1)].$$

The energy levels E_i for $\cos\theta = 0, 0.25, 0.50, 0.75, 1.00$ were evaluated, and are listed in Table II. The total π-electron energies and the resonance energies (E_R) due to interaction between the nitro group and the aromatic π-electrons were calculated and are included in the table. The final values of E_R in kcal were obtained by taking $\beta = -20$ kcal/mole.

The variation of E_R with θ is shown in Fig. 2, which indicates that E_R is approximately proportional to $\cos^2\theta$. The curve shows that at a nitro-group tilt of about 60° the energy of resonance interaction between a nitro group and the aromatic π-electrons is about $1\frac{1}{2}$ kcal/mole, compared with about $6\frac{1}{2}$ kcal/mole in a completely planar aromatic nitro compound, so that it is small but not negligible. Guy (6) has calculated for diphenyl

TABLE II

π-Electron molecular-orbital energy levels (E_i) in order of increasing energy, for various θ

$\theta°$	0	41.4	60	75.5	90
cos θ	1.000	0.750	0.500	0.250	0.000
$i = 1$	$\alpha+3.2098\beta$	$\alpha+3.1214\beta$	$\alpha+3.0552\beta$	$\alpha+3.0140\beta$	$\alpha+3\beta$
2	$\alpha+1.9554\beta$	$\alpha+1.9726\beta$	$\alpha+1.9869\beta$	$\alpha+1.9966\beta$	$\alpha+2\beta$
3	$\alpha+\beta$	$\alpha+\beta$	$\alpha+\beta$	$\alpha+\beta$	$\alpha+\beta$
4	$\alpha+\beta$	$\alpha+\beta$	$\alpha+\beta$	$\alpha+\beta$	$\alpha+\beta$
5	$\alpha+\beta$	$\alpha+\beta$	$\alpha+\beta$	$\alpha+\beta$	$\alpha+\beta$
6	$\alpha-0.6432\beta$	—	—	—	$\alpha-\beta$
7	$\alpha-\beta$	—	—	—	$\alpha-\beta$
8	$\alpha-1.4024\beta$	—	—	—	$\alpha-\beta$
9	$\alpha-2.1197\beta$	—	—	—	$\alpha-2\beta$
$2\sum_{i=1}^{5} E_i$	$10\alpha+16.3305\beta$	$10\alpha+16.1879\beta$	$10\alpha+16.0842\beta$	$10\alpha+16.0211\beta$	$10\alpha+16\beta$
E_R	0.3305β	0.1879β	0.0842β	0.0211β	0
E_R (kcal/mole)	−6.61	−3.76	−1.68	−0.42	0

derivatives a much more rapid decrease in resonance interaction with increasing θ, and in fact his resonance energy is proportional to $\cos^4\theta$, so that it is quite small at $\theta = 60°$ (about 0.4 kcal/mole). However, he makes the initial assumption that the resonance integral $w(\theta)$ is given by $w(\theta) = w(0)[1+\cos 2\theta]/2$, that is β^θ is proportional to $\cos^2\theta$, and hence his resonance energy is inevitably proportional to $\cos^4\theta$. Dewar (7) on the other hand takes β^θ proportional to $\cos\theta$, and shows that the resonance energy is proportional to $\cos^2\theta$.

In nitrobenzene the most stable configuration has $\theta = 0°$, but in a molecule in which the steric effects of neighboring atoms or groups prevent the attainment of a completely coplanar arrangement, the most stable configuration is determined not only by the resonance energy E_R, but also by the repulsive forces between the oxygen atoms and neighboring groups. The energies of van der Waals attraction and electronic repulsion can be represented by a curve of the form

$$E_v = -\frac{a}{r^6} + \frac{b}{r^n} \qquad (n > 6).$$

The variation of this energy with θ in nitro derivatives of mesitylene and durene is shown in Fig. 3; the energy passes through a slight minimum at the angle corresponding to van der Waals separation, and increases very markedly at smaller θ due to rapidly increasing repulsive forces. The variation of the combined energies, E_R and E_v, with θ is also shown in Fig. 3; there is a minimum in the curve in the region of $\theta = 65°$, so that this is the most stable configuration of the isolated molecules.

Inductive Effects

In heterocyclic molecules uncertainty about the exact values of the various coulomb and resonance integrals generally makes the reliability of the calculated energies rather uncertain. In the present calculations, however, while variation of the parameters changes the values of the energy levels E_i, the resonance energies are changed only slightly. The inductive effect of the nitro group on the carbon parameters, for example, can be allowed for by writing the coulomb integrals of the carbon atoms as $\alpha + m\beta$, where m decreases with increase in the number of bonds between the carbon atom and nitro group. The calculations of the energy levels were repeated taking $m = 0.6$ for carbon atom 1, and zero for the other carbon atoms, the results (for $\theta = 0°$ and 90°) being listed in Table III. Comparison with the values of Table II shows that while the energy levels have

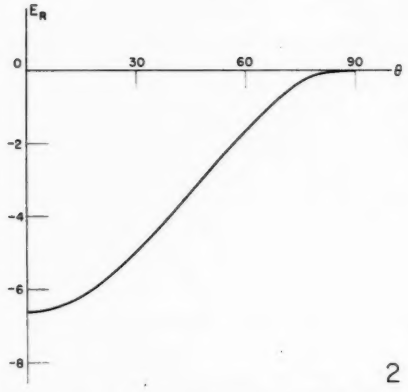

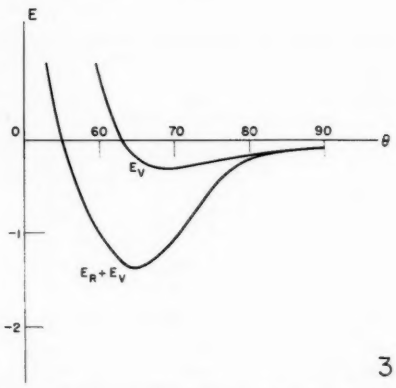

FIG. 2. Energy of resonance interaction (E_R in kcal/mole) between nitro group and aromatic π-electrons as a function of nitro-group tilt (θ).
FIG. 3. Variation of van der Waals energy (E_v) and total energy (E_R+E_v).

TABLE III

Molecular-orbital energy levels, E_i, with allowance for inductive effect

θ / $\cos\theta$	0° / 1.000	90° / 0.000
$i=1$	$\alpha+3.2688\beta$	$\alpha+3\beta$
2	$\alpha+2.0452\beta$	$\alpha+2.1359\beta$
3	$\alpha+1.1845\beta$	$\alpha+1.1995\beta$
4	$\alpha+\beta$	$\alpha+\beta$
5	$\alpha+\beta$	$\alpha+\beta$
6	—	$\alpha-0.8116\beta$
7	—	$\alpha-\beta$
8	—	$\alpha-\beta$
9	—	$\alpha-1.9237\beta$
$2\sum_{i=1}^{5} E_i$	$10\alpha+16.9971\beta$	$10\alpha+16.6707\beta$
E_R	0.3264β	0
E_R (kcal)	−6.53	0

changed, the energy of resonance interaction between a nitro group and aromatic π-electrons differs little from the value calculated neglecting the inductive effect.

Electron Distributions and Mobile Bond Orders

The coefficients c_r^i for each energy level were then evaluated by means of continuants and the π-electron distributions (q_r) and mobile bond orders (p_{rs}) evaluated from the expressions

$$q_r = \sum_i n(c_r^i)^2 \quad \text{and} \quad p_{rs} = \sum_i nc_r^i c_s^i \quad (n = 2).$$

The values for $\theta = 0°$, 60°, 90° are listed in Tables IV and V. The values at $\theta = 0°$ and 90° for $m_1 = 0.6$ are included, and these show that while allowance for the inductive effect of the nitro group changes the charges on the carbon atoms, it produces only quite small differences in the bond orders.

To derive the bond lengths from the calculated bond orders, correlation curves were drawn as described below.

TABLE IV

π-Electron distribution (q_r)

	r	1	2	3	4	5	6	7	8	9
$m_1 = 0$	$\theta = 0°$	1.006	0.973	1.007	0.976	1.007	0.973	1.009	1.530	1.530
	60°	1.002	0.993	1.000	0.994	1.000	0.993	1.003	1.508	1.508
	90°	1.000	1.000	1.000	1.000	1.000	1.000	1.000	1.500	1.500
$m_1 = 0.6$	$\theta = 0°$	1.213	0.893	1.005	0.923	1.005	0.893	1.000	1.534	1.534
	90°	1.232	0.908	1.005	0.940	1.005	0.908	1.000	1.500	1.500

TABLE V

Mobile bond orders (p_{rs})

	$m_1 = 0$			$m_1 = 0.6$	
Bond	$\theta = 0°$	$\theta = 60°$	$\theta = 90°$	$\theta = 0°$	$\theta = 90°$
1–2	0.628	0.656	0.667	0.610	0.648
2–3	0.675	0.669	0.667	0.679	0.670
3–4	0.661	0.665	0.667	0.659	0.664
1–7	0.322	0.167	0	0.318	0
7–8	0.665	0.696	0.707	0.668	0.707

Carbon–Carbon Bonds

Since the carbon–carbon bond orders in nitrobenzene differ only slightly from those in benzene, only the region of the bond order – bond length curve near the benzene point is of importance, and a linear correlation (Fig. 4*a*) between the single-bond distance for sp^2 hybridization (1.50 Å) and the double-bond distance (1.34 Å) was used, this line passing close to the benzene point (0.667, 1.397).

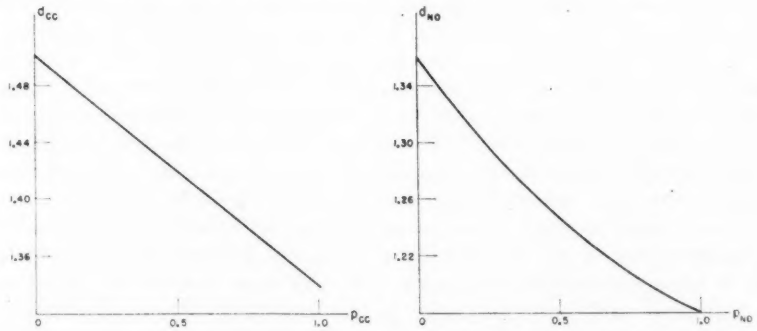

FIG. 4. Bond order – bond length correlation curves for (*a*) C–C bonds and (*b*) N–O bonds.

Nitrogen–Oxygen Bonds

A curve was drawn (Fig. 4*b*) from the point (0, 1.36) representing the single-bond length to (1.0, 1.18) representing the double-bond distance, and passing close to the point for a non-conjugated nitro compound (0.707, 1.21). Only the range of bond orders around 0.7 is of importance in the present computations.

Carbon–Nitrogen Bonds

Since the mobile bond order of the C–N bonds in aromatic nitro compounds changes

considerably with the angle of tilt of the nitro group (Table V), the exact form of this correlation curve is of more importance. The curve shown as a full line in Fig. 5 was

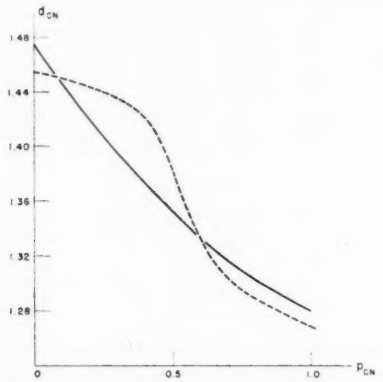

FIG. 5. Correlation curves for C–N bonds.

drawn through (0, 1.475), (0.600, 1.336), and (1.000, 1.280), since Goodwin and Porte (8) have deduced from a consideration of bond orders and lengths in a number of molecules that any reasonable curve must pass close to the point (0.600, 1.336). These authors also suggest that the length of a pure single bond be taken as 1.435 Å to allow for the sp^2 hybridization. However, in aliphatic nitro compounds the C–N distance is about 1.475 Å and since the nitrogen atom is already in a state of sp^2 hybridization, application of a correction for change of hybridization of the carbon atom would give 1.455 Å for the single-bond length to be used in aromatic nitro compounds. An alternative curve using this single-bond distance and of the form suggested by Goodwin and Porte is shown as a broken line in Fig. 5. The two curves differ significantly in the range of bond orders encountered in nitro compounds ($0 \rightarrow 0.3$), and it would be possible to decide between them if some accurate bond length measurements in the bond order range $0 \rightarrow 0.3$ were available. The C–N distance in 9-nitroanthracene (1.482 Å) would suggest that the full curve is more acceptable for nitro compounds, although this length is not known with great accuracy (standard deviation 0.015 Å). An accurate value of the C–N bond length in nitrobenzene would distinguish between the curves, since the lengths corresponding to $p_{CN} = 0.322$ are significantly different (1.391 Å and 1.433 Å) and work is being undertaken to measure this value (and incidentally investigate any possible deviations from exact planarity in this molecule). Meanwhile the full curve will be used in deriving bond lengths, with the bond lengths derived from the broken curve generally being noted for comparison.

The values of the bond lengths for all the bond orders in Table V were read off from the correlation curves, and these are listed in Table VI. The variations of the lengths of the C–C bonds with nitro group tilt are very small, the maximum difference being 0.006 Å (0.009 Å with allowance for the inductive effect, taking $m_1 = 0.6$); similarly the maximum variation for the N–O bonds is 0.007 Å. These variations are generally too small to be measured accurately by X-ray crystal analyses. For the C–N bonds, however, the lengths are 1.475 Å for $\theta = 90°$ and 1.391 Å for $\theta = 0°$ (using the full curve of Fig. 5) and it should be possible to detect this type of variation quite readily. (If the broken correlation curve is used the range is only 1.455 Å to 1.433 Å, but even this variation could be detected by accurate X-ray analysis.)

TABLE VI

Calculated bond lengths (Å)

Bond	$m_1 = 0$			$m_1 = 0.6$	
	$\theta = 0°$	$\theta = 60°$	$\theta = 90°$	$\theta = 0°$	$\theta = 90°$
1–2	1.399	1.395	1.393	1.402	1.396
2–3	1.392	1.393	1.393	1.392	1.393
3–4	1.394	1.393	1.393	1.394	1.394
1–7	1.391	1.428	1.475	1.391	1.475
7–8	1.220	1.215	1.213	1.219	1.213
Alternative					
1–7	1.433	1.446	1.455	1.434	1.455

MESONITROANTHRACENES

The application of the methods described above to aromatic nitro compounds in which resonance between nitro group and aromatic π-electrons is inhibited due to steric effects requires that some estimation of the C–N resonance integral be made, and this integral is approximately proportional to $\cos\theta$. The angle θ has been accurately measured for 9,10-dinitroanthracene and 9-nitroanthracene in the solid state using X-ray diffraction methods (1, 2), and these values may now be used in computing bond orders, and hence in deriving bond lengths for comparison with those measured by the X-ray methods.

9,10-Dinitroanthracene

In 9,10-dinitroanthracene (Fig. 6) each carbon and oxygen atom contributes one p_z

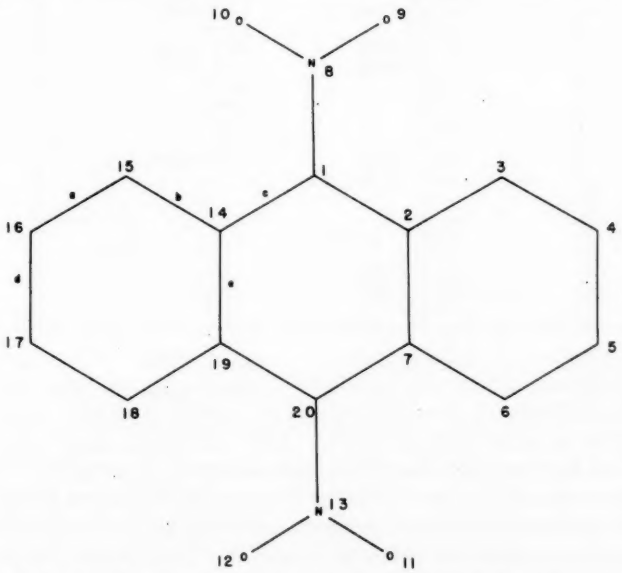

FIG. 6. Numbering used in the computations for 9,10-dinitroanthracene.

electron to the π-molecular-orbital system, while the nitrogen atoms each contribute two, so that 20 molecular orbitals accommodate 22 electrons. The secular equations were set up in the usual way. X-ray analysis has shown that $\theta = 63.7°$, so that the C–N resonance integrals are 0.44β. Overlap integrals were taken as zero, and the inductive

effects of the nitro groups were neglected since, as shown above, their inclusion causes only small variations in the bond orders and bond lengths.

The secular determinant is of the 20th order, but since the molecule has a center of symmetry, the 20th-order determinant was at once factorized into two 10th-order determinants according as $c_r = \pm c_{21-r}$. Using continuants these determinants were readily expanded to

$$\Delta_{\text{symmetrical}} = (x+1)^2(x-1)^2(x-2)[(P_5+5P_4+7P_3+2P_2+P_1+3P_0) - 0.20(P_3+4P_2+7P_1+6P_0)]$$

$$\Delta_{\text{antisymmetrical}} = (x+1)^2(x-1)^2(x+2)[(P_5+P_4-5P_3-2P_2+P_1+3P_0) - 0.20(P_3-P_1-2P_0)].$$

The π-electron molecular-orbital energy levels, E_i, were evaluated for 9,10-dinitroanthracene, and also, for comparison, for anthracene and the nitro groups separately, corresponding to no resonance interaction ($\theta = 90°$). The energy levels are listed in Table VII, together with the total π-electron energy and resonance energy due to reso-

TABLE VII

π-Electron molecular-orbital energy levels, E_i, for 9,10-dinitroanthracene, in order of increasing energy

i	Anthracene + 2 nitro groups	9,10-Dinitroanthracene	Symmetry
1	$\alpha+3\beta$	$\alpha+3.0537\beta$	S
2	$\alpha+3\beta$	$\alpha+3.0397\beta$	A
3	$\alpha+2.4142\beta$	$\alpha+2.3908\beta$	S
4	$\alpha+2\beta$	$\alpha+2\beta$	A
5	$\alpha+1.4142\beta$	$\alpha+1.4118\beta$	S
6	$\alpha+1.4142\beta$	$\alpha+1.4077\beta$	A
7	$\alpha+\beta$	$\alpha+\beta$	S
8	$\alpha+\beta$	$\alpha+\beta$	A
9	$\alpha+\beta$	$\alpha+\beta$	S
10	$\alpha+\beta$	$\alpha+\beta$	A
11	$\alpha+0.4142\beta$	$\alpha+0.4260\beta$	A
12	$\alpha-0.4142\beta$	—	S
13	$\alpha-\beta$	—	S
14	$\alpha-\beta$	—	A
15	$\alpha-\beta$	—	S
16	$\alpha-\beta$	—	A
17	$\alpha-1.4142\beta$	—	S
18	$\alpha-1.4142\beta$	—	A
19	$\alpha-2\beta$	—	S
20	$\alpha-2.4142\beta$	—	A
$2\sum_{i=1}^{11} E_i$	$22\alpha+35.3137\beta$	$22\alpha+35.4596\beta$	
E_R	0	0.1459β	
E_R (kcal/mole)	0	−2.92	

nance interaction between the nitro groups and the anthracene nucleus. Taking $\beta = -20$ kcal/mole this resonance energy is 2.92 kcal/mole (1.46 kcal/nitro group).

The c_r^i were then evaluated for each energy level and the π-electron distribution and mobile bond orders are listed in Tables VIII and IX. The calculated bond lengths were then derived, using the C–N and N–O correlation curves of the previous section; for C–C bonds however, a best linear correlation was drawn through the points representing the calculated bond orders and observed bond lengths for anthracene (Fig. 7).

9-Nitroanthracene

In 9-nitroanthracene 17 molecular orbitals accommodate 18 electrons, and the secular equations were set up using similar parameters to those for the dinitro derivative. X-ray

TABLE VIII

π-Electron distributions (q_r) in 9,10-dinitroanthracene

r	Anthracene + 2 nitro groups	9,10-Dinitroanthracene
1	1.000	0.994
2	1.000	0.996
3	1.000	0.999
4	1.000	0.998
8	1.000	1.004
9	1.500	1.508

TABLE IX

Mobile bond orders (p_{rs}) in 9,10-dinitroanthracene

Bond	Anthracene + 2 nitro groups	9,10-Dinitroanthracene
a	0.737	0.736
b	0.535	0.538
c	0.606	0.596
d	0.586	0.587
e	0.485	0.487
C–N	0	0.163
N–O	0.707	0.695

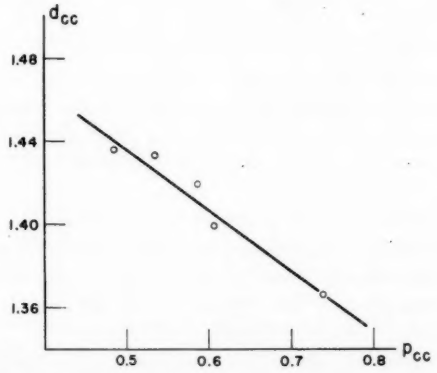

FIG. 7. Correlation curve for C–C bonds, based on the points for anthracene.

analysis has shown that the nitro group is tilted 84.7° out of the aromatic plane so that the C–N resonance integral is 0.09β. The secular determinant is of the 17th order, but since $\cos^2\theta$ is quite small, the energy levels differ little from those in anthracene and a non-conjugated nitro group, and the complete calculations were not carried out. The energy of resonance interaction between the nitro group and the aromatic π-electrons is 0.06 kcal/mole, the C–C and N–O bond orders do not differ significantly from those in the separate, non-conjugated anthracene molecule and nitro group, and the C–N bond order (approximately proportional to $\cos\theta$) is about 0.034. The calculated bond lengths were derived from the same curves as those for 9,10-dinitroanthracene.

DISCUSSION

The energy of resonance interaction between the nitro groups and the anthracene nucleus in 9,10-dinitroanthracene is 2.92 kcal/mole. When the variation of resonance

energy with nitro-group tilt is combined with the energies of van der Waals attraction and electronic repulsion between the oxygen atoms and neighboring carbon and hydrogen atoms, a curve of the type shown in Fig. 3 is obtained, with a minimum in the region of $\theta = 65°$, in good agreement with the measured tilt (64°). This structure is about 3 kcal/mole more stable than that with $\theta = 90°$. The most stable configuration for 9-nitroanthracene should have the nitro group tilted 64° out of the anthracene plane, but in the solid state crystal forces apparently give minimum energy when $\theta = 85°$.

The calculated bond lengths for anthracene, 9,10-dinitroanthracene, and 9-nitroanthracene are compared in Table X with the distances measured by X-ray crystal

TABLE X

Measured and calculated bond lengths in anthracene, 9,10-dinitroanthracene, and 9-nitroanthracene (Å)

	Anthracene			9,10-Dinitroanthracene			9-Nitroanthracene		
Bond	Meas.	Calc.	Δ	Meas.	Calc.	Δ	Meas.	Calc.	Δ
a	1.366	1.366	0	1.356	1.366	−0.010	1.399	1.366	+0.033
b	1.433	1.426	+0.007	1.414	1.425	−0.011	1.434	1.426	+0.008
c	1.399	1.405	−0.006	1.389	1.408	−0.019	1.400	1.405	−0.005
d	1.419	1.411	+0.008	1.400	1.410	−0.010	1.413	1.411	+0.002
e	1.436	1.440	−0.004	1.452	1.440	+0.012	1.437	1.440	−0.003
C–N	—	—	—	1.450	1.430	+0.020	1.482	1.465	+0.017
Alternative C–N	—	—	—		1.446	+0.004		1.453	+0.029
N–O	—	—	—	1.241	1.215	+0.026	1.216	1.213	+0.003
R.M.S. Δ			0.006			0.016			0.015
						(0.015)			(0.017)

analyses, the differences (Δ) and root mean square Δ being included in the table. For anthracene the measured and calculated distances for the various bonds are of course very similar, since the calculated bond orders and observed bond lengths in anthracene have been used in deriving the carbon–carbon correlation curve. The agreement for the C–C bonds in the nitro derivatives is quite satisfactory; only for the *a* bond in 9-nitroanthracene is the difference apparently greater than the estimated experimental error (4), and this latter has probably been slightly underestimated (2). The calculated N–O bond length in 9-nitroanthracene is in very good agreement with the measured value. For 9,10-dinitroanthracene the agreement is not quite so good, although the difference is just within the limits of experimental error.

For the C–N bonds, while the agreement is reasonable, it is still not possible to decide between the two correlation curves shown in Fig. 5. In 9-nitroanthracene the agreement is significantly better when the full curve is used for bond order – bond length correlation, but the broken curve gives better agreement for the dinitro derivative. Further accurate measures of C–N bond lengths in the bond order range $0 \rightarrow 0.3$ are required to establish better correlation for the C–N bonds in nitro compounds, and present investigations by X-ray diffraction methods of the crystal structures of nitro derivatives of mesitylene and durene, and of nitrobenzene, may supply some useful data.

REFERENCES

1. Trotter, J. Acta Cryst. **11**, 564 (1958).
2. Trotter, J. Acta Cryst. (In press).
3. Trotter, J. Can. J. Chem. **37**, 351 (1959).
4. Trotter, J. Can. J. Chem. **37**, 825 (1959).
5. Goodwin, T. H. and Vand, V. J. Chem. Soc. 1683 (1955).
6. Guy, J. J. chim. phys. **46**, 469 (1949).
7. Dewar, M. J. S. J. Am. Chem. Soc. **74**, 3345 (1952).
8. Goodwin, T. H. and Porte, A. L. J. Chem. Soc. 3595 (1956)

THE KINETICS OF HYDROGEN CHEMISORPTION ON AN IRIDIUM CATALYST[1]

MANFRED J. D. LOW AND H. AUSTIN TAYLOR

ABSTRACT

The kinetics of the chemisorption of hydrogen on an iridium catalyst have been studied at various temperatures and pressures. The rate of adsorption is well defined by the Elovich equation. Isothermal anomalies have been observed and were found to be a function of temperature and initial gas pressure.

Recently it has been shown (1) that the Elovich equation,

$$dq/dt = a\, e^{-\alpha q},$$

will accurately reflect the variation of the amount adsorbed, q, with time, t, in many chemisorption processes. The constants (a) and α were found to vary with temperature, but there was no indication of a pressure dependence. More recently (2, 3) such a pressure dependence has been found in several systems and, in order to investigate further the influence of initial gas pressure on the Elovich parameters, the present investigation was undertaken.

EXPERIMENTAL

The measurements of rates of adsorption were carried out by admitting a known amount of hydrogen to a sample of the catalyst which had been suitably evacuated, and measuring the change of pressure in the constant-volume system. A commercial hydrogenation catalyst, purchased from Baker and Co., Inc., was used as adsorbent. The catalyst consisted of 0.5% iridium supported on the surface of 3×5-mm γ-alumina extrudates.

The catalyst (20.10 g) was placed in a Vycor tube and sealed to the all-Pyrex system. A copious evolution of water and of gas took place on heating the catalyst to 500° C. After an overnight pumping period at that temperature the pressure within the system had fallen to 10^{-6} mm Hg. The catalyst was then treated with palladium-filtered hydrogen at 500° C at a pressure of 60 cm dibutyl phthalate (DBP). After 2 hours the gas was removed, and the adsorbent was pumped on overnight at 500°. This hydrogen treatment was repeated six times. It was found that on pumping at 500°, a vacuum of 10^{-6} mm Hg, or less, could be obtained and maintained after a period of about 6 hours. A minimum pump-off period of 10 hours at 500° was therefore chosen.

It was noticed that the color of the untreated catalyst was black. After pumping, but before the hydrogen treatment, the color was still black. After the first contact with hydrogen, however, the catalyst had turned gray, and remained that color until the end of the series of experiments.

Dead spaces were measured by expansion of helium purified by passage through a charcoal trap cooled with liquid nitrogen. The catalyst was thermostatted at a desired temperature by surrounding the chamber with a Dewar flask filled with solid CO_2, ice, or with the vapors of a boiling liquid. The experiments reported here were made at different initial pressures, P_0, at any one temperature, T, and were numbered consecutively in order of their execution.

[1]*Manuscript received January 28, 1959.*
Contribution from The Nichols Laboratory, New York University, New York 53, New York.

RESULTS AND DISCUSSION

A total of 38 experiments at seven different temperatures were made. It was found that the data of each experiment could be precisely described by use of the Elovich equation. Isothermal anomalies (1) were found. The $q - \log t$ plots of the data appeared as straight lines which, after a certain time, t_b, abruptly changed in slope. These discontinuities, or "breaks", are illustrated by Fig. 1. The data of three sample runs are

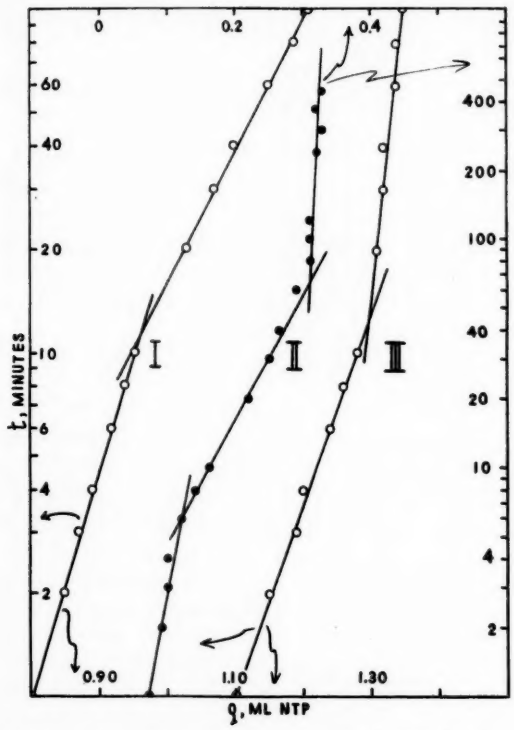

FIG. 1. Adsorption of H_2 on $Ir.Al_2O_3$. Typical runs: I. Run 2, 147°, 34.5 cm DBP; II. Run 28, 257°, 10.4 cm DBP; III. Run 38, −78.5°, 8.8 cm DBP.

shown to be internally consistent. Circles represent experimental points, and the lines were calculated using the equation,

$$q = (2.3/\alpha) \log_{10} (1+a\alpha t).$$

Constants were calculated by a previously described method (4), and are summarized in Table I. The subscripts 1, 2, and 3 identify the parameters corresponding to the 1st, 2nd, or 3rd branches of the curve. The co-ordinates of the break, q_b and t_b, result from the intersection of the 1st and 2nd branches.

It is to be noted that, with the exception of run 38, the slopes of the $q - \log t$ plots increased after t_b. In a few cases, notably with experiments at low pressures, this region of increased slope was followed by one of decreased slope (plot II, Fig. 1). This is not unexpected, since the slope must eventually become zero. The fact that these 3rd branches

TABLE I

Run No.	P_0 cm DBP	$T°$ C	α_1	α_2	α_3	ln $a_1\alpha_1$	ln $a_2\alpha_2$	ln $a_3\alpha_3$	q_b	t_b
1	68.9		11.5	5.1	—	5.50	1.65	—	1.39	27
2	34.5		15.2	8.7	—	5.30	3.58	—	0.96	11
3	25.8		17.4	11.1	—	5.13	2.96	—	0.79	7
4	59.8	147	12.8	5.1	—	5.34	1.33	—	1.20	21
5	43.2		14.3	7.6	—	4.87	2.07	—	0.96	13
6	9.8		20.0	13.5	19.7	3.83	2.46	4.25	0.50	3
7	18.3		18.1	12.9	—	4.33	2.91	—	0.63	4
8	51.9		15.9	7.4	—	5.94	2.26	—	1.03	11
15	5.9		23.0	9.5	25.6	2.50	0.85	3.56	0.28	2
9	26.0		16.4	8.9	13.5	4.63	2.06	3.87	0.76	6
10	10.0		20.0	10.0	17.7	3.13	1.30	3.08	0.43	3.5
11	4.9	100	35.0	31.0	128.0	1.67	0.40	10.96	0.15	3
12	72.5		10.9	4.8	—	5.27	1.61	—	1.38	18
13	42.5		15.3	8.9	—	5.19	2.52	—	0.93	12
14	26.5		15.2	7.7	—	4.61	1.84	—	0.85	10
16	74.8		14.9	4.1	—	5.51	0.54	—	1.05	19
17	43.7		18.7	9.3	—	4.72	1.81	—	0.71	11
18	26.7		19.5	—	—	3.73	—	—	—	—
19	10.2	200	23.0	11.2	20.4	2.11	0.84	2.60	0.25	2
20	18.4		20.5	10.3	—	3.92	1.73	—	0.51	3
21	5.0		23.0	13.9	37.7	1.30	0.66	3.62	0.16	2
22	60.8		14.8	3.8	—	5.08	0.34	—	0.98	17
23	35.3		20.0	10.3	—	4.22	1.78	—	0.57	6
24	5.0		23.0	14.1	40.0	1.30	0.63	3.73	0.17	2.5
25	61.0		11.5	2.8	—	3.60	−0.19	—	0.99	25
26	35.4		23.0	8.4	—	3.90	0.96	—	0.50	7
27	18.9		33.0	10.4	13.8	3.15	0.67	1.28	0.25	3
28	10.4	257	35.0	12.6	115.0	1.07	−0.12	13.60	0.12	6
29	75.2		12.9	5.2	—	4.00	0.96	—	0.90	12
30	44.4		23.0	9.6	—	4.60	1.47	—	0.54	6
31	31.5		30.2	20.2	—	3.60	2.20	—	0.33	5
32	5.5		37.4	18.0	72.0	0.83	0.41	5.57	0.11	3
33	71.8		12.8	5.2	—	7.12	2.12	—	1.52	21
34	9.6	56	21.0	10.4	17.7	3.93	1.71	3.77	0.49	4
35	68.4		15.3	7.0	—	10.81	4.23	—	1.82	20
36	9.2	0	35.0	13.5	26.4	11.26	3.96	8.97	0.78	4
37	64.2		17.7	2.9	—	12.89	4.22	—	4.15	10
38	8.8	−78.5	12.8	38.0	—	6.12	20.31	—	1.30	13

are linear on a $q - \log t$ plot may be of significance, and suggests that rate measurements be continued to zero rate. Most of the present experiments were terminated after about 100 minutes because the rate of adsorption became quite slow. Thus in run 28, 0.309 ml was adsorbed at 100 minutes, and only 0.325 ml was adsorbed after 420 minutes.

Breaks of a similar nature are to be found in the plots of P_0 versus q_t, the amount adsorbed at time t at 100° C. The plots of Fig. 2 show breaks in the region of $P_0 \sim 10$ cm. This phenomenon was previously observed in the case of the systems H_2 – Ni. kieselguhr (2) and H_2 – Ru. Al_2O_3 (3).

Effect of Initial Pressure

From the data in Table I it can be seen that both α_1 and α_2 are dependent on the initial pressure at each temperature. These dependencies are representable by the equations

$$\alpha_1 = B_1 + C_1 P_0$$

$$\alpha_2 = B_2 + C_2 P_0$$

and Table II lists the values of the constants B and C at the four principal tempera-

TABLE II

	100° C	147° C	200° C	257° C
B_1	18.871	20.690	23.590	38.126
$-C_1$	0.106	0.129	0.125	0.354
B_2	10.719	14.979	14.030	15.573
$-C_2$	0.075	0.155	0.139	0.167
D	0.460	0.320	0.141	0.00682
E	0.0124	0.0153	0.9129	0.0133
F	1.807	1.740	−0.329	0.932
G	0.228	0.361	0.257	0.211
K	4.330	4.007	3.159	3.367
L	0.0142	0.0261	0.0317	0.0099
M	3.038	3.583	1.566	2.984
N	0.0175	0.0139	0.0381	−0.00651
$-m$	1.504	1.778	1.112	1.842
n	0.331	0.496	0.197	0.175

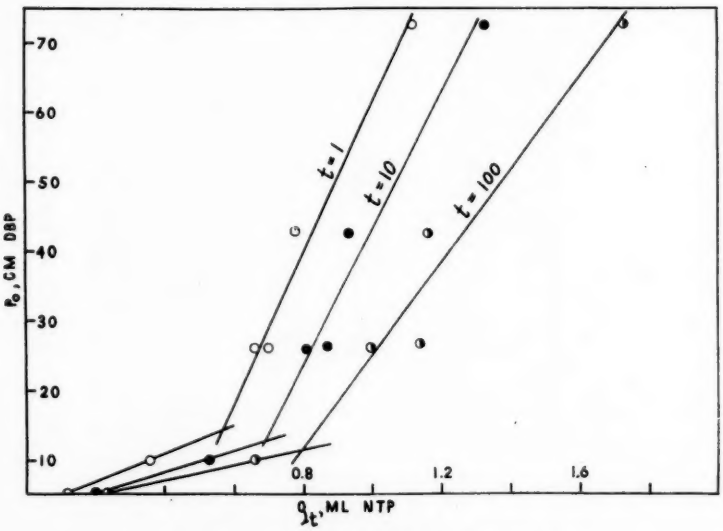

FIG. 2. The variation of q_t with P_0 at 100° C.

tures. In previous studies (2, 3) discontinuities were usually observed in such $\alpha - P_0$ plots, the slope changing abruptly at lower pressures. In the present study a discontinuity was found only at 100° C. Figure 3 shows a plot of both α_1 and α_2 as a function of P_0 at 100°. The data in Table II for 100° refer to the data above 10 cm. Below 10 cm at 100°, $\alpha_1 = 49.41 - 2.94P_0$ and $\alpha_2 = 51.18 - 4.12P_0$. At the other temperatures the constants in Table II cover the whole pressure range studied.

The variation of $\log a_1$ and $\log a_1\alpha_1$ with P_0 followed a pattern similar to that of α, and may be represented by the equations;

$$\log_{10} a_1\alpha_1 = K + LP_0$$

$$\log_{10} a_1 = M + NP_0,$$

the values of the constants at four temperatures being given in Table II. Breaks occurred in the low-pressure region. At 100°, $\log_{10} a_1\alpha_1 = 0.269 + 0.286P_0$; at 200°, $\log_{10} a_1\alpha_1 = 0.522$

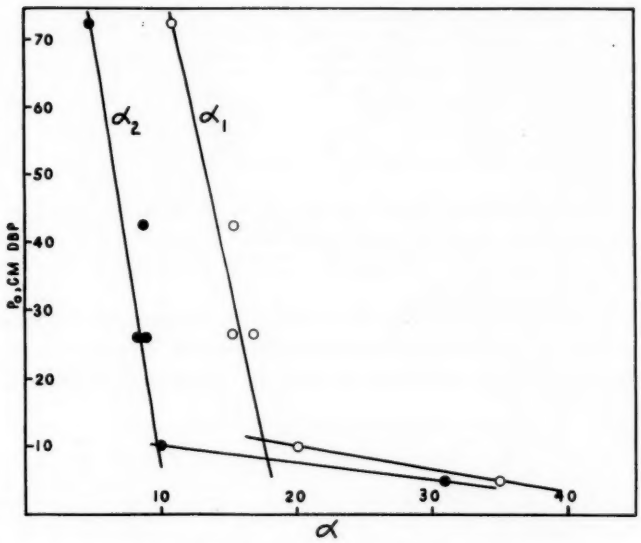

FIG. 3. The variation of α with P_0 at 100° C.

$+0.156P_0$. Since α showed breaks only at 100° but log $a_1\alpha_1$ has breaks at all temperatures, plots of log a_1 vs. P_0, as expected, showed breaks at all temperatures. The constants of the equation,

$$\log_{10} a_1 = m+nP_0,$$

describing the low-pressure region, are given in Table II. The variation of log a_2 and log $a_2\alpha_2$ with P_0 is not clearly defined.

It has been noted that breaks occurred in all isotherms. It is interesting that the time of occurrence of the break, t_b, as well as the amount adsorbed at the time of occurrence, q_t, increase linearly with increasing P_0 according to the equations,

$$t_b = F+GP_0,$$
$$q_b = D+EP_0.$$

The values of the constants of these equations at four temperatures are given in Table II. The data at 100° show a break at a P_0 of about 10 cm in a fashion similar to that of α_1 and α_2. Below 10 cm, $q_b = -0.122+0.0554P_0$.

The Influence of Temperature on Parameter Values

In the previous studies it was found that α and log $a\alpha$ were linear in the reciprocal of the temperature. Since the pressure dependencies of both parameters are more marked in the present study, values of α_1 and log $a_1\alpha_1$ have been calculated from the previous equations for P_0 values of 60 and 40 cm DBP at each of the four highest temperatures. Since only two runs were made at each of the three lowest temperatures, the pressure dependence is too uncertain to justify a similar treatment. The least square straight line through the four points at each initial pressure expresses the relations, $\alpha_1 = U+V/T$, and $\log_{10} a_1\alpha_1 = X+Y/T$. The values of U, V, X, and Y at each of the initial pressures 60 and 40 cm DBP are given in Table III. The energy of activation of adsorption as

TABLE III

	P_0 = 60 cm	P_0 = 40 cm
U	28.68	44.13
$-V$	6194	11461
X	1.58	1489
Y	0.564	1741

usually calculated has previously been shown to be expressible as: $E = R(Vq - Y)$, where R is the gas constant. From the values of V and Y it is found that at $P_0 = 60$ cm, $E = -12.36q - 2.97$, and at $P_0 = 40$ cm, $E = 22.88q - 3.48$. Over the whole range of adsorption values of q, E is negative.

Comparison with previous studies on Ni and Ru shows that the values of V and Y may be either positive or negative. The magnitude and the direction of variation of E with coverage, q, present four possibilities which are illustrated in Fig. 4. Case I with

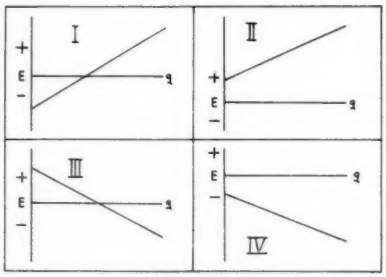

FIG. 4. Linear variation of activation energy with coverage.

V and Y both positive was found in the Ni.kieselguhr system. Case III, with V and Y both negative, was found with Ru.Al_2O_3. Case IV, with V negative and Y positive, is the present study. Case II is approximated by the data of Burwell and Taylor (5) for the adsorption of H_2 on Cr_2O_3. Taking their data, treated by the Elovich equation, given in Table IV of Taylor and Thon (1), for 0.5 atm it is found that $\alpha = (23700/T) - 45.5$, and $\log_{10} a\alpha = (1000/T) - 6$, whence $E = 47q - 2$ kcal. Although V and Y are both positive, the low value of Y leaves E positive except for very small values of q, thus approximating Case II. It is obvious that the interpretation of E as a simple energy of activation is not necessarily an argument for multiplicity of adsorption sites. On the other hand, it would appear inescapable that the changes in adsorption rate, here accentuated as "breaks," as well as the pressure dependencies found, cannot be attributed to a single type of adsorption site. Two or possibly three such types, rather than a spectrum of types, would appear sufficient to account for the observations.

The change in magnitude of a parameter with temperature may be connected with the region of the isobar under consideration. Figure 5 shows estimates of amounts adsorbed at 100 minutes, suggesting that the present experiments were made on the decreasing portion of the isobar. In view of the complexity of the relations it seems too early to comment on the possible physical significance of parameters such as a_2, the mathematical initial rate of the 2nd kinetic stage, or to attempt a general interpretation, much less to attempt to identify the sites concerned. Additional work on other gas–solid systems seems to be required.

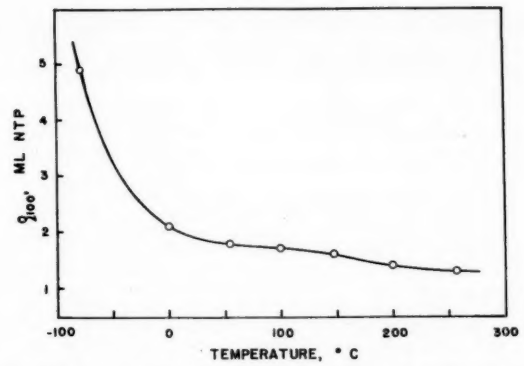

FIG. 5. The "100-minute isobar" of H_2 adsorption on $Ir.Al_2O_3$ at $P_0 = 75$ cm DBP.

REFERENCES

1. TAYLOR, H. A. and THON, N. J. Am. Chem. Soc. **74**, 4169 (1952).
2. LEIBOWITZ, L., LOW, M. J. D., and TAYLOR, H. A. J. Phys. Chem. **62**, 471 (1958).
3. LOW, M. J. D. and TAYLOR, H. A. Can. J. Chem. **37**, 544 (1959).
4. SARMOUSAKIS, N. J. and LOW, M. J. D. J. Chem. Phys. **25**, 178 (1956).
5. BURWELL, R. L. and TAYLOR, H. S. J. Am. Chem. Soc. **58**, 697 (1936).

THE CONSTITUTION OF A METHYL GLUCURONOXYLAN FROM KAPOK (CEIBA PENTANDRA)[1]

A. L. Currie and T. E. Timell

ABSTRACT

The seed hairs of kapok (*Ceiba pentandra*) on alkaline extraction have yielded a hemicellulose composed of xylose and uronic acid residues. Partial hydrolysis of the polysaccharide gave 2-*O*-(4-*O*-methyl-α-D-glucopyranosyluronic acid)-D-xylopyranose, 4-*O*-methyl-D-glucuronic acid, and, probably, galacturonic acid. Hydrolysis of the fully methylated hemicellulose yielded a mixture of 2-*O*- and 3-*O*-methyl-D-xylose, 2,3-di-*O*-methyl-D-xylose, 2,3,4-tri-*O*-methyl-D-xylose, and 2-*O*-(2,3,4-tri-*O*-methyl-α-D-glucopyranosyluronic acid)-3-*O*-methyl-D-xylopyranose in a molar ratio of 1.1:38:1:6. The number-average D.P. of the native and the methylated polysaccharides was 177 and 124, respectively. On the basis of this and other evidence it is suggested that the average hemicellulose molecule contains approximately 180 1,4-linked β-D-xylopyranose residues, one eighth of which carry a single terminal side chain of 4-*O*-methyl-D-glucuronic acid, attached through an α-glycosidic bond to C_2 of the xylose. The xylan framework contains, on the average, slightly less than two branching points per macromolecule, most of them probably originating from C_3. The number of acid side chains and branches is twice as large as that of the otherwise similar 4-*O*-methyl glucuronoxylan present in the seed hairs of milkweed floss.

In previous investigations the general chemical composition of the seed hairs of kapok was studied (1) as well as the molecular characteristics of their cellulose component (2, 3). The present paper is concerned with the structure and properties of the main hemicellulose constituent.

RESULTS AND DISCUSSION

The high pentosan content (24.4%) of the extractive-free seed hairs indicated that the predominant hemicellulose was based on xylose residues. The considerable amounts of acetyl (8.0%) and uronic anhydride (6.6%) groups present as well as the formation of a methylated glucuronic acid on hydrolysis of the fibers suggested that the polysaccharide in its native state was a partially acetylated methyl glucuronoxylan. When kapok fibers were extracted with aqueous alkali a deacetylated product was obtained in a yield of 18.8%, containing 83.3% pentosan and with $[\alpha]_D^{20}$ −68° in water. Its content of ash, methoxyl, and uronic anhydride indicated the presence of an average of 7.8 anhydroxylose units per methylated uronic acid.

Partial acid hydrolysis of the hemicellulose gave a mixture of sugars which was resolved into a neutral and an acidic portion on a column of anion exchange resin. The neutral part contained mostly D-xylose which crystallized but also traces of glucose, mannose, arabinose, and rhamnose. Elution of the column with dilute acetic acid yielded three sugar acids, namely a monouronic acid, chromatographically identical with galacturonic acid, an aldobiouronic acid, and a mono-*O*-methyl monouronic acid.

The methoxyl content and equivalent weight of the aldobiouronic acid suggested that it consisted of a methoxyuronic acid linked to a pentose residue. A portion of the acid was converted to the corresponding methyl ester methyl glycoside, which was reduced with lithium aluminum hydride and hydrolyzed to yield D-xylose, which crystallized, and 4-*O*-methyl-D-glucose, which was identified through its crystalline osazone (4, 5). The methyl ester methyl glycoside of the aldobiouronic acid was completely methylated, reduced, and hydrolyzed. The mixture of methylated sugars obtained was resolved on a cocoanut charcoal column to yield 3,4-di-*O*-methyl-D-xylose and 2,3,4-tri-

[1]*Manuscript received January 6, 1959.*
Contribution from McGill University and Pulp and Paper Research Institute of Canada, Montreal, Quebec.

O-methyl-D-glucose, both of which were identified through their crystalline aniline derivatives (6, 7). The methylated and reduced glycoside of the aldobiouronic acid was therefore methyl 2-*O*-(2,3,4-tri-*O*-methyl-α-D-glucopyranosyl)-3,4-di-*O*-methyl-D-xylopyranoside. This evidence shows that the aldobiouronic acid was 2-*O*-(4-*O*-methyl-α-D-glucopyranosyluronic acid)-D-xylopyranose. Its high positive rotation (+100° in water) in conjunction with other evidence (8, 9) indicated that the biose linkage was present in the α-configuration.

Reduction and subsequent hydrolysis of the methyl ester methyl glycoside of the mono-*O*-methyl uronic acid gave 4-*O*-methyl-D-glucose, thus showing that the compound was 4-*O*-methyl-D-glucuronic acid.

The hemicellulose was methylated to completion and hydrolyzed with dilute acetic acid. The acidic and neutral sugars formed were separated on an anion exchange resin. The acid fraction contained only one component, namely a partially methylated aldobiouronic acid. Reduction of its methyl ester methyl glycoside yielded a crystalline compound, which was identified through its melting point, specific rotation, infrared spectrum, and X-ray powder diagram as methyl 2-*O*-(2,3,4-tri-*O*-methyl-α-D-glucopyranosyl)-3-*O*-methyl-α,β-D-xylopyranoside, previously isolated from western hemlock (10), sugar maple, and yellow birch (11) wood. Methanolysis of the disaccharide followed by hydrolysis gave a mixture of methylated sugars which was resolved by fractional extraction with chloroform of its aqueous solution. The two sugars obtained were 2,3,4-tri-*O*-methyl-D-glucose and 3-*O*-methyl-D-xylose, both of which were characterized through their aniline derivatives.

The aqueous solution of the neutral sugars was fractionally extracted with chloroform. The first compound removed was chromatographically identical with 2,3,4-tri-*O*-methyl-D-xylose and was tentatively characterized through its infrared spectrum. The second and main portion was 2,3-di-*O*-methyl-D-xylose, identified as its crystalline aniline derivative. The residual aqueous solution contained a mixture of sugars which was resolved by paper ionophoresis to give 2-*O*-methyl-D-xylose together with a smaller quantity of 3-*O*-methyl-D-xylose. A portion of the mixture of neutral sugars was resolved by paper chromatography and subjected to quantitative analysis (12). The molar ratio of mono-, di-, and tri-*O*-substituted xyloses was 1.1:38:1. The yield of the partially methylated aldobiouronic acid indicated the presence of 6 moles of aldobiouronic acid per mole of tri-*O*-methyl xylose, corresponding to 8 moles of xylose residues per acid group, in accordance with the above evidence.

The large quantity of 2,3-di-*O*-methyl-D-xylose isolated showed that the backbone of the polysaccharide was composed of D-xylopyranose residues linked through positions 1 and 4 and this conclusion was corroborated by results obtained on periodate oxidation of the hemicellulose. The high negative rotation of the original and of the methylated (−57° in chloroform) polysaccharide strongly suggested that the xylose residues were present in the β-configuration. The 2,3,4-tri-*O*-methyl-D-xylose apparently originated from the non-reducing end groups. The fact that the 4-position was unsubstituted in the crystalline, partly methylated aldobiouronic acid, obtained on partial hydrolysis of the methylated hemicellulose, whereas the methylated aldobiouronic acid itself was substituted in this position, indicated that the 4-*O*-methyl-D-glucuronic acid residues were attached *directly* to the framework of the 1,4-linked xylose residues. The structure of the aldobiouronic acid showed that the side chains were present in the α-configuration and were linked to C_2.

None of the acid side groups were evidently removed during the hydrolysis of the

methylated hemicellulose. The presence of the two mono-*O*-methyl xyloses was therefore due to either incomplete methylation, demethylation, or branching. While some demethylation probably occurred (13, 14), the possibility of branching could not be excluded, especially in view of the fact that one of the mono-*O*-methyl xyloses predominated.

When the number-average molecular weight of the methylated hemicellulose was determined by osmometry (13, 15), a value of 23,400 was obtained. With one 4-*O*-methyl-D-glucuronic acid residue present for every eighth anhydroxylose unit, this corresponded to a degree of polymerization (number of xylose residues in the main chain) of 124. Each methylated macromolecule thus contained on the average 3.0 mono-*O*-methylated, 118 di-*O*-methylated, and 2.7 tri-*O*-methylated xylose residues. This corresponded to the presence of 1.7 branch points per molecule, most of them probably originating from the 3-position of the xylose residues.

A portion of the hemicellulose was converted to the fully substituted acetate derivative which was soluble in chloroform–ethanol. Osmotic pressure measurements gave a number-average molecular weight of 43,700, corresponding to a $\bar{P}_n$ of 177 for the native polymer.

From the above evidence a simplified structure can now be suggested for the main hemicellulose component of the seed hairs of kapok. The xylan framework of this polysaccharide contains an average number of approximately 180 β-D-xylopyranose residues, connected by 1,4-glycosidic bonds and with, on the average, slightly less than two branching points per molecule, most of them probably located at C_3. Every eighth xylose residue has a single, terminal side chain of 4-*O*-methyl-D-glucuronic acid, linked by an α-glycosidic bond to C_2. The exact nature of the branching is unknown.

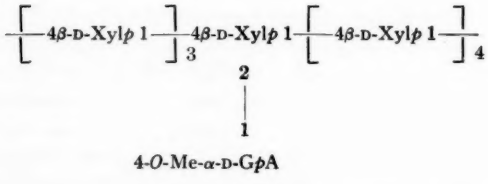

4-*O*-Me-α-D-G*p*A

The only other seed hair hemicellulose hitherto investigated appears to be that present in the floss of the common milkweed (16). This 4-*O*-methyl glucuronoxylan is similar to, albeit not identical with, that found in kapok, the latter polysaccharide having almost twice as many side chains and branching points as the former. Hemicelluloses containing a branched framework of 1,4-β-linked anhydroxylose units have been isolated also from corncob (17), esparto grass (18), and wheat straw (19, 20). In the dicotyledons, however, the 4-*O*-methyl glucuronoxylans are almost invariably linear (21). Whether the same applies to the related gymnosperm xylans is still uncertain (22). Many xylans have been found to contain single side chains of L-arabofuranose residues, for example those present in cereal straws and in coniferous woods. The absence of such groups in the seed hair xylans so far studied is notable. The molecular weight of the native kapok xylan is approximately the same as that of the corresponding polysaccharides present in milkweed floss (16) and in deciduous woods (21).

EXPERIMENTAL

All specific rotations are equilibrium values and melting points are corrected. Evaporations were carried out *in vacuo* at 40–50° C.

Paper Chromatography

Solvents (v/v) used for separating the sugars were (*a*) ethyl acetate – acetic acid – water (9:2:2), (*b*) butan-1-ol–pyridine–water (10:3:3), (*c*) butan-2-one–ethanol–water (20:5:2), (*d*) butan-1-ol–ethanol–water (40:11:19), and (*e*) butan-1-ol–benzene–ethanol–water (6:3:2:1). Whatman No. 1 and No. 3MM filter papers were used and *o*-aminodiphenyl was the preferred spray reagent (12).

Isolation of the Hemicellulose

Kapok seed hairs (1) were exhaustively extracted with ethanol–benzene (1:2, v/v) and subsequently with cold water. The fibers (400 g) were cut into small pieces and shaken with 24% (w/w) aqueous potassium hydroxide (7.6 liters) in an atmosphere of nitrogen for 2 hours. After filtration through sintered glass, the filtrate and the washings were added to a mixture of ethanol (30 liters) and acetic acid (2.6 liters). The precipitate was washed successively on the centrifuge with 80% aqueous methanol, anhydrous methanol, and petroleum ether (b.p. 30–60° C). The product was dried over calcium chloride *in vacuo* for 1 week to yield 75 g of a white, fluffy material, corresponding to 18.8% of the original extractive-free fibers.

Hydrolysis, followed by examination by paper chromatography indicated the presence of mostly xylose and uronic acids. Anal. Pentosan, 83.3%; uronic anhydride, 14.0%; methoxyl, 2.45%; sulphate ash (as potassium), 3.15%; $[\alpha]_D^{20}$ −68° (*c*, 1.0 in 5% sodium hydroxide).

Isolation of Neutral Sugars

The hemicellulose (51 g) was treated with 72% sulphuric acid (120 ml) at room temperature for 2 hours, after which the solution was diluted to 3 liters and boiled under reflux for 6 hours. The solution was neutralized with barium hydroxide, filtered through Celite, and treated with Amberlite IR-120 cation exchange resin for removal of barium ions. Half of the hydrolyzate was slowly passed through a column (5.5×110 cm) of Dowex 1-X4 anion exchange resin. Washing with water removed neutral sugars. On evaporation of the eluate, crystals were obtained which, after recrystallization from 80% ethanol, yielded D-xylose, m.p. and mixed m.p. 144–145° C, $[\alpha]_D^{20}$ +19 (*c*, 1.1 in water). The remaining sirup was resolved on the paper chromatogram (solvent A) to give xylose together with minor quantities of glucose, mannose, arabinose, and rhamnose.

Separation of Sugar Acids

The mixture of sugar acids remaining on the column of exchange resin was resolved by elution with *N* acetic acid to yield two compounds, one being an aldobiouronic acid and the other corresponding in rate of movement on the paper chromatogram (solvent A) and in color produced with the spray reagent to galacturonic acid. Evaporation of the former fraction gave a white, amorphous powder (2.00 g), the infrared spectrum of which was indistinguishable from that of an authentic specimen of 2-*O*-(4-*O*-methyl-α-D-glucopyranosyluronic acid)-D-xylopyranose. Anal. Calc. for $C_{12}H_{20}O_{11}$: OCH_3, 9.1%; equiv. wt., 340. Found: OCH_3, 8.9%; equiv. wt., 351; $[\alpha]_D^{20}$ +100° (*c*, 2.4 in water).

Further elution of the column with 3 *N* acetic acid gave a third sugar acid, chromatographically identical with 4-*O*-methyl glucuronic acid. Anal. Calc. for $C_7H_{12}O_7$: OCH_3, 14.9%; equiv. wt., 208. Found: OCH_3, 13.9%; equiv. wt., 209; $[\alpha]_D^{20}$ +48° (*c*, 1.4 in water).

Reduction and Hydrolysis of the Aldobiouronic Acid

The aldobiouronic acid (0.80 g) was boiled under reflux with 2% methanolic hydrogen

chloride (50 ml) for 11 hours. After neutralization with silver carbonate and treatment with hydrogen sulphide, filtration through Celite and evaporation yielded a clear sirup which was dissolved in dry tetrahydrofuran (100 ml) and reduced with lithium aluminum hydride (2.4 g) in 100 ml of the same solvent. The reduced glycoside was recovered in the usual way and hydrolyzed with *N* sulphuric acid.

Identification of Hydrolysis Products

The mixture of reducing sugars obtained after the hydrolysis was added to a cocoanut charcoal (23) column (3.5×23 cm). Elution with 3% and 10% aqueous ethanol yielded two compounds, corresponding in rate of movement on the paper chromatogram (solvent C) to xylose and 4-*O*-methyl glucose. The xylose (210 mg) crystallized, m.p. 143–144° C, $[\alpha]_D^{20}$ +19° (*c*, 0.8 in water). The 4-*O*-methyl-D-glucose (300 mg), $[\alpha]_D^{20}$ +68° (*c*, 3.0 in water) was converted to the phenylosazone derivative, m.p. and mixed m.p. 156–157° C.

Methylation, Reduction, and Hydrolysis of the Aldobiouronic Acid

A portion of the aldobiouronic acid (1.13 g) was converted to the methyl ester methyl glycoside. The dry sirup obtained was dissolved in dry dimethyl formamide (20 ml) according to Kuhn (24) and methyl iodide (5 ml) and silver oxide (5 g) were added. After shaking for 24 hours, the product was recovered in the usual way and the methylation procedure was repeated twice. The final product had an infrared spectrum which indicated the absence of hydroxyl groups. The sirup (1.02 g) was reduced in ethyl ether (65 ml) with lithium aluminum hydride (2.5 g) to yield a sirup (1.00 g) which was boiled under reflux for 12 hours with 5% methanolic hydrogen chloride followed by refluxing for 10 hours with 0.5 *N* hydrochloric acid.

*Identification of 3,4-Di-O-methyl-*D*-xylose and 2,3,4-Tri-O-methyl-*D*-glucose*

The acid hydrolyzate was added directly to a cocoanut charcoal column (2×13 cm) which was washed with water until the eluate was neutral. Elution with 6% and 10% ethanol gave two compounds, chromatographically (solvent B and D) indistinguishable from 3,4-di-*O*-methyl xylose and 2,3,4-tri-*O*-methyl glucose, respectively. The di-*O*-methyl xylose, electrophoretically (25, 26) identical with the 3,4-di-*O*-methyl derivative, $[\alpha]_D^{20}$ +15° (*c*, 1.1 in chloroform), was converted to the aniline derivative by treatment with aniline dissolved in absolute ethanol at room temperature. After recrystallization from petroleum ether, the 3,4-di-*O*-methyl-*N*-phenyl-D-xylosylamine had m.p. 122.5–123.5° C. The tri-*O*-methyl glucose, $[\alpha]_D^{20}$ +78° (*c*, 2.0 in water), gave crystalline 2,3,4-tri-*O*-methyl-*N*-phenyl-D-glucosylamine, m.p. and mixed m.p. 144–145° C.

*Identification of 4-O-Methyl-*D*-glucuronic Acid*

The mono-*O*-methyl hexuronic acid obtained from the column of anion exchange resin was converted to the ester glycoside, reduced with lithium aluminum hydride in tetrahydrofuran, and hydrolyzed with *N* sulphuric acid. Evaporation yielded a sirup, chromatographically (solvent B) identical with 4-*O*-methyl-D-glucose, $[\alpha]_D^{20}$ +56° (*c*, 1.7 in water). The 4-*O*-methyl-D-glucosazone had m.p. and mixed m.p. 156–157° C.

Methylation of the Hemicellulose

The hemicellulose (20 g) was stirred overnight with water (75 ml) and 40% (w/w) sodium hydroxide (100 ml) in an atmosphere of nitrogen, after which dimethyl sulphate (90 ml) was added dropwise over a period of 12 hours. The treatment with alkali and dimethyl sulphate was repeated nine times. The recovered, partially methylated hemicellulose was suspended in tetrahydrofuran (500 ml) and dried over anhydrous sodium sulphate. After removal of the drying agent by filtration, dry dimethyl formamide (500 ml), methyl iodide (5 ml), and silver oxide (5 g) were added (24) and the mixture was

shaken for 12 hours, after which the same quantities of methylating agents were added and methylation was allowed to proceed for another 12 hours. Tetrahydrofuran was removed by evaporation, chloroform (1000 ml) was added, and dimethyl formamide was removed by continuous extraction with water for 3 days. The dry chloroform extract was concentrated, centrifuged, and poured into petroleum ether (4 liters) to yield a methylated hemicellulose, OCH_3, 37.3% (17.7 g, 80%). Another methylation according to Kuhn (24) failed to raise the methoxyl content of the product. Anal. OCH_3, 37.3%; ash, 0.33%; $[\alpha]_D^{20}$ −57° (*c*, 1.0 in chloroform). The infrared spectrum indicated the absence of hydroxyl groups.

Hydrolysis and Separation of Acidic and Neutral Sugars

A portion of the methylated hemicellulose (7.0 g) was dissolved in glacial acetic acid (75 ml). After addition of water (75 ml), the solution was boiled under reflux for 33 hours, when its rotation was constant. Acetic acid was removed by evaporation and an aqueous solution (500 ml) of the hydrolyzate was added to a column of Dowex 1-X4 exchange resin (acetate form). Neutral sugars were eluted with water after which an acidic compound was removed with 3 *N* acetic acid (1.62 g). Anal. Calc. for $C_{15}H_{26}O_{11}$: OCH_3, 32.5; equiv. wt., 382. Found: OCH_3, 32.3; equiv. wt., 382.

Preparation and Identification of Methyl 2-O-(2,3,4-Tri-O-methyl-α-D-glucopyranosyl)-3-O-methyl-α,β-D-xylopyranoside

The partially methylated aldobiouronic acid (1.38 g) was converted to its methyl ester methyl glycoside, which was reduced with lithium aluminum hydride (1.5 g) in diethyl ether (50 ml). After addition of ethyl acetate and water, the reduced disaccharide was recovered by extraction with chloroform to yield a sirup (1.18 g, 86%) which crystallized on standing. After recrystallization from ethyl acetate, it had a m.p. of 166.5–167.5° C, undepressed on admixture with an authentic specimen of methyl 2-*O*-(2,3,4-tri-*O*-methyl-α-D-glucopyranosyl)-3-*O*-methyl-D-xylopyranoside.* The melting point, infrared spectrum, and X-ray diagram of the material were also identical with those of another authentic specimen, isolated from yellow birch wood (27). Anal. Calc. for $C_{16}H_{30}O_{10}$: OCH_3, 40.6%. Found: OCH_3, 39.0%; $[\alpha]_D^{20}$ +95° (*c*, 0.7 in water). The compound was probably a mixture of the α- and β-xylopyranosides.

A portion (160 mg) of the disaccharide was subjected to methanolysis and subsequent hydrolysis to give an aqueous solution, which, on chromatographic resolution (solvent B), appeared to contain equal amounts of a mono-*O*-methyl xylose and a tri-*O*-methyl glucose. Extraction with chloroform gave a sirup, chromatographically identical with 2,3,4-tri-*O*-methyl-D-glucose (solvent E). The 2,3,4-tri-*O*-methyl-*N*-phenyl-D-glucosylamine had m.p. and mixed m.p. 146–147° C. Evaporation of the remaining aqueous solution gave a compound which was chromatographically identical with 3-*O*-methyl-D-xylose (solvent E). The aniline derivative had an infrared spectrum indistinguishable from that of an authentic specimen. Anal. Calc. for $C_6H_{12}O_5$: OCH_3, 18.9%. Found: OCH_3, 18.8%; $[\alpha]_D^{20}$ +18° (*c*, 1.6 in water).

Separation of the Neutral Components of the Methylated Hemicellulose

The aqueous solution of the neutral sugars from the column of exchange resin was reduced to 500 ml and shaken with chloroform (50 ml) for 3 hours. After having been shaken with water for another 3 hours, the chloroform layer contained only a tri-*O*-methyl xylose (166 mg). The original aqueous solution was extracted continuously with chloroform for 18 hours, the extract was discarded and extraction was continued for another

*The authors are thankful to Professor Fred Smith, University of Minnesota, for providing this sample.

3 days, yielding a chromatographically pure di-*O*-methyl xylose (1.86 g). The remaining aqueous solution was extracted three times with 20-ml portions of hot ethanol to yield a mixture of mono-*O*-methylated xyloses (154 mg).

Preliminary Characterization of Mono-O-methyl Xyloses

This fraction, $[\alpha]_D^{20}$ +23° (*c*, 2.8 in water), had a methoxyl content (16.3%) somewhat lower than that required for a mono-*O*-methyl xylose. Results obtained on ionophoresis in a borate buffer solution suggested the presence of 2-*O*- and 3-*O*-methyl-D-xylose in an approximate ratio of 2:1.

Identification of 2,3-Di-O-methyl-D-xylose

When seeded with authentic crystals of 2,3-di-*O*-methyl-D-xylose (28), this fraction appeared to crystallize, but the m.p. was 20° higher than expected (96–99° C). Anal. Calc. for $C_7H_{14}O_5$: OCH_3, 34.8%. Found: OCH_3, 33.1%; $[\alpha]_D^{20}$ +26° (*c*, 1.0 in water). The 2,3-di-*O*-methyl-*N*-phenyl-D-xylosylamine, when recrystallized once from ethyl acetate, had m.p. 126–127° C. Slow evaporation of an ethyl acetate – petroleum ether solution gave needles, m.p. 130–131° C. The material is known to be dimorphic (29).

Partial Identification of 2,3,4-Tri-O-methyl-D-xylose

Neither the original compound nor its aniline derivative could be induced to crystallize. The infrared spectra of both were indistinguishable from those of authentic samples.

Quantitative Analysis of the Neutral Components

A small portion of the mixture of neutral sugars was resolved on the paper chromatogram with solvent mixture D. The appropriate paper strips were eluted with water and the concentration of each sugar solution was determined by the *o*-aminodiphenyl method (12). The average value of six determinations was used.

Periodate Oxidation of the Hemicellulose

Periodate oxidations were carried out in the dark with 0.05 *M* sodium metaperiodate containing 2 mg of hemicellulose per ml of solution. Aliquots were taken every day for 6 days and the amount of periodate consumed was determined by the arsenite method. The average consumption after 3–4 days was 8.2 moles per repeating unit, corresponding to a calculated value of 7.8.

Preparation of the Acetylated Hemicellulose

Dry hemicellulose (2 g) was swollen or partially dissolved in dry formamide (40 ml) by shaking for 5 hours. Dry pyridine (80 ml) was added, followed by redistilled acetic anhydride (60 ml). The reaction mixture was cooled with tap water for the first half hour and then shaken mechanically at room temperature for 5 hours, after which it was kept at +4° C for 3 days, the reaction flask being opened occasionally during this time. The mixture was poured into ice water (3 liters) with vigorous stirring and washed on a large Buechner funnel, first with ice-cold 2% hydrochloric acid (30) and subsequently with cold distilled water until neutrality. After the water had been replaced by ethanol and the alcohol by petroleum ether (b.p. 30–60° C), the white product was dried *in vacuo* over calcium chloride for 1 week. A second esterification was carried out in the same way although without the addition of formamide. Anal. Calc. for the fully acetylated hemicellulose: acetyl, 37.3%. Found: acetyl, 37.0% (31).

Determination of the Molecular Weight of the Methyl and Acetyl Derivatives of the Hemicellulose

The osmometer used was of the Zimm–Myerson (15) type as modified by Stabin and

Immergut (32). Gel cellophane membranes were used, the solvent was a mixture of chloroform and ethanol (9:1, v/v), and the temperature was 30±0.01° C. The osmotic height was measured at five different concentrations by the static method and the values of h/w, the reduced osmotic pressure, were linearly extrapolated to zero concentrations. The results are presented in Table I. The number-average molecular weight and degree of polymerization were calculated as described elsewhere (28).

TABLE I

Osmometry data for the methylated and acetylated hemicelluloses

Methyl derivative			Acetyl derivative		
w*	h†	h/w	w	h	h/w
3.484	4.625	1.328	3.707	2.188	0.590
2.850	3.630	1.274	3.546	2.098	0.592
2.043	2.430	1.189	2.998	1.747	0.583
1.774	2.138	1.205	2.257	1.341	0.594
1.483	—	1.253	1.872	1.136	0.607
0	—	1.10	0	—	0.588

*Concentration in g/kg solution.
†Osmotic height in cm solvent.

ACKNOWLEDGMENTS

The authors are thankful to Dr. R. St. J. Manley for providing the X-ray data. One of them (A.L.C.) also wishes to express his gratitude to the Allied Chemical Corporation for a fellowship and to the Pulp and Paper Research Institute of Canada for a summer stipend.

REFERENCES

1. Timell, T. E. Textile Research J. **27**, 854 (1957).
2. Timell, T. E. Svensk Papperstidn. **60**, 836 (1957).
3. Timell, T. E. Textile Research J. **28**, 270 (1958).
4. Smith, F. J. Chem. Soc. 2646 (1951).
5. Schinle, R. Ber. **65**, 315 (1932).
6. James, S. P. and Smith, F. J. Chem. Soc. 739 (1945).
7. Peat, S., Schlüchterer, E., and Stacey, M. J. Chem. Soc. 581 (1939).
8. Bishop, C. T. Can. J. Chem. **31**, 154 (1953).
9. Gorin, P. A. J. and Perlin, A. S. Can. J. Chem. **36**, 999 (1958).
10. Dutton, G. G. S. and Smith, F. J. Am. Chem. Soc. **78**, 3744 (1956).
11. Timell, T. E. J. Am. Chem. Soc. (In press).
12. Timell, T. E., Glaudemans, C. P. J., and Currie, A. L. Anal. Chem. **28**, 1916 (1956).
13. Glaudemans, C. P. J. and Timell, T. E. J. Am. Chem. Soc. **80**, 941, 1209 (1958).
14. Lindberg, B. Personal communication.
15. Zimm, B. H. and Myerson, I. J. Am. Chem. Soc. **68**, 911 (1946).
16. Barth, F. W. and Timell, T. E. J. Am. Chem. Soc. **80**, 6320 (1958).
17. Whistler, R. L. and Lauterbach, G. E. J. Am. Chem. Soc. **80**, 1987 (1958).
18. Chanda, S. K., Hirst, E. L., Jones, J. K. N., and Percival, E. G. V. J. Chem. Soc. 1289 (1950).
19. Ehrenthal, I., Montgomery, R., and Smith, F. J. Am. Chem. Soc. **76**, 5509 (1954).
20. Adams, G. A. Can. J. Chem. **30**, 698 (1952).
21. Timell, T. E., Glaudemans, C. P. J., and Gillham, J. K. Pulp Paper Mag. Can. **59** (No. 10) 242 (1958).
22. Painter, T. J. and Jones, J. K. N. (In press).
23. Barth, F. W. and Timell, T. E. Can. J. Chem. **36**, 1321 (1958).
24. Kuhn, R., Trischmann, H., and Löw, I. Angew. Chem. **67**, 32 (1955).
25. Foster, A. B. J. Chem. Soc. 982 (1953).
26. Bouveng, H. and Lindberg, B. Acta Chem. Scand. **10**, 1283 (1956).
27. Timell, T. E. Unpublished results.
28. Gillham, J. K. and Timell, T. E. Can. J. Chem. **36**, 1467 (1958).
29. Ehrenthal, I., Rafique, M. C., and Smith, F. J. Am. Chem. Soc. **74**, 1341 (1952).
30. Carson, J. F. and Maclay, W. D. J. Am. Chem. Soc. **68**, 1015 (1946).
31. Genung, L. B. and Mallat, R. C. Ind. Eng. Chem. Anal. Ed. **15**, 319 (1943).
32. Stabin, J. V. and Immergut, E. H. J. Polymer Sci. **14**, 209 (1954).

PHOTOCHEMICAL SEPARATION OF MERCURY ISOTOPES

III. THE REACTION OF $Hg^{202}6(^3P_1)$ ATOMS, PHOTOEXCITED IN NATURAL MERCURY VAPOR, WITH HYDROGEN CHLORIDE[1]

C. C. McDonald,[2] J. R. McDowell,[3] and H. E. Gunning[3]

ABSTRACT

An investigation has been made of the reaction of $Hg^{202}6(^3P_1)$ atoms, photoexcited in natural mercury vapor, with flowing hydrogen chloride at 28–30° C. Emphasis has been placed on the effect of reaction parameters on the Hg^{202} content of the calomel product of the reaction.

Under fast-flow conditions it has been found that the calomel product contains 44% Hg^{202}, corresponding to an enrichment of 48% over the normal abundance of 29.8%.

In the presence of unsaturated compounds such as butadiene and benzene the enrichment is markedly increased. With butadiene and benzene as addends, the maximum enrichments were 98% and 85% respectively.

The reaction with pure hydrogen chloride can be explained in terms of the sequence:

$$Hg^{202}6(^3P_1) + HCl \rightarrow Hg^{202}Cl + H \quad [1]$$

$$Hg^{202}6(^3P_1) + HCl \rightarrow Hg^{202} + Cl + H \quad [2]$$

$$Cl + Hg^N + M \rightarrow Hg^NCl + M \quad [3]$$

$$H + HCl \rightarrow H_2 + Cl \quad [4]$$

$$H + Cl + M \rightarrow HCl + M \quad [5]$$

where Hg^N is natural mercury and M is a third body, including the wall.

In the presence of unsaturated compounds (U), additional reactions are postulated to occur:

$$Cl + U \rightarrow \text{products} \quad [6]$$

$$H + U \rightarrow \text{products}. \quad [7]$$

The increased enrichment in the presence of unsaturated addends is explained by the reduced rate of formation of Hg^NCl through cleanup of chlorine and hydrogen atoms by reactions [6] and [7].

Under static conditions, the pure hydrogen chloride reaction formed a calomel product of normal Hg^{202} abundance. This finding is explained as a localized depletion of the unexcited mercury in Hg^{202}, through reaction [1]. With increasing linear flow rate the depletion effect gradually disappears and enrichments maximize at high flow rates.

The Hg^{202} enrichment was found to be very sensitive to the wall temperature of the Hg^{202} source. In a 50:50 v/v mixture of hydrogen chloride and butadiene the enrichment was found to decrease from 68% to 24% as the lamp temperature was raised from 25.5° C to 50° C. The effect is explained by temperature broadening of the emission line leading to overlap of the emission line on absorption contours adjacent to that of Hg^{202}.

Both the rate of deposition of the calomel product and the Hg^{202} enrichment were found to depend upon the concentration of natural mercury in the gas stream for hydrogen chloride – butadiene mixtures. Optimum conditions corresponded to a slight supersaturation of the stream with mercury vapor.

INTRODUCTION

In previous studies in this series (1), conditions have been experimentally defined for the photoexcitation, in natural mercury vapor (Hg^N), of a single isotopic species to the $6(^3P_1)$ state. This technique has been recently applied in a study of the reaction of $Hg^{202}6(^3P_1)$ atoms in Hg^N with water vapor (2, 3). In the water reaction it has been found that the HgO product of the reaction contains 80–90% Hg^{202} when addends are present, such as butadiene-1,3, to suppress the secondary formation of Hg^NO.

The present paper reports the first in a series of studies on the reaction of $Hg^{202}6(^3P_1)$ atoms in Hg^N with hydrogen chloride. Emphasis has been placed on the effects of reaction

[1]*Manuscript received December 29, 1958.*

Joint contribution from the Department of Chemistry, Illinois Institute of Technology, Chicago 16, Illinois, and the Department of Chemistry, University of Alberta, Edmonton, Alberta. This work was supported in part by the U.S. Atomic Energy Commission, under Contract AT(11-1)-43. This support is gratefully acknowledged.

[2]*Present address: Chemical Department, E.I. du Pont de Nemours Company, Wilmington, Delaware.*

[3]*Present address: Department of Chemistry, University of Alberta, Edmonton, Alberta.*

parameters on the Hg^{202} content of the calomel product of the reaction. Enrichment in Hg^{202} in this product would be evidence for primary formation of calomel, presumably by the reaction:

$$Hg^{202}6(^3P_1) + HCl \rightarrow Hg^{202}Cl + H. \quad [1]$$

The details of the investigation follow.

EXPERIMENTAL

The general experimental procedure has been previously described (1, 3). In this study a special rectangular reaction cell was used with faces 2.5×8.0 cm, and an internal path length of 0.10 cm. The cell had two side-arms, terminating in 2/5-spherical joints, for attachment to the flow system. The entire cell was fashioned of Vycor 7910 glass to prevent radiation of wavelength less than 2200 Å from entering the cell.

The source consisted of a quartz electrodeless discharge lamp containing mercury, 98.3 atom per cent in Hg^{202}. The lamp was maintained at 25.5±0.1° C unless otherwise specified. The lamp-cooling assembly has been described (1). The intensity of the radiation at 2537 Å incident upon the cell was monitored by a Westinghouse WL-775 phototube. The photometric unit was identical with that used in the mercury isotope analysis system previously described (4).

The mercury saturator consisted of a 500-cc bulb partially filled with mercury, to which two Liebig condensers were sealed in reflux position. The inner tube of the gas entrance condenser extended into the flask to a point about 1 cm above the mercury surface. In operation the gases entered at the top of the entrance condenser, passed over the refluxing mercury, and left the saturator through the top of the exit condenser. The reaction cell was connected to the exit condenser via a scratched stopcock. The temperatures of the water circulating through exit and entrance condensers were separately controlled from thermostats. The condensers were normally maintained at 30.0±0.1° C.

The gases used in the investigation were the highest-purity grades obtainable from the Matheson Company, East Rutherford, N.J. The benzene used was Fisher A.C.S. grade.

RESULTS

For pure hydrogen chloride a large number of exploratory runs were first performed to determine whether the calomel product of the reaction contained more than the normal abundance of Hg^{202}.

Several runs were first made under static conditions. Analysis showed that the calomel product contained the normal abundance (29.8%) of Hg^{202}, within the experimental error. Under flow conditions, however, the calomel product was found to be consistently enriched in Hg^{202}. The enrichments obtained in these runs varied from 20 to 40%. A systematic study was therefore made of the effect of reaction parameters on the Hg^{202} content of the calomel product.

In Table I the results are given for a series of runs at varying pressures of hydrogen chloride. The linear flow rate was held constant at 600 cm/sec. The light intensity was measured relatively by the photocell response as in the analytical system (4). For this series the incident intensity was 60 units.

Throughout this investigation difficulty was encountered in obtaining good reproducibility for runs done under apparently identical conditions. While the actual absorption measurements were reproducible to ±0.5%, maximum variations of ±5% were encountered, at times, for identical runs.

TABLE I

The effect of varying substrate pressure on the Hg^{202} enrichment in the solid product of the reaction of $Hg^{202}6(^3P_1)$ atoms, photoexcited in Hg^N, with flowing hydrogen chloride (Linear flow rate = 600 cm/sec. Incident light intensity = 60 units)

Pressure, mm	% Hg^{202}	Fractional enrichment
0.4	37	1.2
1.0	37	1.2
3.0	40	1.3
11.0	38	1.3
17.0	40	1.3
50.0	38	1.3

From Table I, it can be seen that the enrichment is constant within the experimental error over the pressure range, 0.4 to 50 mm. Pressures exceeding 50 mm were avoided to prevent Lorentz-broadening of the hyperfine absorption contours (1).

For the data given in Table I, the mercury saturator was operated under very gentle reflux. With the mercury boiling vigorously, it was found that the enrichments increased by approximately 10%. All ensuing runs were therefore performed under vigorous reflux conditions.

For the data in Table II, the pressure was maintained essentially constant, while

TABLE II

The effect of varying linear flow rate on the Hg^{202} enrichment in the solid product of the reaction of $Hg^{202}6(^3P_1)$ atoms, photoexcited in Hg^N, with flowing hydrogen chloride (Incident light intensity = 60 units)

Pressure, mm	Linear flow rate, cm/sec	% Hg^{202}	Fractional enrichment
4.0	375	41	1.4
1.4	425	43	1.4
1.1	475	43	1.4
1.4	1500	42	1.4
2.3	1500	44	1.5
2.8	1500	44	1.5

the linear flow rate was varied from 375 to 1500 cm/sec. It will be observed that there is a slight increase in enrichment with increasing linear flow rate to a maximum value of 48% at 1500 cm/sec.

Since it was suspected that $Hg^{202}6(^3P_0)$ atoms might be involved in the isotopically specific primary process, the effect of added nitrogen on the enrichment was studied. Representative data are given in Table III. While there appears to be a slight increase in enrichment with increasing nitrogen concentration in the stream, the effect is only slightly larger than the experimental reproducibility.

The failure to obtain pure $Hg^{202}Cl$ in the hydrogen chloride reaction implies that Hg^NCl is also being formed by some mechanism. On the hypothesis that the Hg^NCl arose by the interaction of free chlorine atoms with unexcited Hg^N, various additives were studied to reduce the chlorine-atom concentration.

In Table IV it can be seen that benzene has a marked effect on the Hg^{202} enrichment. With benzene concentrations exceeding approximately 30 mole per cent, the minimum enrichment was 70%. The benzene additive appears maximally effective at concentrations of 70 mole per cent, corresponding to an enrichment of 85%.

TABLE III

The effect of varying nitrogen concentration on the Hg^{202} enrichment in the solid product of the reaction of $Hg^{202}6(^3P_1)$ atoms, photoexcited in Hg^N, with flowing hydrogen chloride (Linear flow rate = 1500 cm/sec. Incident light intensity = 60 units)

Pressure, mm	Comp. mole %		% Hg^{202}	Fractional enrichment
	HCl	N_2		
2.3	100	0	44	1.5
8.3	80	20	44	1.5
4.8	50	50	47	1.6
6.0	34	66	44	1.5
10.0	20	80	48	1.6

TABLE IV

The effect of varying benzene concentration on the Hg^{202} enrichment in the solid product of the reaction of $Hg^{202}6(^3P_1)$ atoms, photoexcited in Hg^N, with flowing hydrogen chloride (Linear flow rate = 485 cm/sec. Incident light intensity = 60 units)

Pressure, mm	Comp. mole %		% Hg^{202}	Fractional enrichment
	HCl	C_6H_6		
2.3	100	0	44	1.5
3.8	65	35	51	1.7
4.3	37	63	50	1.7
3.6	30	70	55	1.8
8.4	18	82	51	1.7

A number of runs were also done with chlorobenzene as additive. The data are summarized in Table V. The effect of chlorobenzene is quite the reverse of benzene, leading

TABLE V

The effect of varying chlorobenzene concentration on the Hg^{202} enrichment in the solid product of the reaction of $Hg^{202}6(^3P_1)$ atoms, photoexcited in Hg^N, with flowing hydrogen chloride (Linear flow rate = 375 cm/sec. Incident light intensity = 60 units)

Pressure, mm	Comp. mole %		% Hg^{202}	Fractional enrichment
	HCl	C_6H_5Cl		
2.3	100	0	44	1.5
5.0	80	20	44	1.5
6.0	66	34	40	1.3
5.4	50	50	38	1.3
4.0	34	66	38	1.3
6.7	20	80	35	1.2

to a decreased enrichment with increasing mole fraction of chlorobenzene. It is apparent that the photoexcited mercury isotope is being quenched by chlorobenzene with the formation of chlorine atoms. The rate of Hg^NCl formation would therefore be increased over that for pure hydrogen chloride, with a resulting decrease in the Hg^{202} enrichment.

As might be expected, butadiene-1,3 proved to be even more effective than benzene in enhancing the Hg^{202} enrichment. Since butadiene was the most efficient additive encountered in this investigation, it was studied in some detail.

In Table VI, the effect of total pressure on the enrichment is recorded for a mixture containing 50 mole per cent butadiene. The data show clearly that the enrichment reaches a maximum of 98% at a pressure of 5–6 mm. These data were measured at a flow rate of 1500 cm/sec. At lower flow rates the butadiene is less effective. In Table

TABLE VI

The effect of varying total pressure on the Hg^{202} enrichment in the solid product of the reaction of $Hg^{202}6(^3P_1)$ atoms, photoexcited in Hg^N, with flowing hydrogen chloride containing 50 mole per cent of butadiene (Linear flow rate = 1500 cm/sec. Incident light intensity = 65 units)

Pressure, mm	% Hg^{202}	Fractional enrichment
2.1	53	1.8
4.4	56	1.9
5.6	59	2.0
8.0	54	1.8
16.0	50	1.7
32.0	50	1.7

TABLE VII

The effect of varying total pressure on the Hg^{202} enrichment in the solid product of the reaction of $Hg^{202}6(^3P_1)$ atoms, photoexcited in Hg^N, with flowing hydrogen chloride, containing 50 mole per cent of butadiene (Linear flow rate = 94 cm/sec. Incident light intensity = 65 units)

Pressure, mm	% Hg^{202}	Fractional enrichment
4.0	41	1.4
6.7	52	1.7
10.7	50	1.7
32.0	50	1.7

VII the enrichments are given as a function of total pressure for the same mixture, at a flow rate of 94 cm/sec. The maximum enrichment of 74% occurs at 6–7 mm.

There are many isotopically degradative secondary processes which can be adduced to explain the fact that pure $Hg^{202}Cl$ is not obtained even in the presence of Cl-atom acceptors, such as butadiene. The most obvious of these degradative processes would be the gas phase exchange between $Hg^{202}Cl$ and Hg^N. Some information on the importance of this reaction was obtained by determining the effect upon the enrichment of subliming the calomel deposit a number of times during reaction. This sublimation procedure was carried out for a number of runs, and no difference could be detected, within the experimental error, from those runs in which the calomel product was allowed to accumulate during reaction. An example of the effect of sublimation is given in Table VIII.

The results of a number of runs at various butadiene concentrations and total reaction pressures are given in Table VIII. In none of the runs did the Hg^{202} content of the solid product exceed 59%, corresponding to an enrichment of 98%. From Table VIII it can be seen that higher butadiene concentrations are required at higher total pressures to achieve maximum enrichment.

In order to prevent overlap of the emission line on adjacent hyperfine absorption contours, the temperature of the lamp must be kept below 30° C (1). In this investigation the lamp temperature was maintained constant at 25.5±0.1° C. The uncooled lamp was found to operate at a temperature of approximately 50° C. The decrease in enrichment caused by using an uncooled source is shown in Table VIII. For a mixture containing 50 mole per cent of butadiene, at a total pressure of 4 mm, the enrichment dropped from 68% to 24%, when the cooling water to the lamp was shut off.

TABLE VIII

The effect of varying butadiene concentration and reaction pressure on the Hg^{202} enrichment in the solid product of the reaction of $Hg^{202}6(^3P_1)$ atoms, photoexcited in Hg^N, with flowing hydrogen chloride (Linear flow rate = 1500 cm/sec. Incident light intensity = 65 units)

Pressure, mm	Comp. mole %		% Hg^{202}	Fractional enrichment
	HCl	C_4H_6		
3.4	90	10	48	1.6
2.0	66	34	47	1.6
4.1	66	34	52	1.7
4.1	66	34	51	1.7*
2.8	50	50	45	1.5
4.0	50	50	37	1.2†
4.1	50	50	50	1.7
4.4	50	50	53	1.8
5.6	50	50	59	2.0
6.3	33	67	48	1.6
8.0	38	62	59	2.0

*Deposit sublimed three times during reaction.
†Lamp uncooled.

Since traces of air are difficult to eliminate completely in fast-flow systems, a study was made of the effect of adding known concentrations of dry air to various mixtures of hydrogen chloride and butadiene. The results are summarized in Table IX. It is

TABLE IX

The effect of varying concentrations of dry air on the Hg^{202} enrichment in the solid product of the reaction of $Hg^{202}6(^3P_1)$ atoms, photoexcited in Hg^N, with flowing hydrogen chloride – butadiene mixtures (Linear flow rate = 1500 cm/sec. Incident light intensity = 65 units)

Pressure, mm	Comp. mole %			% Hg^{202}	Fractional enrichment
	HCl	C_4H_6	Air		
4.2	67	16	17	48	1.6
4.5	59	31	10	52	1.7
4.9	54	29	17	55	1.8
4.9	41	41	18	50	1.7
4.8	28	57	15	44	1.5
7.7	19	71	10	39	1.3

apparent that concentrations of air in the 10–20 mole per cent range decrease slightly the maximum enrichment obtained. However, the effect is only slightly greater than the experimental reproducibility. It is therefore unlikely that traces of air would have any detectable effect on the enrichment values.

In Table X, the effect of varying linear flow rate is shown, for a mixture containing 50 mole per cent of butadiene, at a total reaction pressure of 16.0 mm. In comparing these data with those in previous tables for hydrogen chloride – butadiene mixtures, it should be noted that the light intensity is 60 units for the runs reported in Table X. Previous runs were made at a light intensity of 65 units. It will be noted from Table X that the Hg^{202} enrichment is independent of flow rate up to 750 cm/sec, at a value of $51 \pm 3\%$. However, at 1500 cm/sec, the enrichment has increased to 67%. The enrichment-enhancing effect of increasing linear flow rate is also apparent in comparing the

TABLE X

The effect of varying linear flow rate on the Hg^{202} enrichment in the solid product of the reaction of $Hg^{202}6(^3P_1)$ atoms, photoexcited in Hg^N, with flowing hydrogen chloride, containing 50 mole per cent of butadiene (Total pressure = 16.0 mm. Incident light intensity = 60 units)

Linear flow rate, cm/sec	% Hg^{202}	Fractional enrichment
188	46	1.5
375	45	1.5
750	44	1.5
1500	50	1.7

data in Tables VI and VII. The effect is most marked for pressures in the 4- to 6-mm range.

The effect of increasing incident light intensity was studied on a hydrogen chloride – butadiene mixture containing 50 mole per cent of butadiene. The total pressure was 4.0 mm and the linear flow rate, 1500 cm/sec. The light intensity was changed by interposing varying thicknesses of Vycor 7910 glass between lamp and cell. The data are given in Table XI. It can be seen that the enrichment increases, with increasing incident

TABLE XI

The effect of increasing incident light intensity on the Hg^{202} enrichment in the solid product of the reaction of $Hg^{202}6(^3P_1)$ atoms, photoexcited in Hg^N, with flowing hydrogen chloride, containing 50 mole per cent of butadiene (Total pressure = 4.0 mm. Linear flow rate = 1500 cm/sec)

Relative incident light intensity	% Hg^{202}	Fractional enrichment
22	48	1.6
30	50	1.7
34	51	1.7
57	53	1.8
68	56	1.9
95	58	1.9

intensity over the entire range of intensities studied.

The final reaction parameter studied was the effect of mercury saturation conditions on the enrichment. In the runs reported to this point in this study the condensers of the mercury saturator were maintained at 30.0±0.1° C. Six feet of pyrex tubing connected the top of the exit condenser to the reaction cell. In order to vary saturation conditions, the 6 ft of connecting tubing were enclosed in a water jacket. To abbreviate the description, the temperature of the exit condenser of the saturator will be referred to as T_c and that of the water-jacketed connecting tubing as T_T.

Normal procedure would correspond closely to $T_c = T_T = 30°$ C, since the uncooled connecting tubing was operated at laboratory temperature, which varied in our case from 28–30° C.

For the mercury saturation studies, a 50:50 v/v mixture of hydrogen chloride and butadiene was used, at a reaction pressure of 4.3 mm, a linear flow rate of 1500 cm/sec, and an incident light intensity of 60 units.

At $T_c = T_T = 30°$ C, sufficient calomel for analysis was obtained in 30 minutes. The average of four runs gave an Hg^{202} abundance of 56±2%. However, as the temperatures

of the water jackets were reduced the rate of deposition of calomel in the reaction zone was observed to decrease markedly. Thus with $T_c = T_T = 16°$ C, no calomel deposit was observed in four hours of irradiation. With $T_c = T_T = 20°$ C, two hours of irradiation were required before deposition was observed. With $T_c = 20°$ C, and $T_T = 28°$ C, sufficient calomel for analysis was obtained in 80 minutes of irradiation. The Hg^{202} content of the product was 50%. When both T_c and T_T were again raised to 30° C, sufficient calomel for analysis was again obtained in 30 minutes. The Hg^{202} content of the calomel was 58%.

In the final experiment on mercury saturation, the water was drained from the exit condenser of the saturator, and the water-jacketed connecting tubing was replaced by a short piece of uncooled tubing. Under these conditions droplets of mercury formed in the reaction cell, indicating supersaturation of the gas stream with mercury vapor. The average of three runs gave an Hg^{202} abundance of 56±1.5%.

DISCUSSION

In the reaction of $Hg^{202}6(^3P_1)$ atoms, photoexcited in Hg^N, with flowing hydrogen chloride, the fact that a calomel product is formed which is enriched in Hg^{202} can most obviously be explained by a dual primary process mechanism:

$$Hg^{202}6(^3P_1) + HCl \rightarrow Hg^{202}Cl + H \quad [1]$$

$$Hg^{202}6(^3P_1) + HCl \rightarrow Hg^{202} + H + Cl \quad [2]$$

$$Cl + Hg^N + M \rightarrow Hg^NCl + M. \quad [3]$$

Reaction [3] would of course require a third body M to remove heat of recombination.

On the basis of the above sequence, the relative rates of the two primary processes can be estimated from the enrichment data. From the mechanism it follows that the relative rate ratio:

$$R_{Hg^{202}Cl}/R_{Hg^NCl} = \Phi_1/\Phi_2$$

where Φ_1 and Φ_2 are the fractions of the absorbed radiation partitioned to reactions [1] and [2] respectively. The ratio Φ_1/Φ_2 can be calculated from the abundance data, since

$$R_{Hg^{202}Cl}/R_{Hg^NCl} = (A-29.8)/(100-A)$$

where A is the percentage abundance of Hg^{202} in the calomel, and 29.8 is the normal Hg^{202} abundance. From our data, the maximum value for $A = 44\%$, whence $\Phi_1/\Phi_2 = 0.25$. In short, reaction [2] is four times more important than reaction [1] at laboratory temperature.

The above calculations are based on the assumption that no isotopic degradation occurs either during reaction or during the recovery of the mercury for analysis. If we allow a maximum uncertainty of ±10% in the A value, the ratio of Φ_2/Φ_1 must be in the range of 3–6. A more detailed investigation of the hydrogen chloride reaction is now in progress in the laboratories of one of us (H.E.G.), as one result of which this ratio should be established more precisely.

The results, given in Table III, indicate that the Hg^{202} enrichment is unaffected by added nitrogen in concentrations up to 80 mole per cent. Although the quenching cross section of hydrogen chloride for $Hg6(^3P_1)$ atoms has not been measured, its value should be at least as large as that for methyl chloride. For methyl chloride and nitrogen, values of 24×10^{-16} cm^2 and 0.274×10^{-16} cm^2 respectively have been obtained (5). Assuming hydrogen chloride to have a quenching cross section of 24×10^{-16} cm^2, hydrogen chloride would be responsible for approximately 96% of the quenching in a mixture containing

80 mole per cent of nitrogen. Hence it would be necessary to study mixtures very much richer in nitrogen before the role of $Hg^{202}6(^3P_0)$ atoms in the reaction could be assessed.

The three-step sequence proposed for the reaction in pure substrate takes no specific cognizance of the fate of the H atoms produced in reactions [1] and [2]. Rodebush and Speakman (6) have postulated the reaction

$$H + HCl \rightarrow H_2 + Cl \qquad [4]$$

in the mechanism of recombination of H atoms in the presence of hydrogen chloride. If reaction [4] is included in the mechanism, the ratio Φ_1/Φ_2 would be increased from 0.25 to 0.67, since the steady-state calculation leads to the relation:

$$R_{Hg^{202}Cl}/R_{Hg^{N}Cl} = \Phi_1/(1+\Phi_2).$$

If we assume further that a recombination process of the type

$$H + Cl + M \rightarrow HCl + M \qquad [5]$$

occurs, the ratio Φ_1/Φ_2 will lie between 0.25 and 0.67. Studies now in progress should shed light on the importance of steps [4] and [5] to the isotopically specific reaction.

The marked enhancement of the enrichment occurring upon the addition of unsaturated compounds (U), such as butadiene and benzene, to the hydrogen chloride stream could involve reactions of both H atoms and Cl atoms with the unsaturated compounds:

$$Cl + U \rightarrow \text{Products}, \qquad [6]$$
$$H + U \rightarrow \text{Products}. \qquad [7]$$

The rapid reaction of H atoms with unsaturated compounds would be very important if reaction [4] has an appreciable effect on the Cl-atom concentration.

The fact that maximum enrichments of 98% were obtained with butadiene as addend, whereas benzene gave a maximum value of 85%, may indicate that reactions [6] and [7] are faster for butadiene than benzene.

When the lamp–wall temperature was raised from 25 to 50° C, a marked decrease in enrichment occurred. This effect is now being systematically investigated. Since the Doppler-broadening is proportional to the square root of the absolute temperature, it can be shown that an increase of 25° in lamp temperature would result in an increase of emission line width of only 0.1 mÅ. The separation of adjacent hyperfine absorption contours from that of Hg^{202} is about 10 mÅ (1). Hence, at this time, it is apparent that Doppler-broadening alone is insufficient to explain the effect of lamp temperature on the enrichment.

The fact that the addition of chlorobenzene to the hydrogen chloride stream depresses the enrichment indirectly substantiates the proposed mechanism. Quenching of the photoexcited mercury atoms by chlorobenzene apparently leads to the formation of chlorine atoms. The rate of $Hg^{N}Cl$ formation by reaction [3] would therefore be increased, and the over-all enrichment would be reduced.

Since sublimation of the calomel product during reaction did not significantly alter the enrichment, it appears unlikely that exchange reactions of the type:

$$Hg^{202}Cl + Hg^{N} \rightarrow Hg^{N}Cl + Hg^{202} \qquad [8]$$

are important in degrading the isotopic calomel before dimerization on the wall.

The failure to obtain enrichment under static conditions can be explained simply on the basis of the proposed mechanism. Under static conditions the unexcited mercury will become impoverished in Hg^{202} through reaction [1]. Hence the calomel formed in

reaction [3] will contain less than the normal abundance of Hg^{202}. The enrichment caused by reaction [1] will just correspond to the depletion by reaction [3]. The recovered calomel will therefore contain the normal abundance of Hg^{202}. Now as the linear flow rate is increased the Hg^{202}-depleting effect of reaction [1] on the unexcited mercury will become less and less important. The increase in enrichment with increasing linear flow rate therefore follows from this explanation.

Our findings indicate that, at high flow rates, the enrichment increases with increasing incident light intensity for the hydrogen chloride – butadiene mixtures. The explanation of this effect is not readily forthcoming from the proposed mechanism. It would appear wiser to postpone comment on the light intensity dependence until a more detailed study has been made of the hydrogen chloride – butadiene reaction.

The dependence of both the rate of calomel deposition and the Hg^{202} enrichment on the mercury concentration in the stream for the hydrogen chloride – butadiene reaction again emphasizes the complexity of this system. Since maximum enrichment and efficient calomel deposition are obtained only when the stream is slightly supersaturated with mercury vapor it appears that a layer of natural mercury must be adsorbed on the walls of the reaction vessel before the calomel can deposit. Further studies must be carried out on this system before an adequate explanation can be given for this behavior.

CONCLUSIONS

As a result of this investigation it has been firmly established that a fraction of the quenching collisions between $Hg^{202}6(^3P_1)$ atoms and hydrogen chloride forms a solid mercury compound. From stability considerations it is likely that the primary compound is $Hg^{202}Cl$ rather than $Hg^{202}H$.

From the Hg^{202}-enrichment data, and an assumed mechanism, it can be calculated that the isotopically specific portion of the primary reaction at 28–30° C is in the range 20–40%. It is likely that the two primary processes involve a common intermediate, Hg^{202}–Cl–H*. It would be expected that increasing reaction temperature would favor Cl-atom formation. Studies are now under way at the University of Alberta on the temperature coefficient of the primary reaction.

Further investigations are also in progress on the kinetics of the hydrogen chloride reaction in the presence of unsaturated addends.

ACKNOWLEDGMENTS

The authors would like to express their deep appreciation to Dr. Kenton R. Osborn, Dr. Willard F. Allen, and Mr. John A. Poole for many valuable discussions.

REFERENCES

1. OSBORN, K. R., McDONALD, C. C., and GUNNING, H. E. J. Chem. Phys. **26**, 124 (1957).
2. PERTEL, R. and GUNNING, H. E. J. Chem. Phys. **26**, 219 (1957).
3. PERTEL, R. and GUNNING, H. E. Can. J. Chem. **37**, 35 (1959).
4. OSBORN, K. R. and GUNNING, H. E. J. Opt. Soc. Am. **45**, 552 (1955).
5. DARWENT, B. and PHIBBS, M. J. Chem. Phys. **22**, 110 (1954).
6. RODEBUSH, W. H. and SPEAKMAN, M. L. J. Am. Chem. Soc. **57**, 1040 (1935).

REARRANGEMENT STUDIES WITH C^{14}

VII. THE ACETOLYSIS OF METHYL-C^{14}-ISOPROPYLCARBINYL *p*-TOLUENESULPHONATE[1]

A. J. Finlayson and C. C. Lee

ABSTRACT

Acetolysis of methyl-C^{14}-isopropylcarbinyl *p*-toluenesulphonate (I) at reflux temperature gave a mixture of 2-methyl-2-butene (II), 2-methyl-1-butene (III), and 3-methyl-1-butene (IV) with no isolatable quantity of substitution product. The relative amounts of olefins II, III, and IV were measured by gas–liquid chromatography to be 80%, 18%, and 2%, respectively, and these were substantially verified by estimations with the isotope dilution technique. When the acetolysis was carried out at 50° C, besides olefins II, III, and IV, present in relative amounts of 83%, 16%, and 1%, respectively, as determined by gas–liquid chromatography, a small quantity of substitution product, *t*-amyl acetate (V), was obtained. Under the conditions of acetolysis at reflux temperature, however, V was found to decompose to olefins II and III. Degradation of the olefinic products of acetolysis gave, among other compounds, radioactive acetone. Since acetone was derived from the chief product, II, its activity could be attributed to an isotope position rearrangement resulting from a 1,2-methide shift as one of the processes that gave rise to olefin II. This rearrangement amounted to about 2.5% and 0.9%, respectively, in olefin II from acetolysis at reflux temperature and at 50° C. Considering all these results, it may be concluded that both substitution and elimination reactions could take place during acetolysis of I. The substitution reaction proceeded with neighboring hydrogen participation to yield *t*-amyl acetate, which would decompose to olefins II and III at reflux temperature under the acetolysis conditions. In the E_1 reaction during acetolysis of I, processes involving no neighboring group participation to give olefins II and IV, with neighboring hydrogen participation to give olefins II and III, and with neighboring methyl participation to give isotopically rearranged olefins II and IV, all occurred, the process with neighboring hydrogen participation being predominant.

First-order reaction rates for the formolysis of methylisopropylcarbinyl *p*-toluenesulphonate and the acetolysis and formolysis of methylisopropylcarbinyl *p*-bromobenzenesulphonate have been reported by Winstein and Marshall (1) in connection with their studies on neighboring hydrogen and carbon participation. From considerations of relative rates for a series of related secondary sulphonates, it was concluded that there is some assistance to ionization from neighboring group participation during solvolyses of methylisopropylcarbinyl derivatives, though the driving force associated with participation in this system was said to be small (1). No clear-cut differentiation was made on whether participation was from neighboring hydrogen or carbon, nor were any reaction products isolated. In the present work, the acetolysis of methyl-C^{14}-isopropylcarbinyl *p*-toluenesulphonate (I) was carried out, the reaction products identified, and the degrees of isotope position rearrangement determined so as to shed some light on the different routes the reaction may follow during acetolysis.

RESULTS AND DISCUSSIONS

Methyl-C^{14}-isopropylcarbinol was prepared from reaction of isobutyraldehyde with methyl-C^{14}-magnesium iodide. On subjecting this carbinol to the haloform reaction, non-radioactive isobutyric acid was obtained, indicating that all the C^{14} activity was on the methyl carbon. Conversion of the carbinol to sulphonate I was effected by treatment with *p*-toluenesulphonyl chloride in pyridine.

Acetolysis of I at reflux temperature yielded only olefinic products. No acetate fraction could be isolated. The olefins were shown by gas–liquid chromatographic analysis (2), and verified by isotope dilution, to be a mixture of 2-methyl-2-butene (II), 2-methyl-1-

[1]*Manuscript received January 16, 1959.*
Contribution from the Department of Chemistry, University of Saskatchewan, Saskatoon, Saskatchewan.

butene (III), and 3-methyl-1-butene (IV), the relative proportions of these are given in Table I. When the acetolysis was carried out at 50° C, besides olefins II, III, and IV (Table I), a small amount of *t*-amyl acetate (V), but no methylisopropylcarbinyl acetate (VI), was obtained. On subjecting V to treatment under conditions as in the acetolysis at reflux temperature, V decomposed to olefins II and III. There was no decomposition of VI under a similar treatment.

TABLE I

Relative amounts of olefins from acetolyses of methyl-C^{14}-isopropylcarbinyl *p*-toluenesulphonate

Reaction	Olefin	% Composition		
		Analyzed by gas chromatography	Analyzed by radioactivity	
			Run 1	Run 2
Acetolysis at reflux temp.	2-Methyl-2-butene	80	82.8	82.5
	2-Methyl-1-butene	18	14.8	13.8
	3-Methyl-1-butene	2	2.4	3.7
Acetolysis at 50° C	2-Methyl-2-butene	83	79	76
	2-Methyl-1-butene	16		
	3-Methyl-1-butene	1		

Degradations of olefins II, III, and IV are shown by reaction sequences 1–3, the C^{14} labels being indicated on positions as if there were no isotope position rearrangement.

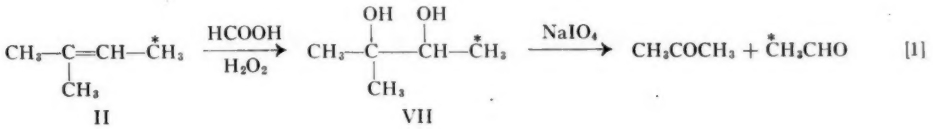

II VII [1]

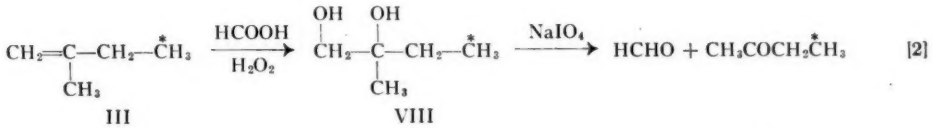

III VIII [2]

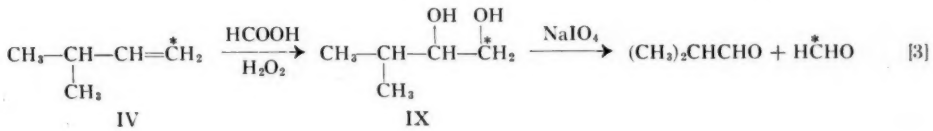

IV IX [3]

When a mixture of II, III, and IV was degraded according to these schemes, the products consisted of a mixture of formaldehyde, acetaldehyde, isobutyraldehyde, acetone, and methyl ethyl ketone. Separation of these carbonyl compounds as their 2,4-dinitrophenylhydrazones was effected by adsorption chromatography in a column packed with a 2:1 mixture of silicic acid and celite (3). Desired bands of individual 2,4-dinitrophenylhydrazones were recovered by elution with petroleum ether containing some diethyl ether. Alternatively, the aldehydes in the mixture of carbonyl compounds were first oxidized with potassium permanganate (4) before the chromatographic separation of acetone and methyl ethyl ketone as their 2,4-dinitrophenylhydrazones.

For measurements of relative amounts of II, III, and IV by isotope dilution, non-labeled olefin II was obtained by distillation of the commercial material through a long column. Non-labeled olefins III and IV were prepared by the Chugaev reaction with *sec*-butylcarbinol and isobutylcarbinol, respectively (5). From these olefins, inactive glycols VII, VIII, and IX were obtained. The purity of each of these glycols was demonstrated by their cleavage with sodium metaperiodate to give only the expected carbonyl compounds.

The isotope dilution experiments were carried out by adding a known quantity of inactive glycol VII, VIII, or IX to a weighed mixture of VII, VIII, and IX derived from the olefins obtained in an acetolysis. The diluted mixture was cleaved with sodium metaperiodate and the 2,4-dinitrophenylhydrazones of the most abundant products isolated from the chromatographic column. Radioactivity assays of these diluted products of degradation provided data from which the relative amounts of II, III, and IV in the original products of acetolysis can be calculated. For example, in isotope dilution run No. 1, the mixture of olefins II, III, and IV from an acetolysis at reflux temperature was converted to a mixture of glycols VII, VIII, and IX. To 0.0580 g of this glycol mixture, 0.2279 g of inactive VII was added. After degradation and separation by adsorption chromatography, the 2,4-dinitrophenylhydrazones of acetaldehyde and acetone were isolated. Radioactivity assay gave specific activity of 8704 c.p.m. on a molar basis[2] for the 2,4-dinitrophenylhydrazone of acetaldehyde. Since gas–liquid chromatography indicated 80% II in the olefin mixture from acetolysis at reflux temperature, it is reasonable to assume that of the 0.0580 g of undiluted active glycol mixture, 80% was VII. Hence the total activity of the acetaldehyde from 0.0580 g of undiluted glycol mixture is equivalent to $8704\times(0.2279+0.80\times0.0580)$ c.p.m. Correcting to a common basis of 1 g of undiluted active glycol mixture, the corrected activity for the acetaldehyde fraction would be

$$\frac{8704\times(0.2279+0.80\times0.0580)}{0.0580} = 41{,}200 \text{ c.p.m.}$$

Similarly, the corrected activity for the acetone was found to be 1120 c.p.m.

In an analogous way, the active glycol mixture was diluted with inactive VIII or IX. From dilution with VIII, the 2,4-dinitrophenylhydrazones of methyl ethyl ketone and formaldehyde were isolated, while from dilution with IX, only the 2,4-dinitrophenylhydrazone of formaldehyde was eluted for activity assay. Radioactivity data from these experiments as well as from a duplicate run are summarized in Table II.

Since formaldehyde is formed from degradation of both VIII and IX, the activity in the formaldehyde would be derived from both VIII and IX in the undiluted active glycol mixture. The corrected activity for formaldehyde from dilution experiment with either inactive VIII or IX should, therefore, be identical. The actual data (Table II) showed small differences in corrected activities calculated for the two formaldehyde samples from each run. Possibly, in the chromatographic separation of the 2,4-dinitrophenylhydrazones, slight contamination of the formaldehyde derivative by the more highly active derivative of acetaldehyde may contribute to these differences. In any case, the magnitude of the differences between corrected activities of formaldehyde samples, of the order of 300 c.p.m. compared to the total corrected activities for all fractions of around 40,000 to 50,000 c.p.m., should not materially affect the over-all calculation of the relative amounts of olefins II, III, and IV.

[2]*See footnote* †, *Table II.*

TABLE II

Data from isotope dilution of the mixture of glycols derived from the olefins obtained in acetolyses at reflux temperature

Wt. of active glycols (g)		Wt. of inactive diluent (g)		Inactive diluent used	Degradation product assayed	Specific activity (c.p.m. on molar basis†)		Corrected activity per gram of glycol mixture (c.p.m.)		Percentage of total activity‡		Percentage rearrangement in 2-methyl-2-butene	
Run 1	Run 2	Run 1	Run 2			Run 1	Run 2	Run 1	Run 2	Run 1	Run 2	Run 1	Run 2
0.0580	0.0732	0.2279	0.3113	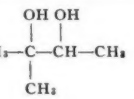	CH_3CHO	8704	6310	41200	31900	80.6	80.5		
					CH_3COCH_3	236	157	1120	800	2.2	2.0	2.6	2.4
0.1078	0.0210	0.1853	0.3105	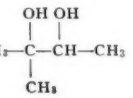	CBr_4*	567	69	1370	1070	2.7	2.7		
0.0845	0.0877	0.1734	0.2177	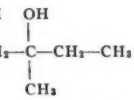	$CH_3COCH_2CH_3$	3400	2052	7580	5470	14.8	13.8		
					HCHO	689	658	1550	1770	3.0	4.5		
0.0975	0.0666	0.1355	0.1079	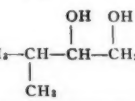	HCHO	781	796	1240	1450	2.4	3.7		

*From reaction of ketonic products with bromine and sodium hydroxide.

†Specific activities in c.p.m. on a molar basis were determined by converting all compounds to barium carbonate and counted as infinitely thick samples of constant geometry in a gas flow Geiger counter. Correction for the presence of non-labeled carbon atoms was made by multiplying the observed activity with the number of carbon atoms per molecule in the compound assayed (6). In the case of CBr_4, the observed activity was multiplied by 2, since acetone has two equivalent methyl groups. All samples were counted for sufficient lengths of time so that statistical errors were within ±2% of the observed activities.

‡The total activity was taken as the sum of the corrected activities of CH_3CHO, CH_3COCH_3, $CH_3COCH_2CH_3$, and HCHO from dilution with inactive 3-methyl-1,2-butanediol. The percentage of total activity in CH_3CHO and CH_3COCH_3 is a measure of the amount of 2-methyl-2-butene in the mixture of olefins from the acetolysis. The percentage of total activity in $CH_3COCH_2CH_3$ and in HCHO from dilution with inactive 3-methyl-1,2-butanediol is taken as measures of 2-methyl-1-butene and 3-methyl-1-butene, respectively.

For the estimation of the relative amounts of olefins II, III, and IV in the original acetolysis products, the total corrected activities of acetaldehyde, acetone, methyl ethyl ketone, and one sample of formaldehyde were taken as representing the total activity of olefins II, III, and IV. The sum of the corrected activities of acetaldehyde and acetone was used as a measure of II, while the corrected activities of methyl ethyl ketone and formaldehyde were used as measures of III and IV, respectively. Since formaldehyde could actually be derived from both III and IV, and since any active formaldehyde from III would have to arise from an isotopically rearranged III, it may be reasonably assumed that any activity of the formaldehyde from III would be small compared to the activity of methyl ethyl ketone. The use of the corrected activity of methyl ethyl ketone alone as a measure of III is, therefore, an acceptable approximation. For these same reasons, the use of the corrected activity of formaldehyde as a measure of IV is also only a good approximation. Furthermore, it should also be pointed out that although the degradation of IV should give rise to formaldehyde and isobutyraldehyde, the activity in the isobutyraldehyde, if any, should be negligibly small, as active isobutyr-

aldehyde could only result from an isotopically rearranged IV. In Table II, the corrected activities of a number of degradation products are expressed as percentages of total activity. The percentage of total activity for both acetaldehyde and acetone together would be equivalent to the amount of II and the percentages of total activity for methyl ethyl ketone and formaldehyde would be equivalent to the amounts of III and IV, respectively, in the original acetolysis products. These estimated relative amounts of II, III, and IV are also given in Table I for comparison with results from gas–liquid chromatography.

The fact that there was some activity in the acetone fraction from these isotope dilution experiments indicated that there was some isotope position rearrangement in the major acetolysis product, 2-methyl-2-butene (II). For acetolysis at reflux temperature run No. 1, this rearrangement amounted to

$$\frac{1120}{1120+41200}\times 100 = 2.6\%.$$

In the duplicate run, the rearrangement was 2.4% (Table II). This rearrangement very likely arose from a 1,2-methide shift, or neighboring methyl participation, resulting in an acetone with C^{14} on the methyl carbons:

$$CH_3{-}\underset{\displaystyle CH_3}{\underset{|}{CH}}{-}\overset{+}{C}H{-}\overset{*}{C}H_3 \xrightleftharpoons{CH_3\ \text{shift}} CH_3{-}\overset{+}{C}H{-}\underset{\displaystyle CH_3}{\underset{|}{CH}}{-}\overset{*}{C}H_3$$

Collaboration of such a reaction path may be deduced from the following experiment. A sample of the active mixture of glycols VII, VIII, and IX derived from the products of an acetolysis at reflux temperature was diluted with inactive VII and then cleaved with sodium metaperiodate. The resulting mixture of carbonyl compounds was treated with neutral potassium permanganate to destroy the aldehydes (4). An aqueous solution of the remaining acetone and methyl ethyl ketone was recovered by distillation and then treated with bromine and sodium hydroxide to give carbon tetrabromide. The corrected activities of the carbon tetrabromide samples are also included in Table II. If much of the acetone activity were located on the carbonyl carbon, one would expect the corrected activity of the carbon tetrabromide to be less than that of the acetone. Actually, for a given run, carbon tetrabromide showed somewhat greater activity than acetone (Table II). This extra activity in the carbon tetrabromide very likely was derived from the methyl group of methyl ethyl ketone, indicating that there was also a small degree of isotope position rearrangement in 2-methyl-1-butene (III), another product from the acetolysis of I.

When acetolysis of I was carried out at 50° C, as mentioned earlier, a small amount of *t*-amyl acetate was obtained besides a mixture of olefins II, III, and IV. The relative amounts of II, III, and IV, as measured by gas–liquid chromatography, are given in Table I. In addition, the major product, II, was estimated by radioactivity measurements. As before, olefins II, III, and IV from a given run were converted to the glycol mixture, VII, VIII, and IX. This mixture, without dilution, was degraded in the usual manner and the 2,4-dinitrophenylhydrazones of acetaldehyde and acetone isolated from the adsorption chromatographic column. Activity assays on these degradation products as well as on the glycol mixture were carried out. The results from duplicate acetolyses at 50° C are tabulated in Table III. From these results, the isotope position rearrangement in II, as indicated by the activity of the acetone, was calculated (Table III). The sum of

the activities of acetaldehyde and acetone in a given run is, of course, a measure of the amount of II in the original mixture of olefins II, III, and IV. This estimate of II is also listed in Table I for comparison with gas–liquid chromatographic data.

TABLE III

Radioactivity data from acetolyses at 50° C

	Specific activity (c.p.m. on molar basis)		Percentage of total activity		Percentage rearrangement in 2-methyl-2-butene	
Compound assayed	Run 1	Run 2	Run 1	Run 2	Run 1	Run 2
Glycol mixture from olefinic products	8790	10860	100	100		
CH_3CHO	6900	8125	79	76	0.9	0.9
CH_3COCH_3	62	74				

CONCLUSIONS

From the results presented in the foregoing sections and summarized in Tables I, II, and III, it is clear that a number of reaction routes may be followed in the acetolysis of methyl-C^{14}-isopropylcarbinyl *p*-toluenesulphonate (I). At 50° C, some substitution involving neighboring hydrogen participation took place, giving rise to *t*-amyl acetate (V) as depicted in reaction [4]:

$$\underset{\text{I}}{CH_3{-}CH(CH_3){-}CH(OTs){-}{}^{*}CH_3} + HOAc \longrightarrow \underset{\text{V}}{CH_3{-}C(CH_3)(OAc){-}CH_2{-}{}^{*}CH_3} + TsOH \qquad [4]$$

At reflux temperature, if such a substitution reaction did occur, the product, V, would decompose to olefins II and III. By far the major part of the acetolysis products resulted from elimination reactions. To explain the formation of the various elimination products, processes similar to some of those involved in the E_1 reaction in the acetolysis of the diastereoisomers of 3-phenyl-2-butyl *p*-toluenesulphonate (7) may be postulated. Three processes, depicted by reaction sequences 5, 6, and 7, definitely occurred.

$$\text{I} \xrightarrow{-OTs^-} \underset{\text{X}}{CH_3{-}CH(CH_3){-}{}^{+}CH{-}{}^{*}CH_3} \xrightarrow{-H^+} \underset{\text{II}}{CH_3{-}C(CH_3){=}CH{-}{}^{*}CH_3} + \underset{\text{IV}}{CH_3{-}CH(CH_3){-}CH{=}{}^{*}CH_2} \qquad [5]$$

$$\text{I} \xrightarrow{-OTs^-} \underset{\text{XI}}{CH_3{-}{}^{+}C(CH_3){-}CH_2{-}{}^{*}CH_3} \xrightarrow{-H^+} \underset{\text{II}}{CH_3{-}C(CH_3){=}CH{-}{}^{*}CH_3} + \underset{\text{III}}{CH_2{=}C(CH_3){-}CH_2{-}{}^{*}CH_3} \qquad [6]$$

$$\text{I} \xrightarrow{-OTs^-} \underset{\text{X}_r}{CH_3{-}{}^{+}CH{-}CH({}^{*}CH_3){-}CH_3} \longrightarrow \underset{\text{II}_r}{CH_3{-}CH{=}C({}^{*}CH_3){-}CH_3} + \underset{\text{IV}_r}{CH_2{=}CH{-}CH({}^{*}CH_3){-}CH_3} \qquad [7]$$

(Subscript r is used to denote isotopically rearranged X, II, and IV.)

Reaction [5] involves ionization of I without anchimeric assistance to secondary carbonium ion X, which gave rise to olefins II and IV. Reaction [6] involves ionization of I with anchimeric assistance from neighboring hydrogen participation resulting in tertiary carbonium ion XI, which gave olefins II and III. Reaction [7] involves ionization of I with anchimeric assistance from neighboring methyl participation to give isotopically rearranged X_r, which resulted in the formation of isotopically rearranged olefins II_r and IV_r. According to Saytzeff's rule (8), one would expect a greater amount of II (or II_r) formed in each of these processes. It is, therefore, not surprising to have found that olefin II was the chief isolatable product from the acetolysis mixture. Of these processes of elimination, reaction [6] may be considered as most important, or as having occurred to the greatest extent, since olefin IV, a measure of reaction [5], and isotopically rearranged II_r, a measure of reaction [7], each amounted to only 2–4% of the over-all reaction products for acetolysis at reflux temperature. Still less IV and II_r, in the order of 1%, were found in the products of acetolysis at 50° C.

On the basis of the present results, it is, of course, not possible to differentiate, that in the neighboring hydrogen and methyl participations, whether the processes involved a series of 1,2-shifts in concrete stages with ion X as the first intermediate (reaction sequences 8 and 9), or whether ions XI and X_r were formed directly from I. Nor can one decide whether non-classical carbonium ions XII and XIII play any role in these reactions, for the present results can be explained with or without postulating the existence of XII and XIII.

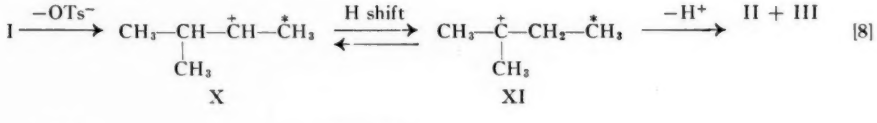

[8]

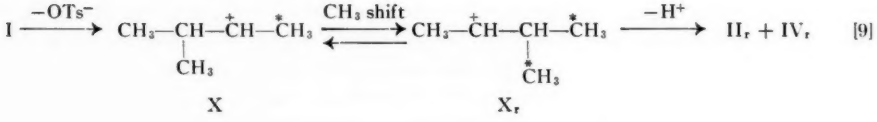

[9]

It may be recalled that in the degradation of acetone and methyl ethyl ketone to carbon tetrabromide in acetolysis runs 1 and 2 at reflux temperature (Table II), the corrected activity of the carbon tetrabromide was somewhat higher than that of the corresponding acetone. If one were to consider this difference significant and attribute the extra activity in the carbon tetrabromide as arising from the methyl carbon of methyl ethyl ketone, a process involving first a 1,2-methide shift followed by a 1,2-hydride shift would have to be postulated (reaction sequence [10]):

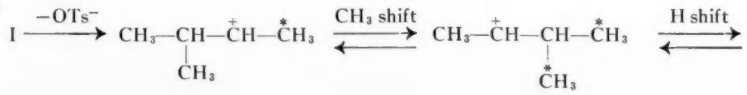

$$CH_3-CH_2-\overset{+}{C}(\overset{*}{CH_3})-\underset{*}{CH_3} \xrightarrow{-H^+} CH_3-CH=C(\overset{*}{CH_3})-\underset{*}{CH_3} + CH_3-CH(\underset{*}{CH_3})-C=\overset{*}{CH_2} \qquad [10]$$

XI$_r$ II$_r$ III$_r$

Methyl ethyl ketone with C^{14} activity on the methyl carbon would thus result from the isotopically rearranged olefin III$_r$.

In summary, it may be concluded that in the acetolysis of methyl-C^{14}-isopropylcarbinyl *p*-toluenesulphonate (I), both substitution and elimination reactions take place. The substitution proceeds with neighboring hydrogen participation, resulting in the formation of *t*-amyl acetate, which will decompose to olefins at reflux temperature under the acetolysis conditions. In the E_1 reaction during the acetolysis of I, processes involving no neighboring group participation, neighboring hydrogen participation, and neighboring methyl participation all occur, with neighboring hydrogen participation predominant. A process involving first a 1,2-methide shift followed by a 1,2-hydride shift before olefin formation may also take place, though the experimental results only indicate a probability, without an unequivocal proof, of such a reaction route. These conclusions are in excellent agreement with the recent finding of Winstein and Takahashi (9) that the acetolysis of I has a relatively high value of k_Δ/k_s, the ratio of rate constants for anchimerically assisted and unassisted solvolysis processes. These workers attributed k_Δ to neighboring hydrogen participation and accounted for the earlier observation of a low degree of rate acceleration (1) on conformational considerations. Their kinetic studies, however, failed to show the smaller contribution to k_Δ from neighboring methyl participation clearly demonstrated by the present data.

EXPERIMENTAL

Methyl-C^{14}-isopropylcarbinol

Methyl-C^{14}-isopropylcarbinol was prepared by the reaction of isobutyraldehyde with methyl-C^{14}-magnesium iodide. The procedure used was similar to that described for the synthesis of 2-butanol-1-C^{14} (10). A typical preparation is as follows:

Methyl-C^{14}-magnesium iodide, prepared from 13.0 g (0.092 moles) of methyl-C^{14} iodide and 2.9 g (0.12 moles) of magnesium in 180 ml of anhydrous ether, was maintained at −20° C in a dry-ice bath. A solution of 10.8 g (0.15 moles) of freshly distilled isobutyraldehyde in 180 ml of anhydrous ether was added dropwise over a period of 2 hours. The mixture was brought to 0° C and 20 ml of a saturated solution of ammonium chloride was added. The ether layer was separated and the aqueous layer and the precipitated salts were extracted several times with ether. The combined extract was dried over magnesium sulphate, the ether removed, and the residue distilled to give 5.30 g (66%) of the carbinol, b.p. 107–109° C (uncorrected), 3,5-dinitrobenzoate derivative, m.p. 74–75° C (lit. (11*a*), m.p. 76° C).

Isobutyric Acid from Methyl-C^{14}-isopropylcarbinol

A haloform reaction between the carbinol and bromine in sodium hydroxide solution was carried out using a procedure analogous to that employed in the preparation of trimethylacetic acid from pinacolone (12). From 2.80 g (0.032 moles) of methyl-C^{14}-isopropylcarbinol, 1.85 g (65%) of isobutyric acid was obtained. A derivative, the *p*-bromophenacyl ester, showed a m.p. of 77° C (lit. (11*b*), m.p. 77° C). Radioactivity assay showed that this isobutyric acid contained no activity, indicating that all the C^{14} was located on the methyl carbon of methylisopropylcarbinol.

Methyl-C^{14}-isopropylcarbinyl p-Toluenesulphonate

Methyl-C^{14}-isopropylcarbinyl *p*-toluenesulphonate was prepared from the carbinol by treatment with *p*-toluenesulphonyl chloride in pyridine (13). The product, recrystallized twice from petroleum ether chilled in a dry-ice bath, melted at 20–21° C (lit. (1), m.p. 20.1–20.8° C); the yields obtained were in the order of 60% of theoretical.

Acetolysis of Methyl-C^{14}-isopropylcarbinyl p-Toluenesulphonate

Anhydrous acetic acid containing 0.1 *M* potassium acetate was prepared by refluxing freshly distilled acetic acid, acetic anhydride, and potassium carbonate as described by Cram and Allinger (14). This solution was used for all acetolysis runs. Duplicate acetolyses at reflux temperature and at 50° C were carried out. Typical procedures are given below:

A. Acetolysis at Reflux Temperature

A mixture of 7.15 g (0.030 moles) of methyl-C^{14}-isopropylcarbinyl *p*-toluenesulphonate, 60 ml of anhydrous acetic acid containing 0.1 *M* potassium acetate, and an additional 3.0 g (0.031 moles) of potassium acetate sufficient to neutralize all liberated *p*-toluenesulphonic acid was heated under reflux for 3.5 hours. During the refluxing, the system was flushed with dry nitrogen and any condensable products entrained by the nitrogen were recovered in a dry-ice cooled trap. After the refluxing, the reaction mixture was cooled and extracted with a 3:1 mixture of petroleum ether and ether. The extract was washed with dilute sodium carbonate solution and dried, and the solvent removed. No residue remained, indicating no isolatable quantity of substitution product.

The olefin mixture recovered in the dry-ice cooled trap weighed 1.70 g (82%). It decolorized bromine in carbon tetrachloride very readily. It was distilled once, b.p. 35–38° C, before being used for subsequent analyses by gas chromatography and isotope dilution.

B. Acetolysis at 50° C

A mixture of 13 g (0.054 moles) of methyl-C^{14}-isopropylcarbinyl *p*-toluenesulphonate, 130 ml of anhydrous acetic acid containing 0.1 *M* potassium acetate, and an additional 6.0 g (0.061 moles) of potassium acetate was maintained at 50±1° C and constantly stirred for 14 hours. The olefins formed (1.25 g) were swept out by nitrogen and collected in a dry-ice cooled trap. These olefins were also distilled once, b.p. 35–38° C, before being analyzed.

For the recovery of the product of substitution, the reaction mixture from the acetolysis was poured into 250 g of ice and water and extracted with ether. The extract was washed with water and with dilute sodium carbonate until the washing remained basic. The washed extract was dried and the ether removed. From the colorless residue, a fraction (0.220 g) boiling at 117–118° C was obtained. Its infrared spectrum was identical with that of *t*-amyl acetate and different from that of methylisopropylcarbinyl acetate.

The residue remaining after the distillation of the acetate weighed 4.6 g. On crystallization, 4.0 g of unreacted methyl-C^{14}-isopropylcarbinyl *p*-toluenesulphonate was recovered. Based on the 9.0 g of sulphonate that was not recovered, the yield of olefins was 48% and the yield of *t*-amyl acetate was 4.6%.

Treatment of t-Amyl Acetate in Refluxing Acetolysis Mixture

A mixture of 6.0 g (0.046 moles) of *t*-amyl acetate, prepared from a reaction of *t*-amyl alcohol with acetic anhydride in the presence of zinc chloride (15), 60 ml of anhydrous acetic acid containing 0.1 *M* potassium acetate, and an additional 3.0 g of potassium acetate was gently refluxed for 3.5 hours. The volatile product, which proved to be a

60:40 mixture of 2-methyl-2-butene (II) and 2-methyl-1-butene (III) according to gas–liquid chromatographic analysis, was swept out by nitrogen and collected in a dry-ice cooled trap as in the acetolysis. The appearance of this olefinic mixture at various time intervals is recorded below:

Time (hours)	Weight of olefins (g)	% Yield
1.5	0.54	17
2.5	0.81	25
3.5	0.97	30

From the reaction mixture, 2.31 g (39%) of unchanged *t*-amyl acetate was recovered.

Treatment of Methylisopropylcarbinyl Acetate in Refluxing Acetolysis Mixture

Methylisopropylcarbinyl acetate was prepared from acetylation of the alcohol with acetyl chloride in pyridine. Treatment of this acetate in the refluxing acetolysis mixture as described for *t*-amyl acetate gave no olefinic product in 3 hours. On working up of the resulting mixture, unchanged acetate was recovered in 80% yield.

Gas–Liquid Chromatography

The olefinic mixture from acetolysis at reflux temperature or at 50° C was analyzed by gas–liquid chromatography. The column was packed with dinonyl phthalate supported on ground firebrick. The olefins passed through the column with helium as carrier gas. The effluent was analyzed by a thermal conductivity cell with the results automatically recorded. Three peaks were obtained corresponding to the three olefins, 2-methyl-2-butene (II), 2-methyl-1-butene (III), and 3-methyl-1-butene (IV). The areas under these peaks were used as measures of the relative amounts of these olefins. The results are tabulated in Table I.

The olefinic product from the treatment of *t*-amyl acetate in the refluxing acetolysis mixture was also analyzed. Only two peaks, corresponding to a 60:40 mixture of II and III, were observed.

Preparations of Non-radioactive Olefins II, III, and IV

2-Methyl-2-butene (II) was obtained from a commercial sample by careful fractionation through an efficient column (16). 2-Methyl-1-butene (III) and 3-methyl-1-butene (IV) were prepared from *sec*-butylcarbinol and isobutylcarbinol, respectively, by the Chugaev reaction according to the modified method described by Whitmore and Simpson (5). These authors (5) reported the details on the reaction with isobutylcarbinol. In the reaction with *sec*-butylcarbinol, from 22.5 g (0.26 moles) of the carbinol treated with equimolar quantities of sodium hydroxide, carbon disulphide, and methyl iodide, the methylxanthate of *sec*-butylcarbinol obtained weighed 32.8 g (73%), b.p. 107–110° C at 15–17 mm, n_D^{25} 1.5225. Anal. Calc. for $C_7H_{14}OS_2$: C, 47.2%; H, 7.92%; S, 36.0%. Found: C, 47.1%; H, 7.72%; S, 35.8%. This xanthate was decomposed at reflux temperature to give a 42% yield of 2-methyl-1-butene (III).

Degradation of Olefins II, III, and IV

Olefin II, III, or IV was degraded by conversion to the corresponding glycol with performic acid (formic acid and hydrogen peroxide) followed by the cleavage of the glycol with sodium metaperiodate to give carbonyl compounds. The procedures used were similar to those described by Roberts, McMahon, and Hine (4) for their degradation

of isotopically labeled 2-methyl-2-butene (II). The carbonyl compounds, recovered as an aqueous solution by distillation after the reaction with sodium metaperiodate, were converted to the 2,4-dinitrophenylhydrazones which were, in turn, separated by adsorption chromatography. A typical chromatographic separation is as follows:

The chromatographic column, 2.2 cm in diameter and 25 cm in length, was packed with a mixture of silicic acid and celite (2:1 by weight) as described by Gordon and co-workers (3). A 20-mg sample of the 2,4-dinitrophenylhydrazones derived from the degradation of 2-methyl-1-butene (III) was dissolved in 3 ml of chloroform and placed on the top of the column. After the material was adsorbed, 100 ml of low-boiling petroleum ether was added and allowed to percolate into the column under a slight nitrogen pressure. The bands of 2,4-dinitrophenylhydrazones were developed with a 2% solution of diethyl ether in petroleum ether and then eluted by gradually increasing the diethyl ether concentration to 12%. Flow of the solvent was aided by maintaining a nitrogen pressure of about 2 p.s.i.g. on the reservoir of solvent on top of the column. Two bands were eluted. The eluant containing each band was concentrated to about 10 ml whereby the 2,4-dinitrophenylhydrazone crystallized. From the first band, 12.5 mg (90%) of methyl ethyl ketone – 2,4-dinitrophenylhydrazone was recovered. It melted alone and on admixture with an authentic sample at 116–117° C. The second band gave 5.0 mg (80%) of formaldehyde – 2,4-dinitrophenylhydrazone which melted at 161° C. It did not show any melting-point depression when mixed with an authentic sample. No other material was recovered from the column, indicating that the 2-methyl-1-butene (III) degraded was pure.

Similarly, degradation of 2-methyl-2-butene (II) or 3-methyl-1-butene (IV) gave only the 2,4-dinitrophenylhydrazones of the expected carbonyl compounds after the chromatographic separation.

Isotope Dilutions and Degradations of Olefinic Products from Acetolyses at Reflux Temperature

The mixture of radioactive olefins II, III, and IV obtained from each of the duplicate acetolyses at reflux temperature was converted to the corresponding mixture of active glycols, 2-methyl-2,3-butanediol (VII), 2-methyl-1,2-butanediol (VIII), and 3-methyl-1,2-butanediol (IX) by treatment with performic acid (4). Known quantities of this mixture were diluted with weighed amounts of non-radioactive glycol VII, VIII, or IX and then cleaved to give carbonyl compounds. The cleavage was effected by the method of Reeves (17) instead of that of Roberts and co-workers (4) because the former method gave better yields. Details of a typical dilution and degradation are given below:

To 0.0580 g (0.00056 moles) of the mixture of active glycols, derived from acetolysis at reflux temperature run No. 1, was added 0.2279 g (0.0022 moles) of inactive 2-methyl-2,3-butanediol (VII). This diluted glycol mixture was dissolved in 10 ml of water and treated with 10 ml of 0.03 *N* periodic acid and 10 ml of 1 *N* sodium bicarbonate. After it had been left standing at room temperature for 1 hour, the reaction mixture was treated with 10 ml of 1 *N* hydrochloric acid and 10 ml of 1 *N* sodium arsenite solution to destroy the iodine formed. The resulting solution was distilled and the distillate containing the carbonyl compounds was trapped in a dry-ice cooled receiver. This distillate was poured into 250 ml of 2 *N* hydrochloric acid containing 1.20 g (0.006 moles) of 2,4-dinitrophenylhydrazine and allowed to stand for 1 hour at 0° C. The 2,4-dinitrophenylhydrazones formed weighed 1.00 g (79% of the theoretical calculated on the assumption that the diluted glycol mixture was pure 2-methyl-2,3-butanediol). Part of

these 2,4-dinitrophenylhydrazones was separated, in 50-mg lots, by chromatography in the silicic acid – celite column as previously described. In this particular dilution experiment in which the diluent was inactive VII, the 2,4-dinitrophenylhydrazones of the major degradation products, acetaldehyde and acetone, were isolated from the column and assayed for radioactivity.

Similarly, other portions of the same mixture of active glycols were diluted with inactive glycol VIII or IX and cleaved to give carbonyl compounds which were separated as their 2,4-dinitrophenylhydrazones by chromatography. A fresh silicic acid – celite column was used for each separation. In the dilution with inactive 2-methyl-1,2-butanediol (VIII), the 2,4-dinitrophenylhydrazones of formaldehyde and methyl ethyl ketone were recovered for radioactivity assays. In the dilution with inactive 3-methyl-1,2-butanediol (IX), only the 2,4-dinitrophenylhydrazone of formaldehyde was recovered and its radioactivity measured.

The entire process was repeated using the mixture of active glycols derived from acetolysis at reflux temperature run No. 2.

The radioactivity data are summarized in Table II.

Carbon Tetrabromide from the Ketonic Degradation Products

A portion (0.1078 g) of the mixture of active glycols derived from acetolysis at reflux temperature run No. 1 was diluted with 0.1853 g of inactive 2-methyl-2,3-butanediol (VII) and then cleaved with periodic acid as described above. The solution of carbonyl compound obtained was treated with dilute potassium permanganate solution until the purple color persisted for 1 hour. The excess permanganate was reduced by a few drops of 4% sodium bisulphite and the manganese dioxide removed by filtration. This treatment effectively destroyed all the aldehydes (4). The filtrate was distilled to give a solution containing only the ketonic degradation products, acetone and methyl ethyl ketone. This distillate was added dropwise to a stirred solution of 3.5 g of bromine in 65 ml of 10% sodium hydroxide maintained at 5° C. After the addition, stirring was continued at room temperature for 3 hours. The precipitated carbon tetrabromide was recovered by steam distillation and purified by sublimation. The yield was 0.25 g, m.p. 91–92° C (lit. (11*c*), m.p. 92° C).

A similar reaction using the mixture of active glycols derived from acetolysis at reflux temperature run No. 2 was also carried out.

The radioactivity data are included in Table II.

Degradation of the Olefinic Products from Acetolyses at 50° C

The mixture of active olefins II, III, and IV obtained from each of the duplicate acetolyses at 50° C was converted to the corresponding mixture of active glycols VII, VIII, and IX. Without any dilution with inactive glycol, this mixture was cleaved with periodic acid and the resulting carbonyl compounds subjected to chromatographic separation as their 2,4-dinitrophenylhydrazones. The chief components, the 2,4-dinitrophenylhydrazones of acetaldehyde and acetone, were recovered. Radioactivity assays were carried out on these two 2,4-dinitrophenylhydrazones and on the original mixture of active glycols VII, VIII, and IX. The results are summarized in Table III.

ACKNOWLEDGMENT

The financial assistance given by the National Research Council of Canada is gratefully acknowledged.

REFERENCES

1. WINSTEIN, S. and MARSHALL, H. J. Am. Chem. Soc. **74**, 1120 (1952).
2. KEULEMANS, A. I. M. Gas chromatography. Reinhold Publishing Corp., New York, N.Y. 1957.
3. GORDON, B. E., WOPAT, F., BURNHAM, H. D., and JONES, L. C. Anal. Chem. **23**, 1754 (1951).
4. ROBERTS, J. D., MCMAHON, R. E., and HINE, J. S. J. Am. Chem. Soc. **72**, 4237 (1950).
5. WHITMORE, F. C. and SIMPSON, C. T. J. Am. Chem. Soc. **55**, 3809 (1933).
6. ROBERTS, J. D., BENNETT, W., HOLROYD, E. W., and FUGITT, C. H. Anal. Chem. **20**, 904 (1948).
7. CRAM, D. J. J. Am. Chem. Soc. **74**, 2137 (1952).
8. INGOLD, C. K. Structures and mechanism in organic chemistry. Cornell University Press, Ithaca, N.Y. 1953. p. 443.
9. WINSTEIN, S. and TAKAHASHI, J. Tetrahedron, **2**, 316 (1958).
10. ROBERTS, J. D., BENNETT, W., MCMAHON, R. E., and HOLROYD, E. W. J. Am. Chem. Soc. **74**, 4283 (1952).
11. SHRINER, R. L., FUSON, R. C., and CURTIN, D. Y. The systematic identification of organic compounds. 4th ed. John Wiley & Sons, Inc., New York, N.Y. 1956. (*a*) p. 280; (*b*) p. 276; (*c*) p. 312.
12. SANDBORN, L. T. and BOUSQUEL, E. W. Organic synthesis, Collective Vol. I. 2nd ed. John Wiley & Sons, Inc., New York, N.Y. 1947. pp. 526–528.
13. MARVEL, C. S. and SEKERA, V. C. Org. Synthesis, **20**, 50 (1940).
14. CRAM, D. J. and ALLINGER, J. J. Am. Chem. Soc. **79**, 2858 (1957).
15. VOGEL, A. I. Practical organic chemistry. Longmans, Green and Company, London. 1948. p. 379.
16. DHAR, M. L., HUGHES, E. D., and INGOLD, C. K. J. Chem. Soc. 2065 (1948).
17. REEVES, R. E. J. Am. Chem. Soc. **63**, 1476 (1941).

THE EFFECT OF MOLECULAR OXYGEN ON THE REACTION OF OXYGEN ATOMS WITH *cis*-2-PENTENE[1]

S. SATO[2] AND R. J. CVETANOVIĆ

ABSTRACT

The effect of the presence of nitrogen, oxygen, and nitric oxide on the reaction between *cis*-2-pentene and oxygen atoms has been investigated at room temperature (25±2° C). For production of oxygen atoms use was made of mercury-photosensitized decomposition of nitrous oxide and of the photolysis of nitrogen dioxide at 3660 Å.

In the N_2O work, the presence of molecular oxygen induced the formation of acetaldehyde, propanal, methanol, and ethanol. In the NO_2 work, the amounts of acetaldehyde, propanal, and ethyl nitrate formed increased rapidly with increasing pressure of molecular oxygen. Possible reaction mechanisms for the formation of these compounds are discussed.

Additional information was obtained on the pressure-independent fragmentation in the reaction of oxygen atoms with *cis*-2-pentene.

INTRODUCTION

The reactions of oxygen atoms with various mono-olefins have been extensively investigated in this laboratory and the main features of the reactions have been established (1). As the source of oxygen atoms use was made of mercury-photosensitized decomposition of nitrous oxide (1), photolysis of nitrogen dioxide (2), and activation of oxygen molecules by electrical discharge (3). In the last method, however, excess oxygen molecules present participated in the reaction and led to considerable complexities. Ozone formation was postulated to explain the formation of some of the observed products.

In the photo-oxidation of hydrocarbons by nitrogen dioxide in the air, Haagen-Smit demonstrated the formation of large amounts of ozone (4). Possible mechanisms have been recently reviewed and discussed in some detail by Leighton and Perkins in connection with "smog" formation in the Los Angeles area (5).

The authors have briefly mentioned in a previous paper (2) that photo-oxidation of 1-butene, isobutene, and 2-butene by nitrogen dioxide in the presence of oxygen gives large amounts of propionaldehyde, acetone, and acetaldehyde, respectively, under certain conditions (for example, 3 mm NO_2, 3 mm olefin, and 50 mm oxygen), although the amounts of the main addition products formed remain almost constant in the presence of either nitrogen or oxygen.

A study of the reactions of ozone with a number of olefins in the gas phase is in progress in this laboratory (6). It has been established that ozone produces mainly propanal and formaldehyde from 1-butene, acetone and formaldehyde from isobutene, and propanal and acetaldehyde from 2-pentene. It appears possible then that an intermediate formation of ozone is responsible for some of the major products in the photochemical oxidation of olefins by nitrogen dioxide in the presence of molecular oxygen.

According to Benson and Axworthy (7) and Herron and Schiff (8), the formation of ozone by the third-body reaction

$$O + O_2 + M \rightarrow O_3 + M \qquad [1]$$

is very slow compared with the reactions of oxygen atoms with olefins under conditions stated above. If the aldehydes observed in the photo-oxidation of butenes by nitrogen

[1]*Manuscript received February 3, 1959.*
Contribution from the Division of Applied Chemistry, National Research Council, Ottawa, Canada.
Issued as N.R.C. No. 5146.
[2]*National Research Council Postdoctorate Fellow 1956–1958. Present address: Laboratory of Physical Chemistry, Tokyo Institute of Technology, Tokyo, Japan.*

dioxide in the presence of molecular oxygen result from the reactions between ozone and the butenes, there must be another mechanism of formation of ozone. This, perhaps, may involve some radicals (R·) formed in these processes and the following reaction sequence (4, 5):

$$R\cdot + O_2 \rightarrow RO_2\cdot, \quad [2]$$

$$RO_2\cdot + O_2 \rightarrow RO\cdot + O_3. \quad [3]$$

The object of the present work has been to obtain further experimental information on these processes. *cis*-2-Pentene was chosen for the study because the main features of its reaction with oxygen atoms are known and the major products of the reaction with ozone in the gas phase are acetaldehyde and propionaldehyde, both of which are easily measured quantitatively. Photo-oxidation of this olefin by nitrogen dioxide in the presence of nitrogen, nitric oxide, and oxygen was investigated at room temperature and using the wave length of 3660 Å. Also, some additional aspects of the reaction with oxygen atoms produced by mercury-photosensitized decomposition of nitrous oxide were investigated with and without molecular oxygen added with a view of gaining further insight into the mechanism of formation of free radicals by pressure-independent fragmentation in this reaction.

EXPERIMENTAL

The experimental arrangements employed in the two methods of production of oxygen atoms, the mercury-photosensitized decomposition of nitrous oxide (1) and the photolysis of nitrogen dioxide (2), have been reported in the previous papers.

cis-2-Pentene was obtained from the National Bureau of Standards, Washington (impurity 0.07±0.02 mole %). This olefin, nitrogen (Linde Air Products Co.), and nitric oxide (Matheson Co., Inc.) were used without further purification. Oxygen (Dominion Oxygen Co.) was passed through a tube packed with molecular sieve granules to remove traces of water. The method of purification of nitrogen dioxide was the same as reported previously (2).

In the N_2O work, the reaction products were transferred to a LeRoy still (9), and the fraction condensable at −140° C was analyzed by means of gas chromatography (GLC) (10). In the NO_2 work, the products were pumped off at liquid nitrogen temperature and were transferred to a sampling tube containing a drop of mercury. After completion of the reaction of the excess nitrogen dioxide present with mercury, the products were again pumped off at liquid nitrogen temperature and analyzed by GLC. The identity of the reaction products separated by GLC was further confirmed by infrared and mass spectrometric analyses. The amounts of products were measured from the GLC peak areas.

Since a variety of reaction products are formed in these reactions, several GLC columns were used: dimethyl sulpholane (DMS) on glass beads (3 wt. % DMS, 8 ft), dinonyl phthalate (DNP) on glass beads (4 wt. % DNP, 8 ft), and Tricresyl phosphate (TCP) on firebricks (40 wt. % TCP, 40 ft). The last column was used at 90° C and the others at room temperature. The carrier gas was helium.

When the reaction products were passed through the DMS column first, several pairs of compounds remained unresolved: *cis*-2-pentene and acetaldehyde, *trans*-β-pentene oxide and ethyl alcohol, *cis*-β-pentene oxide and methyl nitrate. The first pair was then separated on the TCP column and the last two on the DNP column.

The isolation and identification of *n*-butane formed in the N_2O work was kindly done by Dr. N. F. Foster on a 40-ft GLC column (40 wt. % DMS on firebrick) operated at

room temperature. Figure 1 shows typical GLC peaks obtained by the DMS column (8 ft).

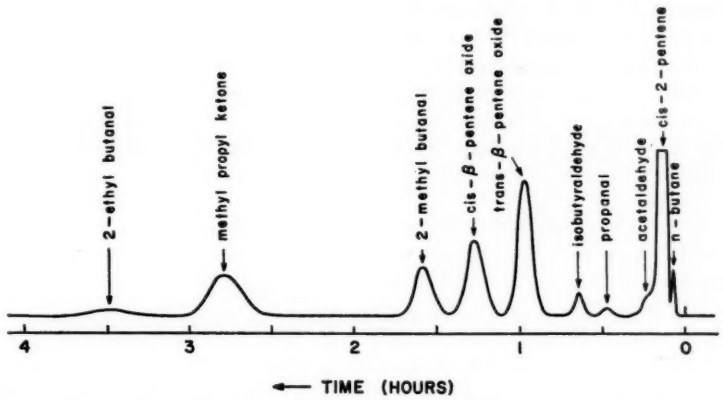

FIG. 1. Typical GL chromatogram obtained using the 8-ft DMS column for the analysis of products of the reaction of oxygen atoms with *cis*-2-pentene.

RESULTS AND DISCUSSION

The Nature of the Pressure-independent Fragmentation in the Reaction of Oxygen Atoms with cis-2-Pentene

As already reported (1), the principal products of the reaction between oxygen atoms and *cis*-2-pentene are *trans*- and *cis*-β-pentene oxide, methyl propyl ketone, and 2-methyl butanal. The first three compounds are produced by internal rearrangements (non-radical mechanisms), while 2-methyl butanal is partly formed by "external" rearrangement (free-radical mechanism). This last process is a consequence of a certain amount of pressure-independent fragmentation which occurs in these reactions (1). (The pressure-dependent fragmentation of the "hot" addition products formed is suppressed already at relatively quite low pressures, except in the case of ethylene and propylene (1, 2).)

In order to obtain further information on the nature of the pressure-independent fragmentation, additional experiments with *cis*-2-pentene and oxygen atoms produced by mercury-photosensitized decomposition of N_2O have been carried out with and without molecular oxygen added. The particular object has been to establish more thoroughly the type of the minor products formed. The results are shown in Table I.

TABLE I

The products of the reaction of oxygen atoms with *cis*-2-pentene
(Oxygen atoms produced by mercury-photosensitized decomposition of N_2O, irradiation time 15 minutes, 25±2° C)

N_2O, mm	*c*-Pe, mm	O_2, mm	GLC peak areas of the products (arbitrary units)											
			t-PO	*c*-PO	2MB	MPK	But	AcA	PrA	*i*-BA	2EB	MeOH	EtOH	H_2O
245	2.7	0	642	462	364	505	53	5	25	87	63	0	0	0
245	2.9	4.4	604	435	100	499	n.d.	535	240	0	0	129	249	ind.
0	6.8	10.2	(10)	8	10	10	n.d.	17	18	0	0	19	(2)	0

c-Pe = *cis*-2-pentene, *t*-PO = *trans*-β-pentene oxide, *c*-PO = *cis*-β-pentene oxide, 2MB = 2-methyl butanal, MPK = methyl propyl ketone, But = *n*-butane, AcA = acetaldehyde, PrA = propanal, *i*-BA = isobutyraldehyde, 2EB = 2-ethyl butanal, MeOH = methyl alcohol, EtOH = ethyl alcohol, n.d. = not determined, ind. = indication. The values in parentheses are of low accuracy.

In the absence of oxygen, small amounts of butane, propanal, isobutyraldehyde, and 2-ethyl butanal[3] are formed besides the large amounts of the four main addition products. It is significant that these minor products clearly indicate formation not only of free CH_3 but also of free C_2H_5 radicals in the pressure-independent fragmentation. This is also confirmed by the results in the presence of molecular oxygen, which will be discussed further below. In view of this it is suggested that the pressure-independent fragmentation probably results from the decomposition of a very short-lived excited epoxide molecule ($C_2H_5 \cdot CH—CH \cdot CH_3$**), i.e. reactions [8] and [9] in the following scheme:

$$C_2H_5CH{=}CHCH_3 + O \rightarrow C_2H_5\dot{C}H—CH(O)CH_3 \qquad [4]$$

$C_2H_5\dot{C}H—CH(O)CH_3$

$\rightarrow C_2H_5CH_2—C(=O)\dot{C}H_3^{*} \xrightarrow{(M)} C_2H_5CH_2C(=O)CH_3$ [5]

$\rightarrow C_2H_5CH(CH_3)—C(=O)H^{*} \xrightarrow{(M)}$ [6]

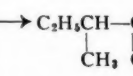

$\rightarrow C_2H_5CH—CH(O)CH_3^{*} \xrightarrow{(M)} C_2H_5CH—CH(O)CH_3$ [7]

(*cis*- and *trans*-) (*cis*- and *trans*-)

$C_2H_5CH—CH(O)CH_3^{**} \rightarrow C_2H_5 + CHC(=O)CHCH_3$ [8]

$\rightarrow CH_3\cdot + CHC(=O)CHC_2H_5$ [9]

The formation of 2-methyl butanal by "external" rearrangement (1) is then due to the radical combinations

$$\left.\begin{array}{l} C_2H_5\cdot + CH(=O)\dot{C}HCH_3 \\ CH_3\cdot + CH(=O)\dot{C}HC_2H_5 \end{array}\right\} \longrightarrow \begin{array}{c} C_2H_5 \\ CH_3 \end{array}\!\!>\!CH—CH(=O) \qquad [10]$$

The above mechanism is identical with the general mechanism of addition of oxygen atoms to olefins given previously (1), except that a more detailed course is now postulated for the pressure-independent fragmentation, i.e. reactions [8] and [9]. The presence of both free CH_3 and C_2H_5 radicals is thus accounted for, and the formation of the minor products can then be readily explained by the reactions

$$C_2H_5\cdot + C_2H_5\cdot \rightarrow C_4H_{10} \qquad [11a]$$

$$C_2H_5\cdot + CH_3\cdot \rightarrow C_3H_8 \qquad [11b]$$

$$CH_3\cdot + CH_3\cdot \rightarrow C_2H_6 \qquad [11c]$$

$$CH(=O)\dot{C}HCH_3 \xrightarrow{(RH)} CH(=O)CH_2CH_3 \qquad [12]$$

[3]*Mass spectrometer analysis of the fraction isolated by GLC as 2-ethyl butanal indicated also the presence of some unidentified impurities.*

$$\begin{matrix}\mathrm{CH}\\ \|\\ \mathrm{O}\end{matrix}\begin{matrix}\mathrm{CH}\\ \cdot\end{matrix}\mathrm{CH_2} + \mathrm{CH_3}\cdot \rightarrow \begin{matrix}\mathrm{CH_3}\\ \mathrm{CH_3}\end{matrix}\!\!>\!\mathrm{CH{-}CH}\begin{matrix}\\ \|\\ \mathrm{O}\end{matrix} \qquad [13]$$

$$\begin{matrix}\mathrm{CH}\\ \|\\ \mathrm{O}\end{matrix}\begin{matrix}\mathrm{CH}\\ \cdot\end{matrix}\mathrm{C_2H_5} + \mathrm{C_2H_5}\cdot \rightarrow \begin{matrix}\mathrm{C_2H_5}\\ \mathrm{C_2H_5}\end{matrix}\!\!>\!\mathrm{CH{-}CH}\begin{matrix}\\ \|\\ \mathrm{O}\end{matrix} \qquad [14]$$

Since ethane has been observed in the previous work (1) and no analysis for propane could be made in the presence of the huge excess of N_2O, essentially all the observed products are predicted by this scheme.[4]

In the presence of oxygen, large amounts of methyl alcohol, ethyl alcohol, acetaldehyde, and propanal were observed instead of the larger part of 2-methyl butanal (the part formed by "external", free-radical rearrangement), *n*-butane, isobutanal, and 2-ethyl butanal, as shown in Table I. These products did not result from the quenching reaction of oxygen molecules, although the table shows that some quenching reactions involving oxygen molecules in the absence of nitrous oxide occurred, perhaps

$$\mathrm{Hg^*} + \mathrm{O_2} \rightarrow \mathrm{Hg} + \mathrm{O_2^*}, \qquad [15]$$

$$\mathrm{C_2H_5CH{=}CHCH_3} + \mathrm{O_2^*} \rightarrow \mathrm{C_2H_5}\begin{matrix}\mathrm{CH}\\ \|\\ \mathrm{O}\end{matrix} + \begin{matrix}\mathrm{CH}\\ \|\\ \mathrm{O}\end{matrix}\mathrm{CH_3}, \qquad [16]$$

or

$$\mathrm{O_2^*} + \mathrm{O_2} \rightarrow \mathrm{O} + \mathrm{O_3}. \qquad [17]$$

These reactions (and further reactions of O and O_3) could explain the small amount of products formed in the absence of N_2O.

In the presence of a large amount of nitrous oxide, excited mercury atoms are essentially exclusively quenched by nitrous oxide and the molecular oxygen acts as an efficient scavenger for the free radicals formed in the pressure-independent fragmentation reactions [8] and [9].

The processes which occur in the presence of molecular oxygen are of considerable complexity and are as yet not fully understood. The formation of the alcohols and the aldehydes may be explained tentatively by the following reactions:

$$\mathrm{R}\cdot + \mathrm{O_2} \rightarrow \mathrm{RO_2}\cdot \qquad [2]$$

$$\begin{matrix}\mathrm{CH}\\ \|\\ \mathrm{O}\end{matrix}\begin{matrix}\mathrm{CH}\\ \cdot\end{matrix}\mathrm{CHR} + \mathrm{O_2} \rightarrow \begin{matrix}\cdot\mathrm{CH}\\ \|\\ \mathrm{O}\end{matrix} + \mathrm{O_2CHR} \qquad [18]$$

$$\mathrm{RO_2}\cdot + \mathrm{RO_2}\cdot \rightarrow \mathrm{RO}\cdot + \mathrm{O_2} + \mathrm{RO}\cdot \qquad [19]$$

$$\mathrm{RO_2}\cdot + \mathrm{O_2CHR} \rightarrow \mathrm{RO}\cdot + \mathrm{O_2} + \begin{matrix}\mathrm{CHR}\\ \|\\ \mathrm{O}\end{matrix} \qquad [20]$$

$$\mathrm{O_2CHR} + \mathrm{O_2CHR} \rightarrow \begin{matrix}\mathrm{CHR}\\ \|\\ \mathrm{O}\end{matrix} + \mathrm{O_2} + \begin{matrix}\mathrm{CHR}\\ \|\\ \mathrm{O}\end{matrix} \qquad [21]$$

$$\mathrm{RO}\cdot + \mathrm{RO}\cdot \rightarrow \text{alcohol} + \text{aldehyde} \qquad [22]$$

$$\mathrm{RO}\cdot + \begin{matrix}\cdot\mathrm{CH}\\ \|\\ \mathrm{O}\end{matrix} \rightarrow \mathrm{ROH} + \mathrm{CO} \qquad [23]$$

[4] *Undoubtedly some disproportionation of ethyl radicals occurs as well, but the amount of ethylene thus formed must be relatively quite small and difficult to estimate with certainty by mass spectrometric analysis of the ethane fraction.*

$$O_2CHR + O_2 \rightarrow \underset{\underset{O}{\|}}{CHR} + O_3 \qquad [24]$$

$$RCH{=}CHR + O_3 \rightarrow \underset{\underset{O}{\|}}{RCH} + O_2CHR \qquad [25]$$

Here R· stands for CH_3· or C_2H_5. Reaction [18] is somewhat similar to the generally assumed initial splitting of an olefin molecule on interaction with ozone (reaction [25]), and O_2CHR is the "zwitter ion" assumed to be formed in this latter process (5). An inspection of the amounts of products in Table I indicates that reactions [2] and [18–23] are capable of explaining the aldehydes and alcohols formed in the presence of oxygen. There is no need then to assume in this case chain processes involving ozone, such as sequences of reactions [2], [3], and [25], or [24] and [25].

Experiments with higher pressures of oxygen have not been attempted in the nitrous oxide work because the quenching reaction [15] is very likely to become important and some additional complications could affect the quantitative aspect of the results.

Photo-oxidation of cis-2-Pentene by Nitrogen Dioxide

Light of wave length of 3660 Å dissociates nitrogen dioxide into nitric oxide and a ground-state oxygen atom (^3P), and the reaction scheme outlined in the previous section should, therefore, be applicable. In this case, however, nitrogen dioxide competes with *cis*-2-pentene for oxygen atoms and also acts as an efficient scavenger for the free radicals formed by the pressure-independent fragmentation, reactions [8] and [9]. As a result a greater complexity of products has to be expected. Figure 2 shows the results of experiments with 3 mm of nitrogen dioxide and 3 mm of *cis*-2-pentene at various irradiation

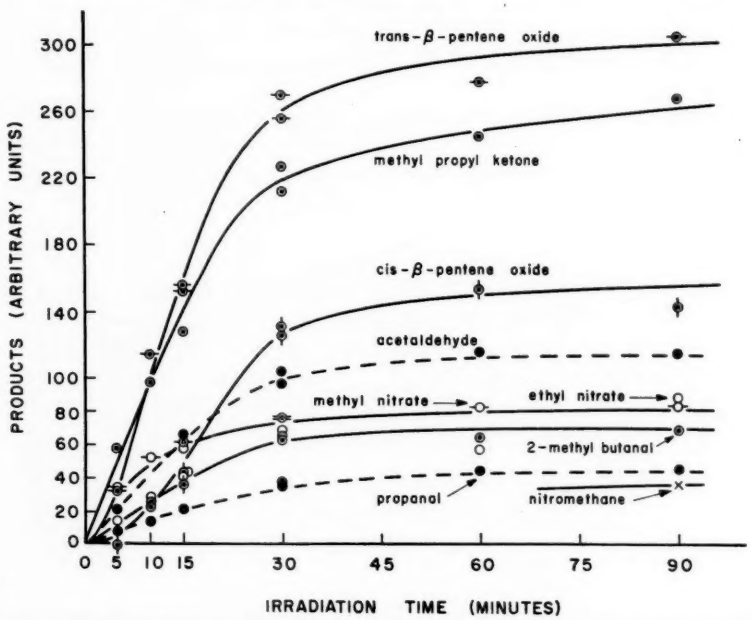

FIG. 2. Yield of the products as a function of irradiation time in the photo-oxidation of *cis*-2-pentene (3 mm) by nitrogen dioxide (3 mm), 25±2° C.

times. The products formed are *trans*- and *cis*-β-pentene oxide, 2-methyl butanal, methyl propyl ketone, acetaldehyde, propanal, methyl nitrate, ethyl nitrate, nitromethane, and probably nitroethane. The first four compounds are the main products observed in the N_2O work. The curves for *trans*- and *cis*-β-pentene oxide in Fig. 2 show apparent induction periods. These are explainable by a certain amount of thermal reaction between nitrogen dioxide and the pentene oxides formed in the photo-oxidation, as discussed previously (2). The rates of the thermal reactions of butene oxides with nitrogen dioxide are believed to be in the following order: isobutene oxide > *cis*-β-butene oxide > *trans*-β-butene oxide > α-butene oxide. β-Pentene oxides are believed to behave similarly to β-butene oxides.

In order to obtain information on the consumption of nitrogen dioxide under various conditions, a RCA 935 vacuum phototube was placed behind the reaction cell and the intensity of the transmitted light was measured by means of an electronic circuit. Figure 3 shows the fraction of the initially taken 3 mm of nitrogen dioxide consumed at various

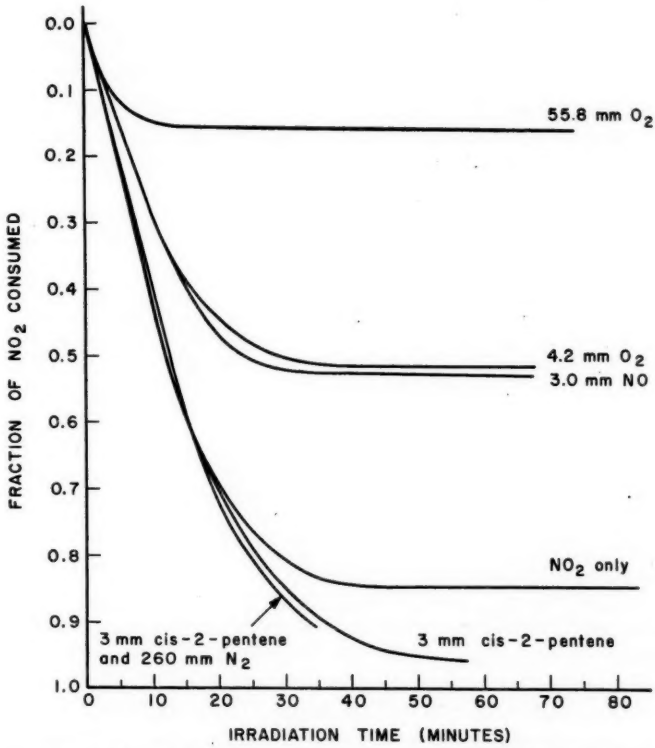

FIG. 3. Consumption of NO_2 as a function of irradiation time. (Initial NO_2 pressure 3 mm, the pressures of added gases are indicated on the curves.)

irradiation times. The greatest part of nitrogen dioxide (in the absence of other compounds) was consumed in about 20 to 30 minutes. In the presence of oxygen or nitric oxide, the consumption was much slower because of more rapid regeneration of nitrogen dioxide when excess of either of these two compounds was added initially.

Figure 4 shows that pressure effects in the photo-oxidation of *cis*-2-pentene are negligible in the investigated range from 6 to 400 mm, while the photo-oxidations of 1-butene and isobutene showed pressure effects below about 10 mm. Yet, the amounts of acetaldehyde and propanal are seen in Fig. 4 to increase appreciably at pressures below about 10 mm without a noticeable compensating decline in the addition products. This could perhaps be ascribed to a reaction between *cis*-2-pentene and excited oxygen molecules formed in the reaction

$$O + NO_2 \rightarrow NO + O_2^*. \qquad [26]$$

However, nothing definite is known about reactions of this type. There is some scatter of points for the addition products formed, Fig. 4, and some pressure-dependent fragmentation at very low pressures is not ruled out. This view is supported by the observation that the amount of methyl nitrate also increases below about 10 mm.

According to Ford and Endow (11) the three-body reaction

$$O + NO_2 + M \rightarrow NO_3 + M \qquad [27]$$

can successfully compete with reaction [26]. From the values of the rate constants given by these authors for these two reactions, R_{26}/R_{27} is about unity at a pressure of 400 mm when nitrogen is the third body. However, no pressure effect is shown in Fig. 4 at higher pressures, suggesting that reaction [27] is relatively unimportant. These two findings are obviously contradictory except if NO_3 molecules produced in reaction [27] react with *cis*-2-pentene in the same manner as oxygen atoms. This appears somewhat unlikely in view of the following.

Since NO_3 presumably reacts very rapidly with nitric oxide, the effect of additions of nitric oxide was examined as shown in Table II. It is evident from Fig. 3 that with the

TABLE II

Yield of the reaction products as a function of the pressure of nitric oxide
(Oxygen atoms produced by photolysis of NO_2 at 3660 Å, irradiation time 5 minutes, 25±2° C)

NO_2, mm	*c*-Pe, mm	NO, mm	GLC peak areas of the products (arbitrary units)								
			t-PO	*c*-PO	2MB	MPK	AcA	PrA	$MeNO_2$	$MeNO_3$	$EtNO_3$
3.0	3.0	0	394	126	72	341	132	42	(21)	193	131
3.0	3.0	30.4	283	47	99	355	(118)	17	(120)	0	11
3.0	3.0	100	121	20	83	284	(72)	ind.	(130)	0	ind.

c-Pe = *cis*-2-pentene, *t*-PO = *trans*-β-pentene oxide, *c*-PO = *cis*-β-pentene oxide, 2MB = 2-methyl butanal, MPK = methyl propyl ketone, AcA = acetaldehyde, PrA = propanal, $MeNO_2$ = nitromethane, $MeNO_3$ = methyl nitrate, $EtNO_3$ = ethyl nitrate, ind. = indication. The values in parentheses are of low accuracy.

short irradiation times of 5 minutes used in these experiments there could be little variation in the average concentration of nitrogen dioxide as the amount of NO added is varied. The amounts of methyl propyl ketone and 2-methyl butanal remained relatively little affected as the pressure of NO was increased. The observed variations introduce some uncertainty into the quantitative validity of this argument, although they are explainable by the experimental errors and a certain amount of competitive consumption of oxygen atoms in the reaction

$$O + NO + M \rightarrow NO_2 + M.$$

The rapid decline in the two epoxides with increasing amounts of NO added may be ascribed to the considerable reactivity of these compounds. The trends in the amounts of the other products in Table II are of interest for the understanding of the mechanism of their formation and will be discussed further below.

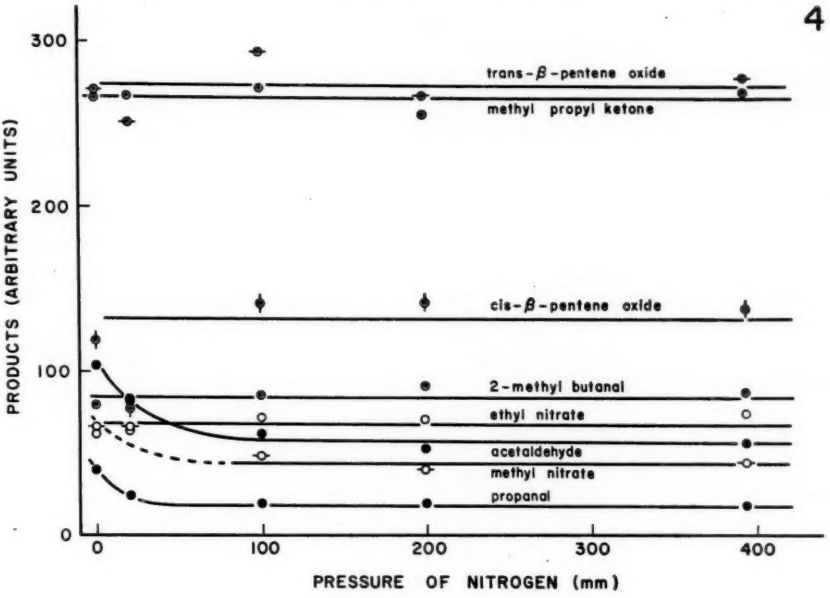

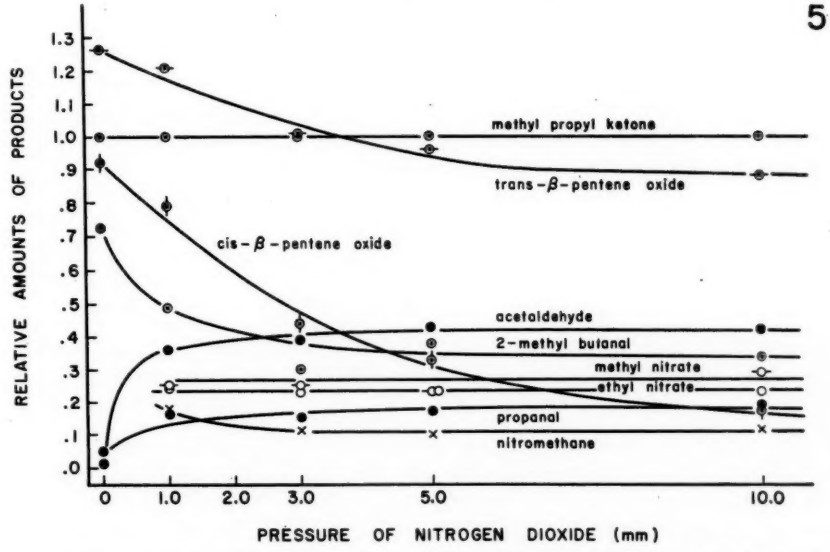

FIG. 4. The effect of pressure on the products formed in the photo-oxidation of *cis*-2-pentene (3 mm initially) by nitrogen dioxide (3 mm initially). Irradiation time 30 minutes, 25±2° C.

FIG. 5. Relative yields of products as a function of initial pressures of nitrogen dioxide in the photo-oxidation of *cis*-2-pentene (3 mm initially). The amounts of methyl propyl ketone formed are taken as unity. Irradiation time 30 minutes, 25±2° C. The points on the ordinate represent the relative amounts of acetaldehyde, propionaldehyde, and the four major addition products observed in the N_2O work, as given in Table I.

The dependence of the relative amounts of products formed (taking methyl propyl ketone as unity) on the pressure of the initially taken nitrogen dioxide is shown in Fig. 5. The decrease in pentene oxides is explained by the thermal reaction of these products with excess nitrogen dioxide. With decreasing NO_2 pressure the relative amounts of these two products tend, within the experimental error, to the relative values found in the N_2O work. The latter are indicated on the ordinate together with the relative values for 2-methyl butanal, acetaldehyde, and propanal (methyl propyl ketone is again taken as unity). The part of 2-methyl butanal formed by external migration (free-radical combination) is completely suppressed already at quite low NO_2 pressure and the part formed by internal migration of methyl radicals remains unaffected by further increasing NO_2 pressure. This is in full agreement with the internal rearrangements described previously (1) and there is no need to discuss here again the mechanism of formation of the four direct addition products. A mechanism for the formation of the products resulting from fragmentation can be proposed with much less certainty and the following scheme is of a tentative character (R· stands for CH_3 and C_2H_5):

$$R\cdot + NO_2 \rightarrow RNO_2, \qquad [28]$$

$$R\cdot + NO_2 \rightarrow RO\cdot + NO, \qquad [29]$$

$$RO\cdot + NO_2 \rightarrow RONO_2, \qquad [30]$$

$$\underset{\cdot}{\overset{\|}{\underset{O}{RCHCH}}} + NO_2 \rightarrow \underset{}{\overset{\|}{\underset{O}{RCH}}} + CHO\cdot + NO, \qquad [31]$$

$$\underset{\cdot}{\overset{\|}{\underset{O}{RCHCH}}} + NO_2 \rightarrow \underset{NO_2}{\overset{\|}{\underset{O}{RCHCH}}}, \qquad [32]$$

$$CHO\cdot + NO_2 \rightarrow CO + HNO_2. \qquad [33]$$

The radicals are initially formed in the pressure-independent fragmentation reactions [8] and [9]. The products of the last two reactions and nitroethane have not been identified. The observed products are consistent with the reaction scheme. In the presence of added excess NO the following reactions are assumed to occur:

$$R\cdot + NO \rightarrow RNO, \qquad [34]$$

$$RNO + NO_2 \rightarrow RNO_2 + NO, \qquad [35]$$

$$\underset{\cdot}{\overset{\|}{\underset{O}{RCHCH}}} + NO \rightarrow \underset{NO}{\overset{\|}{\underset{O}{RCHCH}}}. \qquad [36]$$

These reactions explain the observed increase in CH_3NO_2 and suppression of the nitrates, propanal, and acetaldehyde (Table II). The product of reaction [36] has not been identified.

The Effect of Molecular Oxygen on the Photo-oxidation of cis-2-Pentene by Nitrogen Dioxide

Photolysis of nitrogen dioxide in the presence of olefins and oxygen in air has been shown to be responsible for "smog" formation in some places on this continent (4, 5). This process is characterized by a remarkable complexity of the recoverable condensable material and is accompanied by appreciable ozone formation. The photolysis of nitrogen dioxide in the presence of *cis*-2-pentene and molecular oxygen studied in the present work is superficially similar to the conditions in polluted atmosphere leading to smog formation. However, the concentrations of NO_2 and the olefin have been very much larger and, as a result, it is difficult to say how much there is in common between the two processes. Nevertheless, it is considered of some interest to report briefly the results of

the experiments carried out inasmuch as they show the type of products formed under the particular conditions employed.

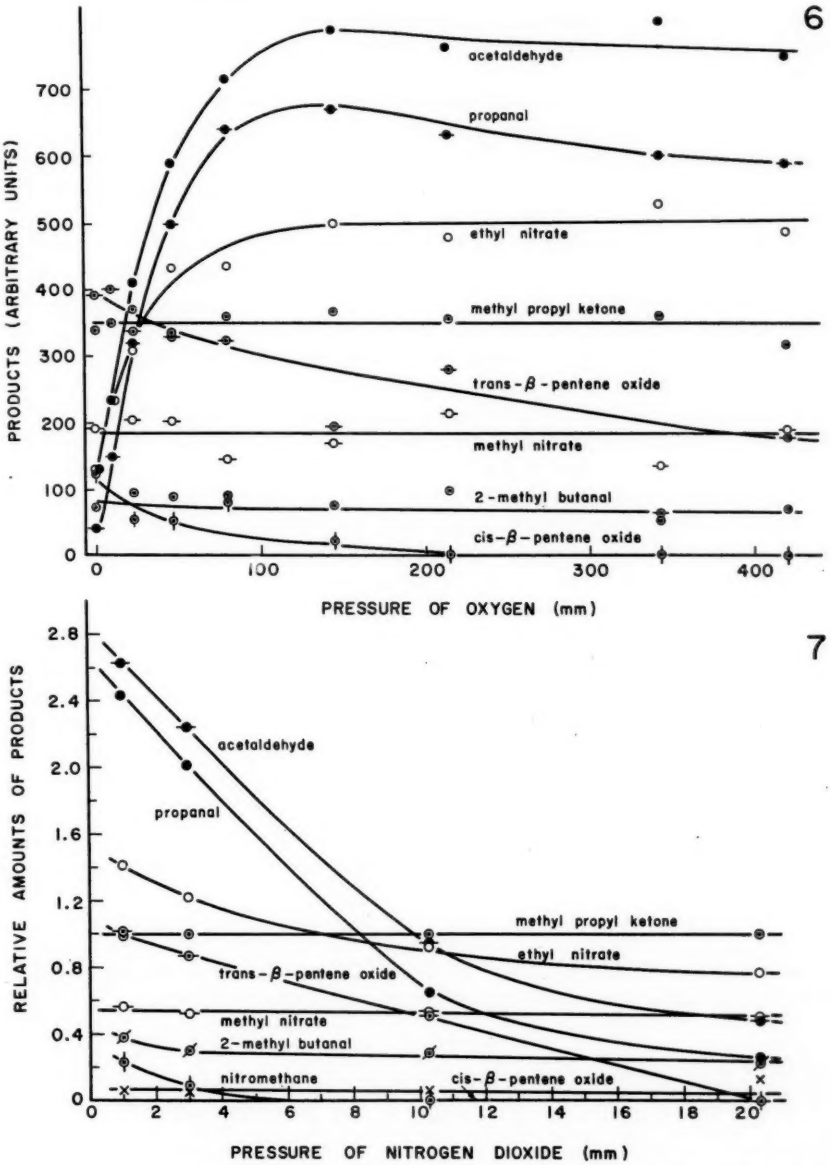

FIG. 6. The amounts of products formed as a function of oxygen pressure (3 mm NO_2, 3 mm *cis*-2-pentene, 25±2° C).

FIG. 7. Relative yields of products in the presence of 100 mm of oxygen as a function of initial pressures of nitrogen dioxide. The amounts of methyl propyl ketone formed are taken as unity (3 mm *cis*-2-pentene, irradiation time 15 minutes, 25±2° C).

The experimental results are plotted in Figs. 6 and 7, which should be contrasted with Figs. 4 and 5, respectively. It is clear from Fig. 6 that the presence of molecular oxygen induces formation of large amounts of acetaldehyde, propionaldehyde, and ethyl nitrate, although the amounts of the other compounds formed, with the exception of the epoxides, remain constant. The amounts of the two epoxides decrease with increasing oxygen pressure.

The effect of the initial pressure of nitrogen dioxide on the relative yields of products in the presence of 100 mm of oxygen is shown in Fig. 7. It is clear that the formation of acetaldehyde, propionaldehyde, and ethyl nitrate is particularly large at smaller nitrogen dioxide concentrations. The amounts of the two epoxides decline again with increasing NO_2 pressure.

As has already been mentioned, reaction of ozone with 2-pentene in the vapor phase leads to the predominant formation of acetaldehyde and propionaldehyde (6). It is significant that in the photo-oxidation of 1-butene, 2-butene, and isobutene, respectively, in the presence of molecular oxygen large amounts of propionaldehyde, of acetaldehyde, and of acetone are formed and the same compounds are again the predominant products (observed by GLC analysis) in the vapor-phase reaction of ozone with these olefins (6). In view of this, it is probable that in the photo-oxidation experiments carried out in the presence of large amounts of molecular oxygen there was an intermediate formation of ozone, which was, in the case of 2-pentene, responsible for the major part of acetaldehyde and propionaldehyde formed. Here again it is most likely that ozone is not formed to any extent directly from oxygen atoms and molecular oxygen. In the vapor-phase reaction of ozone with *cis*-2-pentene in addition to large amounts of propionaldehyde and acetaldehyde a residue of lower volatility is also formed, the nature of which is being further investigated (6). In one experiment, this residue[5] (after removal of acetaldehyde and propionaldehyde at $-80°$ C) was transferred to the reaction cell containing 3 mm of NO_2. The two were allowed to react thermally for 5 minutes at room temperature and then the product analysis was carried out in the usual manner. The GLC analysis showed peaks in the position of methyl nitrate, ethyl nitrate, *cis*-β-pentene oxide, and methyl propyl ketone and no *trans*-β-pentene oxide nor 2-methyl butanal. This experiment suggests that there are perhaps two potential sources of methyl propyl ketone and gives an example of the complex character of the studied process. In view of the observed complexities it is felt that a detailed discussion of the experimental results will become possible only after considerable additional background knowledge on the reactions of this type is accumulated.

ACKNOWLEDGMENTS

The authors are indebted to Dr. A. W. Tickner for the mass spectrometer analyses and to the Analytical Section of this Division for the infrared analyses.

REFERENCES

1. CVETANOVIĆ, R. J. J. Chem. Phys. **25**, 376 (1956); Can. J. Chem. **36**, 623 (1958); J. Chem. Phys. **30**, 19 (1959).
2. SATO, S. and CVETANOVIĆ, R. J. Can. J. Chem. **36**, 279, 970, 1668 (1958).
3. JARVIE, J. M. S. and CVETANOVIĆ, R. J. Can. J. Chem. **37**, 529 (1959).
4. HAAGEN-SMIT, A. J. and FOX, M. M. Ind. Eng. Chem. **48**, 1484 (1956). HAAGEN-SMIT, A. J., BRADLEY, C. E., and Fox, M. M. Proceedings of the Second National Air Pollution Symposium, Pasadena, Calif. 1952. p. 54.
5. LEIGHTON, P. A. and PERKINS, W. A. Photochemical Secondary Reactions in Urban Air. Report No. 24 of the Air Pollution Foundation, San Marino, Calif. August 1958.

[5]*The authors are thankful to Dr. T. Vrbaški for carrying out the reaction between 2-pentene and ozone.*

6. VRBAŠKI, T. and CVETANOVIĆ, R. J. To be published.
7. BENSON, S. W. and AXWORTHY, A. E., JR. J. Chem. Phys. **26**, 1718 (1957).
8. HERRON, J. T. and SCHIFF, H. I. Can. J. Chem. **36**, 1159 (1958).
9. LEROY, D. J. Can. J. Research, B, **28**, 492 (1950).
10. CALLEAR, A. B. and CVETANOVIĆ, R. J. Can. J. Chem. **33**, 1256 (1955).
11. FORD, H. W. and ENDOW, H. J. Chem. Phys. **27**, 1156, 1277 (1957).

THE TEMPERATURE DEPENDENCE OF THE HYDROLYSIS OF METHYL ESTERS OF CERTAIN ALKYL-SUBSTITUTED BENZENESULPHONATES IN WATER[1]

G. A. HAMILTON[2] AND R. E. ROBERTSON

ABSTRACT

Rate data for the hydrolysis of a series of alkyl-substituted methyl benzenesulphonates are presented and the resulting differences in derived parameters are compared and discussed in an analysis of substituent effects.

Coincident with the hydrolysis studies to be reported on toluenesulphonates (1) a survey was made of the changes in rate and derived parameters for a series of alkyl-substituted benzenesulphonates with the aim of discovering the effect of systematic increase in the size of the anion being produced while the "mechanism" was kept constant through use of the methyl ester. With the realization that the solvent reorganization accompanying the activation process did not necessarily include the total initial solvation shell of the ester (2), the more extensive study of the effect of such groups on solvation was discontinued and the data already determined are published here.

The importance of solvation on the rates of reactions in solution has long been recognized in principle (3) and the general trends analyzed in terms of charge development or distribution. While far from optimum, the benzenesulphonic system provides a means of examining the effect of a substituent on the rate and thermodynamic parameters where there is no steric interference with solvation (para substitution) and where the solvation is altered through the competition of more effective intramolecular interaction (ortho substitution). It is recognized that the latter is not equivalent to the simple screening of a charge by an alkyl group as considered by Everett and Wynne-Jones (4) in discussing the changes in solvation of anions with alkyl substitution but is more closely allied to the effect considered by Evans (5) and Franklin (6) in calculating the heat of solvation of the series $\overset{+}{\text{Me}} \rightarrow t\text{-}\overset{+}{\text{Bu}}$ carbonium ions, where the loss of solvation through solvent exclusion was compensated for by internal resonance effects.

TABLE I

Effect of methyl substituents on relative rates of solvolysis in ethanol and water at 80° C

	Ethanol		Water		Acetic acid	
Ester	$k_1 \times 10^4$	Rel. rate	$k_1 \times 10^3$	Rel. rate	$k_1 \times 10^6$	Rel. rate
Me-*p*-H	1.67_3*	1.0	3.07†, ‡	1.0	1.89	1.0
Me-*p*-Me	1.09_5	0.65	2.19§	0.71	1.27	0.67
Me-*o*-Me	1.41	0.84	2.39	0.78	1.44	0.76
Me-2,4-diMe	0.877	0.52	1.62	0.53	—	—
Me-3,4-diMe	0.905	0.54	1.85	0.60	1.06	0.55
Me-2,4,6-triMe	0.426	0.25	0.309	0.27	—	—

*Ref. 9.
†Ref. 2.
‡Rates calculated from constants Table I, above, and Table V ref. 2.
§Ref. 11.

[1]*Manuscript received November 4, 1958.*
Contribution from the Division of Pure Chemistry, National Research Council, Ottawa, Canada.
Issued as N.R.C. No. 5145.
[2]*Summer Student.*

Whether an alkyl substituent group in a benzenesulphonate will be expected to interfere or in fact increase the solvation of the developing sulphonic anion in the activation process leading to hydrolysis will depend not only on its position and size, but also on the electronic nature of its effect, i.e., whether the effect is simply inductive, or shows evidence of hyperconjugation, or both. To evaluate the possible effect of hyperconjugation one must look for stabilizing influences arising from this cause both in the initial and in the transition states. Formal presentation of typical resonance contributors to the stabilization of these two states are as follows:

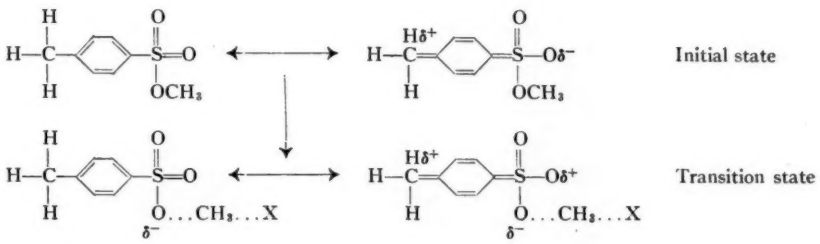

It will be obvious from the above that resonance contributors will be more important in the initial state than in the transition state, since in the latter the developing negative charge will oppose any such electronic shift. Thus we anticipate the initial state for the para-methyl-substituted ester will be stabilized compared to the corresponding state for the unsubstituted ester, and the rate correspondingly reduced. This does not exclude the operation of an inductive effect toward the same end, but evidence that a hyperconjugative effect is present may be gained from a comparison of the relative rates of solvolysis for a series of esters in ethanol and in water (Table I).

If the effect of the methyl group were purely inductive the rate for the meta methyl ester would be the same or slower than that for the para methyl ester. Were the effect purely hyperconjugative, the substituent effect of the meta methyl should be negligible. From Table I it is seen that the relative effect of the para methyl and ortho methyl are about additive to give the value for the 2,4-dimethyl hydrolyzing in ethanol and water of 0.49 (calc.) in both cases and 0.52 and 0.53 (obs.) respectively. If the effect of the para methyl were completely inductive, then the meta methyl should have approximately the same effect and we would anticipate the relative rate values for the 3,4-dimethyl to be 0.30 and 0.42 (calc.) compared with the observed values of 0.53 and 0.60 in ethanol and water, respectively. Hence it may be argued that some considerable fraction of the effect of the para methyl group must be attributed to hyperconjugative stabilization of the initial state.

For the 2,4,6-trimethyl ester, it might be expected the second ortho methyl would not interact with the sulphonic group to the same extent as the first ortho methyl but would have an effect somewhat like an additional para methyl group. Thus the relative rate for the 2,4,6-trimethyl ester might be expected to be intermediate between that calculated assuming the second ortho methyl to duplicate the first (calculated relative rate in ethanol 0.33, in water 0.27) and assuming it is a para methyl (calculated relative rate in ethanol 0.14 and in water 0.20). The observed values of 0.25 and 0.27 in ethanol and water respectively are in fair agreement with this analysis.

The fact that the para methyl substituent may be changed to other para alkyl sub-

stituents with no change in relative rates (Table II) compared with the unsubstituted ester may be taken as further evidence of compensation between the inductive and hyperconjugative effects. Taft (13) has explained the apparent constancy of the ionization constants of the 4-alkyl-substituted pyridines by a similar balancing of inductive and hyperconjugative effects and our results are in qualitative as well as quantitative agreement with his.

TABLE II

Effect of para alkyl groups on rate of hydrolysis of methyl benzenesulphonates in water at 60° C*

Compound	$k_1 \times 10^4$ sec^{-1}	k_x/k_H
Me-*p*-H†	5.33±1.01	1
Me-*p*-Me‡	3.77±0.01	0.71
Me-*p*-Et	3.80±0.02	0.71
Me-*p*-isoPro	3.77±0.02	0.71
Me-*p*-*t*-Bu	3.80±0.06	0.71
Me-*p*-*n*-Pro	3.68±0.02	0.69

*Actual temperature 60.14° C.
†Ref. 2.
‡Ref. 11.

While comparisons of relative rates such as above give a valuable indication of trends, and largely provide the basis for our knowledge of the relation between structure and reaction rates, the fact that these ratios are temperature dependent encourages a more detailed examination in terms of the parameters derived from the temperature dependence of the rate. In Table III are given the rate data for three methyl esters over a range of

TABLE III

Kinetic data for the hydrolysis of three methyl-substituted benzenesulphonic esters in water

Temp.	Me-3,4-dimethyl benzenesulphonate, $k_1 \times 10^5$ sec^{-1}	Me-2,4-dimethyl benzenesulphonate, $k_1 \times 10^5$ sec^{-1}	Me-2,4,6-trimethyl benzenesulphonate, $k_1 \times 10^5$ sec^{-1}
353.172	$185._8$	$161._7$	83.1_9
348.164	$121._7$	$107._9$	54.2_4
343.166	79.3_1	$70._2$	35.8_3
338.168	50.5_1	45.3_8	22.4_0
333.158	31.3_7	28.5_5	14.1_1
323.159	11.6_4	10.78	5.2_5
313.173	3.97_4	3.79_5	1.80_9
308.170	2.23_2	2.16_4	1.02_5
303.173	1.231	1.21_0	0.57
Standard deviation* $\log k_{obs} - \log k_{calc}$	0.00096	0.0012	0.0010

*The average deviation from the mean of 3 or 4 separate kinetic runs is shown directly after the corresponding rate. The standard deviations between this observed value and the rate calculated from the derived equation [1] are shown here.

temperature. These data fit an empirical equation of the form

$$[1] \qquad \log_{10} k = A/T + B \log_{10} T + C$$

within experimental error and values of the corresponding constants are summarized

in Table IV. These constants may be interpreted as follows:

$$A = -(\Delta H_0^{\ddagger}/2.303\ R),$$
$$B = (\Delta C_p^{\ddagger}/R)+1,$$
$$C = (\Delta S_0^{\ddagger}-\Delta C_p^{\ddagger})/2.303\ R + \log_{10} k/h,$$

but it is well to recall that this interpretation finally rests on the assumption that an equilibrium exists between the initial and the transition state. Further, in our evaluation of $\Delta S^{\ddagger}$ we assume a frequency factor of $\log kT/h$ which is constant throughout a series and in fact throughout all series. Since we normally are considering $\Delta\Delta S^{\ddagger}$ values within a given series such an assumption is probably acceptable at this preliminary stage of comparison.

TABLE IV

Summary of constants for equation [1]

Benzenesulphonate	*A*	*B*	*C*
Me-3,4-dimethyl	−7408.282	−19.3250	67.48493
Me-2,4-dimethyl	−7067.916	−17.7061	62.33737
Me-2,4,6-trimethyl	−6776.710	−15.1235	54.64063

The thermodynamic parameters calculated from the above data are given in Table V.

TABLE V

Thermodynamic constants at 25° C

Benzenesulphonate	Me-3,4-diMe	Me-2,4-diMe	Me-2,4,6-triMe
k_1 sec$^{-1}\times10^5$	0.660	0.6596	0.309
$\Delta F^{\ddagger}$ cal/mole	24,514	24,512	24,962
$\Delta H_0^{\ddagger}$ cal/mole	33,898	32,340	31,010
$\Delta H^{\ddagger}_{298.16}$ cal/mole	21,855	21,257	21,455
$-\Delta C_p^{\ddagger}$ cal/mole deg	40.39	37.17	−32.04
$-\Delta S^{\ddagger}$	8.94	10.95	11.64

In Table VI are given the difference functions with unsubstituted methyl benzenesulphonate as the standard. From these a much clearer picture can be gained of the effect of the substituent on the detailed mechanism than was possible from a consideration of relative rates.

TABLE VI

Effect of methyl substitution on thermodynamic constants for the hydrolysis of benzenesulphonic esters in water at 25° C

Ester	k_1 sec$^{-1}\times10^5$	$\delta_z\Delta H^{\ddagger}_{cal}$	$\delta_z\Delta C_p^{\ddagger}$	$\delta_z\Delta S^{\ddagger}$
Me-*p*-H	1.166 (1)	0	0	0
Me-*p*-Me	0.799 (0.69)	+197	−2.0	−0.03
Me-*o*-Me	0.998 (0.86)	−540	+6.4	−2.46
Me-3,4-diMe	0.660 (0.57)	+435	−7.0	+0.35
Me-2,4-diMe	0.660 (0.57)	−163	−3.8	+1.66
Me-2,4,6-triMe	0.309 (0.27)	+ 35	+1.4	−2.35

We have noted elsewhere (1) that the *p*-Me raises $\Delta H^{\ddagger}$ by ∼200 cal while *o*-Me lowers $\Delta H^{\ddagger}$ by ∼−500 cal. If we may assume, on the basis of the above evidence, that the solvation of the para alkyl group is not altered during the activation process, aside from the possibility of a small hyperconjugation effect (and the small $\Delta\Delta S^{\ddagger}$ supports this assumption), then the effect of the *p*-group is to increase the bond energy requiring

greater thermal activation to achieve the critical charge level characteristic of the transition state. The 3-Me group probably has a somewhat greater inductive effect (7), say $\Delta\Delta H^{\ddagger}$ +225 cal, while if the trend is maintained ortho methyl would be expected to raise $\Delta H^{\ddagger}$ by 275∼300 cal (8). On this basis, the shift to be expected in $\Delta H^{\ddagger}$ for the 2,4-dimethyl will be (+200−500) = −300 compared to the observed value of −175 cal. To rationalize the value of $\Delta H^{\ddagger}$ for the 2,4,6-trimethyl ester we note from an examination of models that if a single ortho methyl interacts with the sulphonic group, the second ortho methyl will not be orientated for interaction. The second ortho methyl will then resemble a more effective (275∼300 cal) para methyl. The interaction of the first ortho methyl will cause a decrease in rotational entropy ($\delta_z\Delta S^{\ddagger}$ ∼2 e.u.) but this will not be duplicated by the second. Thus the predicted $\delta_z\Delta H^{\ddagger}$ will be (+200+275−500) = −25 cal; observed +24 cal, and the $\delta_z\Delta S^{\ddagger}$ is of the same sign and magnitude as for a single ortho methyl. It will be noted that these results are in essential agreement with the additivity relations noted for the relative rates.

Qualitatively, the differences in the heat capacity of activation are in accord with this analysis, but the crude state of our knowledge of the factors influencing this term limits interpretation of small differences. If the $\Delta C_p^{\ddagger}$ observed in hydrolysis arises from the temperature dependence of the $\Delta H^{\ddagger}$ required to break the solvation shell, then it is probable that the observed differences in $\Delta C_p^{\ddagger}$ reflect differences in the degree of involvement of the solvent. As has been noted elsewhere, such large heat capacity differences can hardly be attributed to the solute alone. The changes in $\Delta C_p^{\ddagger}$ are approximately additive. However, even considering the larger experimental error characterizing this parameter, the 2,4-dimethyl value for $\Delta C_p^{\ddagger}$ appears anomalous.

EXPERIMENTAL

Solvents.—Ethanol (absolute) and water were as previously described (9, 2). To acetic acid (reagent) was added sufficient acetic anhydride so that after heating overnight at 100° C approximately 0.05% remained according to analysis of S. Bruckstein (10).

Esters.—The constants characterizing the sulphonyl chloride and the esters are recorded in Table VII. There was no kinetic evidence (non-linear plots) of the presence of any competing impurity in the esters studied.

TABLE VII

Physical constants of methyl esters

Ester	M.p.	M.p. of amide*	Refractive index	Density	Neutral equivalent
Me-*p*-Et		108.5–109.5	1.5148	1.19562	200.9
Me-*p*-*n*-Pro		109.5–111	1.5105	1.16036	—
Me-*p*-isoPro		106–107	1.5116	1.16482	210
Me-*p*-*t*-Bu	68–69	137	—	—	211
Me-2,4-diMe		138.5–139.5	1.5213	1.2055	200.2
Me-3,4-diMe		145.5–146	—	—	200
Me-2,4,6-triMe	43–43.7	143.5–145	—	—	212

*Of corresponding sulphonyl chlorides. These are in essential agreement with values found by previous workers and summarized by Suter (ref. 14).

Kinetic studies.—The rates in water were determined by a conductance method. Details of the method, calculations, and assumptions have been discussed in detail in previous communications (11). The rate data in ethanol and in acetic acid followed the method described by Robertson (9) and Winstein (12) respectively.

REFERENCES

1. ROBERTSON, R. E. Unpublished work.
2. ROBERTSON, R. E. Can. J. Chem. **35**, 613 (1957).
3. INGOLD, C. K. Structure and mechanism of organic chemistry. Cornell University Press, Ithaca, N.Y. 1951. p. 345 et seq.
4. EVERETT, D. H. and WYNNE-JONES, W. F. K. Trans. Faraday Soc. **35**, 1380 (1939).
5. EVANS, A. G. Reactions of organic halides in solution. Manchester University Press. 1946.
6. FRANKLIN, J. L. Trans. Faraday Soc. 443 (1952).
7. TAFT, R. Steric effects in organic chemistry. John Wiley & Sons, Inc., New York, N.Y. 1956. Chap. 13. Sec. 5.
8. JAFFE, H. Chem. Revs. **53**, 191 (1953).
9. ROBERTSON, R. E. Can. J. Chem. **31**, 589 (1953).
10. BRUCKSTEIN, A. Anal. Chem. **28**, 1920 (1956).
11. ROBERTSON, R. E. Can. J. Chem. **33**, 1536 (1955).
12. WINSTEIN, S., GRUNWALD, E., and INGRAHAM, L. I. J. Am. Chem. Soc. **70**, 821 (1948).
13. TAFT, R. W. Private communication.
14. SUTER, C. M. The organic chemistry of sulphur. John Wiley & Sons, Inc., London. 1944. p. 458 et seq.

THE ACETOLYSIS OF SOME HYDROXYTETRAHYDRO-2-PYRANS[1]

THOMAS FRANCIS[2] AND E. VON RUDLOFF

ABSTRACT

The reaction between acetic anhydride and several hydroxytetrahydropyrans in the presence of boron trifluoride has been studied. 2-Methyl-3-hydroxytetrahydropyran, 2-hydroxymethyl-4,5-dihydroxytetrahydropyran, and 3,4-dihydroxytetrahydropyran all underwent normal acetolysis to the expected straight-chain polyol acetates. Optically active forms of *cis*- and *trans*- 3,4-dihydroxytetrahydropyran gave the same, inactive pentanetetrol, showing that racemization of the active centers had accompanied ring cleavage. 2-Hydroxymethyltetrahydropyran gave 1,3,6-hexanetriol besides the expected 1,2,6-isomer. The reagent did not cleave 4-hydroxytetrahydropyran nor dihydro-D-galactal, but the latter underwent hydroxyl inversion to give dihydro-D-altral. 1,5-Anhydro-D-sorbitol (polygalitol) appeared to undergo both ring fission and inversion.

INTRODUCTION

The isolation of several hydroxylated derivatives of tetrahydro-2-pyran from the hydrogenolysis of methyl glycopyranosides (1, 2, 3) stimulated an interest in ring cleavage of this type of cyclic ether as a possible aid in determining their structure and configuration. Relatively few examples of this reaction are cited in the literature (4), in contrast to extensive studies on tetrahydrofurans (4, 5), but it is generally accepted that tetrahydropyrans are much more resistant to cleavage than are their five-membered ring analogues (4, 5). Of the reagents generally used to effect fission of cyclic ethers (4), those involving the use of acetic anhydride and an acid catalyst appeared most attractive, since the cleavage products could be deacetylated readily and the free polyols thus obtained conveniently examined by paper chromatography and periodic acid oxidation.

In preliminary experiments, several different catalysts were used to study the acetolysis of 2-hydroxymethyltetrahydropyran and 3,4-dihydroxytetrahydropyran. The cleavage of 2-hydroxymethyltetrahydropyran using zinc chloride and acetic anhydride for 8 hours at reflux temperature has been reported (6) to yield 1,2,6-hexanetriol triacetate. Re-examination of this reaction now showed that 85% of the starting material was recoverable as its acetate after 4 hours' refluxing and 75% with a reaction period of 28 hours. No trace of cleavage was detected when 3,4-dihydroxytetrahydropyran was subjected to the same conditions for 4 hours. Mixtures of sulphuric acid and acetic anhydride were found to cause some cleavage of 2-hydroxymethyltetrahydropyran but decomposition was extensive and the effect of these reagents on other tetrahydropyrans was not investigated. Trifluoroacetic anhydride promoted acetylation of each of these tetrahydropyrans but there was no evidence of ring opening. However, boron trifluoride was found to catalyze the cleavage without too much general decomposition and its use in the acetolysis of hydroxytetrahydropyrans was, therefore, examined in detail.

DL-*trans*-3,4-Dihydroxytetrahydropyran, treated with excess acetic anhydride saturated with boron trifluoride, split to an extent of 25% with a reaction time of 18 hours at room temperature and to 50% at 100° C for 1 hour, whereas at the higher temperature fission was virtually complete in 4 hours. The cleavage product, after deacetylation and purification, was the expected 1,2,3,5-pentanetetrol. D-*trans*-3,4-Dihydroxytetrahydropyran

[1]*Manuscript received January 23, 1959.*
Contribution from the National Research Council of Canada, Prairie Regional Laboratory, Saskatoon, Saskatchewan.
Issued as N.R.C. No. 5144.
[2]*National Research Council of Canada Postdoctorate Fellow, 1958.*

and L-*cis*-3,4-dihydroxytetrahydropyran were found to yield the same optically inactive pentanetetrol, showing that racemization of the optically active centers had accompanied ring fission. Under similar reaction conditions the triacetate of 2-hydroxymethyl-4,5-dihydroxytetrahydropyran gave a 25% yield of the expected 1,2,3,5,6-hexanepentol, which did not give a solid benzoate or *p*-nitrobenzoate and formed a sirupy pentaacetate.

Cleavage of 2-hydroxymethyltetrahydropyran was complete in 2 hours at room temperature, whilst at 100° C decomposition was extensive. The product from the reaction at room temperature, or lower, was an oil which could not be separated into more than one component by counter-current distribution (210 transfers). The deacetylated product was shown to be a sirupy hexanetriol. However, when oxidized with periodic acid, the material consumed only 0.4 moles of oxidant with the release of 0.4 moles of formaldehyde, indicating that it was a mixture of the expected 1,2,6-hexanetriol and an isomer having no vicinal hydroxyl groups. This mixture of isomers could not be resolved by column chromatography, nor by counter-current distribution (120 transfers), but the isomeric triol was isolated from the mixture by decomposition of the 1,2,6-isomer with periodate. The sirupy product had an infrared spectrum which was similar to that of the 1,2,6-isomer and formed a crystalline tris-*p*-nitrobenzoate having similar spectral properties to those of the 1,2,6-derivative. These data, together with the results from C-methyl determinations, suggested that the compound was most likely 1,3,6-hexanetriol. 1,3,6-Triacetoxyhexane was prepared from tetrahydrofuran-2-acetic acid (7) by lithium aluminum hydride reduction to tetrahydrofuran-2-ethanol and subsequent ring cleavage (8). The triol obtained on deacetylation was shown to be identical with that obtained from 2-hydroxymethyltetrahydropyran. The formation of 1,3,6-hexanetriol besides the 1,2,6-isomer is unexpected, since tetrahydrofuranyl carbinols have given rise to only one triacetate on acetolysis with zinc chloride as catalyst (5). Since the starting material was found to be pure, it could not have been derived from a major impurity, such as tetrahydrofuran-2-ethanol.

Cleavage of a fraction isolated from the hydrogenolysis of α-methyl-D-glucopyranoside and thought to be a hydroxytetrahydropyran derivative (2) was readily effected with the reagent at room temperature in 18 hours. The product, after deacetylation, was 1,4,5-hexanetriol, since it consumed 1.0 mole of periodic acid with the production of 1.0 mole of acetaldehyde, and yielded a tris-*p*-nitrobenzoate. Thus, if no rearrangement had taken place during acetolysis (this assumption is justified, since no isomeric products were isolated) the starting material must have been 2-methyl-3-hydroxytetrahydropyran, a product not unexpected from the hydrogenolysis reaction. The ready cleavage of this 2-alkyl derivative is in accord with the findings on 2-alkyl tetrahydrofurans by Paul (5). The formation of olefinic intermediates presumably was suppressed by the 3-hydroxyl substituent.

4-Hydroxytetrahydropyran was not cleaved to any extent at room temperature, at 65° C, or at 100° C, charring being extensive at the latter temperature. This result was unexpected and cannot be explained by the proposed mechanisms of ether cleavage (4). Similar results were obtained with dihydro-D-galactal and dihydro-D-glucal. When dihydro-D-galactal was first acetylated and then treated with excess reagent at 100° C ring cleavage was also not obtained, showing that the formation of acetic acid in the initial acetylation of the free polyol is not the cause of this failure to cleave the ether. However, after a 10-hour treatment at 100° C dihydro-D-galactal yielded a small amount of dihydro-D-altral. Paper chromatographic analysis of the deacetylated product obtained from dihydro-D-glucal showed the presence of compounds with R_f values corre-

sponding to dihydrogalactal and dihydroaltral. A similar examination of the reaction product from a small amount of 1,5-anhydro-D-sorbitol (polygalitol) indicated the presence of both fission products (hexitols) and inversion products, besides unreacted starting material.

Burwell (4) proposed as the first step in the catalytic acetolysis of aliphatic ethers the addition of an acetyl cation to the ether oxygen. Presumably this mechanism is also operative in the acetolysis of tetrahydropyrans in the presence of boron trifluoride. The subsequent cleavage of a carbon–oxygen bond of the ether linkage and addition of an acetyl anion to the residual carbonium ion is more difficult to reconcile with the divergent results obtained. An intermediate cation, having the positive charge distributed between the oxygen atom and the carbon atoms in positions 2 and 3, analogous to the cation proposed in the acid-catalyzed cyclization of terpenes (11), would explain, for example, the formation of 1,3,6-hexanetriol in addition to the 1,2,6-isomer from 2-hydroxymethyltetrahydropyran. Such a cation could either cleave directly to such end products, or produce an intermediate olefin, analogous to those isolated by Paul (5) from 2-alkyl tetrahydrofurans. The olefinic diacetate could then be acetylated in the presence of boron trifluoride (12), or might recyclize to tetrahydrofuran-2-ethanol, which would undergo readily ring fission to 1,3,6-hexanetriol. Hydroxyl groups in the 3 position would prevent the formation of such intermediates and lead only to a single, expected product, which is in agreement with the present findings. However, such a mechanism would not explain the resistance to cleavage of the dihydroglycals and 4-hydroxytetrahydropyran. The failure of the former compounds to undergo ring fission may be explained (9) by boron complex formation of the type reported by Angyal and McHugh (10). Aliphatic ethers are known to form stable complexes with boron trifluoride (4) and it is conceivable that complex formation of one type or another prevents the cleavage reaction with some hydroxytetrahydropyrans.

It is concluded that although boron trifluoride is an excellent catalyst for the acetolysis of some tetrahydropyrans, the unexpected results obtained in other cases show that its action is not of a general nature.

EXPERIMENTAL

Paper chromatography was carried out using Whatman No. 1 paper and 1-butanol – ethanol – water (40:11:19, v/v) as solvent. The chromatograms were developed with ammoniacal silver nitrate spray reagent (13) and the distances travelled by compounds relative to rhamnose (R_{Rh}) were measured. Column chromatography was carried out on cellulose using benzene–ethanol–water (500:50:1, v/v) (A), 1-butanol (B), or 1-butanol $\frac{1}{4}$ saturated with water (C) as solvents. In counter-current distribution, a modified 100-tube E.C. Apparatus Co. fractionator was used (14). Deacetylation of polyol acetates was carried out in the manner previously described (2).

3,4-Dihydroxytetrahydropyran

(*a*) DL-*trans-3,4-Dihydroxytetrahydropyran* (*Dihydro*-DL-*xylal*)

A mixture of the diol (1.1 g) and acetic anhydride (10 ml) was saturated with boron trifluoride at such a rate that the internal temperature did not exceed 60° C. The reaction mixture was then heated on a steam bath for 4 hours, cooled, and poured into an ice-cold excess of saturated aqueous sodium carbonate or bicarbonate solution. The mixture was filtered and the residue and filtrate were extracted thoroughly with chloroform which was washed once with water, dried over calcium chloride, and evaporated. After distillation at 170–180° C and 0.5 mm, the cleavage product (2.05 g) was deacetylated.

Paper chromatography of the residue indicated a major component, R_{Rh} 1.14, and a minor component, R_{Rh} 1.73, the latter corresponding to unchanged starting material. The mixture was resolved by column chromatography using solvent B, and the cleavage product was thus obtained as a colorless sirup (0.9 g, 72%), b.p. 175–185° C (air bath) at 0.1 mm. Calculated for $C_5H_{12}O_4$: C, 44.11%; H, 8.88%. Found: C, 44.18%; H, 8.83%. The tetrol consumed 2.0 moles of periodic acid with the liberation of 1.0 mole of formaldehyde (15). The tetraacetate of the tetrol, prepared with sodium acetate and acetic anhydride, was a colorless oil, b.p. 175–180° C (air bath) at 0.5 mm; n_D^{20} 1.4442. Calculated for $C_5H_8(OCOCH_3)_4$: C, 51.31%; H, 6.63%; $COCH_3$, 56.6%. Found: C, 51.64%; H, 6.77%; $COCH_3$, 57.1%. The derived tetra-*p*-nitrobenzoate separated as light yellow crystals, m.p. 187° C, from acetone – ethyl acetate. Calculated for $C_{33}H_{24}N_4O_{16}$: C, 54.10%; H, 3.30%; N, 7.65%. Found: C, 54.47%; H, 3.54%; N, 7.68%.

When the cleavage reaction was carried out at 0° C for 18 hours and at room temperature for 24 hours, the product contained about 25% and 50%, respectively, of the tetrol.

(*b*) D-*trans-3,4-Dihydroxytetrahydropyran* (*Dihydro*-D-*xylal*)

Diacetyldihydro-D-xyla! (2.0 g) was treated with acetic anhydride (7.5 ml) and boron trifluoride and the resulting tetrol (0.9 g, 67%) was isolated and purified as described above. Periodic acid oxidation of the polyol and analyses of the free polyol and its tetraacetate were consistent with a 1,2,3,5-pentanetetrol structure. The tetrol had no optical rotation in saturated aqueous sodium borate and its derived tetra-*p*-nitrobenzoate was shown by melting point, mixed melting point, and X-ray powder diagram comparison to be identical with that of the tetrol from dihydro-DL-xylal.

(*c*) L-*cis-3,4-Dihydroxytetrahydropyran* (*Dihydro*-L-*arabinal*)

Dihydro-L-arabinal (0.5 g) was cleaved and the derived tetrol (0.3 g, 52%) isolated and purified as described above. The tetrol had no optical rotation in saturated aqueous sodium borate and its tetra-*p*-nitrobenzoate derivative was identical with those of the tetrols from dihydro-D- and dihydro-DL-xylal (melting point, mixed melting point, infrared spectrum, and X-ray powder diagram).

2-Hydroxymethyl-4,5-dihydroxytetrahydropyran

The triacetate of this triol (3.8 g) was treated with acetic anhydride (5 ml) and boron trifluoride at 100° C for 4 hours and the product isolated and purified in the usual way. Paper chromatography of the product indicated that it was a mixture of the starting material and a hexanepentol (R_{Rh} 0.66). The pentol was isolated by column chromatography using solvent C and was a colorless sirup (0.58 g, 25%), n_D^{20} 1.4860. Calculated for $C_6H_{14}O_5$: C, 43.36%; H, 8.49%. Found: C, 43.60%; H, 8.48%. The substance consumed 3.2 moles of periodic acid with the production of 1.8 moles of formaldehyde showing that it was essentially 1,2,3,5,6-hexanepentol. It failed to give a solid benzoate or *p*-nitrobenzoate. The pentaacetate, prepared with sodium acetate and acetic anhydride, was a pale yellow sirup, n_D^{20} 1.4488. Calculated for $C_6H_9(OCOCH_3)_5$: C, 51.06%; H, 6.43%; $COCH_3$, 57.1%. Found: C, 51.08%; H, 6.80%; $COCH_3$, 57.4%.

2-Methyl-3-hydroxytetrahydropyran

One gram of a tetrahydropyran fraction obtained from hydrogenolysis of α-methyl-D-glucopyranoside (2) was treated with acetic anhydride (6 ml) and boron trifluoride at room temperature for 18 hours. The crude product was distilled at 160–170° C (air bath) and 12 mm and was then deacetylated. Paper chromatography of the product indicated that cleavage was complete and that the product was a hexanetriol (R_{Rh} 1.73). The triol was purified by column chromatography in solvent A and by distillation at

130–135° C (air bath) and 0.1 mm giving a colorless sirup (0.64 g, 55%), n_D^{20} 1.4738. Calculated for $C_6H_{14}O_3$: C, 53.71%; H, 10.52%; C-methyl, 20.2%. Found: C, 53.43%; H, 10.50%; C-methyl, 20.2%. The triol consumed 1.0 mole of periodic acid and yielded 1.0 mole of acetaldehyde (16).

The triacetate was a colorless oil, b.p. 105° C (air bath) and 0.1 mm with n_D^{20} 1.4366 (Paul (5) reported n_D^{10} 1.44029; found n_D^{10} 1.4403). Calculated for $C_6H_{11}(OCOCH_3)_3$: C, 55.37%; H, 7.75%; $COCH_3$, 49.6%. Found: C, 54.97%; H, 7.90%; $COCH_3$, 50.7%.

The derived tris-*p*-nitrobenzoate, after several recrystallizations from methanol–acetone, had m.p. 149–150° C. Calculated for $C_{27}H_{23}O_{12}N_3$: C, 55.77%; H, 3.99%; N, 7.23%. Found: C, 55.95%; H, 3.90%; N, 7.24%.

4-Hydroxytetrahydropyran

γ-Pyrone (12.5 g) was hydrogenated in ethanol (75 ml) with Raney nickel (0.6 g) at 100° C and 80 atmospheres pressure for 10 hours. The residual oil, after evaporation of the solvent, was fractionally distilled, yielding 4-hydroxytetrahydropyran (8.5 g), b.p. 90–92° C at 12 mm, n_D^{20} 1.4590. This tetrahydropyran was recovered unchanged from the reaction with boron trifluoride and acetic anhydride at room temperature for 18 hours, at 65° C and at 100° C for 2 hours. At the elevated temperatures charring took place and at 100° C a very small amount of an oil, b.p. 125–130° C (air bath) and 0.1 mm was obtained. The deacetylated product had R_{Rh} 1.62, corresponding to a hexanetriol. The amount obtained was too small for further identification.

Dihydro-D-galactal

Dihydro-D-galactal (0.5 g) was treated with acetic anhydride (5.0 ml) and boron trifluoride at 100° C for 10 hours. The crude product, after deacetylation, showed two major spots, R_{Rh} 1.12 and 1.37, and a weak spot, R_{Rh} 0.74, on paper chromatography. Unchanged dihydrogalactal (0.15 g, R_{Rh} 1.12) was removed from the reaction product by crystallization from methanol – ethyl acetate and the residue was then chromatographed using solvent A. By this means, the material with R_{Rh} 1.37 was isolated and after crystallization from ethyl acetate was identified as dihydro-D-altral by means of mixed m.p. 101–103° C, and by comparison of its X-ray powder diagram with that of an authentic specimen (3). A similar result was obtained using triacetyldihydro-D-galactal and a large excess of acetic anhydride and boron trifluoride.

Dihydro-D-glucal and 1,5-Anhydro-D-sorbitol (Polygalitol)

The product from the reaction of dihydro-D-glucal (R_{Rh} 1.24) with excess acetic anhydride and boron trifluoride at 100° C for 4 hours was deacetylated and paper chromatography of the product showed two major components having R_{Rh} 1.37 and 1.12 and a trace component, R_{Rh} 0.76.

Polygalitol (R_{Rh} 0.74), when similarly treated, yielded a mixture of substances having R_{Rh} values of 0.85, 0.74, 0.45, corresponding to an isomerization product, unchanged starting material, and a hexitol respectively.

2-Hydroxymethyltetrahydropyran

The reaction between 2-hydroxymethyltetrahydropyran (5 g) and acetic anhydride (15 ml) and boron trifluoride was complete in 2 hours at room temperature. The crude acetate mixture was distilled at 117–128° C and 0.5 mm to give a pale yellow oil (6.4 g, 57%) n_D^{20} 1.4472, which failed to separate into more than one component when subjected to counter-current distribution between 70% acetone/petrol (b.p. 60–70° C) when 210 transfers were applied (14). The same oil resulted when the reaction was carried out at

room temperature for 24 hours and also when the acetate of the starting material (6.5 g) was similarly reacted with acetic anhydride (9 ml) and boron trifluoride. At 100° C, decomposition was extensive and only a small amount of the oil was isolated. Calculated for $C_6H_{11}(OCOCH_3)_3$: C, 55.37%; H, 7.75%. Found: C, 55.40%; H, 7.85%.

Deacetylation of the above oil yielded a pale yellow sirup, n_D^{20} 1.4720, which did not separate into more than one component on column chromatography using solvent A or on counter-current distribution between water and *n*-butanol with 120 transfers. On paper chromatography it showed a single spot R_{Rh} 1.73, corresponding to a hexanetriol. Calculated for $C_6H_{14}O_3$: C, 53.71%; H, 10.52%. Found: C, 53.89%; H, 10.40%. Oxidation of the sirup with periodic acid resulted in the uptake of 0.4 mole of oxidant and the formation of 0.4 mole of formaldehyde.

The triol mixture (0.5 g) in water (20 ml) and periodic acid (0.5 g) in water (10 ml) was left to stand at room temperature for 2 hours and was then treated with Dowex-1 – bicarbonate until it gave a negative reaction to starch/KI paper. The mixture was filtered and evaporated and formaldehyde removed from the residue by steam distillation. The residue was then dissolved in water, extracted several times with ether, and recovered by evaporation of the aqueous solution. Distillation of the residual material afforded a colorless sirup (0.2 g), b.p. 135° C (air bath) at 0.1 mm, having R_{Rh} 1.73, n_D^{20} 1.4696, and low reducing power to the silver nitrate spray. C alculated for $C_6H_{14}O_3$: C, 53.71%; H, 10.50%. Found: C, 53.40%; H, 10.58%.

The derived tris-*p*-nitrobenzoate, m.p. 130–131° C, crystallized from ethyl acetate. Calculated for $C_{27}H_{23}O_{12}N_3$: C, 55.77%; H, 3.99%; N, 7.23%. Found: C, 56.09%; H, 3.89%; N, 7.23%.

Synthesis of Tetrahydrofuran-2-ethanol

A solution of tetrahydrofuran-2-acetic acid, prepared from tetrahydrofurfuryl bromide (17) by the method of Barger *et al.* (7), (10.5 g) in dry ether (200 ml) was added slowly with stirring to a mixture of lithium aluminum hydride (3.59 g) and dry ether (150 ml). When addition was complete, the mixture was stirred at room temperature for 18 hours and the excess lithium aluminum hydride was then decomposed by careful addition of water. The mixture was then shaken with excess dilute sulphuric acid and the ethereal phase was extracted with aqueous sodium bicarbonate and the aqueous phase again extracted with ether for 18 hours. The ethereal solution of the neutral products was evaporated and the residue distilled at 115–120° C (air bath) and 20 mm giving tetrahydrofuran-2-ethanol (8.0 g, 85%) as a colorless mobile oil n_D^{20} 1.4545. Calculated for $C_6H_{12}O_2$: C, 62.04%; H, 10.41%. Found: C, 61.66%; H, 10.56%.

1,3,6-Hexanetriol from Tetrahydrofuran-2-ethanol

Tetrahydrofuran-2-ethanol (4.06 g) in acetic anhydride (5 ml) was added slowly with stirring to a refluxing mixture of acetic anhydride (15 ml) and zinc chloride (0.3 g) (8). The mixture was refluxed for a further 18 hours and most of the excess anhydride was removed by distillation. The residue was cooled and poured into cold saturated aqueous sodium carbonate. The product was extracted into chloroform, which was washed once with water and dried over calcium chloride and evaporated. The residue was distilled at 120–130° C and 0.5 mm to give 6.5 g (71%) of an oil having n_D^{20} 1.4408. Calculated for $C_6H_{11}(OCOCH_3)_3$: C, 55.37%; H, 7.75%; $COCH_3$, 49.6%. Found: C, 55.58%; H, 7.52%; $COCH_3$, 49.5%.

The oil was deacetylated in the usual way and the triol was purified by column chromatography in solvent A and by distillation at 135° C (air bath) and 0.1 mm. The infrared

spectrum of the sirup, n_D^{20} 1.4753, was indistinguishable from that of the triol of 2-hydroxymethyltetrahydropyran. Confirmation of this identity was obtained by mixed melting point determination and infrared spectra comparison of the derived *p*-nitrobenzoate.

ACKNOWLEDGMENTS

We are grateful to Mr. M. Granat for infrared analyses, to Mr. T. M. Mallard for X-ray powder diagram determinations, to Mr. M. Mazurek and Mr. J. A. Baignée for microanalyses, and also to Dr. A. S. Perlin for his advice and criticism.

REFERENCES

1. BAUER, H. F. and STUETZ, D. E. J. Am. Chem. Soc. **78**, 4097 (1956).
2. RUDLOFF, E. VON, STUETZ, D. E., and BAUER, H. F. Can. J. Chem. **35**, 315 (1957).
3. RUDLOFF, E. VON and TULLOCH, A. P. Can. J. Chem. **35**, 1504 (1957).
4. BURWELL, R. L. Chem. Revs. **54**, 615 (1954).
5. PAUL, R. Bull. soc. chim. France, **8**, 369 (1941).
6. SOCIÉTÉ DES USINES CHIMIQUES RHÔNE-POULENC. Brit. Pat. No. 606,564, Aug. 17, 1943; cf. Chem. Abstr. **43**, 1435f (1949).
7. BARGER, G., ROBINSON, R., and SMITH, H. L. J. Chem. Soc. 718 (1937).
8. GRUMMITT, O., STEARNS, J. A., and ARTERS, A. A. *In* Organic syntheses. Vol. 29. *Edited by* C. S. Hamilton. John Wiley & Sons, Inc., New York. 1949. p. 89.
9. DEAN, F. M. Private communication.
10. ANGYAL, S. J. and MCHUGH, D. J. J. Chem. Soc. 1423 (1957).
11. RE, L. and SCHINZ, H. Helv. Chim. Acta, **41**, 1695 (1958).
12. ZAVGORODINII, S. V. Otdel. Khim. Nauk, 872 (1955); cf. Chem. Abstr. **50**, 9329f (1956); **33**, 5805[9] (1939).
13. PARTRIDGE, S. M. Nature, **158**, 270 (1946).
14. RAYMOND, S. Anal. Chem. **30**, 1214 (1958).
15. LAMBERT, M. and NEISH, A. C. Can. J. Research, B, **28**, 83 (1950).
16. DESNUELLE, P. and NAUDET, M. Bull. soc. chim. France, **12**, 871 (1951).
17. SMITH, L. H. *In* Organic syntheses. Vol. 23. *Edited by* L. I. Smith. John Wiley & Sons, Inc., New York. 1943. p. 88.

THE DECOMPOSITION OF SOLID POTASSIUM CHLORATE BY X RAYS[1]

H. G. HEAL[2]

ABSTRACT

Potassium chlorate irradiated with X rays has been found to contain chloride, chlorite, hypochlorite, and occluded oxygen, and probably also substantial amounts of dichlorine hexoxide and a trace of chlorine dioxide. The chlorite and hypochlorite appear to decompose during irradiation to chloride. *G* values are given for 25° and −196°. They vary little with temperature or dose rate.

INTRODUCTION

There has been no previous detailed study of the decomposition of solid potassium chlorate by ionizing radiation. In 1953, however, Hennig, Lees, and Matheson (9) published *G* values for the formation of oxygen when this salt is irradiated in a nuclear reactor, and in the same year the present writer published a brief note mentioning the finding of chlorite, hypochlorite, and chloride in X-irradiated potassium chlorate (6). One of the aims of the investigation reported here was to determine the nature of the decomposition products, which had not been more than tentatively identified. This is not a particularly straightforward matter, since the usual analytical methods only show what is present in a *solution* of the irradiated salt; the substances present in the original crystal are quite likely to be different (7, 8). We have now tried to identify these by examining the absorption spectra of the crystals, in conjunction with ordinary analysis. The other main purpose of this study was to learn what we could about the reaction mechanisms from a rough survey of the kinetics of decomposition.

EXPERIMENTAL

Reagent grade potassium chlorate was recrystallized once by cooling a hot aqueous solution. Rapid cooling gave small platelets, averaging 0.02 mm thick. These were dried for a week at 160°; they then melted quietly when heated, without any trace of decrepitation, showing the absence of water. These crystals were employed in studies of chemical decomposition. Slower cooling gave larger plates from 0.04 mm to 0.15 mm thick, selected specimens of which were used for plotting absorption spectra.

A Machlett OEG-60 X-ray tube, with tungsten target, was the source of radiation employed in the work on chemical decomposition. It was run at 50 kvp, 28 ma, with rectified but not filtered 60-cycle high voltage supply. The sample holder is shown in Fig. 1. Each sample weighed 1.2 to 1.6 mg. It was spread out over the bottom (5 mm in diameter) of a dish pressed from 0.017-mm aluminum foil. Typical samples were seen under the microscope to consist of platelets 0.01 mm to 0.03 mm thick, stacked two or three deep in many places. In order to achieve reasonably uniform rates of energy absorption in such samples, it was necessary to filter out the softer X radiation from the beam. The more filtration is used, the more uniform the rate of energy absorption through the sample, but the lower the dose rate. In the best series of irradiations, only negligible portions of the sample received energy at rates differing by more than 6% from the average for the whole sample. This entailed heavy filtration (294 mg/cm² of aluminum) and long irradiations (up to 75 hours). In another series of irradiations with filtration 84 mg/cm² of aluminum, the average dose rate was three times as great, but

[1]*Manuscript received January 23, 1959.*
Contribution from the Chemistry Department, University of British Columbia, Vancouver.
[2]*Present address: Chemistry Department, Queen's University, Belfast, Ireland.*

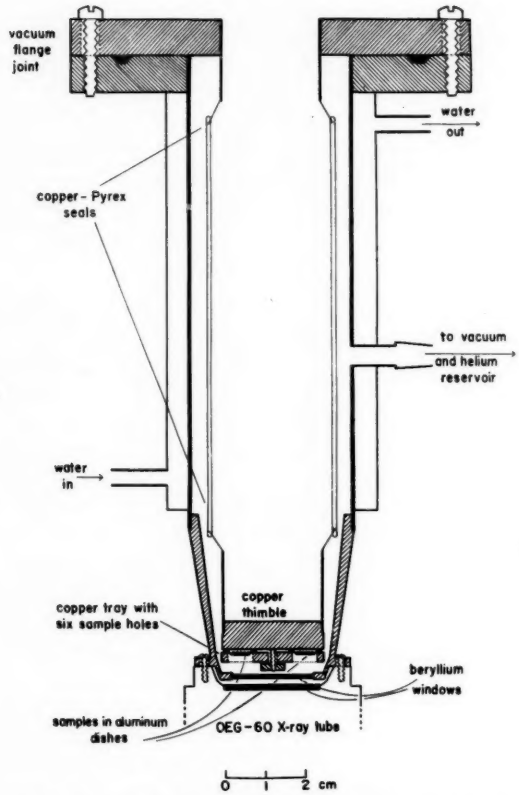

FIG. 1. Irradiation vessel for chemical decomposition studies. The filters are omitted for the sake of clarity. They consisted of aluminum disks which were placed between the two beryllium windows.

some parts of the sample received energy at rates up to 15% different from the average. Most irradiations were performed at 25°±1° under 0.5–1.0 mm of dry helium, which served to conduct away heat generated in the sample by the radiation, and prevented any appreciable rise of temperature. Results quoted for −196° were obtained from single crystals about 0.1 mm thick, which were cemented along one edge to the bottom of the central copper thimble of the irradiation vessel. The vessel was evacuated and the thimble filled with liquid nitrogen.

The absolute energy flux at the position of the samples was measured calorimetrically as described in an earlier publication (6), and the rate of energy absorption in the samples computed using tables of mass absorption coefficients, along with De Waard's formula for the spectral energy distribution of the X rays (1).

The apparatus used for plotting absorption spectra is shown in Fig. 2. The sample, a single crystal plate, was cemented across a hole 3 mm square in a copper block, which was maintained at the desired temperature. This crystal could be made to face either a small beryllium window through which the X-ray beam entered, or, by rotation through 90° on a standard taper joint, a pair of quartz windows through which the light beam of the spectrophotometer passed. The apparatus could be coupled to the

X-ray tube, a Machlett AEG-50-T, or fitted into the cell compartment of a Cary Model 14 recording spectrophotometer, by arrangements not shown in the diagram. As in the chemical work, the radiation was heavily filtered to ensure a nearly uniform dose rate throughout the crystal.

All sample weighings were done with a Cahn electrobalance sensitive to ± 2 μg.

For the spectrophotometric determination of chlorite and hypochlorite in solutions of irradiated chlorate, the solutions were placed in special quartz optical cells with a light path of 1 cm, but requiring only 0.5 ml of solution. The spectrophotometer was again the Cary Model 14. For the turbidimetric determination of chloride, the transmission of the samples was measured with a Bausch and Lomb Spectronic 20 calorimeter, run from a constant voltage transformer. For convenience, the other details of these procedures are described in the next section.

In order to minimize analytical errors when the degree of decomposition was small, up to six similarly irradiated samples were often combined for one analysis.

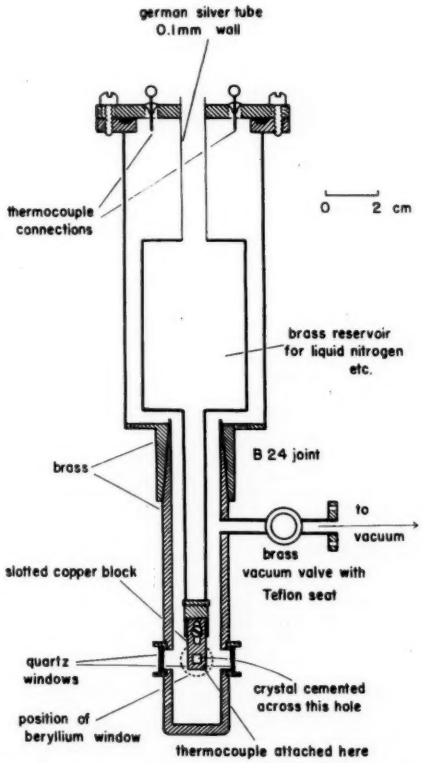

FIG. 2. Irradiation vessel used in the study of absorption spectra.

RESULTS

During irradiation at 25° the crystals darken gradually to a golden-brown tint. Up to about 8% decomposition, practically all the oxygen gas formed remains occluded within the crystals, as shown by the constancy of their weight. Above about 10% decompo-

sition the crystals "pop" or decrepitate at the slightest touch, presumably because of the oxygen pressure. Hennig, Lees, and Matheson also observed this phenomenon (9). With continued irradiation the crystals disintegrate to a light, fluffy, nearly white powder.

The decomposition products identified with reasonable certainty in irradiated potassium chlorate were oxygen, chloride, chlorite, and hypochlorite ions. Perchlorate ion was probably also present. Other products present in smaller amounts were tentatively identified as dichlorine hexoxide and chlorine dioxide. The methods by which these substances were identified and analyzed for will now be described.

Gas occluded in the irradiated crystals was determined by the microscope slide method described in an earlier publication (5). The crystals were dissolved in 0.025 *M* sodium carbonate which had been saturated with oxygen gas, by bubbling, immediately beforehand, with the object of minimizing errors due to the solubility of oxygen. The gas collected was assumed to be *oxygen*, since chlorine and all its oxides would have dissolved in or reacted with the sodium carbonate solution.

Considering next the *chlorite* and *hypochlorite*, Fig. 3 shows the absorption spectrum of a typical sample of irradiated chlorate, dissolved in 0.025 *M* sodium carbonate (pH

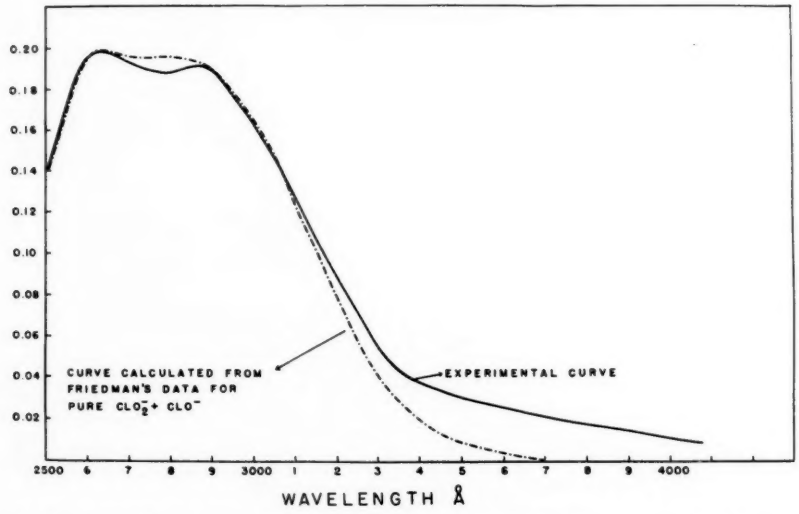

FIG. 3. Spectrum of a solution of irradiated $KClO_3$ in 0.025 *M* Na_2CO_3, compared with the spectrum for an appropriate ClO^-/ClO_2^- mixture from Friedman (ref. 2).

11 approximately). The peak at 2610 Å probably arises from chlorite ion, and the one at 2900 Å from hypochlorite ion. As the figure shows, the experimental spectrum agrees well with that calculated for an appropriate mixture of chlorite and hypochlorite, using Friedman's data for these ions (2). The only serious divergence is in the region 3300 Å to 4000 Å, where the samples always showed a weak absorption not attributable to chlorite or hypochlorite. This disappeared gradually over an hour or so. We attribute it to *chlorine dioxide*, which has an absorption maximum at about 3600 Å and is stated to hydrolyze slowly. The spectra appeared as depicted immediately after the samples were dissolved, suggesting that the chlorite was mostly present as such in the crystals,

and was not formed by the hydrolysis of chlorine dioxide present in the crystals. The absorption spectra of irradiated crystals themselves support this conclusion. Figure 4 shows a series of spectra for a crystal irradiated at 25°. Peaks developed at 2600 Å and

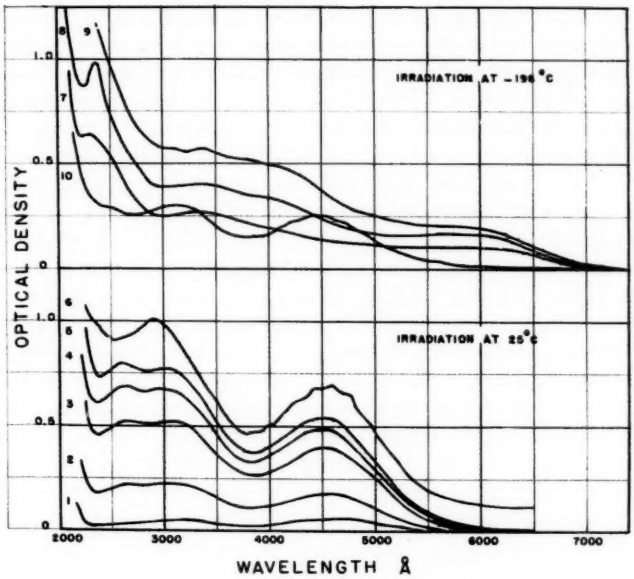

FIG. 4. Absorption spectra of irradiated $KClO_3$ crystals. (All optical densities relative to the unirradiated crystal.)

Below (curves 1 to 6) for crystal irradiated at 25° C. Crystal 0.12 mm thick. (All spectra measured at 25°, except (6).)

(1) After 3.08 hours, irradiation (0.38×10^{23} ev/mole).
(2) After 10.42 hours (1.28×10^{23} ev/mole).
(3) After 25.6 hours (3.15×10^{23} ev/mole).
(4) After 35.7 hours (4.4×10^{23} ev/mole).
(5) After 47.4 hours (5.8×10^{23} ev/mole).
(6) As in (5), but spectrum measured at −196°. The ordinate for this curve has been raised 0.1 unit of optical density for clarity.

Above (curves 7 to 10) for crystal irradiated at −196° C. Crystal 0.04 mm thick. (All spectra measured at −196°.)

(7) After 1 hour and 40 minutes' irradiation (0.86×10^{23} ev/mole).
(8) After 2 hours and 50 minutes' irradiation (1.46×10^{23} ev/mole).
(9) After 4 hours and 50 minutes' irradiation (2.49×10^{23} ev/mole).
(10) After 8 hours' irradiation at −196°, crystal warmed to room temperature for 2 hours, then cooled to −196° again for plotting spectrum (total dose 4.14×10^{23} ev/mole).

3100 Å, which we attribute to chlorite and hypochlorite respectively. The optical densities at the peaks agree within 15% with the values expected from the amounts of chlorite and hypochlorite found by analysis in the crystal, assuming the extinction coefficients in the solid to be the same as in solution. Quantitative analyses for chlorite and hypochlorite were carried out by dissolving the irradiated sample in 0.5 ml of 0.025 *M* sodium carbonate, and measuring optical densities at 2610 Å and 2900 Å. The absorption bands of the two ions overlap, so the amounts of chlorite and hypochlorite were calculated as solutions of a pair of simultaneous equations, using molar extinction coefficients from Friedman's paper.

Chloride could not be tested for by the usual reagent, silver ion in nitric acid solution, since the chlorite already known to be there disproportionates to an uncertain extent to chloride in acid pH's; moreover, silver ion is stated to precipitate silver chloride from

hypochlorite solutions (3). Instead, the chloride was allowed to react with silver ion in a weakly alkaline medium (0.01 *M* borax, pH about 9). At this pH, neither silver oxide nor silver borate precipitates, and we established spectrophotometrically that chlorite–hypochlorite mixtures are stable indefinitely. We ascertained by trial that after adding excess silver nitrate, in a very small volume, to a solution of irradiated chlorate in 0.01 *M* borax, and allowing the precipitate of silver chloride to settle, the chlorite and hypochlorite bands appeared in the absorption spectrum of the supernatant liquid exactly as they had been before adding the silver nitrate. This shows that silver nitrate precipitates chloride alone, without interference from chlorite or hypochlorite, in 0.01 *M* borax. For the quantitative estimation of chloride, the sample was dissolved in 1.0 ml 0.01 *M* borax. Water (0.5 ml) was added, followed by 1.5 ml of millimolar silver nitrate, shaking well at each stage. At the same time, a reference solution and two standards were made up. Each contained unirradiated potassium chlorate equal in weight to the sample. The standards contained, in addition, appropriate volumes of millimolar potassium chloride in place of some or all of the water. The quantities of chloride in the standards were chosen to "bracket" that expected for the sample, which had been roughly determined in earlier runs. All solutions were in 10-ml colorimeter test tubes which we had matched. After the solutions were shaken and left to stand for half an hour in the dark, the optical densities of all suspensions were measured at 375 mμ. Control experiments had established that the optical densities in the range we worked with were proportional to the amount of chloride, and (in confirmation of published work (11)) that they reached a maximum steady value in a few minutes less than the half-hour waiting period, at the laboratory temperature (26°).

The amount of gaseous oxygen recovered was less than equivalent to the hypochlorite, chloride, and chlorite, by an amount exceeding any likely experimental error. The most obvious explanation is that some *perchlorate* was formed. This ion could not be directly determined because there appears to be no simple micromethod applicable in the given circumstances. The infrared absorption spectrum of an irradiated sample believed from the material balance to contain 2 mole % of perchlorate was taken by the potassium chloride disk method. It showed a small peak at 1113 cm^{-1} not visible in the spectrum of unirradiated potassium chlorate. This falls close to the main maximum in the spectrum of pure potassium perchlorate (about 1100 cm^{-1}). This observation cannot be considered reliable evidence of perchlorate, since the side of the very strong main chlorate band extends into this region and tends to obscure small structural features. Nevertheless, we consider the formation of perchlorate to be the most likely explanation of the oxygen deficiency, especially in view of Sharman and McCallum's observation that pile-irradiated sodium chlorate contains substantial amounts of perchlorate (14).

The evidence for *dichlorine hexoxide* in irradiated potassium chlorate is derived solely from the absorption spectra of crystals. This substance hydrolyzes to chloric and perchloric acids when dissolved in water, so could not have been detected by any simple chemical method. Figure 4 shows the spectra in question. Besides the bands attributed to chlorite and hypochlorite already mentioned, irradiation at 25° produced a strong band with maximum at 4500 Å, which was responsible for the brown color of the crystals. When the crystal was cooled to −196°, this band developed a structure, as shown. Since this structure only appeared on cooling, it cannot have been an optical effect arising from polarization as described by Pringsheim (13), but must have been a true vibrational structure. The spacing of the subsidiary maxima was irregular and ranged from 570 to 680 cm^{-1}. The structure shows that this band came from a molecular

species, and not a color center. According to published information, no band anywhere near this position is to be found in the spectrum of chlorine or of any of the chlorine oxyanions or oxides, with the exception of Cl_2O_6 (12). The spectrum of this oxide has not been fully investigated, but the long wavelength edge of its absorption band, as described by Goodeve and Richardson (4) corresponds with the long wavelength side of our 4500 Å band.

The spectrum of crystals irradiated at −196°, and then allowed to warm up to 25°, was quite different (Fig. 4). The 4500 Å band was missing, and there was absorption over a considerable range of wavelengths, with one well-defined maximum at 2400 Å and several other ill-defined maxima. When the crystals were warmed to room temperature, the 2400 Å maximum and most of the remaining absorption disappeared, being replaced by a spectrum very similar to that obtained by irradiation at room temperature, including a strong band at 4500 Å. This developed structure on cooling of the crystal, and was obviously due to the same substance as the 4500 Å band produced by irradiation at 25°.

Our data on the *kinetics* of the decomposition are summarized in Fig. 5 and Table I. The figure shows the results of the best series of runs at 25°, viz. those done with the most heavily filtered radiation, and consequently the most nearly uniform dose rate. The main facts about Fig. 5 are as follows. Chlorite and hypochlorite were generated

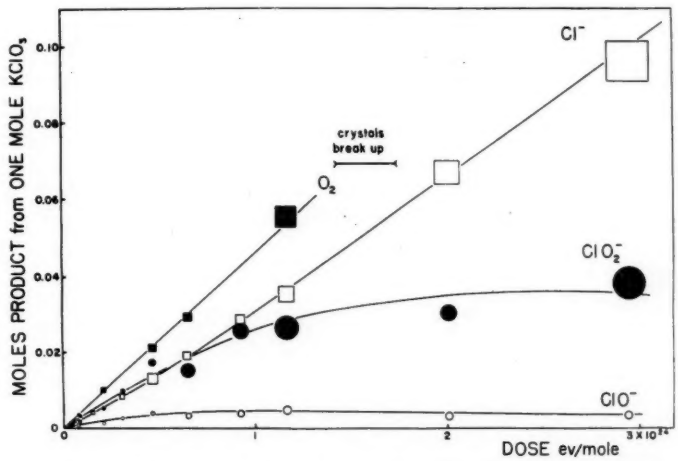

FIG. 5. Yields of chloride, hypochlorite, chlorite, and oxygen on dissolving $KClO_3$ irradiated for various times at 25° (dose rate 0.39×10^{23} ev/mole per hour). Sizes of experimental points represent possible analytical errors.

at rates which decreased with time until their concentrations became roughly steady. Chloride was formed at a rate increasing somewhat with time at first, and then (after a dose of about 10^{24} ev/mole) roughly constant. The final slope of the chloride line is about 25% greater than the initial slope. The rate of formation of oxygen was approximately constant up to the point where it began to escape from the crystals, and could no longer be determined. Some of the points of the chlorite curve are scattered more widely than would be expected from analytical errors alone; the reason is unknown. The general picture for the higher dose rate at 25°, and for the runs at −196° (not plotted, but data given in Table I), was very similar in all respects.

TABLE I

Initial G values (molecules per 100 ev absorbed) for the formation of products in the X irradiation of potassium chlorate

Temp., °C	Dose rate, ev/mole per hour	G_{Cl^-}	G_{ClO^-}	$G_{ClO_2^-}$	G_{O_2}	$G_{Cl_2O_6}$	G_{ClO_2}
25	1.24×10^{23}	1.9	0.7	2.6	2.9	—	≈0.2
	0.39×10^{23}	1.3	0.5	2.0	2.5	—	
	0.12×10^{23}	—	—	—	—	1.4*	
−196	0.38×10^{23}	1.1	0.5	1.5	2.0	Not formed	

*Value estimated from optical density of crystal at 5460 Å, using $\epsilon = 80$ (Goodeve and Richardson, ref. 4) (see also ref. 10).

DISCUSSION

Chloride, hypochlorite, and chlorite all appear to be formed at the earliest stages of decomposition accessible to our measurements, viz. a few tenths of one per cent. Probably they all arise directly from chlorate by alternative processes of excitation and subsequent breakdown. The bodies decomposing cannot be positively identified, but are probably not ClO_3 molecules or radicals in their ground state, which are stable. The reactions occurring are likely to be:

$$ClO_3^{-*} \rightarrow Cl^- + O_2 + O \quad [1]$$
$$ClO_3^{-*} \rightarrow ClO^- + O_2 \quad [2]$$
$$ClO_3^{-*} \rightarrow ClO_2^- + O. \quad [3]$$

The perchlorate thought from the material balance to be present might be formed by a reaction between unexcited chlorate ions and O atoms from [1] and [3]:

$$ClO_3^- + O \rightarrow ClO_4^-. \quad [4]$$

The maximum possible yield of perchlorate (taking for discussion the figures for the lower dose rate at 25°) which could be associated with the observed oxygen deficiency is $G_{ClO_4^-} = 1.9$. The yield of O atoms from [1] and [3] is given by $G_O = 3.3$, considerably more than adequate to account for any perchlorate present.

The other main reaction product, thought to be Cl_2O_6, might arise as follows. Irradiation gives rise to positive holes (equivalent to ClO_3 radicals) and electrons in the conduction band. We suggest that at −196° these positive holes do not migrate rapidly, and that the strong ultraviolet absorption observed at this temperature is partly due to ClO_3, which is known to absorb with a maximum just below 3000 Å (12). The spectrum, however, gives no indication of the usual types of trapped electron centers, which would absorb in the region upwards of 5000 Å, and there is a question as to the fate of the electrons. We suggest that these are trapped by some of the O atoms from [1] and [3], which are not accounted for by [4], giving O^- or $O^=$ ions. The oxygen atom has an electron affinity of about 2.2 v, so that it should trap electrons efficiently. The wavelength at which the resulting O ion begins to absorb light would depend on its environment, but is not outside the range of the optical absorption observed in crystals irradiated at −196°. When the crystals are warmed up, some of the positive holes would be annihilated by electrons, while others may migrate together in pairs, forming Cl_2O_6 molecules, which are known to be very stable.

The drop in the net rates of formation of chlorite and hypochlorite as irradiation continues (Fig. 5) can best be explained by the secondary decomposition of these ions to chloride by the radiation:

$$\left.\begin{aligned} ClO_2^{-*} &\rightarrow Cl^- + O_2 \\ ClO^{-*} &\rightarrow Cl^- + O. \end{aligned}\right\} \quad [5]$$

This might be expected to lead to an increase in the total rate of formation of chloride as irradiation continues. Such an increase is observed, but cannot be given any simple quantitative interpretation. Examination of the data of Fig. 5, for example, discloses that when the concentrations of ClO_2^- and ClO^- are steady, the rates of destruction, and hence also the rates of formation, of these ions must be considerably less than their initial rates of formation; for in this region, the total G_{Cl^-} is only 1.6. If the initial rates of formation of ClO_2^- and ClO^- persisted into the steady state, the rate of formation of chloride from reactions [5] alone would equal $(G_{ClO_2^-}+G_{ClO^-})_{initial} = 2.5$. It seems that the excitons produced by the radiation are used at first mainly in reactions [1] to [3]. Soon, however, the ClO^- and ClO_2^- ions formed in [2] and [3] begin to trap a considerable proportion of the excitons, and use them in reactions [5], causing the yields from [1], [2], and [3] to diminish. ClO^- and ClO_2^- should trap excitons efficiently, since their excitation energies (as shown by their optical absorption) are lower than the minimum excitation energies of ClO_3^- and ClO_4^-. The experimental data do not suffice to give a more detailed picture of exciton utilization. It is interesting to note that the variation of chlorite and hypochlorite concentration with dose in potassium perchlorate (reported in an earlier paper (6)) is very much like that found in potassium chlorate, probably for similar reasons.

The assumption made in the preceding discussion, that all the primary chemical steps are initiated by single excitons, is justified by the small effect of dose rate on the G values (Table I). Reactions involving pairs of excitons would usually proceed at rates proportional to intensity squared, or, what is equivalent, their G values would be proportional to dose rate. Experimentally, all the G values do seem to increase somewhat with dose rate, but not nearly in proportion to it. Since the dose rate was regulated by varying the filtration, this small apparent variation of G values may well be due to systematic errors in the calculations of energy absorption, due among other causes to insufficiently accurate knowledge of the spectral energy distribution of the X rays. The variation of G with temperature over the enormous range from 25° to −196° is so small that none of the reactions can require thermal activation in the ordinary sense.

Our G values for the generation of oxygen (2.5 and 2.9 at 25°) agree well with the values 2.5 and 2.6 reported for pile-irradiated potassium chlorate by Hennig, Lees, and Matheson (9).

ACKNOWLEDGMENT

It is a pleasure to acknowledge the generous support for this investigation received from the Defence Research Board of Canada.

REFERENCES

1. De Waard, R. H. Proc. Acad. Sci. Amsterdam, **49**, 944, 1011 (1946).
2. Friedman, H. L. J. Chem. Phys. **21**, 319 (1953).
3. Gmelin's Handbuch der anorganischen Chemie. System-nummer 6(Chlor). Verlag Chemie G.M.B.H., Berlin. 1927. p. 290.
4. Goodeve, C. F. and Richardson, F. S. Trans. Faraday Soc. **33**, 453 (1937).
5. Heal, H. G. Nature, **172**, 30 (1953).
6. Heal, H. G. Can. J. Chem. **31**, 91 (1953).
7. Heal, H. G. Can. J. Chem. **31**, 1153 (1953).
8. Heal, H. G. Trans. Faraday Soc. **53**, 210 (1957).
9. Hennig, G., Lees, R., and Matheson, M. S. J. Chem. Phys. **21**, 664 (1953).
10. Kalina, M. H. and Spinks, J. W. T. Can. J. Research, B, **16**, 381 (1938).
11. Lamb, A. B., Carleton, P. W., and Meldrum, W. B. J. Am. Chem. Soc. **42**, 253 (1920).
12. Supplement to Mellor's comprehensive treatise of inorganic and theoretical chemistry. The halogens. Vol. I (18). Longmans, Green, & Co., Ltd., London. 1956.
13. Pringsheim, P. J. Chem. Phys. **23**, 369 (1955).
14. Sharman, L. J. and McCallum, K. J. J. Chem. Phys. **23**, 597 (1955).

PREPARATION OF SOME FLUORINE-CONTAINING TRISUBSTITUTED AROMATIC HYDROXYLAMINES[1]

B. A. GINGRAS AND C. H. BAYLEY

ABSTRACT

The preparation and properties of aryl dialkyl hydroxylamines in which the aryl group is a fluorobenzene derivative, and the two alkyl substituents are 2-cyano-2-propyl groups, are described.

Fluorine and its inorganic derivatives have been known for some time to be toxic to many live species (1) and, more recently, the high toxicity of fluoroacetic acid and many of its derivatives has been demonstrated (2). Although aromatic fluorine compounds have been prepared in good yields since 1927 (3), it was not until 1949 that the first systematic investigation of their fungistatic properties was undertaken (4). It was found that a number of monofluorinated quinones and nitrophenols showed good activity against the organisms *A. niger*, *A. terreus*, *M. verrucaria*, and *C. globosum*, the last two being cellulolytic. Addition of a second fluorine atom resulted in a decrease in potency and, for the fluoronitrophenols, a loss of activity was obtained by addition of another nitro group. However, in the aromatic hydrocarbon series, addition of a second nitro group markedly increased the potency, the most powerful compound being 2,4-dinitro-5-fluorotoluene (5). There are some indications that with multiple halogen dissimilar halogens give higher potencies, the most effective of all the compounds studied being 1-fluoro-3-bromo-4,6-dinitrobenzene, which, in concentration of 0.8 p.p.m., prevented growth of *A. niger* (6).

Most aromatic fluorinated nitro compounds have a yellow color and impart this to materials to which they are applied. This may be an objectionable feature, especially in the treatment of textile fibers for the suppression of microbiological attack. In the search for new antifungal compounds for this latter type of application, a series of colorless derivatives of fluoronitrobenzene have been prepared. These are O,N,N-trisubstituted hydroxylamines (I), similar to those reported by Gingras and Waters (7).

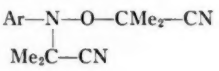

I

They are prepared through a free radical reaction from aromatic *C*-nitroso compounds and 2-cyano-2-propyl free radicals as follows. An aromatic amine (II) is first diazotized and then transformed into the fluorine derivative (IV) through a Schiemann reaction (3, 8). Nitration, followed by mild reduction gives the nitroso compound (VI), which is in turn reduced to the tertiary hydroxylamine (VIII) with two 2-cyano-2-propyl radicals (VII), the latter being produced by thermal dissociation of 2,2′-azo-bis-isobutyronitrile (IX) in solution (9).

In some instances, especially when the resulting mixture from nitration was difficult to separate into pure products, a nitroamine was used as starting material. In these

[1]*Manuscript received February 5, 1959.*
Contribution from the Division of Applied Chemistry, National Research Council, Ottawa, Canada. Issued as N.R.C. No. 5148.

Can. J. Chem. Vol. 37 (1959)

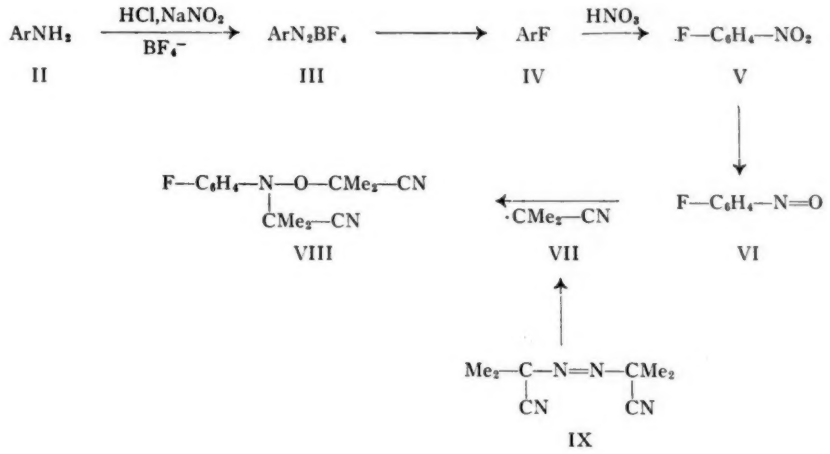

II III IV V VIII VII VI IX

cases, special precautions had to be taken as thermal decomposition of benzene diazonium fluoborates (III) containing a nitro group is difficult to control with resultant possibility of poor yields (8).

The tertiary hydroxylamines together with the intermediate nitro compounds are listed in the table. Except for 2,4-dimethyl-6-nitrofluorobenzene, all the nitro compounds had been previously described.

TABLE

	Fluoronitro compounds: Ar—NO_2			Fluoro tertiary hydroxylamines: Ar—N(CMe_2CN)—O—CMe_2CN		
Starting material	Ar- groups	M.p. or b.p., °C at mm Hg	Lit. m.p. or b.p., °C at mm Hg	M.p., °C	Found, %	Required, %
p-Nitroaniline	4-FC_6H_4—	95/22	95–97.5/22 (11)	121	C, 64.3 H, 6.4 N, 16.0	64.4 6.1 16.0
o-Nitroaniline	2-FC_6H_4—	110/21	110–112/22 (11)	117.5	C, 64.7 H, 6.3 N, 16.2	64.4 6.1 16.0
2-Methyl-5-nitroaniline	3,4-F(Me)C_6H_3—	m.p. 34	m.p. 34 (12)	79	C, 65.2 H, 6.5 N, 15.0	65.5 6.5 15.3
2,4-Dimethyl-6-nitroaniline	2,3,5-F(Me_2)C_6H_2—	m.p. 70	—	88	N, 14.4	14.5
o-Fluorotoluene*	3,4-Me(F)C_6H_3—	m.p. 42 120/25	m.p. 41.5 99.4/13 (13)	86.5	C, 65.9 H, 7.0 N, 15.4	65.5 6.5 15.3
m-Toluidine	2,4-Me(F)C_6H_3—	111/21 †	78.5/3 216/775 (14)	100	C, 65.2 H, 6.5 N, 15.3	65.5 6.5 15.3
p-Fluoroanisole*	2,5-OMe(F)C_6H_3—	m.p. 62	m.p. 61.5 (15)	97.5	C, 61.9 H, 6.3 N, 14.8	61.8 6.2 14.4

*Eastman organic chemical used without further purification.
†Boiling point arrived at by extrapolation.

The fluorohydroxylamines are white solids, easily purified by chromatography and crystallization. They are practically insoluble in water, but dissolve in most organic solvents. Infrared spectra are of requisite character and, as expected, they are very similar to those obtained for the corresponding chlorine analogs (7). They all show the typical nitrile band at 4.5 μ, a band at 6.25 μ due to vibrations of the aromatic ring, and among others, a medium or strong band in the 9 μ region. Although the latter is indicative of $\rangle$C—F grouping (10), no conclusion can be drawn here, as this region is also characteristic of the C—O and N—O stretching frequencies. Furthermore, the chlorine analogs also show a strong band in this region (7) and hence, it is probable that this is due to some covalencies of the system $\begin{matrix} C \\ \diagdown \\ C \diagup \end{matrix}$N—O—C of the hydroxylamines.

Preliminary examination shows that reduction of the nitro compounds to the substituted hydroxylamines resulted in a decrease of potency. Other types of fluorine compounds are being examined simultaneously and it is hoped that a full discussion of the biological results will be published elsewhere.

EXPERIMENTAL

2,2′-Azo-bis-isobutyronitrile was the commercial product Porophor N, (Westville laboratories) and was recrystallized before use, from ethyl acetate, to m.p. 104° C; lit. m.p. 103–104° (16). Diazonium fluoborates were prepared and decomposed by the method of Balz and Schiemann (3, 8). Nitro compounds were reduced to the corresponding nitroso compounds by the method of Lutz and Lytton (17). All melting points were taken on a Fisher–Johns apparatus and are corrected.

p-Fluoronitro- and p-Fluoronitroso-benzene

p-Nitroaniline (34.6 g, 0.25 mole) was converted into *p*-fluoronitrobenzene (15.2 g, 45%) by the Schiemann reaction (8). The preparation of *p*-fluoronitrosobenzene is typical and is described in detail. *p*-Fluoronitrobenzene (14.1 g, 0.1 mole) was dissolved in a mixture of alcohol (42 ml) and water (24 ml) and powdered calcium chloride (1.5 g) was added. The mixture was heated to boiling and zinc dust (20 g) was added in small portions. At the end, the solid residue was removed by filtration and the filtrate was poured into an ice-cold solution of ferric chloride (37 g) in water (600 ml). The dark green precipitate of nitroso compound that formed was separated by filtration, and washed with ice-cold water. The product was purified by steam distillation; yield: 6.5 g (52%).

Reaction between p-Nitrosofluorobenzene and 2,2′-Azo-bis-isobutyronitrile

p-Nitrosofluorobenzene (6.5 g, 0.05 mole) and 2,2′-azo-bis-isobutyronitrile (16.4 g, 0.1 mole) were dissolved in toluene (150 ml) and the solution was heated to 80° C. The azo compound was decomposed and the green color of the nitroso compound soon disappeared. Heating was continued under reflux for 2 hours to assure complete decomposition of the azobutyronitrile. The toluene and radical dimer (tetramethylsuccinonitrile formed by combination of two free radicals VII) (9) were distilled with steam and the residue taken up in ether and dried. After evaporation of the ether, the residue was chromatographed through a column of silica gel. A mixture of benzene and ethyl ether 9:1 eluted ON-di-(2-cyano-2-propyl)-N-(*p*-fluorophenyl) hydroxylamine (5.31 g, 40% from the nitroso compound; 8% over-all yield from original amine; m.p. 121°). The product was recrystallized from aqueous alcohol 80%.

o-Fluoronitro- and o-Fluoronitroso-benzene

o-Nitroaniline (34.6 g, 0.25 mole) gave 4.4 g (14%) of *o*-fluoronitrobenzene. This gave, by the method previously described, 1.8 g (46%) *o*-fluoronitrosobenzene.

Reaction between o-Fluoronitrosobenzene and 2,2'-Azo-bis-isobutyronitrile

This reaction was carried out as above using 1.8 g (0.15 mole) *o*-fluoronitrosobenzene, 5 g (0.03 mole) azobutyronitrile, and 50 ml toluene. The solution was heated during 2½ hours under reflux and then steam-distilled. The residue from the steam distillation weighed 1.2 g. Chromatographic separation of this residue yielded ON-di-(2-cyano-2-propyl)-N-(*o*-fluorophenyl) hydroxylamine (0.75 g, 20% from the nitroso compound). After recrystallization from aqueous alcohol it had m.p. 117.5°.

3-Fluoro-4-methylnitro- and 3-Fluoro-4-methylnitroso-benzene

2-Methyl-5-nitroaniline (38 g, 0.25 mole) gave 2-methyl-5-nitrobenzenediazonium fluoborate (58 g, 93%) which when decomposed yielded 2-methyl-5-nitrofluorobenzene (25.5 g, 70%). The corresponding 2-methyl-5-nitrosofluorobenzene was obtained in 50% yield (*ca.* 7 g) from 15.5 g (0.1 mole) of nitro compound.

Reaction between 2-Methyl-5-nitrosofluorobenzene and 2,2'-Azo-bis-isobutyronitrile

The nitroso compound (7 g, 0.05 mole) and the azonitrile (16.4 g, 0.1 mole) were dissolved in toluene (100 ml). After the usual 2½ hours' reflux and steam distillation, the residue (4.8 g) was chromatographed. There was obtained from mixtures of benzene: ethyl ether, 4:1 and 2:1, ON-di-(2-cyano-2-propyl)-N-(3-fluoro-4-methylphenyl) hydroxylamine (3.8 g, 28%) which was recrystallized from *n*-hexane to constant m.p. 79°.

2-Fluoro-3,5-dimethylnitro- and 2-Fluoro-3,5-dimethylnitroso-benzene

2,4-Dimethyl-6-nitroaniline (41.5 g, 0.25 mole) gave the corresponding diazonium fluoborate (36.5 g, 55%). The latter decomposed at 220° C to give 2-fluoro-3,5-dimethylnitrobenzene (7.8 g, 25%; m.p. 70°). Calc. for $C_8H_8FNO_2$, mol. wt. 169: C, 56.8; H, 4.8; N, 8.3. Found: C, 57.8; H, 5.2; N, 8.3. Reduction of 5.6 g (0.03 mole) of the nitro compound gave 2-fluoro-3,5-dimethylnitrosobenzene (*ca.* 5 g).

ON-*Di*-(*2-cyano-2-propyl*)-N-(*2-fluoro-3,5-dimethylphenyl*) *Hydroxylamine*

Reaction of 2-fluoro-3,5-dimethylnitrosobenzene (*ca.* 5 g, 0.03 mole) and 2,2'-azo-bis-isobutyronitrile (11.5 g, 0.07 mole) in toluene (125 ml) gave 1 g (12%) of the tertiary hydroxylamine. The product was recrystallized from aqueous alcohol; m.p. 88°.

3-Methyl-4-fluoronitro- and 3-Methyl-4-fluoronitroso-benzene

Nitration of *o*-fluorotoluene (60 g, 0.54 mole) with fuming nitric acid (66 ml, sp. gr. 1.5) by the method of Schiemann (11) afforded 3-methyl-4-fluoronitrobenzene (57 g, 67%, b.p. 120° at 25 mm Hg). Reduction of the nitro compound (15.5 g, 0.1 mole) gave the corresponding nitroso compound (*ca.* 7 g, 50%).

ON-*Di*-(*2-cyano-2-propyl*)-N-(*3-methyl-4-fluorophenyl*) *Hydroxylamine*

This reaction was carried out as above using 3-methyl-4-fluoronitrosobenzene (*ca.* 7 g, 0.05 mole) and 2,2'-azo-bis-isobutyronitrile (16.4 g, 0.1 mole) in toluene (150 ml). After usual heating, steam distillation, and chromatography, there was obtained the tertiary hydroxylamine (4.8 g, 35%) which was recrystallized from absolute ethyl alcohol to constant m.p. 86.5°.

2-Methyl-4-fluoronitro- and 2-Methyl-4-fluoronitroso-benzene

m-Fluorotoluene (13.4 g) was nitrated with nitric acid (15 g, sp. gr. 1.42) and concen-

trated sulphuric acid (45 g) to give 2-methyl-4-fluoronitrobenzene (12 g, 70%, b.p. 111° at 21 mm). This was reduced to the corresponding nitroso compound by the usual method.

Reaction between 2-Methyl-4-fluoronitrosobenzene and 2,2'-Azo-bis-isobutyronitrile

This reaction was carried out as before and gave the expected ON-di-(2-cyano-2-propyl)-N-(2-methyl-4-fluorophenyl) hydroxylamine (2.9 g, 25%) which was best recrystallized from ethyl alcohol; m.p. 100°.

2-Methoxy-5-fluoronitro- and 2-Methoxy-5-fluoronitroso-benzene

p-Fluoroanisole (20 g, 0.15 mole) was nitrated by the method of Swarts (15) to give 2-methoxy-5-fluoronitrobenzene (15.7 g, 60%, m.p. 62°). Reduction of the latter (15.7 g, 0.09 mole) gave 2-methoxy-5-fluoronitrosobenzene (7.7 g, 54%).

ON-*Di*-(*2-cyano-2-propyl*)-N-(*2-methoxy-5-fluorophenyl*) *Hydroxylamine*

Reaction of 2-methoxy-5-fluoronitrosobenzene (7.7 g, 0.05 mole) with 2,2'-azo-bis-isobutyronitrile (16.4 g, 0.1 mole) gave the expected tertiary hydroxylamine (5 g, 33%), which was recrystallized from *n*-hexane; m.p. 97.5°.

REFERENCES

1. FREAR, D. E. H. Chemistry of the pesticides. 3rd ed. D. Van Nostrand Company Inc., New York. 1955. p. 271.
2. PATTISON, F. L. M. Nature, **172**, 1139 (1953). PATTISON, F. L. M. and MILLINGTON, J. E. Can. J. Chem. **34**, 757 (1956).
3. BALZ, G. and SCHIEMANN, G. Chem. Ber. **60**, 1186 (1927).
4. FINGER, G. C., FINNERTY, J. L., and SCHNEIDER, H. G. Am. Chem. Soc. Abstr. of Papers, 116th Meeting (Atlantic City). p. 17K (1949).
5. FINGER, G. C. and REED, F. H. Wright Air Development Center, Tech. Rept. 54–148, Wright-Patterson A.F.B., Ohio. (1954).
6. FINGER, G. C., REED, F. H., and DUNBAR, J. E. Wright Air Development Center, Tech. Rept. 52–214 (1952).
7. GINGRAS, B. A. and WATERS, W. A. Chem. & Ind. 615 (1953); J. Chem. Soc. 1920 (1954).
8. ROE, A. Organic reactions. Vol. V. John Wiley & Sons, Inc., New York. 1949. p. 193.
9. BICKEL, F. A. and WATERS, W. A. Rec. trav. chim. **69**, 312 (1950).
10. MILLER, F. A. Organic chemistry. Vol. III. *Edited by* Henry Gilman. John Wiley & Sons, Inc., New York. 1953. p. 148.
11. SCHIEMANN, G., PILLARSKY, R., and SCHÜTH, W. Chem. Ber. **62**, 3040 (1929).
12. SCHMELKES, F. C. and RUBIN, M. J. Am. Chem. Soc. **66**, 1631 (1944).
13. SCHIEMANN, G. Chem. Ber. **62**, 1804 (1929).
14. OSTASZYNSKI, A. Bull. soc. sci. lettres Lódź, Classe III, **3**, No. 15, 10 (1952); Chem. Abstr. **49**, 203*i* (1955).
15. SWARTS, F. Bull. acad. roy. Belg. 241 (1913); Chem. Abstr. **8**, 681 (1914).
16. OVERBERGER, C. G., O'SHAUGHNESSY, M. T., and SHALIT, H. J. Am. Chem. Soc. **71**, 2661 (1949).
17. LUTZ, R. E. and LYTTON, M. R. J. Org. Chem. **2**, 68 (1937).

NOTES

SZILARD CHALMERS REACTION IN POTASSIUM MANGANATE

R. A. MACKENZIE AND K. J. MCCALLUM

Several investigators have studied the chemical effects following neutron capture by the manganese nucleus in potassium permanganate. Libby (1) showed that when the irradiated solid was dissolved in water, most of the radioactive manganese could be separated with manganese dioxide, but a certain percentage, termed the retention, remained in the form of permanganate ion. The retention was observed to increase when the pH of the solution in which the solid was dissolved was high. Libby postulated that, while some of the radioactive manganese was present in the solid as permanganate ion, some existed as species formed by the loss of one or more oxygen ions from the permanganate ion, such as MnO_3^+ or MnO_2^{+++}. He assumed that these would be reduced to manganese dioxide by water, but would react with hydroxyl ions to form permanganate, thus leading to the observed increase in retention in basic solutions. Later investigations (2, 3) have verified the nature of the observed changes in retention, and have given results which are consistent with the reactions postulated by Libby.

If similar changes occur following neutron capture in potassium manganate, the species trapped in the solid would be of the type MnO_3 or MnO_2^{++}. Libby (1) made preliminary measurements of retention, following the neutron activation of sodium manganate dissolved in basic solution. The retention was less than that observed for permanganates under the same conditions, indicating that the recoil species differed in their behavior under these conditions.

The present note reports the results of a study on the effect of the normality of sodium hydroxide in the solvent on the retention for solid potassium manganate.

Potassium manganate was prepared by boiling a solution of potassium permanganate and potassium hydroxide. The compound was recrystallized from potassium hydroxide solution, the crystals being washed with absolute methanol containing a small amount of dissolved potassium hydroxide, and then with anhydrous ether. The oxidation equivalent of the product corresponded to 95–98% K_2MnO_4 in different preparations.

The solid was exposed to neutrons from a Ra–Be neutron source in a paraffin block. It was then dissolved in sodium hydroxide solutions of known normality, the retention then being determined by methods previously used for studies on potassium permanganate (2).

The results are given in Table I.

TABLE I

Retention in potassium manganate

Solution	% Retention	Solution	% Retention
1 *N* NaOH	46	7.5 *N* NaOH	87
3 *N* NaOH	55	8.5 *N* NaOH	92
5 *N* NaOH	66	10 *N* NaOH	97

The results indicate that the retention increases with increase in concentration of the hydroxyl ion, as was found for potassium permanganate. The recoil species then show

the same general chemical behavior for both salts. Measurements of retention in acid solutions might serve to reveal differences between the species. The disproportionation of manganate ion that occurs in such solutions makes necessary a different method of determining retentions. Attempts to establish a satisfactory method are in progress.

The financial assistance of the National Research Council of Canada is gratefully acknowledged.

1. LIBBY, W. F. J. Am. Chem. Soc. **62**, 1930 (1940).
2. MCCALLUM, K. J. and MADDOCK, A. G. Trans. Faraday Soc. **49**, 1150 (1953).
3. RIEDER, W., BRODA, E., and ERBER, J. Monatsh. **81**, 657 (1950).

RECEIVED FEBRUARY 2, 1959.
DEPARTMENT OF CHEMISTRY,
UNIVERSITY OF SASKATCHEWAN,
SASKATOON, SASKATCHEWAN.

ELECTRON SPIN RESONANCE ABSORPTION OF ULTRAMARINE: EFFECT OF CATIONS

YOSHIO MATSUNAGA*

Although the origin of the intense blue color of ultramarine is still unexplained, it has been generally accepted that the color is associated with the presence of regulated amounts of alkali and sulphur and the latter seems to be in the form of polysulphide sulphur (1). Gardner and Fraenkel (2) found that ultramarines show E.S.R. absorption and suggested that the paramagnetism arises from some type of sulphur radical. On the other hand, it is well known that the alkali in ultramarine is exchangeable for other bases and the color depends on the kind and the amount of bases. Here we wish to present the results of a study of the effect of cations on E.S.R. absorption of ultramarine.

The synthetic ultramarine supplied by Fisher Scientific Co. (Catalog No. U-1) was used as starting material and treated with large excess of silver nitrate and small amount of water in a sealed tube at 120–140° C for 15 hours. By this method we can replace sodium nearly completely with silver (3, 4). The other ultramarines were prepared by the treatment of the silver derivative with the halide of the desired metal as described by Jaeger (4). E.S.R. absorption was measured at room temperature at a frequency of 9 k Mc/s. The results are given in Table I. The line width is given by the distance in gauss between the points of maximum slope.

TABLE I

E.S.R. absorption of substituted ultramarines

Cation	Color	Line width	*g*-Value	Intensity
Na (original)	Blue	22	2.030	Very strong
Li	Dark violet grey	*ca.*30	2.030	Strong
Na	Dark blue	*ca.*30	2.030	Strong
K	Dark blue	*ca.*30	2.030	Strong
Ag	Brownish yellow	*ca.*35	2.026	Weak
Ca	Green	*ca.*30	2.024	Medium
Sr	Greenish brown	*ca.*30	2.026	Weak
Ba	Brown	*ca.*35	2.027	Weak
Zn	Brown	*ca.*30	2.026	Weak
Cd	Greenish brown	*ca.*30	2.024	Medium

**N.R.C. Postdoctoral Fellow 1957–.*

Contrary to the replacement of sodium with silver, the exchange of cation in the reverse direction is incomplete. In addition, the loss of a part of the sulphur and the change of oxidation state by the prolonged treatments must be taken into consideration. Although the quantitative explanation of the results is thus complicated by these facts, we can conclude that the concentration of unpaired electrons and the *g*-value depend on the kind of cation. The intensity of E.S.R. absorption is decreased by a factor of 20 to 30 accompanying the replacement of sodium by silver, but the paramagnetism of silver ultramarine can be increased about ten times by treatment with alkali halide. The color of ultramarine also changes nearly reversibly by these replacements. As to the ultramarines containing divalent cations, the replacement of silver seems to be more incomplete (4). However, generally the color of these ultramarines is far from blue and the concentration of unpaired electrons in these samples is less than alkali ultramarines.

It appears that not only the color of ultramarine but also the concentration of unpaired electrons depends on the kind of cation. Besides, the shift of *g*-value by cation exchange suggests that the spin–orbit interaction can be modified by the cation. Therefore, the paramagnetic species is not an isolated sulphur radical but is a complex containing cations. In accordance with the view which regards the color as being due to incompletely oxidized sulphur, it is very likely that unpaired electrons arise from polysulphide ions, however, they can apparently interact with each other through cations. The ability of the cation to couple unpaired electrons seems to be related to its polarizability and its valency. Alkali ions are not so effective for such an interaction.

The author wishes to thank Professor C. A. McDowell and Dr. J. B. Farmer for their interest and encouragement.

1. Emeleus, H. J. and Anderson, J. S. Modern aspects of inorganic chemistry. D. Van Nostrand Company, Inc., New York. 1954. pp. 251–257.
2. Gardner, D. M. and Fraenkel, G. K. J. Am. Chem. Soc. **77**, 6399 (1955).
3. Heumann, K. Ann. **199**, 253 (1879).
4. Jaeger, F. M. and Van Melle, F. A. Proc. Acad. Sci. Amsterdam, **30**, 479, 885 (1927); **32**, 156 (1929).

Received December 15, 1958.
Department of Chemistry,
The University of British Columbia,
Vancouver 8, B.C.

THE ADDITION OF ETHYL RADICALS TO ETHYLENE

F. W. Lampe and F. H. Field

In a recent study (1) of the reaction of ethyl free radicals generated by the photolysis of diethyl ketone, James and Steacie reported the activation energy (assuming zero activation energy for radical coupling) for addition to 1-alkene-type olefins to be 7.0 ± 0.2 kcal/mole. This value is consistent with the value of 7 kcal/mole found by Mandelcorn and Steacie (2) for the addition of methyl radicals to ethylene but is somewhat higher than the value found by Pinder and LeRoy (3) for ethyl radical addition to ethylene. These latter authors generated ethyl radicals by utilizing the mercury-photosensitized decomposition of hydrogen in the presence of ethylene and found an activation energy of 5.5 kcal/mole and a steric factor ratio of 5.0×10^{-5}. A "low" value of 4.6 kcal/mole for the addition of methyl radicals to ethylene can be derived (2) from the data of Raal and Danby (4).

We wish to report here the results of some studies, on the photolysis of azoethane in the presence of ethylene, that support the lower values for the activation energy of the addition reactions.

EXPERIMENTAL

Azoethane was prepared by the method of Leitch (5). Ethylene was Phillips Research Grade, had a stated purity of 99.9+ mole %, and was used without further purification.

The photolyses were carried out in an annular reaction vessel constructed entirely of quartz. The annular space which contained the reacting gases had a thickness (light-path distance) of about 1.5 cm and a length of about 25 cm. The light source, positioned in the center of the vessel, consisted of two 8-watt G.E. "Black-lights" connected in series. The emitted radiation of the "Black-light" peaks at 3660 Å and emits negligible intensity below 3000 Å, thus eliminating the possibility of mercury-sensitized reactions. The gases were circulated by a two-stage Toepler pump, with the dead-space volume being about 20% of the total volume of reaction system.

In all experiments the azoethane pressure was held constant at 40 mm of Hg while the ethylene pressure was varied from 5 to 25 mm of Hg. Nitrogen was measured by assuming it to be the only noncondensible gas at −195° C. After its measurement the nitrogen was removed and the gases condensible at −195° C were analyzed by vapor–liquid partition chromatography.

RESULTS AND DISCUSSION

In all photolyses the only major reaction products observed were nitrogen, ethane, *n*-butane, and *n*-hexane. At the highest conversions in the runs at 175° C, small amounts of butylene were detected. No appreciable amounts of octane or higher hydrocarbons were found.

The main features of the mechanism involved in the photolysis of azoethane have been established (6, 7). The reactions of most importance to this discussion are:

$$C_2H_5N{=}NC_2H_5 + h\nu \rightarrow 2C_2H_5 + N_2 \qquad [R1]$$

$$C_2H_5 + C_2H_5N{=}NC_2H_5 \rightarrow C_2H_6 + C_2H_5N{=}NCH_2CH_2\cdot \qquad [R2]$$

$$C_2H_5 + C_2H_5 \rightarrow C_4H_{10} \qquad [R3]$$

$$C_2H_5 + C_2H_5 \rightarrow C_2H_4 + C_2H_6. \qquad [R3']$$

If ethylene is added to the system, some of the ethyl radicals formed in [R1] will add to it to form butyl radicals, i.e.,

$$C_2H_5 + C_2H_4 \rightarrow C_4H_9. \qquad [R4]$$

The absence of significant amounts of octane indicates, under our experimental conditions, that there is no appreciable addition of butyl radicals to ethylene nor coupling of butyl radicals. Since there is no appreciable addition of butyl radicals to ethylene, it seems reasonable to assume that butyl radicals will not abstract hydrogen from azoethane under these conditions. Also, since there is no appreciable coupling of butyl radicals, it is reasonable to assume that butyl radicals do not couple appreciably with the azoethyl radicals produced in [R2]. Thus, as an approximation, we assume that butyl radicals react only with ethyl radicals, i.e.,

$$C_2H_5 + C_4H_9 \rightarrow C_6H_{14} \qquad [R5]$$

$$C_2H_5 + C_4H_9 \rightarrow C_2H_6 + C_4H_8 \qquad [R6]$$

$$C_2H_5 + C_4H_9 \rightarrow C_2H_4 + C_4H_{10}. \qquad [R7]$$

The usual steady state approximation leads to

$$[E1] \qquad (1/[C_2H_4])(R_{C_6H_{14}}/R^{\frac{1}{2}}_{C_4H_{10}}) = P_C(k_4/k_3^{\frac{1}{2}})$$

when the R's denote rates of formation, k's specific reaction rates, and P_C is the probability that in [R5]–[R7] coupling occurs, i.e.,

[E2] $$P_C = k_5/(k_5+k_6+k_7).$$

In Table I we show the results of the photolyses. Each value of $P_C(k_4/k_3^{\frac{1}{2}})$ is the average obtained from at least five experiments with irradiation times varying from 15 to 70 minutes. In the calculation of $P_C(k_4/k_3^{\frac{1}{2}})$, initial ethylene concentrations were used.

TABLE I

Addition of ethyl radicals to ethylene

Temp. (° K)	$[C_2H_4]_0$ (mm at T° K)	$P_C(k_4/k_3^{\frac{1}{2}})\times10^{12}$ (cc/molecule-sec)$^{\frac{1}{2}}$
398	10.2	2.54
398	15.5	2.67
398	20.0	2.64
398	25.0	2.47
423	5.0	3.79
423	10.1	3.71
423	15.0	3.81
423	20.0	3.88
448	5.0	5.62

This does not introduce any error greater than that involved in the analyses, because in all runs the ethylene conversion was below 10% and generally of the order of 2–6%.

The absence of significant amounts of butylene and the fact that [R6] is thermodynamically favored over [R7] suggests that P_C is very close to unity. Assigning P_C a value of unity (an approximation that is not in error by more than 5 or 10%) enables us to make the usual type Arrhenius plot of the rate constant ratios in Table I. Such a plot is shown in Fig. 1 and leads to a value for the activation energy difference, $E_4-\frac{1}{2}E_3$, of 5.5 kcal/mole. The ratio of the pre-exponential factors, $A_4/A_3^{\frac{1}{2}}$, is 2.6×10^{-9} which, upon assumption of a mean collision diameter of 4.0 Å, leads to a steric factor ratio, $P_4/P_3^{\frac{1}{2}}$, of 1.3×10^{-4}.

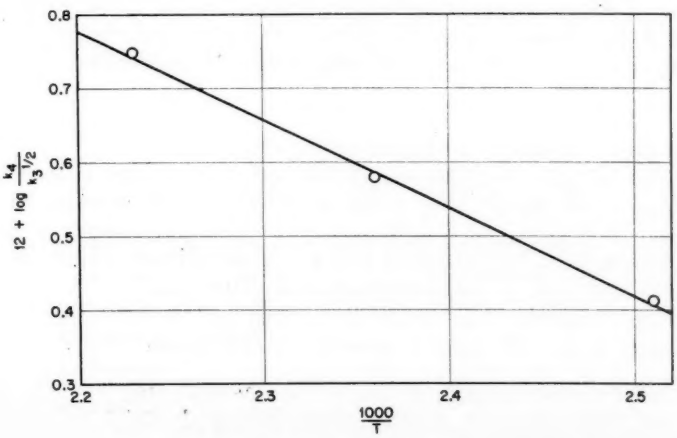

FIG. 1. Arrhenius plot for the addition of ethyl radicals to ethylene.

The activation energy difference of 5.5 kcal/mole is in excellent agreement with the results of Pinder and LeRoy (3), and consistent with the low value of 4.6 kcal/mole found by Raal and Danby (4) for the addition of methyl radicals to ethylene. Our value of the steric factor ratio is larger than that found by Pinder and LeRoy (3) by a factor greater than two. We can advance no explanation for this difference.

ACKNOWLEDGMENTS

We are indebted to Dr. D. E. Bown for the synthesis of the azoethane and to Mr. J. C. Leutwyler for assistance in the measurements.

1. JAMES, D. G. L. and STEACIE, E. W. R. Proc. Roy. Soc. A, **244**, 297 (1958).
2. MANDELCORN, L. and STEACIE, E. W. R. Can. J. Chem. **32**, 474 (1954).
3. PINDER, J. A. and LEROY, D. J. Can. J. Chem. **35**, 588 (1957).
4. RAAL, F. A. and DANBY, J. C. J. Chem. Soc. 2219 (1949).
5. RENAUD, R. and LEITCH, L. C. Can. J. Chem. **32**, 545 (1954).
6. AUSLOOS, P. and STEACIE, E. W. R. Bull. soc. chim. Belges, **63**, 87 (1954).
7. WEININGER, J. L. and RICE, O. K. J. Am. Chem. Soc. **74**, 6216 (1952).

RECEIVED DECEMBER 29, 1958.
RESEARCH AND DEVELOPMENT DIVISION,
HUMBLE OIL AND REFINING COMPANY,
BAYTOWN, TEXAS.

NOTE ON THE DETERMINATION OF CRYSTALLINITY INDEX OF CELLULOSE

M. KOURIS, H. RUCK, AND S. G. MASON

In a recent communication (1) it was shown that the maximum intensity of air scattering can be used as a reference intensity in determining the X-ray crystallinity index of cellulose. The successful application of the method requires that the following conditions are met:

1. The sample mass must be kept constant to within $\pm 3\%$.
2. I_{as} must be comparable with I_{002}, the intensity of the A_4 cellulose interference.

It now appears that in the earlier work the correct experimental conditions for satisfying the second requirement were fortuitously established.

The purpose of the present note is to draw attention to the recently discovered fact that the second requirement above is satisfied when the thickness of the irradiated sample is about one-third of the optimum thickness as defined by the relation (2)

$$t_m = 1/\mu$$

where μ is the linear absorption coefficient of the sample.

If the optimum sample thickness is used, the absorption of the primary beam will be at a maximum, and the intensity of the air scattering will therefore be disproportionately weak with respect to I_{002} to be used as a reference interference. By reducing the sample thickness to $t_m/3$ the relative intensity of air scattering with respect to I_{002} is increased threefold and I_{as} becomes comparable with I_{002}.

It may also be of interest to point out that preliminary experiments were unable to detect any change in I_{as} with normal variations in atmospheric pressure.

1. KOURIS, M., RUCK, H., and MASON, S. G. Can. J. Chem. **36**, 931 (1958).
2. KLUG, H. P. and ALEXANDER, L. E. X-Ray diffraction procedures for polycrystalline and amorphous materials. John Wiley & Sons, Inc., New York. 1954. pp. 204–206.

RECEIVED JANUARY 21, 1959.
PHYSICAL CHEMISTRY DIVISION,
PULP AND PAPER RESEARCH INSTITUTE OF CANADA,
MONTREAL, QUEBEC.

STRUCTURE AND REACTIVITY OF C_3H_3 RADICAL*

G. GIACOMETTI†

Recent mass spectroscopic work by Collin and Lossing (1) on the mercury photosensitized decomposition of allene led to the production of the C_3H_3 radical. The latter was then allowed to react with CH_3 radicals, produced thermally from $Hg(CH_3)_2$, and the analysis of the products showed that all the radicals react to form 1-butyne ($CH_3—CH_2—C\equiv C—H$) and none of the allenic isomer $CH_2=C=CH—CH_3$.

This fact is to be considered evidence for the structure of the C_3H_3 radical being of the resonant type

$$\dot{C}H_2—C\equiv CH \longleftrightarrow CH_2=C=\dot{C}H \qquad [I]$$

rather than of the pure allenic type

$$CH_2=C=\dot{C}H. \qquad [II]$$

The structure of the radical is actually going to be different in the two cases because if [I] is correct, the two bonds have certainly different lengths, while if [II] is valid, the two bond distances must be approximately the same.

Though one might feel intuitively that resonance is making structure [I] more stable, it is of interest to show that structure [I] is indeed predicted by a very crude molecular orbital approach.

We shall assume that the simple LCAO, MO theory (2) is applicable, neglecting overlap and also π_x–π_y electron interaction. We shall consider equal all the coulomb integrals and take the exchange integrals as a decreasing function of the bond distance (in absolute value).

Indicating by a the C—C bond in [II] and by b and c those in [I], we have:

$$|\beta_b| < |\beta_a| \leqslant |\beta_c|.$$

The total π electron energy for [II] is simply:

$$E_{II} = 4\beta_a$$

while for [I] we have:‡

$$E_I = 2\beta_c + 2\beta_c \left|\sqrt{\left(1+\frac{\beta_b^2}{\beta_c^2}\right)}\right| \approx 4\beta_c + \beta.$$

Structure [I] is lower in energy than [II] by an amount at least of the order of β, which corresponds to approximately 20–30 kcal/mole. It is then quite clear that the C_3H_3 radical formed from an excited allene molecule is best represented by formulation [I] and has two different bond lengths.

*Issued as N.R.C. No. 5139.
†National Research Council Postdoctorate Fellow 1957–58. Present address: Instituto di Chimica Fisica, Università di Padova, Padova, Italy.
‡The β's are negative quantities. The coulomb integral is taken as zero of the energy scale.

The experimentally found reactivity at carbon 1 follows in a straightforward way. Both the free valence index and the localization energy criteria, as used for radical addition to unsaturated molecules (3), agree with addition to carbon 1.

Indicating by k the ratio $\frac{\beta_c}{\beta_b} > 1$ we have the free valence indices:

$$f_1 = N_{max} - \frac{1}{\sqrt{(1+k^2)}}, \qquad f_3 = N_{max} - \frac{k}{\sqrt{(1+k^2)}}, \qquad \text{hence } f_1 > f_3$$

and the localization energies (in units of β):

$$E_1 = \sqrt{(1+k^2)} - k, \qquad E_3 = \sqrt{(1+k^2)} - 1, \qquad \text{hence } E_1 < E_3.$$

Of course, this simple theory does not exclude completely addition to carbon 3, the extent of the latter reaction depending mainly on the value to be attributed to k.

Addition to position "three" actually occurs in the case of the cyanoisopropyl radicals:

whose π electron system is similar to the one for C_3H_3 radical. They have been found to recombine mainly carbon to carbon but some of the products correspond also to recombination carbon to nitrogen, the ratio being approximately 2:1 (4). In this case, however, the different electronegativities of nitrogen and of the methyl-substituted carbon atom may also play an important role.

1. COLLIN, J. E. L. and LOSSING, F. P. Can. J. Chem. **35**, 778 (1957).
2. (*a*) HÜCKEL, E. Z. Physik, **70**, 204 (1931).
(*b*) COULSON, C. A. and LONGUET-HIGGINS, H. C. Proc. Roy. Soc. A, **191**, 39 (1947).
3. (*a*) COULSON, C. A. J. Chem. Soc. 1435 (1955).
(*b*) GIACOMETTI, G. Nuovo cimento, (10) **3**, 1488 (1956).
4. TALÂT-ERBEN, M. and BYWATER, S. J. Am. Chem. Soc. **77**, 3710 (1955).

RECEIVED NOVEMBER 7, 1958.
DIVISION OF PURE CHEMISTRY,
NATIONAL RESEARCH COUNCIL,
OTTAWA, CANADA.

THE HALF-LIFE OF Pb^{210} (RaD)

B. D. PATE,* D. C. SANTRY,† AND L. YAFFE

Pb^{210} (RaD), a member of the $4n+2$ series, emits soft β^- radiation (0.020 Mev) to form Bi^{210} (RaE), which has a half-life of 5.0 days and emits energetic β^- rays (1.15 Mev). The half-life of RaD has been measured many times. Values ranged from 16.5

**Present address: Department of Chemistry, Brookhaven National Laboratory, Upton, Long Island, N.Y.*
†*Present address: Department of Chemistry, Cambridge University, Cambridge, England.*

to 23 years and in 1931 the International Radium Standards Commission (1) adopted a value of 22 years.

Since the β^- rays from RaD are so soft, the measurements were not made directly on the RaD, but usually on the Bi^{210} (RaE) daughter in equilibrium with it or on the latter's Po^{210} (RaF) granddaughter, which emits α radiation. A very painstaking measurement of the last type was made by Joliot-Curie (2), who obtained a value of 23 years.

Wagner (3), using an ion chamber, obtained a value of 25 years from a measurement which was carried out for a period of 250 days. In 1955 Tobaillem (4), using a differential ionization chamber, compensated against radium, followed the decay of RaD source for 121 days, and obtained a half-life of 19.4 ± 0.35 years. Merritt, Campion, and Hawkings (5), using a $4\pi\beta$ proportional counter, obtained a value of 22.4 ± 0.4 years for measurements observed over a period of $5\frac{1}{2}$ years. Unfortunately this measurement is not quoted in either the title or the abstract of their paper, and this value became known to us after our series of measurements was completed.

We, in our laboratory, initially used RaD as a standard to monitor the performance of a $4\pi\beta$ proportional counter described previously (6). It soon became apparent that this instrument was sufficiently stable to be used to measure, with good accuracy, the half-lives of long-lived radionuclides.

The Pb^{210} source was chemically purified using standard methods and then sandwiched between aluminum sufficiently thick to absorb all the radiation emitted, other than the β radiation from Bi^{210}. Adequate sealing ensured the exclusion of moisture. This was further checked by intersource comparisons from time to time to ensure source constancy on a short-time basis. The aluminum was thick enough so that no change in geometrical shape could occur which would remove the source from the position of 100% efficiency in the counter (6).

The dead time of the counter was determined from time to time by the well-known 'paired-source' technique, and the correction due to this was of the order of 0.5%. The count rate was great enough so that background and statistical variations in counting rate could be adequately treated.

Activity measurements were carried on for a period of 5 years. Frequency of measurements varied from daily to weekly, so that a large amount of data was accumulated.

The data were analyzed by the method of least squares and yielded a half-life of 23.30 years. The results were broken down into a yearly basis to see whether any consistent variation was occurring which would attest to source impurity. The deviations were random and were of the order of 0.1 year. It is difficult to assess a systematic error to this series of measurements and a value five times this deviation has been used. This yields a value of 23.3 ± 0.5 years in good agreement with Joliot-Curie (2) and Merritt *et al.* (5) but not with Tobaillem (4).

1. International Radium Standards Commission. Revs. Modern Phys. **3**, 427 (1931).
2. Joliot-Curie, I. J. phys. **10**, 388 (1929).
3. Wagner, F. U.S. Atomic Energy Comm. Rept. ANL **4490**, 5 (1950).
4. Tobaillem, J. J. phys. radium, **16**, 235 (1955).
5. Merritt, W. F., Campion, P. J., and Hawkings, R. C. Can. J. Phys. **35**, 16 (1957).
6. Pate, B. D. and Yaffe, L. Can. J. Chem. **33**, 610 (1955).

Received July 7, 1958.
Radiochemistry Laboratory,
Department of Chemistry,
McGill University,
Montreal, Quebec.

LOW TEMPERATURE IRRADIATION OF MIXTURES OF HBr AND C_2H_4

D. A. ARMSTRONG* AND J. W. T. SPINKS

A 90-c Co^{60} source was used to irradiate solid equimolar mixtures of HBr and C_2H_4 in a 0.5-cm diameter Pyrex cell at liquid nitrogen and liquid oxygen temperature. A few irradiations of liquid equimolar mixtures just above their freezing point (−165° C) (1) were also performed.

An addition reaction was observed at all three temperatures. The product was identified from its vapor pressure and refractive index to be virtually pure ethyl bromide. The addition was followed by evaporating the mixture at given time intervals and measuring its total pressure. For successive irradiations of the same sample, the pressure decreased until it had fallen to 50% of the initial value, i.e., until the addition was complete.

The pressure decrease (as a percentage of the initial pressure of the HBr–C_2H_4 mixture) versus time of irradiation curves for samples which were irradiated continuously are given in Fig. 1. From the dose rate, estimated by ferrous sulphate dosimetry,† an initial G value of about 10^5 was calculated for addition in the liquid samples. For the frozen samples the G values were lower and fell off rapidly with increasing time of irradiation, especially for those irradiated at liquid nitrogen temperature.

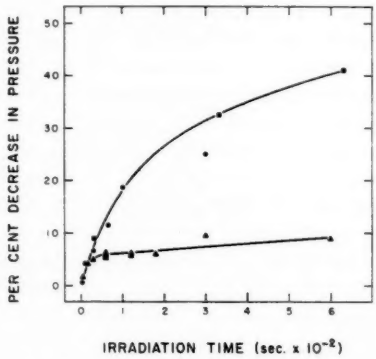

FIG. 1. Percentage decrease in pressure as a function of irradiation time; ■ liquid phase; ● solid phase at liquid oxygen temperature; ▲ solid phase at liquid nitrogen temperature. Dose rate, 450 r per minute.

Unirradiated samples of mixtures of ethylene and hydrogen bromide were stable (cf. (1)), and no addition was observed when an HBr–C_2H_4 mixture was condensed in an empty Pyrex cell which had been previously irradiated.

The high G values are indicative of a chain reaction and it would appear that the radiation produced reactive entities (possibly free radicals, cf. 2, 3, 4, 5) in the liquid and frozen mixtures which subsequently initiated the chain addition. It would seem that for frozen samples the chain reaction must have occurred during melting. In support of this, it was found that the reaction could be initiated in an unirradiated mixture by condensing it onto an irradiated mixture at liquid nitrogen temperature and then melting the combined samples, e.g., when equal amounts of unirradiated and irradiated mixtures

Holder of a Postdoctoral Fellowship.

†We are indebted to Mr. A. L. Riegert for these measurements.

were used, the amount of product formed in the combined sample, on melting, was 60% greater than that formed in the irradiated mixture alone.

We are grateful to the National Research Council and the Atomic Energy of Canada Limited for continued financial support.

1. MAASS, O. and WRIGHT, C. H. J. Am. Chem. Soc. **46**, 2664 (1924).
2. VAUGHAN, W. E., RUST, F. F., and EVANS, T. W. J. Org. Chem. **7**, 477, 491 (1942).
3. NORMAN, L. and PORTER, G. Proc. Roy. Soc. A, **230**, 399 (1955).
4. JONES, T. O., LUEBBE, R. H., WILSON, J. R., and WILLARD, J. E. J. Phys. Chem. **62**, 9 (1958).
5. WILLARD, J. Radiation Research (Abstr.), **9**, 146 (1958).

RECEIVED JANUARY 9, 1959.
CHEMISTRY DEPARTMENT,
UNIVERSITY OF SASKATCHEWAN,
SASKATOON, SASKATCHEWAN.

ELECTRON SPIN RESONANCE ABSORPTION OF BINAPHTHOQUINONES

YOSHIO MATSUNAGA*

Previously we examined the diamagnetic susceptibilities of a number of condensed polycyclic aromatic hydrocarbons and quinones and found that some of them have anomalously small values of susceptibility (1). It was pointed out that this anomaly is characteristic of perylene and its analogues. The localization of π-electrons due to the characteristic molecular structure† and the appearance of a paramagnetic state were suggested as the causes. Although the former suggestion seemed to be in accordance with the predicted tendency for diamagnetic anisotropy given by London's method‡ and no E.S.R. absorption was detected in perylene (2), the existence of unpaired electrons in violanthrone (3, 4) and mesonaphthodianthrene (5) was confirmed by the E.S.R. method. The above-mentioned paramagnetic quinone is dark violet and the hydrocarbon is bluish green; therefore it seemed interesting to know whether the deeply colored polycyclic compounds of a different type can be paramagnetic or not.

Three binaphthoquinones were examined by an E.S.R. spectrometer at a frequency of 9 k Mc/s. Dimethoxybinaphthoquinone (X=OCH_3) was prepared by the oxidation of 1,4-naphthohydroquinone monomethylether with ferricyanide ion as described by Russig (6) and recrystallized from toluene. The sample shows E.S.R. absorption with a line width of 5.6 gauss at a half power. The *g*-value, estimated by comparison with DPPH, is 2.0036±0.0003. There is one unpaired electron for about 400 molecules of quinone. If this compound is analogous to Chichibabin's hydrocarbon type of carbon biradical, as suggested by Leffler (7), the molecule should be more paramagnetic in the dissolved state. However we could not find E.S.R. absorption from a benzene solution of this compound. The appearance of paramagnetism seems to be limited to the solid state. Unlike Chichibabin's hydrocarbon and Bourdon and Calvin's hindered biphenoquinone (8), the present compound is stable towards oxygen in the solid and in the dissolved states. Binaphthoquinone may belong to the same group of paramagnetic organic compounds as violanthrone (3, 4), mesonaphthodianthrene (5), and metal-free phthalocyanine (9, 10).

*N.R.C. Postdoctoral Fellow, 1957–.

†*In the sense of VB theory the central two or more single bonds can be double only in the excited states.*

‡*Among the compounds of this type, only the anisotropy of perylene was examined by London's method. The predicted value is 1.88 times that of naphthalene. The value given in ref. 1 is in arithmetical error.*

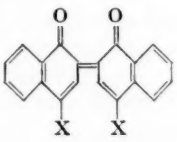

Winslow *et al.* (10) suggested that enough thermal energy can be absorbed at room temperature to produce unpaired electrons in crystals of highly conjugated molecules. However, Akamatu *et al.* (4) found that the spin concentration in violanthrone does not decrease by cooling to liquid nitrogen temperature and considered that the molecules with unpaired electrons are not in excited states. It is well known that polycyclic aromatic compounds are semiconductive and the positive charge carriers in these compounds have high mobility. Therefore, the appearance of unpaired electrons in these cases may have some correlation with the presence of a strong intermolecular charge-transfer force* (11), and unpaired electrons may be trapped at some kind of imperfection in the crystal lattice.

Dichloro- and dibromo-binaphthoquinones (12) were also examined and both of them were found to be paramagnetic to about the same extent as the dimethoxy-derivative. These two compounds are too unstable to be recrystallized, therefore we cannot exclude the possibility that E.S.R. absorption is due to paramagnetic impurities. However, it is very likely that these two quinones have similar magnetic behavior to the well-defined dimethoxy-derivative.

I wish to thank Professor C. A. McDowell for his interest in this work. This research was supported by grants from the National Research Council of Canada.

1. Akamatu, H. and Matsunaga, Y. Bull. Chem. Soc. Japan, **26**, 364 (1953).
2. Yokozawa, Y. and Miyashita, I. J. Chem. Phys. **25**, 796 (1956).
3. Yokozawa, Y. and Tatsuzaki, I. J. Chem. Phys. **22**, 2087 (1954).
4. Akamatu, H., Mrozowski, S., and Wobschall, D. Paper presented at Carbon Conference, Buffalo, N.Y. 1957.
5. Matsunaga, Y. Unpublished.
6. Russig, F. J. prakt. Chem. (2) **62**, 30 (1900). Goldschmidt, S. and Wessbecher, H. Ber. **61**, 372 (1928).
7. Leffler, J. E. The reactive intermediates of organic chemistry. Interscience Publishers, Inc., New York. 1956. p. 54.
8. Bourdon, J. and Calvin, M. J. Org. Chem. **22**, 101 (1957).
9. Ingram, D. J. E. and Bennett, J. E. J. Chem. Phys. **22**, 1136 (1954).
10. Winslow, F. H., Baker, W. O., and Yager, W. A. J. Am. Chem. Soc. **77**, 4751 (1955).
11. Akamatu, H., Inokuchi, H., and Matsunaga, Y. Bull. Chem. Soc. Japan, **29**, 213 (1956). Matsunaga, Y. Bull. Chem. Soc. Japan, **28**, 475 (1955); J. Chem. Phys. To be published.
12. Willstätter, R. and Schuler, L. Ber. **61**, 362 (1928).

Received February 2, 1959.
Department of Chemistry,
University of British Columbia,
Vancouver 8, B.C.

**Aromatic hydrocarbon – iodine, typical charge-transfer complex, was found to be highly conductive and rather strongly paramagnetic.*

SUBSTITUTION AND ELIMINATION REACTIONS DURING ACETOLYSIS OF DERIVATIVES OF 3β,6β-DIHYDROXYALLOCHOLANIC ACID

P. Ziegler

Tosylation of the 3β,6β-dihydroxy grouping in allosteroids has been reported (1, 2) to yield the corresponding 3β-monotosylates. Replacement of this tosyloxy function by

means of a variety of nucleophylic reagents such as ammonia and amines (3), thiophenoxide ion (4), and diethyl malonate ion (2) invariably is accompanied by inversion of configuration at C-3. When 3β,6β-dihydroxyallosteroids were treated (1, 5) with mesyl chloride, the corresponding dimesylates were obtained; acetolysis of the latter compounds with acetate ion in acetic acid proceeded with retention of configuration at C-3, giving rise to 3β-acetoxy-Δ^5-steroids. These results can readily be understood by postulating that the 3β-monotosylates undergo a bimolecular substitution reaction which is accompanied by inversion at C-3. On the other hand, with a 3β,6β-dimesylate, dehydromesylation is the initial event leading to the intermediary 3β-mesyloxy-Δ^5-steroid; this unsaturated derivative, under the influence of the π-electrons, is believed (6) to undergo unimolecular heterolysis to provide the stabilized 3β-cation. The latter finally reacts with the weakly nucleophylic acetate ion to yield, with retention of configuration, the 3β-acetoxy-Δ^5-steroid.

The present study describes an analogous case involving methyl 3β,6β-dihydroxyallocholanate (I*a*). Mesylation of I*a* provided the dimesylate I*c*, which, with potassium acetate in aqueous dimethylformamide and subsequent saponification, was converted to 3β-hydroxy-Δ^5-cholenic acid (II). For further characterization, compound II was transformed to the methyl ester. Tosylation of I*a* provided the monotosylate I*b* as well as smaller amounts of the corresponding 3β,6β-ditosylate; acetolysis of I*b* under the same conditions as were used with I*c* and subsequent saponification of the products afforded 3α,6β-dihydroxyallocholanic acid (III). This acid, derived from 3α-hydroxy-6-oxo-allocholanic acid or its acetate methyl ester by catalytic hydrogenation, was previously reported (7, 8, 9) to have melting points in the range 246–251°. Our product, m.p. 248–252°, did not give a depression on mixed melting point with an authentic specimen of III;* elemental analyses of III, even when the sample was dried at 200° in a high vacuum, indicated that the compound retained half a mole of water.* Chromic acid oxidation of this acid provided 3,6-dioxo-allocholanic acid, identified by mixed melting point and conversion to the corresponding methyl ester.

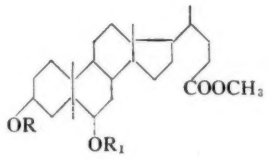

I

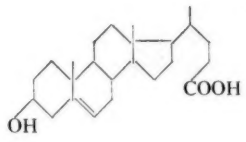

II

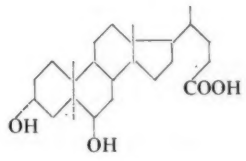

III

a, R = R₁ = H

b, R = H₃C—⟨⟩—SO₂—, R₁ = H

c, R = R₁ = H₃C—SO₂—

EXPERIMENTAL

Methyl 3β,6β-Dimesyloxyallocholanate (I*c*)

Compound I*a* (3 g) dissolved in pyridine (20 ml) was treated at 3° with methanesulphonyl chloride (3.4 g). The mixture was kept at that temperature for 20 hours, the excess reagent was decomposed by addition of a small amount of ice, and the solution was then poured into ice-cold dilute hydrochloric acid. The resulting precipitate was

**Kindly supplied by Dr. A. Schubert of VEB Jenapharm, Jena, East Germany, who also informed us that elemental analyses of his acid III indicated the retention of half a mole of water.*

filtered off, washed with water, dried, and finally recrystallized from ethyl acetate – ether to afford 3.05 g of I*c*, m.p. 125° (decomp.). Two further recrystallizations from the same solvent system gave the analytical specimen, m.p. 125–127° (decomp.). Anal. Calc. for $C_{27}H_{46}O_8S_2$: C, 57.62; H, 8.24; S, 11.39; OCH_3, 5.51. Found: C, 57.54, 57.57; H, 8.32, 8.26; S, 11.50; OCH_3, 5.69, 5.77.

3β-Hydroxy-Δ⁵-cholenic Acid (II)

A solution of I*c* (3 g) and potassium acetate (7.3 g) in water (4 ml) and dimethylformamide (40 ml) was kept at 120–125° for 5 hours. The mixture was then poured into dilute hydrochloric acid, the resulting precipitate was filtered off, and washed with water. Saponification of the wet solid by refluxing with 4% methanolic potassium hydroxide (40 ml) for 2 hours, followed by addition of dilute mineral acid, provided a solid which was separated by filtration. Crystallization from ethyl acetate afforded 680 mg of substance, m.p. 226–228°, giving an insoluble digitonide and a yellow color with tetranitromethane. Two more recrystallizations from the same solvent gave m.p. 231–233°. Methylation of II with diazomethane and crystallization of the product from hexane gave the methyl ester of II, m.p. 142–143° and $[\alpha]_D^{24}$ −36.2° (*c*, 1.02, dioxane).

Tosylation of Methyl 3β,6β-Dihydroxyallocholanate (I*a*)

To I*a* (2.15 g) dissolved in pyridine (10 ml) was added tosyl chloride (3 g). After 22 hours at 25°, the excess reagent was decomposed by a small amount of ice, the mixture was poured into dilute hydrochloric acid, and the products were extracted with ether–chloroform. The solvent extract was washed with water, dried over sodium sulphate, and evaporated. Crystallization of the residue (3.04 g) from ether (20 ml) yielded 690 mg of material, m.p. 135–140° (decomp.); this was recrystallized from ethyl acetate – ether to give the analytical sample of methyl 3β,6β-ditosyloxyallocholanate, m.p. 133–136° (decomp.). Anal. Calc. for $C_{39}H_{54}O_8S_2$: C, 65.51; H, 7.61; S, 8.97; OCH_3, 4.34. Found: C, 65.45, 65.64; H, 7.60, 7.47; S, 9.11; OCH_3, 4.62, 4.60.

The filtrate from the first crop of ditosylate yielded, on refrigeration, 1.85 g of material, m.p. 140–148°. Three recrystallizations from ethyl acetate – hexane gave pure I*b*, m.p. 150–152° (decomp.) and $[\alpha]_D^{24}$ −13.6° (*c*, 1.75, dioxane). Anal. Calc. for $C_{32}H_{48}O_6S$: C, 68.53; H, 8.63; S, 5.72; OCH_3, 5.53. Found: C, 68.66, 68.70; H, 8.57, 8.65; S, 6.02; OCH_3, 5.75, 5.80.

3α,6β-Dihydroxyallocholanic Acid (III)

Potassium acetate (2.6 g), water (1.3 ml), and dimethylformamide (14 ml) were heated to 110°. After addition of I*b* (1.12 g), the solution was kept at that temperature for 4 hours, whereupon the reaction products were treated with dilute mineral acid and extracted with ether. The residue, obtained from the solvent extract after washing, drying, and evaporating, was refluxed for 2 hours with 4% methanolic potassium hydroxide (50 ml). The saponified mixture was then poured into dilute hydrochloric acid, the precipitate was filtered off, washed with water, and dried. Crystallization of the solid from ethyl acetate afforded 596 mg of material, m.p. 243–245°. Successive recrystallization from methanol, acetone, and ethyl acetate yielded the analytical specimen of III, m.p. 248–252° and $[\alpha]_D^{23}$ +10.7° (*c*, 0.991, dioxane). This compound failed to give an insoluble digitonide and did not react with tetranitromethane. Anal. Calc. for $C_{24}H_{40}O_4.\frac{1}{2}H_2O$: C, 71.78; H, 10.29. Found: C, 71.86, 72.06, 71.70, 71.74; H, 10.30, 10.17, 10.05, 10.38. These analytical data remained unchanged after a sample had been boiled with sodium hydroxide solution and, after neutralization, had been dried at

200° in a high vacuum. The methyl ester of III could not be obtained in crystalline form.

Oxidation of III (235 mg) in acetic acid (5 ml) with a solution of chromic acid (150 mg) in water (0.12 ml) and acetic acid (2.5 ml) was carried out at 10° for 1.5 hours. The mixture was then diluted by gradual addition of ice water, whereupon a granular precipitate appeared; this was filtered off, washed with water, dried, and then crystallized twice from ethanol to yield 178 mg of 3,6-dioxo-allocholanic acid, m.p. 206–208°. Methylation of this compound with diazomethane and crystallization of the ester from methanol showed m.p. 149–151.5°. Mixed melting points, both of the acid and the ester, with authentic specimens showed no depressions.

1. REICH, H. and LARDON, A. Helv. Chim. Acta, **29**, 671 (1946).
2. SHOPPEE, C. W. and STEPHENSON, R. J. J. Chem. Soc. 2230 (1954).
3. PIERCE, J. H., RICHARDS, H. C., SHOPPEE, C. W., STEPHENSON, R. J., and SUMMERS, G. H. R. J. Chem. Soc. 694 (1955).
4. SHOPPEE, C. W., RICHARDS, H. C., and SUMMERS, G. H. R. J. Chem. Soc. 4817 (1956).
5. REICHSTEIN, T. U.S. Patent No. 2,520,656 (1950).
6. DAVIES, R. H., MEECHAM, S., and SHOPPEE, C. W. J. Chem. Soc. 679 (1955).
7. SUGIYAMA, G. J. Biochem. (Japan), **25**, 157 (1937).
8. JUSTONI, R. and PESSINA, R. Il Farmaco, **11**, 72 (1956).
9. SCHUBERT, A. and DAMKER, CHR. J. prakt. Chem. **4**, 260 (1957).

RECEIVED DECEMBER 12, 1958.
RESEARCH AND DEVELOPMENT LABORATORIES,
CANADA PACKERS LTD.,
TORONTO, ONTARIO.

HELVETICA
CHIMICA
ACTA

SCHWEIZERISCHE
CHEMISCHE GESELLSCHAFT
Verlag Helvetica Chimica Acta
Basel 7 (Schweiz)

Seit 1918 **40** Jahre

Abonnemente: Jahrgang 1959, Vol. XLII $25.00 incl. Porto

Es sind noch lieferbar:

Neudruck ab Lager
Vol. I–XXIV (1918–1941)
Vol. XXV–XXVII (1942–1944) in Vorbereitung.

Originalausgaben, druckfrisch und antiquarisch.
Vol. XXVIII–XLI (1945–1958)

Diverse Einzelhefte ab Vol. XXII
Preise auf Anfrage. Nur solange Vorrat

Das wissenschaftliche Organ der SCHWEIZERISCHEN CHEMISCHEN GESELLSCHAFT

NOTES TO CONTRIBUTORS

Canadian Journal of Chemistry

MANUSCRIPTS

General.—Manuscripts, in English or French, should be typewritten, double spaced, on paper 8½×11 in. **The original and one copy are to be submitted.** Tables and captions for the figures should be placed at the end of the manuscript. Every sheet of the manuscript should be numbered. Style, arrangement, spelling, and abbreviations should conform to the usage of recent numbers of this journal. Greek letters or unusual signs should be written plainly or explained by marginal notes. Characters to be set in bold face type should be indicated by a wavy line below the characters. Superscripts and subscripts must be legible and carefully placed. Manuscripts and illustrations should be carefully checked before they are submitted. Authors will be charged for unnecessary deviations from the usual format and for changes made in the proof that are considered excessive or unnecessary.

Abstract.—An abstract of not more than about 200 words, indicating the scope of the work and the principal findings, is required, except in Notes.

References.—These should be designated in the text by a key number and listed at the end of the paper, with the number, in the order in which they are cited. The form of the citations should be that used in this journal; in references to papers in periodicals, titles should not be given and only initial page numbers are required. The names of periodicals should be abbreviated in the form given in the most recent *List of Periodicals Abstracted by Chemical Abstracts*. All citations should be checked with the original articles and each one referred to in the text by the key number.

Tables.—Tables should be numbered in roman numerals and each table referred to in the text. Titles should always be given but should be brief; column headings should be brief and descriptive matter in the tables confined to a minimum. Vertical rules should not be used. Numerous small tables should be avoided.

ILLUSTRATIONS

General.—All figures (including each figure of the plates) should be numbered consecutively from 1 up, in arabic figures, and each figure referred to in the text. The author's name, title of the paper, and figure number should be written in the lower left corner of the sheets on which the illustrations appear. Captions should not be written on the illustrations.

Line drawings.—Drawings should be carefully made with India ink on white drawing paper, blue tracing paper, or co-ordinate paper ruled in blue only; any co-ordinate lines that are to appear in the reproduction should be ruled in black ink. Paper ruled in green, yellow, or red should not be used. All lines must be of sufficient thickness to reproduce well. Decimal points, periods, and stippled dots must be solid black circles large enough to be reduced if necessary. Letters and numerals should be neatly made, preferably with a stencil (**do NOT use typewriting**), and be of such size that the smallest lettering will not be less than 1 mm high when the figure is reduced to a suitable size. Many drawings are made too large; originals should not be more than 2 or 3 times the size of the desired reproduction. Wherever possible two or more drawings should be grouped to reduce the number of cuts required. In such groups of drawings, or in large drawings, full use of the space available should be made; the ratio of height to width should conform to that of a journal page (5½×7½ in.) but allowance must be made for the captions. **The original drawings and one set of clear copies (e.g. small photographs) are to be submitted.**

Photographs.—Prints should be made on glossy paper, with strong contrasts. They should be trimmed so that essential features only are shown and mounted carefully, with rubber cement, on white cardboard, with no space between those arranged in groups. In mounting, full use of the space available should be made. **Photographs are to be submitted in duplicate;** if they are to be reproduced in groups one set should be mounted, the duplicate set unmounted.

REPRINTS

A total of 50 reprints of each paper, without covers, are supplied free. Additional reprints, with or without covers, may be purchased at the time of publication.

Charges for reprints are based on the number of printed pages, which may be calculated approximately by multiplying by 0.5 the number of manuscript pages (double-space typewritten sheets, 8½×11 in.) and including the space occupied by illustrations. Prices and instructions for ordering reprints are sent out with the galley proof.

Contents

Gerassimos Frangatos and Alfred Taurins—Pyridinium betaines of 1,3-indandione series - 835

Henry W. Habgood and James F. Hanlan—A gas chromatographic study of the adsorptive properties of a series of activated charcoals - - - - 843

Hans Mayer and Léo Marion—The partial structures of aconitine and aconitoline - 856

Nazih Latif and Ibrahim Fathy—Carbonyl and thiocarbonyl compounds. 1 *a*. Reaction of 9-diazoxanthene with *o*-quinones. *b*. The direct preparation of halogenated cyclic ethers from certain thiones and their molluscicidal activity - 863

R. A. McIvor and C. E. Hubley—Infrared spectra of organo-phosphorus compounds. III. Phosphoramidates, phosphoramidothionates, and related compounds - 869

E. H. Charlesworth, H. J. Campbell, and D. L. Stachiw—The synthesis of 2-ketocyclohexylsuccinic acid and related substances. IV. Studies on some *cis*- and *trans*-fused γ-lactones - - - - - - - - - - - - 877

T. Schaefer—On the coupling between F^{19} and H^{1} nuclei in *p*-fluorotoluene - 882

E. Bock and A. N. Campbell—The limiting conductance of aqueous solutions of potassium iodate, potassium chlorate, and silver nitrate at 35.00° C - 889

T. E. Timell—The constitution of a hemicellulose from sugar maple (*Acer saccharum*) - 893

J. G. Hooley—Isotherms of bromine on graphite - - - - - - - - - 899

James Trotter—Steric inhibition of resonance. III. Calculation of resonance energies and bond lengths - - - - - - - - - - - - - - - - 905

Manfred J. D. Low and H. Austin Taylor—The kinetics of hydrogen chemisorption on an iridium catalyst - - - - - - - - - - - - - - 915

A. L. Currie and T. E. Timell—The constitution of a methyl glucuronoxylan from kapok (*Ceiba pentandra*) - - - - - - - - - - - - - - 922

C. C. McDonald, J. R. McDowell, and H. E. Gunning—Photochemical separation of mercury isotopes. III. The reaction of $Hg^{202}6(^3P_1)$ atoms, photo-excited in natural mercury vapor, with hydrogen chloride - - - - - 930

A. J. Finlayson and C. C. Lee—Rearrangement studies with C^{14}. VII. The acetolysis of methyl-C^{14}-isopropylcarbinyl *p*-toluenesulphonate - - 940

S. Sato and R. J. Cvetanović—The effect of molecular oxygen on the reaction of oxygen atoms with *cis*-2-pentene - - - - - - - - - - - - 953

G. A. Hamilton and R E. Robertson—The temperature dependence of the hydrolysis of methyl esters of certain alkyl-substituted benzenesulphonates in water - 966

Thomas Francis and E. von Rudloff—The acetolysis of some hydroxytetrahydro-2-pyrans - 972

H G. Heal—The decomposition of solid potassium chlorate by X rays - 979

B. A. Gingras and C. H. Bayley—Preparation of some fluorine-containing trisubstituted aromatic hydroxylamines - - - - - - - - - - 988

Notes:

R. A. Mackenzie and K. J. McCallum—Szilard Chalmers reaction in potassium manganate - 993

Yoshio Matsunaga—Electron spin resonance absorption of ultramarine: effect of cations - 994

F. W. Lampe and F. H. Field—The addition of ethyl radicals to ethylene - 995

M. Kouris, H. Ruck, and S. G. Mason—Note on the determination of crystallinity index of cellulose - - - - - - - - - - - - - - - - - - 998

G. Giacometti—Structure and reactivity of C_3H_3 radical - - - - - - 999

B. D. Pate, D. C. Santry, and L. Yaffe—The half-life of Pb^{210} (RaD) - - 1000

D. A. Armstrong and J. W. T. Spinks—Low temperature irradiation of mixtures of HBr and C_2H_4 - - - - - - - - - - - - - - - - 1002

Yoshio Matsunaga—Electron spin resonance absorption of binaphthoquinones - 1003

P. Ziegler—Substitution and elimination reactions during acetolysis of derivatives of 3β,6β-dihydroxyallocholanic acid - - - - - - - - 1004